VOL.
10
1961

THE INTERNATIONAL JOURNAL OF

Applied Radiation and Isotopes

Volume 10 1961

Editorial Board

P. C. AEBERSOLD
Washington

A. H. W. ATEN, Jr.
Amsterdam

M. BRUCER
Oak Ridge

J. COURSAGET
Saclay

V. N. KONDRATIEV
Moscow

M. MAGAT
Paris

B. MANOWITZ
New York

J. L. PUTMAN
Wantage

H. SELIGMAN
Vienna

Editorial Advisory Board

Austria
B. KARLIK, Vienna

Argentina
E. E. GALLONI, Buenos Aires

Belgium
Z. M. BACQ, Liége
P. C. CAPRON, Louvain

France
P. AUGER, Paris
L. BUGNARD, Paris
C. H. FISCHER, Saclay
B. GOLDSCHMIDT, Paris
M. HAISSINSKY, Paris

Germany
H. LANGENDORFF, Freiburg
M. MAIER-LEIBNITZ, Munich
F. STRASSMANN, Mainz
F. WEYGAND, Berlin

Israel
I. DOSTROVSKY, Rehovoth

Italy
E. B. CHAIN, Rome
A. PERUSSIA, Milan
G. TRABACCHI, Rome

Japan
MASAO TSUZUKI, Tokyo

Portugal
H. DE CARVALHO, Lisbon

Scandinavia
G. C. DE HEVESY, Stockholm

Switzerland
H. H. STAUB, Zürich

U.N.E.S.C.O.
P. AUGER, Paris

United Kingdom and Commonwealth
J. S. ANDERSON, Victoria
R. H. BETTS, Chalk River, Ontario
A. CHARLESBY, Shrivenham
Sir JOHN COCKCROFT, Cambridge
V. R. KHANOLKAR, Bombay
Sir HANS KREBS, Oxford
C. P. LEBLOND, Montreal
D. R. LLEWELLYN, Auckland
A. S. MCFARLANE, London
J. STERNBERG, Montreal

U.S.A.
J. C. BUGHER, New York
V. CONQUEST, Chicago
R. D. EVANS, Cambridge, Mass.
M. HARRIS, Spokane, Wash.
W. F. LIBBY, Los Angeles
W. B. MANN, Washington
H. F. MARK, New York
H. R. NELSON, Columbus, Ohio
S. WARREN, Boston

U.S.S.R.
N. A. BACH, Moscow
G. M. FRANK, Moscow
G. V. KURDIUMOV, Moscow

Pergamon Press New York • London • Oxford • Paris

VO
1
19

VOL.
10
1961

CONTENTS OF VOLUME 10

NUMBER 1

W. C. Dewey and W. K. Sinclair: Criteria for evaluating collimators used in *in vivo* distribution studies with radioisotopes 1

L. A. Walker, G. Sparling and H. Mercer: A simple method for the differential counting of radioactive iron (Fe^{59}) and chromium-51 in mixtures 17

E. R. Powsner: Self-absorption of carbon-14 samples on thin paper planchets 22

R. E. Black: Preparation and testing of low-energy radiation sources 30

H. E. Skibitzke, H. T. Chapman, G. M. Robinson and R. A. McCullough: Radiotracer techniques for the study of flow in saturated porous materials 38

W. R. Singleton, A. Caspar and W. S. Flory, Jr.: A cobalt machine for semi-acute irradiation of growing plants 47

Technical Notes

T. W. Sudia and A. J. Linck: Method for autoradiography using individually packaged X-ray film 55

S. V. Nablo and T. C. Martin: Efficiencies and photofractions of some commonly used NaI(Tl) well crystals 55

Book Reviews 61

Book Received 62

International News 63

NUMBERS 2/3

J. W. G. Dale, W. E. Perry and R. F. Pulfer: A beta-gamma ionization chamber for substandards of radioactivity—I. Uses and calibration 65

J. W. G. Dale: A beta-gamma ionization chamber for substandards of radioactivity—II. Instrument response to gamma radiation 72

F. J. Carleton and H. R. Roberts: Determination of the specific activity of tritiated compounds on paper chromatograms using an automatic scanning device 79

G. Rowlands: Solid angle calculations 86

V. Bocci: Proteolysis of I^{131}-labelled gamma-globulin 94

M. Brucer: A total-body irradiator 99

D. O. Cummins and C. F. G. Delaney: Design studies for a Cs-137 irradiator 106

J. R. Puig et J. Dobó: Greffage radiochimique par irradiation à basses temperatures 112

R. L. Platzman: Total ionization in gases by high-energy particles: An appraisal of our understanding 116

Technical Notes

R. C. Palmer, D. K. Davis and W. V. Willis: A remote sampling system for high-level gamma sources 128

H. L. Otto and M. Winand: The preparation of curie quantities of S^{35}-labelled element sulphur 130

P. J. Campion and J. G. V. Taylor: Statistical errors in disintegration rate measurements by the coincidence technique 131

H. J. Born and P. Wilkniss: Zur aktivierungsanalyse von Sauerstoff mit Hilfe der Reaktion $O^{16}(t,n)F^{18}$ 133

Book Reviews 137

International News 139

NUMBER 4

J. Pijck, J. Gillis et J. Hoste: La détermination du Cu, Cr, Zn et Co dans le sérum par radioactivation 149

H. W. Wilson, D. E. Watt and D. Ramsden: A low-background laboratory 158

G. D. Fatzer, J. M. Schroeer and B. E. Blake: The radiotracer testing method in metal cleaning studies 167

Y. Ericsson: Double labelling of sodium monofluorophosphate with P^{32} and F^{18} 177

J. Kivel and A. F. Voigt: Gamma radiolysis of carbon-14 labeled isobutane 181

C. Mechelynck-David et F. Provoost: Etude de l'effet de partenaires solides sur la polymérisation de l'éthylène et sur la télomérisation du tétrachlorure de carbone et de l'éthylène initiées par rayonnement gamma 191

T. S. Osborne and A. O. Lunden: The cooperative plant and seed irradiation program of the University of Tennessee 198

Technical Notes

M. C. Kordecki and M. B. Gandy: Precision plating of stearic acid-1-carbon-14 from benzene solutions 210

W. G. Duncombe: A nomogram for calculating autoradiograph exposures 212

Letter to the Editors

B. Kalab and E. Broda: Assay of radioactive CO_2 in Geiger counters 214

Book Reviews 215

International News 219

AUTHOR INDEX

Black, R. E. 30
Blake, B. E. 167
Bocci, V. 94
Born, H. J. 133
Broda, E. 214
Brucer, M. 99
Campion, P. J. 131
Carleton, F. J. 79
Caspar, A. 47
Chapman, H. T. 38
Cummins, D. O. 106
Dale, J. W. G. 65, 72
David, C. Mechelynck- 191
Davis, D. K. 128
Delaney, C. F. G. 106
Dewey, W. C. 1
Dobó, J. 112
Duncombe, W. G. 212
Ericsson, Y. 177
Fatzer, G. D. 167
Flory, W. S., Jr. 47
Gandy, M. B. 210
Gillis, J. 149
Hoste, J. 149
Kalab, B. 214
Kivel, J. 181
Kordecki, M. C. 210
Linck, A. J. 55
Lunden, A. O. 198
McCullough, R. A. 38
Martin, T. C. 55
Mercer, H. 17
Nablo, S. V. 55
Osborne, T. S. 198
Otto, H. L. 130
Palmer, R. C. 128
Perry, W. E. 65
Pijck, J. 149
Platzman, R. L. 116
Powsner, E. R. 22
Provoost, F. 191
Puig, J. R. 112
Pulfer, R. F. 65
Ramsden, D. 158
Roberts, H. R. 79
Robinson, G. M. 38
Rowlands, G. 86
Schroeer, J. M. 167
Sinclair, W. K. 1
Singleton, W. R. 47
Skibitzke, H. E. 38
Sparling, G. 17
Sudia, T. W. 55
Taylor, J. G. V. 131
Voigt, A. F. 181
Walker, L. A. 17
Watt, D. E. 158
Wilkniss, P. 133
Willis, W. V. 128
Wilson, H. W. 158
Winand, M. 130

International Journal of Applied Radiation and Isotopes, 1961, Vol. 10, pp. 1 to 16. Pergamon Press Ltd. Printed in Northern Ireland

Criteria for Evaluating Collimators used in *In Vivo* Distribution Studies with Radioisotopes

W. C. DEWEY and W. K. SINCLAIR
Physics Department, University of Texas,
M. D. Anderson Hospital and Tumor Institute,
Houston, Texas, U.S.A.

VOL.
10
1961

(*Received* 6 *June* 1960)

In many practical circumstances involving the localization of radioactive regions in the body, the highest resolution is not necessarily desirable because of the accompanying reduction in sensitivity. A compromise must therefore be effected between resolution and sensitivity. Principles are presented for effecting this compromise and a figure of merit is defined in order to determine which collimator–detector system provides the highest probability of detecting a radioactive target located inside a region with a different concentration of radioactivity. A most important factor is the ratio of target-to-nontarget sensitivity which depends on both the shielding of the detector and the collimator construction.

Three different focusing collimators having 91, 19 and 7 holes, respectively, and two single-bore collimators, 3 and 5 in. in length, are studied. It is found that the most suitable collimator for detecting a given target depends on the size of that target. For example, of the compromises available, a collimator with very good resolution and low sensitivity is best for small targets, while for larger targets a collimator with low resolution and high sensitivity is best.

Two other questions of interest are considered. First, the distortion in the representation of the target, which varies with target size, is specified in terms of a parameter called specific resolution. Second, the concentrations of radioactivity needed for given scintiscanning situations can be calculated by means of an equation which is derived. An application of the equation to a practical case in brain-tumor scanning is presented.

DES CRITERES POUR EVALUER LES COLLIMATEURS EMPLOYES DANS LES RECHERCHES SUR LA DISTRIBUTION *IN VIVO* AVEC DES RADIOISOTOPES

En bien des cas actuels comportant la localization de régions radioactives dans le corps, la plus forte résolution n'est pas nécessairement à désirer, vu la diminution de sensibilité qui l'accompagne. Il faut donc faire un compromis entre la résolution et la sensibilité. On présente des principles pour achever ce compromis et on précise un chiffre de mérite pour décider quel système de collimateur/détecteur offre la plus grande probabilité d'observer une cible radioactive située dans une région ayant une différente concentration de radioactivité. Un facteur fort important est la proportion de sensibilité cible—non-cible qui dépend à la fois du blindage du détecteur et de la construction du collimateur.

On étudie trois différents collimateurs ajustables ayant 91, 19 et 7 canaux et deux collimateurs à canal unique de longueur 3 et 5 in. (7,5 et 12,5 cm). On trouve que le meilleur collimateur pour observer une cible particulière dépend de la grandeur de cette cible. Par example, d'entre les compromis possibles, un collimateur de très bonne résolution et de petite sensibilité est le meilleur pour les petites cibles, mais pour les plus grandes un collimateur de petite résolution et de grande sensibilité est le meilleur.

On regarde deux autres questions d'intérêt. D'abord, la distortion dans la représentation de la cible, qui varie avec la grandeur de la cible, se spécifie en termes d'un paramètre dit la *resolution spécifique*. En deuxième place, les concentrations de radioactivité nécessaires pour des situations particulières d'exploration à scintillement peut se calculer au moyen d'une équation que l'on déduit. On présente une application de cette équation à un cas actuel d'exploration d'une tumeur de cervelle.

КРИТЕРИЙ ОЦЕНКИ КОЛЛИМАТОРОВ, ПРИМЕНЯЕМЫХ ДЛЯ ИССЛЕДОВАНИЯ РАСПРЕДЕЛЕНИЯ РАДИОИЗОТОПОВ

Во многих случаях, например при определении местонахождения радиоактивных областей в организме, максимальная разрешающая способность не обязательно необходима, поскольку она связана с уменьшением чувствительности. Следовательно, нужно найти компромисс между разрешением и чувствительностью. Предлагаются способы решения этого компромисса и выводится соответствующая величина, на основании которой можно определить, какая коллиматорно-детекторная система дает максимальную вероятность определения радиоактивности мишени в областях с различной концентрацией радиоактивности. Наиболее существенным фактором является отношение чувствительности внутри и вне мишени, которое зависит как от экранировки детектора, так и от конструкции коллиматора.

Были исследованы три различных фокусирующих коллиматора с 91, 19 и 7 отверстиями и 2 коллиматора с одним отверстием длиной 3 и 5 дюймов. Было найдено, что пригодность коллиматоров для обнаружения мишени определяется размерами последней. Оказалось, например, что из числа возможных вариантов для малых мишеней лучше применять коллиматор с хорошим разрешением и низкой чувствительностью, а для больших мишеней—с низким разрешением и высокой чувствительностью.

Были рассмотрены два других интересных вопроса. Во-первых, искажение графического изображения мишени, меняющееся с ее размерами, было определено параметром, называемым удельным разрешением. Во-вторых, было найдено, что концентрации радиоактивности, необходимые для снятия сцинтиграмм, могут быть вычислены в каждом случае на основании выведенного уравнения. Описано применение этого уравнения для нахождения опухоли мозга.

MERKMALE FÜR DIE AUSWERTUNG VON KOLLIMATOREN BEI UNTERSUCHUNGEN DER VERTEILUNG VON RADIOISOTOPEN *IN VIVO*

Bei der Lokalisierung von radioaktiven Regionen innerhalb des Körpers ist in diesen praktischen Fällen eine hohe Auflösung nicht immer erwünscht, da sie eine Herabsetzung der Empfindlichkeit mit sich bringt. Ein Kompromiss zwischen Auflösung und Empfindlichkeit muss daher gefunden werden. Grundsätze zur Ausfindung eines solchen Kompromisses werden angegeben und optimale Bedingungen werden definiert, um damit jene Kollimator-Detektor-Kombination zu bestimmen, welche die grösste Wahrscheinlichkeit bietet, einen radioaktiven Herd innerhalb eines Gebietes mit verschiedenen Konzentrationen der Radioktivität aufzufinden. Der wichtigste Faktor ist dabei das Verhältnis der Radioaktivität des Herdes und der Hintergrundsaktivität, welches sowohl von der Abschirmung des Detektors als auch von der Konzentration des Kollimators abhängt.

Drei verschiedene fokusierende Kollimatoren mit 91, 19 und 7 Löchern und 2 Kollimatoren mit je einer Bohrung von 3 bzw. 5 in. Länge wurden untersucht. Es wurde gefunden, dass die Grösse des Herdes ausschlaggebend ist, welcher Kollimator sich zur Ausfindung eben dieses Herdes am besten eignet. Z.B. eignet sich ein Kollimator mit hoher Auflösung und kleiner Empfindlichkeit gut zur Ausfindung eines räumlich kleinen Herdes, während für ausgedehnte Herde am besten ein Kollimator mit niederer Auflösung und hoher Empfindlichkeit verwendet wird. Zwei weitere interessante Fragen werden erwähnt: erstens die Verzerrung der Darstellung des Herdes, welcher von der Ausdehnung des Herdes abhängt. Sie wird durch einen Parameter ausgedrückt, der spezifische Auflösung genannt wird. Zweitens wird die Konzentration der Radioaktivität, die für die bestimmte Szintillationsscanning-Situation erforderlich ist mit Hilfe einer Gleichung berechnet, welche abgeleitet wird. Eine Anwendung dieser Gleichung im praktischen Fall eines Gehirn-tumor-Scannings wird vorgeführt.

VOL. 10 1961

INTRODUCTION

COLLIMATORS, in conjunction with scintillation crystals and associated electronic and automatic scanning equipment, are important in determinations of the *in vivo* distribution of gamma emitting radioisotopes. Several papers[1–5] have appeared on design considerations for collimators, and it is apparent that, as the resolution or ability of the collimator to distinguish one radioactive area from an adjacent radioactive area improves, the sensitivity generally decreases. Since both resolution and sensitivity are important in the definition of distributions of radioactive material, a compromise between these two parameters must be considered when designing a collimator. In the literature this problem is frequently considered from a theoretical point of view, sometimes in relation to a point source of radioactivity and often without taking into consideration the gamma rays which penetrate both the shielding around the crystal and the lead walls and partitions of the collimator. In this investigation an evaluation of collimators was made based on experimentally determined values of resolution, sensitivity and the ratio of target sensitivity to nontarget sensitivity. In practical circumstances, the optimum compromise between these factors will depend on the size of the region being studied.

MATERIALS AND METHODS

The scintillation detecting system consisted of a commercial probe with a 2 × 2 in. sodium iodide crystal assembly connected to a spectrometer and a scaler. Additional lead shielding was provided around the crystal as indicated in Fig. 1.

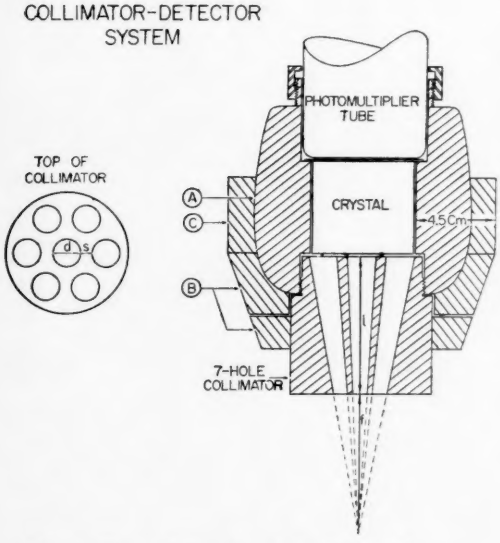

FIG. 1. Plan and elevation views of the collimator–detector system. In this sketch the seven-hole focusing collimator is shown. The other collimators differed only in the number and size of holes. Different sections of lead shielding are designated *A*, *B* and *C*.

Specifications for focusing collimators and two single-bore collimators (one cylindrical hole in the center) which were designed by the authors and fabricated in the physics workshop of this institution are given in Table 1. The focal point, resolution and sensitivity at the focal point as determined with a point source (1·0 mm × 1·0 mm) of I^{131} are also included. These parameters will be defined and discussed later. All the focusing collimators consisted of equally spaced, tapered holes which focused at a point in space. One-half of the crystal face was covered by the septa between the holes. The seven-hole focusing collimator is shown in Fig. 1.

All studies were conducted using I^{131} as the radioactive source. The spectrometer was set to include all of the photopeak, primarily 367 keV gamma rays which had not been scattered. The reproducibility of the spectrometer settings was checked frequently by using a long-lived mock I^{131} standard (mixture of Ba^{133} and Cs^{137}).

Radioactive sources consisted of shallow circular cylinders to which accurately measured volumes and amounts (4–7 $\mu c/cm^2$ of I^{131} were added. The specific activity (microcuries per milliliter) of the I^{131} was determined by assaying each sample of I^{131} in a calibrated well ionization chamber.

TABLE 1. Design specifications and experimental parameters for various collimators

	Collimator	Ninety-one-hole	Nineteen-hole	Seven-hole	¾ × 5 in.* single-bore	¾ × 3 in.* single-bore
Design specifications	Hole diameter at top (d) (cm)	0·38	0·90	1·60	2·0	2·0
	Septa thickness at top (s) (cm)	0·10	0·26	0·59	—	—
	Collimator length (l) (cm)	7·2	8·0	8·0	12·6	7·6
	Hole diameter at bottom (cm)	0·23	0·45	0·80	2·0	2·0
	Septa thickness at bottom (cm)	0·05	0·13	0·30	—	—
	Focal distance (f) (cm)	8·4	8·0	8·0	—	—
	Radius of geometrical penumbra at 8·0 cm distance	0·40	0·90	1·60	4·54	6·20
Experimental parameters	Focal distance (cm)	7·5	6·5	6·8	—	—
	Resolution at focus R_{Pt} (cm)	0·50	0·90	1·65	3·28*	4·0*
	Sensitivity to point source at focus (c.p.m./μc)	2550	2410	2200	730*	1360*
	Shielding parameter†	0·19	0·43	0·65	0·84	0·93

* For single-bore collimators resolution and sensitivity are listed for a source-to-collimator distance of 8·0 cm.

† The shielding parameter is equal to S (Fig. 4), the ratio of target-to-nontarget sensitivities, when the size of the target is equal to the geometrical penumbra as listed above. The size of the nontarget is 30 × 120 cm.

Sources with the following diameters were used: 0·5, 1·0, 2·0, 3·0, 4·0, 6·0, 8·0, 12·0 and 24·0 cm. The latter was the largest diameter that was feasible because of the large amounts of radioactivity involved. The sources were positioned with the plane of the source perpendicular to the axis of the collimator and at various distances from the face of the collimator. The counting rate was determined for each source at various positions, and the response was expressed in counts per minute per microcuries per square centimeter.

The response to sources larger than 24 cm in diameter up to and including a 30 × 120 cm rectangular source representing a frontal section of the human body (Fig. 2) was investigated in the following manner. The response of a small source (a bottle 3·0 cm in diameter containing 2·0 mc of I^{131}) was determined at a distance r from the axis of

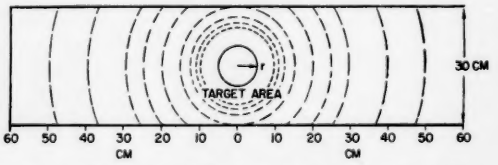

FIG. 2. Diagram of whole-body plane source with a target area of 5 cm radius located at the center. In the analysis described in the text the source was subdivided into rings and segments of rings as indicated.

VOL. 10 1961

the collimator. The response in counts per minute per microcuries per square centimeter for a ring 3 cm in width at this distance was found by multiplying the response in counts per minute per microcuries for the small source by the area of the ring. The responses for successive rings, into which the large source could be divided, were added to give the response for the large source. Note in Fig. 2 that when the distance from the axis of the collimator exceeded 15 cm ($r > 15$), the source was divided into segments of rings.

In order to determine more accurately the response to circular sources smaller than 1·0 cm in diameter, the integration technique just described was used. The response of a point source (1·0 × 1·0 mm) was determined in relation to its distance from the collimator axis. As before, the responses for small rings (0·1 cm in width) were calculated, and these were added to give the response for the circular source. The responses calculated for the 0·5 and 1·0 cm diameter sources corresponded to the responses actually measured for these sources.

For automatic scanning, a commercial scintiscanner with a modified photoscanner was used. The photoscanner consisted of a modulated neon light, the intensity of which increased with the counting rate. It was possible to amplify small differences between counting rates by adjusting the photoscanner such that light and dark areas on the film differed by only 20 per cent in counting rate.

EXPERIMENTAL DETERMINATION OF RESOLUTION AND SENSITIVITY

(1) *Point sources*

The response of each collimator–detector system to the position of a point source of radiation was determined and represented on paper by drawing iso-response lines through the points of equal counting rate. For example, in Fig. 3(A) data are plotted for the ninety-one-hole focusing collimator which has response symmetry radial to the axis. At 7·5 cm below the face of the collimator there is a point of maximum counting rate (2250 c.p.m./μc I^{131}) or a point of focus. On the focal plane and at a lateral distance of 0·25 cm from the focal point, the response decreases to one-half maximum. The resolution is equal to twice this distance or 0·50 cm for the ninety-one-hole collimator. The other collimators were investigated similarly, and the results are listed in Table 1. For the focusing collimators the sensitivities at the focal point are nearly the same; the resolution is approximately equal to the diameter of the hole at the top of the collimator; and the actual focal distance is less than the geometrical focal distance. These relationships were predicted theoretically by BROWNELL[5]. The single-bore collimators do not have a focal point, and the sensitivity continues to increase as the source approaches the collimator.

(2) *Plane sources*

The response of each collimator–detector system was also studied in relation to the position of circular plane sources. In Fig. 3(B) the response of the ninety-one-hole focusing collimator to an I^{131} plane circular source 3·0 cm in diameter is represented. The counting rate in relation to distance from the collimator is rather uniform, and indeed *there is no focusing effect for a large source.* When the source is located on the "focal" plane (as determined with the point source) the crystal "sees" a small part to the source with maximum sensitivity; whereas when the source is located above or below the focal plane the crystal "sees" a larger part of the source with lower sensitivity. This is discussed in more detail by BROWNELL[5]. It is apparent that the response as determined with a point source can be misleading if used to represent the response to larger sources.

(a) *Centers on central axis.* The responses to a range of plane sources placed with their centers on the axis of the collimator were determined for distances of 4·0, 8·0 and 12·0 cm below the collimator face. The counting rates were normalized to the response of the whole-body plane source (a 30 × 120 cm rectangle). The results are plotted in Fig. 4. The normalized value S for a target region of

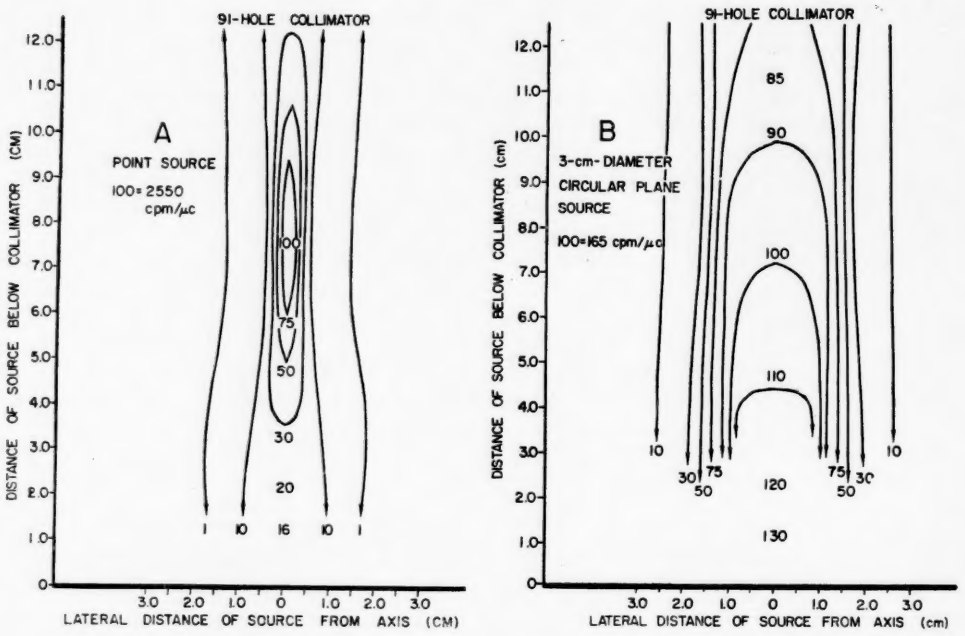

(A)—Determined with point source (1 × 1 mm).

(B)—Determined with circular plane source 3 cm in diameter.

FIGS. 3(A) and 3(B). Relative response for ninety-one-hole focusing collimator vs. position of I^{131} source relative to face of collimator. Iso-response lines are indicated.

radius r is the ratio of the response from the target region to the response from the whole-body plane source. The quantity S is determined principally by the shielding around the crystal assembly. The response K c.p.m. per $\mu c/cm^2$ to radiation emitted from the whole-body source is a sensitivity parameter.

Some important relationships should be noted in the plane-source response curves in Fig. 4.

(i) For focusing collimators, the plots of the normalized response S versus the size of the source r do not depend greatly on the distance of the source from the collimator. For single-bore collimators, however, there is more dependence on source-to-collimator distance.

(ii) The target size determines which collimator has the best target-to-nontarget ratio (i.e. largest value of S): for r less than 0·2 cm the ninety-one-hole is best, for $1{\cdot}0 > r > 0{\cdot}2$ the nineteen-hole is best, for $3{\cdot}0 > r > 1{\cdot}0$ the seven-hole is best, and for $r > 3{\cdot}0$ cm the $\frac{3}{4} \times 3$ in. is best.

(iii) The value of S depends greatly on the amount of lead shielding around the scintillation crystal (Figs. 4 A,B and E); for example adding an extra lead ring 1·5–2·0 cm in thickness (parts B and C of Fig. 1) when the ninety-one-hole collimator was used increased the values of S for sources smaller than 6 cm in radius by 348 per cent.

(iv) The sensitivity parameters K vary greatly from one collimator to another; viz., from 3240 c.p.m. per $\mu c/cm^2$ for the ninety-one-hole collimator to 19,500 c.p.m. per $\mu c/cm^2$ for the $\frac{3}{4} \times 3$ in. single-bore collimator.

The curves in Fig. 4 can be corrected for water absorption by using experimental data obtained by placing a layer of water between the source and the collimator. Absorption measurements indicated that the I^{131} gamma rays (367 keV) were attenuated exponentially according to a linear absorption coefficient of

VOL. 10 1961

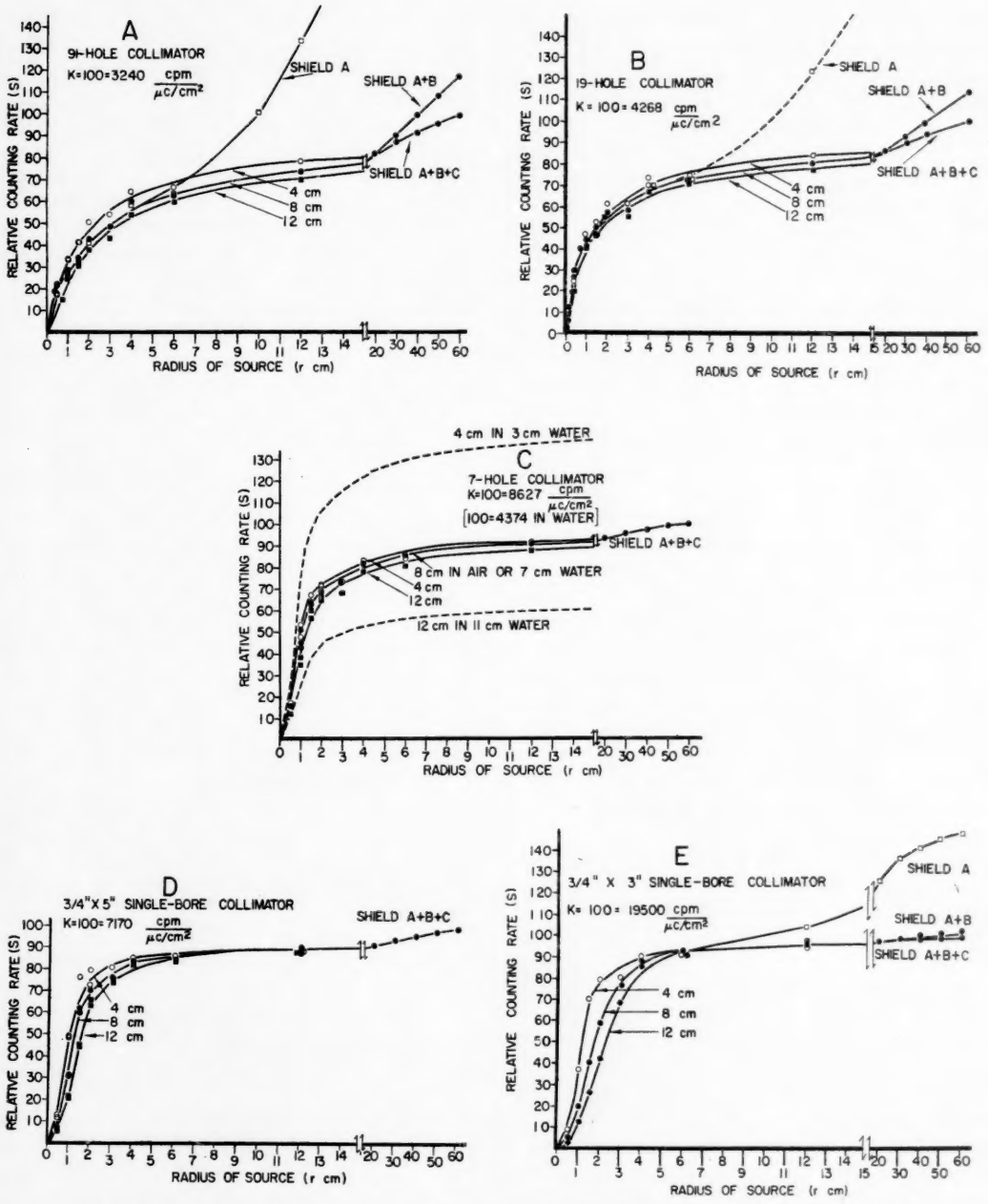

FIGS. 4(A) through 4(E). Relative sensitivity vs. size of I^{131} plane source at 4, 8 and 12 cm distance from face of collimator. Dimensions of plane source are shown in Fig. 2. Different amounts of lead shielding are shown in Fig. 1. For sources smaller than 15 cm in radius there is no difference between shield $A + B$ and shield $A + B + C$, and for sources smaller than 4–5 cm in radius there is no difference between shield A, shield $A + B$, and shield $A + B + C$. After correction for absorption of the gamma-rays by a layer of water, the curves (dotted lines in Fig. 4C) were normalized to the 8 cm distance.

0·10 cm^{-1}. This agrees quite well with the total attenuation coefficient of 0·11 cm^{-1} given by EVANS[9] and corresponds to a half-thickness of 7·1 cm. The effect of water absorption is indicated in Fig. 4(C).

(b) *Shielding parameter.* A parameter can be defined which indicates the effectiveness of the shielding. Ideally, the counting rate should result only from gamma rays which do not penetrate any shielding and which originate from the region of the source intersected by the geometrical umbra and penumbra (i.e. the region "seen" by the crystal). Thus, the shielding parameter is defined as the ratio of this ideal counting rate to the counting rate determined for the whole-body source. (This parameter is approximately equal to S when the target size is equal to the region seen by the crystal, Fig. 4). The radius of the source defined by the geometrical penumbra at a distance of 8·0 cm was determined for each collimator (Table 1), and the shielding parameter was estimated from Fig. 4. Values for each collimator with shields $A + B + C$ are as follows (Table 1): 0·19 for ninety-one-hole, 0·43 for nineteen-hole, 0·65 for seven-hole, 0·84 for $\frac{3}{4} + 5$ in. and 0·93 for $\frac{3}{4} + 3$ in.

Inspection of Figs. 4(A) and 4(B) reveals that the lead of the collimator itself is of primary importance for shielding gamma rays emitted from a circle less than 4·0 cm in radius, while the extra lead (shields $B + C$ in Fig. 1) around the probe and collimator is most important for shielding gamma rays emitted from a circle larger than 4·0 cm in radius. If the extra shielding were infinitely thick, the shielding parameters would be increased from 0·19 to only 0·34 for the ninety-one-hole collimator and from 0·43 to only 0·64 for the nineteen-hole collimator. Therefore the shielding in the septa of the collimators also needs to be increased. This could be accomplished by using material of higher density than lead (11·3), such as tungsten (19·0), mercury (13·5) or gold (19·3). If the extra shielding were infinitely thick and if the collimator were made of gold (assumed to be twice as effective as lead), the shielding parameters would be about 0·51 for the ninety-one-hole collimator and 0·78 for the nineteen-hole collimator.

Considerations of this kind also enable other factors (such as varying the ratio of "hole" to "septum" size) to be evaluated. In the practical case, the importance of analyzing the circumstances according to large sources rather than point sources is clearly evident. Furthermore, it may be possible to carry out such analyses by applying theoretical considerations.[6,7,8]

(c) *Centres moved from axis.* The responses of the collimators to circular plane sources displaced laterally at various distances from the axis of the collimator were determined. The sources were located in a plane at 8·0 cm from the face of the collimator. The results for two different sources determined with the nineteen-hole focusing collimator are plotted in Fig. 5. As for the point source, resolution for circular plane sources (R_{Pl}) is defined as twice the distance the collimator axis must move from the edge of the source in order to decrease the counting rate to one-half the maximum.* The edges of two circular sources must be separated by at least the resolution distance in order to be detected as separate sources. As indicated in Fig. 5, the resolution distance for a particular collimator decreases as the size of the circular source increases. Results for different collimators and sources of different size are plotted in Fig. 6.

(d) *Specific resolution.* Note the size of source for which the resolution is equal to the diameter of the source. This is indicated in Fig. 6 by the intersections of the diagonal line with the resolution curves. The resolution at each point of intersection is designated as the *specific resolution* (SR_{Pl}), which is therefore defined as the resolution when the distance from the edge of the source to the point of half-maximum counting rate equals the radius of the source. Values of SR_{Pl} are listed in Table 2 for each collimator.

The specific resolution is of practical

* The resolution has been defined with reference to the edge of the source instead of with reference to the center of the source. This is preferable because a target representation depends primarily on the counting rate transition across the target–nontarget interface. A similar method of representing resolution was used by FOLICHON and GANDY[10].

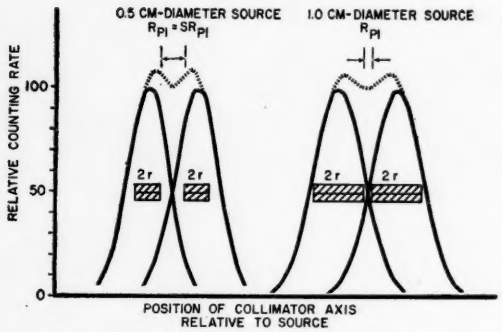

FIG. 5. Relative counting rate for nineteen-hole focusing collimator vs. the lateral displacement of circular plane sources from the collimator axis. The solid line indicates the response to each source considered individually, and the dotted line indicates the response to the two sources considered together. Source positions are indicated by horizontal lines designated by $2r$, the diameter of the source. The resolution, indicated by R_{PI}, decreases as the diameter of the source increases. When the resolution equals the diameter of the source, it is called the specific resolution SR_{PI}.

significance in that it specifies for each collimator the magnitude of the target distortion or sharpness of the interface between the target and nontarget regions in terms of the target size. As the collimator moves over a target with a diameter equal to the specific resolution, the counting rate will decrease to one-half maximum at a distance of one target radius from the edge. Two targets of this size must have their edges separated by a distance equal to their diameter in order to be detected as separate sources. For larger targets, the distance from the edge to one-half the maximum counting rate will be less than the target radius, and the targets can be resolved when they are separated by a distance less than their diameter. Smaller targets, however, can b resolved only when they are separated by a distance larger than their diameter.

It is interesting and useful to note in Table 2 that the specific resolution is approximately one-half (0·47–0·56) the resolution as determined with the point source. This is useful because the resolution for a point source can be determined much easier than the specific resolution. In view of the diversity in collimator design for which this correlation holds, it will probably apply in most cases.

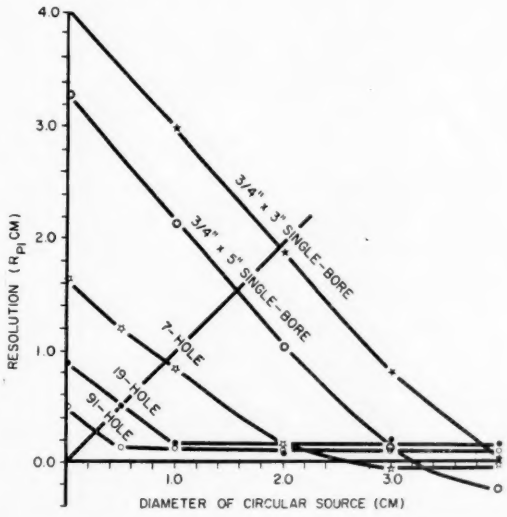

FIG. 6. Resolution as determined with plane circular sources vs. diameter of source. Sources were positioned 8·0 cm from the collimator face. The resolution is equal to twice the distance the collimator must move from the edge of one source in order that the counting rate will decrease to one-half the maximum counting rate; this is shown in Fig. 5. The specific resolution is indicated by the intersection of the diagonal line with the resolution curve; at this intersection the resolution is equal to the diameter of the source.

RESOLUTION VERSUS SENSITIVITY

In general, one is concerned with detecting and defining a target area in which the radioisotope has a higher or lower concentration than in a surrounding nontarget area. The first consideration is the probability of distinguishing the target area from the nontarget area. This depends on the change in counting rate as the collimator moves over the target area, which must be distinguished from the statistical fluctuations in the counting rate. The second consideration is the precision with which the shape of the target area is defined. This depends on the resolution obtainable with the collimator in relation to the target size.

(1) *Best collimator from the criterion of probability of distinguishing the target area from the nontarget area*

(a) *Plane sources.* For simplification the whole-body plane source, a rectangle 30 cm by 120 cm with a target area r (cm) in radius located at the center, will be considered (Fig. 2). Other quantities are defined as follows:

C_T—μc/cm^2 in the target area

C_{NT}—μc/cm^2 in the nontarget area

f—C_T/C_{NT} = the ratio of concentration of radioisotope in the target area to the concentration of radioisotope in the nontarget area

K—sensitivity (c.p.m. per μc/cm^2) to radiation emitted from the whole-body plane source, when the collimator–detector is over the center of the source (values in Fig. 4). Since the source is large, K varies very little as the collimator moves over it and decreases only as it approaches the edges

k—sensitivity (c.p.m. per μc/cm^2) to radiation emitted from the target area, when the collimator is directly over the target area

S—k/K = the ratio of target sensitivity to nontarget sensitivity (values in Fig. 4)

R_T—counting rate (c.p.m.) when the collimator is over the target area.

R_{NT}—counting rate (c.p.m.) when the collimator is over the nontarget area

t—time interval or equivalent pre-set time during which the counts are accumulated. (In most cases it is equal to twice the time constant of the integrating circuit or rate meter.)

The criterion for distinguishing the target area from the nontarget area is defined as follows: as the collimator moves directly over the target area, the change in the counting rate (ΔR) must be equal to or greater than n times the standard error (σ) in the counting rate R_{NT} ($\sigma = \sqrt{R_{NT}/t}$).

$$\Delta R = n\sigma = n\sqrt{\frac{R_{NT}}{t}}^{*}. \qquad (1)$$

If $n = 3$, the target will most certainly be detected.[11]

For a more rigorous statistical criterion of detection, ΔR must be equal to or greater than n' times the standard error in the difference between the target and nontarget counting rates. Then

$$|\Delta R| = n'\sqrt{\frac{R_{NT} + R_T}{t}}.$$

With equations presented in the next paragraph it can be shown that,

$$|\Delta R| = n'\sqrt{2 - S + Sf}\sqrt{\frac{R_{NT}}{t}}. \qquad (2)$$

For simplification, at the expense of statistical rigor, equation (1) instead of equation (2) was used as a criterion of detection. However, by comparing the two equations it is evident that equation (1) can be quite rigorous by putting

$$n = n'\sqrt{2 - S + Sf}.$$

In most scanning situations $0 < S < 0{\cdot}5$ and $0 < f < 2{\cdot}0$; therefore, $1{\cdot}22\,n' < n < 1{\cdot}58\,n'$. When n' equals 2·0, there should be about 95 per cent probability of distinguishing the target area from the nontarget area.

Expressions for ΔR and R_{NT} in equation (1) can be derived from the source and collimator–detector parameters.

$$R_{NT} = KC_{NT} \qquad (3)$$

$$R_T = kC_T + (K - k)C_{NT}. \qquad (4)$$

From the definitions of f, k and S,

$$R_T = KC_{NT}[1 + (f - 1)S] \qquad (5)$$

$$\Delta R = R_T - R_{NT} = KC_{NT}(1 - f)S$$
$$= kC_{NT}(1 - f). \qquad (6)$$

Combine equations (1), (3), and (6):

$$f = 1 \pm \frac{1}{\sqrt{Sk}} \times \frac{n}{\sqrt{C_{NT}t}}. \qquad (7)$$

* Normal room background has been neglected because in most scanning situations the net counting rate will be greater than 500 c.p.m., and the background can be reduced to about 50 c.p.m.. Under these conditions, neglecting background will result in less than 5 per cent error in estimating ΔR which is unimportant.

VOL. 10 1961

The value of f (and therefore of C_T) required to distinguish the target area from the nontarget area is thus determined when all the other factors are known or can be assigned values.

In the practical situation however, more often the value of f may be known or assumed. Rearranging equation (7)

$$C_{NT} = \frac{1}{Sk} \frac{n^2}{(1-f)^2 t} \tag{8}$$

where C_{NT} is the concentration (microcuries per square centimeter) of radioisotope in the nontarget area required to distinguish the target area from the nontarget area. The values of n and t can be chosen arbitrarily, independent of the collimator–detector system and the value of f depends on the ratio of concentration of radioactivity in the target area to concentration of radioactivity in the nontarget area. The values of k and S, however, as indicated in Fig. 4, are dependent on the particular collimator–detector system and on target size. As the value of $1/kS$ decreases, C_{NT} decreases; i.e. the concentration of radioactivity required is inversely proportional to the target sensitivity k and the ratio of target sensitivity to nontarget sensitivity S.* Furthermore, k can be standardized in terms of the sensitivity to the whole-body-plane source (a 30 × 120 cm rectangle) by substituting KS for k in equation (8). Then

$$C_{NT} = \frac{1}{KS^2} \frac{n^2}{(1-f)^2 t}. \tag{9}$$

The expression $1/KS^2$ is a valuable figure of merit for choosing the best collimator–detector system for the detection of a target area of particular size.

Values of this figure of merit are found by substituting the values of S and K from Fig. 4. For simplification, a source-to-target distance of 8·0 cm is considered, and the values $1/KS^2$ are plotted against target size in Fig. 7. For a specified equivalent pre-set time t, for a certain target (radius r, ratio f) and for a certain probability of detection, $1/KS^2$ is clearly proportional to C_{NT}. If equation (9) is solved for n,

$$n = \sqrt{\frac{C_{NT}(1-f)^2 t}{1/KS^2}}, \tag{10}$$

and it is apparent that for given values of C_{NT}, f and t the collimator which has the lowest value of $1/KS^2$ offers the highest probability of detecting this target and is therefore "best". It is clear from Fig. 7 that for

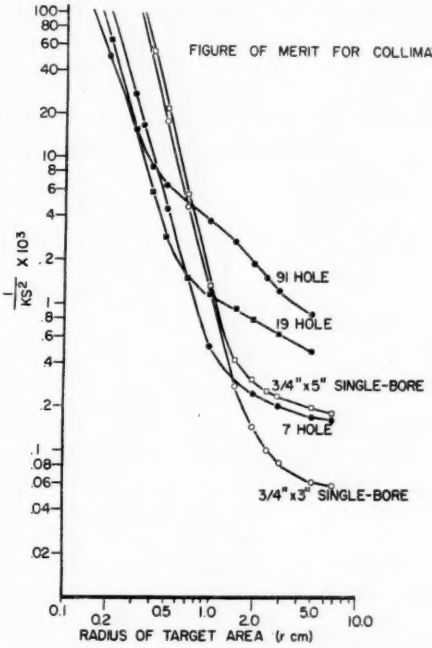

FIG. 7. Figure of merit ($1/KS^2$) vs. target size. The figure of merit is used in equations (9), (10) and (20) in the text, and its values depend on the particular collimator and target size. The collimator which has the lowest value of $1/KS^2$ for a particular target will offer the highest probability of detecting this target. (Source is 8 cm below collimator face.)

targets less than 0·25 cm in radius the ninety-one-hole collimator with low sensitivity and very good resolution is best, whereas for targets from 0·25 to 0·7 cm in radius the nineteen-hole collimator with higher sensitivity and moderate resolution is best. Then, from 0·7 to 1·5 cm the seven-hole collimator with even higher sensitivity and fair resolution is best, and for target radii greater than

* Although the resolution R_{PI} is not included in equation (8), it is interesting to note (Figs. 4 and 6) that as the size of the target increases, S increases while R_{PI} decreases.

1·5 cm the $\frac{3}{4} \times 3$ in. single-bore collimator with the highest sensitivity and low resolution is best. Note that the $\frac{3}{4} \times 5$ in. single-bore collimator is never the best collimator. These results are summarized in Table 2. Although the collimators have been evaluated for a source-to-target distance of 8·0 cm, their relative merits would not change greatly for distances from 4·0 to 12·0 cm (Fig. 4).

(b) *Volume sources.* The figure of merit for collimators which was derived in the last section for plane sources will also apply to volume sources if the parameters C_{NT} and f in equation (9) can be replaced by the equivalent values $(C_{NT})_e$ and f_e obtained for a volume source. Then,

$$(C_{NT})_e = \frac{1}{KS^2} \times \frac{n}{(1 - f_e)^2\, t}. \qquad (11)$$

A volume source can be represented as an infinite number of plane sources, one above the other. It is possible to specify an equivalent plane source which would have the same response as the volume source. For simplification, it is assumed that the difference in response between planes at different distances from the collimator is due only to the self-absorption in the source. Data in Fig. 4 indicate that the error resulting from this assumption will be small, especially for the focusing collimators. Some of the parameters used in the derivation are illustrated in Fig. 8. The following additional quantities are used:

ρ_{NT}—concentration of radioisotope in the nontarget volume (μc/cm^3)
ρ_T—concentration of radioisotope in the target volume (μc/cm^3)
f'—ρ_T/ρ_{NT}
$(C_{NT})_e$—equivalent concentration of radioisotope in the nontarget equivalent plane source (μc/cm^2)
$(C_T)_e$—equivalent concentration (μc/cm^2) of radioisotope in the plane source equivalent to the target.
f_e—$(C_T)_e/(C_{NT})_e$
μ—linear absorption coefficient (0·10 cm^{-1} for I^{131} gammas, 367 keV).

The counting rate when the collimator is

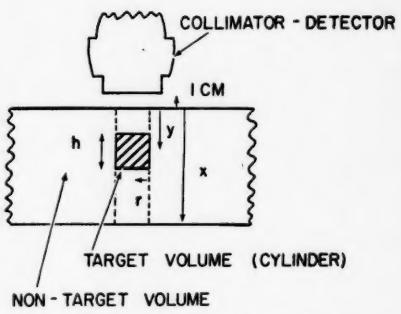

FIG. 8. View of collimator positioned above volume source. Target volume, which is assumed to be a right circular cylinder, has a different concentration of radioactivity than the nontarget volume ($30 \cdot 120 \cdot x$ cm rectangular parallelepiped).

over the nontarget volume is

$$R_{NT} = K\rho_{NT}\int_0^x e^{-\mu x}\, dx$$

and according to equation (3)

$$R_{NT} = K(C_{NT})_e. \qquad (12)$$

Thus,

$$(C_{NT})_e = \frac{\rho_{NT}(1 - e^{-\mu x})}{\mu} \qquad (13)$$

from which the equivalent concentration (μc/cm^2) in the nontarget equivalent plane source can be calculated. Conversely, if the equivalent concentration for the plane source is known, the actual concentration for the volume source can be calculated,

$$\rho_{NT} = \frac{\mu(C_{NT})_e}{1 - e^{-\mu x}}. \qquad (14)$$

The equivalent concentration for the plane source equivalent to the target can be derived similarly. From equations (4) and (5), the counting rate when the collimator is over the target volume is:

$$R_T = k(C_T)_e + (K - k)(C_{NT})_e \qquad (15)$$

and

$$R_T = K(C_{NT})_e[1 + (f_e - 1)S]. \qquad (16)$$

Consider the target area in Fig. 8 as composed of two sources. One source with a concentration ρ_{NT} is a right circular cylinder formed by projecting the target volume from the top to the bottom of the whole-body source. The other source is the target

VOL.
10
1961

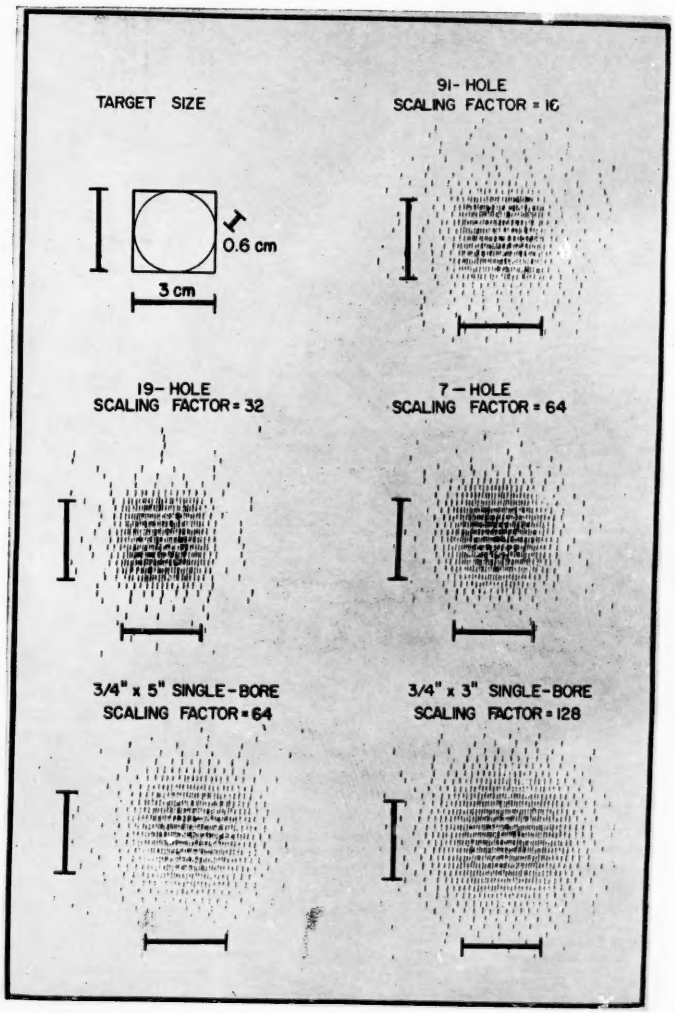

FIG. 9. Scintigrams of a 3 cm cube filled with 100 μc of I^{131} and placed at the center of a 12 cm cube filled with water. Collimators were positioned 8·0 cm above the center of the small cube. Scanning speed was 6·0 mm/sec.

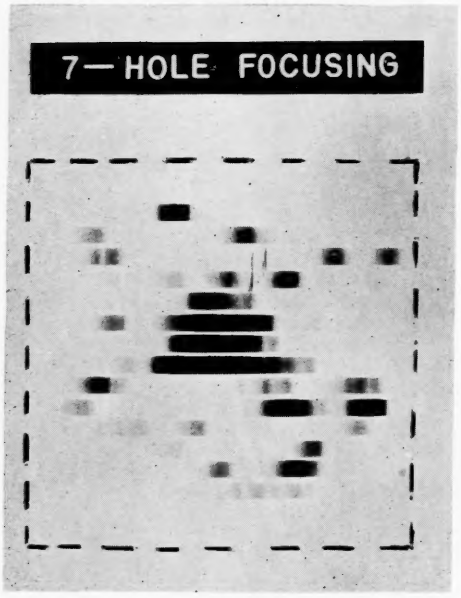

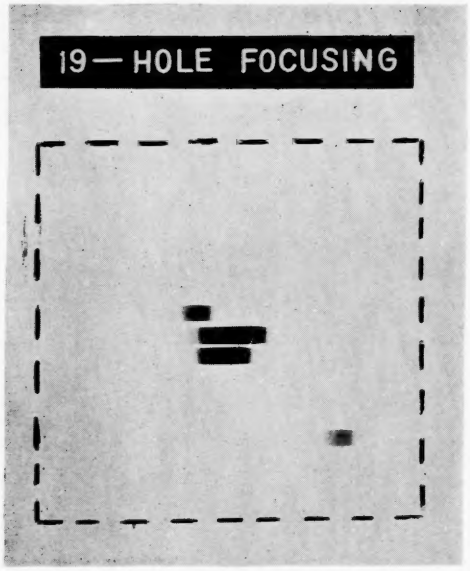

FIG. 10(A)

FIG. 10(B)

FIG. 10(A) and 10(B). Photoscans of a 2 cm cube containing 0·0610 μc/cm^3 or 0·488 μc of I^{131} and placed at the center of a 12 cm cube containing 0·0122 μc/cm^3 or 18·3 μc of I^{131}. Note that I^{131} was 5·0 times more concentrated in the small cube. Scanning conditions were as follows:

scanning speed = 1·25 mm/sec, light spot size = 10 × 5 mm,
rate meter time constant = 4·0 sec (equivalent pre-set time of 8·0 sec),
compensation for memory lag = 6·3 mm.

The "memory lag" between the collimator–detector system and the recording light was compensated for by automatically changing the length of the rod connecting the detector and the light each time the scanning direction was reversed.

volume with a concentration $\rho_T - \rho_{NT}$. Then

$$R_T = k(C_{NT})_e + k(\rho_T - \rho_{NT}) \times \int_{y-h/2}^{y+h/2} e^{-\mu y}\, dy + (K - k)(C_{NT})_e.$$

Comparing with equation (15)

$$(C_T)_e = (C_{NT})_e + \frac{(\rho_T - \rho_{NT}[e^{-\mu(y-h/2)} - e^{-\mu(y+h/2)}]}{\mu}. \quad (17)$$

From equation (17) it can be shown that, when $h = x$ and $y = x/2$ for the situation where the target volume extends from the top to bottom of the source,

$$(C_T)_e/(C_{NT})_e = \rho_T/\rho_{NT}.$$

For small target volumes with a considerable amount of nontarget material above and below them, viz. $h \ll x$, equation (17) can be simplified to

$$(C_T)_e = (C_{NT})_e + (\rho_T - \rho_{NT})h\, e^{-\mu y}.$$

Substituting $f'\rho_{NT}$ for ρ_T,

$$(C_T)_e = (C_{NT})_e + (f' - 1)\rho_{NT} h\, e^{-\mu y} \quad \text{when} \quad h \ll x. \quad (18)$$

The ratio of the equivalent target concentration to the equivalent nontarget concentration is

$$f_e = 1 + \frac{(f' - 1)h\rho_{NT}\, e^{-\mu x}}{(C_{NT})_e}.$$

Combining the above equation with equation (13)

$$f_e = 1 + \frac{(f' - 1)h\mu\, e^{-\mu y}}{1 - e^{-\mu x}}. \quad (19)$$

Combining equations (11), (13) and (19)

$$\rho_{NT} = \frac{1}{KS^2} \times \frac{n^2(1 - e^{-\mu x})}{(1 - f')^2\, t\mu h^2\, e^{-2\mu y})}. \quad (20)$$

Thus, as for the plane source, the concentration of radioactivity in a volume source required for the detection of a particular target volume is proportional to the collimator figure of merit, $1/KS^2$.

(2) *Ability of the collimator–detector system to accurately define the target area and to distinguish one target area from an adjacent target area*

In the last section the collimators were evaluated only on the basis of probability of detecting the target area. The figure of merit did not indicate the distortion with which the collimator–detector system would represent the target area or the minimum distance by which two target areas must be separated in order to be detected as two separate sources. Information on these points can be obtained from the specific resolution which was defined previously. The specific resolution (SR_{Pl}) for circular plane sources specifies the magnitude of the target distortion in terms of target size. In addition, two targets with diameters equal to the specific resolution must have their edges separated by a distance equal to their diameter in order to be detected as separate sources (Fig. 5).

The precision with which a collimator can represent a target area must depend on the specific resolution. This was investigated experimentally as follows. A small 3 cm cube containing 100 μc of I^{131} was placed at the center of a larger 12 cm cube filled with water. The cubes were scanned automatically with the various collimators located 8·0 cm above the center of the small cube. The scintigrams shown in Fig. 9 indicate that all of the collimators provided representations of the small cube which were approximately the same *size* as the actual cube. This would be expected from a consideration of the specific resolutions, the largest of which is 1·94 cm, smaller than the size of the 3 cm cube. However, the *shape* of the cube is accurately represented only in the scintigrams obtained with the nineteen-hole and the ninety-one-hole collimators. To represent the shape accurately it was necessary to resolve the corners of the cube from the rest of the cube; in other words, it was necessary to provide a reasonably accurate representation of a small source about 0·6 cm across. Only the nineteen- and ninety-one-hole collimators, which have

VOL. 10 1961

specific resolutions of 0·50 and 0·28 cm respectively, were capable of providing the resolution needed. Thus, it appears that the specific resolution may be approximately equal to the smallest target size which can be detected with reasonable precision.

The actual distortion will depend on the particular display system and such things as background cut-off circuits, where only counting rates higher than a predetermined level are displayed. Also important is the relationship between the integrating time constant and the scanning speed. If the time constant is too long in relation to the scanning speed, the "memory lag" between the collimator–detector system and the recording device will reduce the size of the target display. Nevertheless, specific resolution specifies distortion in terms of target size by relating to target size the change in counting rate as the collimator passes over the target–nontarget interface. The display of a target equal in size to the specific resolution will probably be less than twice the size of the actual target. Larger targets will be displayed with less distortion, and smaller targets will be displayed with more distortion.

(3) *Comparison of collimators with regard to resolution, sensitivity and size of target*

The specific resolutions as determined in Fig. 6 for the plane circular sources are listed in Table 2. Also listed are the resolutions as determined with the point source (approximately twice the specific resolution), and a range of optimum target sizes for which each collimator is best. The optimum target diameters are taken from Fig. 7. The specific resolution for a particular collimator is always less than the optimum target diameter. For practical purposes, this means that when one of the five collimators studied is used because it gives the highest probability of detecting a particular target size, the collimator will enable a determination of the target size with a reasonable degree of precision.

TABLE 2. Comparison of collimators with regard to resolution, sensitivity and size of target

Collimator	Point source* resolution (R_{Pt}) (cm)	Specific† resolution (SR_{Pt}) (cm)	$\frac{SR_{Pt}}{R_{Pt}}$	K Sensitivity to whole-body source (c.p.m. per $\mu c/cm^2$)	Target diameter‡ for which collimator is best (cm)
Ninety-one-hole	0·50 $\binom{1·12}{1·00}$	0·28	0·56	3240	<0·54
Nineteen-hole	0·90 $\binom{1·05}{1·35}$	0·50	0·55	4268	0·54–1·4
Seven-hole	1·65	0·91	0·55	8627	1·40–3·0
¾ × 5 in. single-bore	3·28	1·55	0·47	7170	Never
¾ × 3 in. single-bore	4·0 $\binom{3·4}{5·4}$	1·94	0·48	19500	>3·0

* Point source resolution specifies the minimum resolving distance between two point sources. It was determined at the focal point (Table 1) for the focusing collimators and at 8·0 cm from the collimator face for the single-bore collimators. Values in parentheses refer to resolutions determined at 4·0 cm (above), and resolutions determined at 12·0 cm (below).

† Specific resolution specifies the distortion in the target size. Circular targets with diameters equal to the specific resolution must have their edges separated by a distance equal to the specific resolution in order to be detected as separate sources (see text).

‡ The collimators were compared on the basis of providing the greatest probability of detection (Fig. 7).

VOL. 10 1961

AN APPLICATION OF THE PRINCIPLES PRESENTED

A sample scanning problem is presented as follows. It is desired to use RISA (radioiodinated serum albumin) to detect brain tumors which are as small as a 2 cm cube and located at the center of the head It is assumed that the concentration of I^{131} will be at least 5 times higher in the tumor than in normal brain tissue; according to KRAMER *et al.*[12] the tumor to brain concentration ratios range from 5 to 30. The problem is (1) which collimator should be used, and (2) what concentration of RISA in the brain is needed?

Additional scanning conditions are as follows. Let the 2 cm target (tumor) be located at the center of the whole-body source ($30 \times 120 \times 12$ cm in depth) and at 6 cm below its surface. (Positioning the brain at the center of the whole-body source instead of at the end simplifies the analysis and makes little difference, Fig. 4). Let the scanning conditions provide an equivalent pre-set time of 8 sec = 0·133 min. (This involves the rate meter time constant, scanning speed and size of light spot on the photoscanner.) Let $n = 3$ in equation (20). Preliminary studies indicate that when $n = 3$ there is a high probability of obtaining a good representation of the target.

To answer the question of the best collimator, refer to Table 2. A 2 cm source is between the target diameters of 1·4 and 3·0, for which the seven-hole collimator is best. Furthermore, the specific resolution (0·91 cm) is acceptable for a 2 cm target.

To obtain the concentration of RISA which is needed, substitute into equation (20) the following values: $f' = 5$, $h = 2$, $\mu = 0{\cdot}10$, $y = 6$, $x = 12$, $n = 3$, $t = 0{\cdot}133$, and $1/KS^2 = 0{\cdot}5(10)^{-3}$ (obtained from Fig. 7). Thus,

$$\rho_{NT} = 0{\cdot}0122 \ \mu c/cm^3$$

where ρ_{NT} is the concentration of RISA in the brain, which is required for detection of the 2 cm tumor. A 1500 cm^3 brain would thus contain 18·3 μc. Preliminary studies indicate that about 500 μc would have to be injected into a 70 kg man for the concentration needed.

Incidentally, the actual counting rates can be obtained by substituting the appropriate values into equations (12), (13), (16) and (19). The values of S (0·48) and K (8627) are obtained from Fig. 4. This gives counting rates of 738 c.p.m. over the nontarget area and 960 c.p.m. (30 per cent higher) over the target area. When these figures were corrected for a 12 cm cube in the example which follows, they were 627 and 849, respectively. (They were corrected by subtracting $(1 - 0{\cdot}85)738$, Fig. 4C.)

The calculations were verified experimentally by filling a 12 cm cube with an I^{131} solution having a concentration of 0·0122 $\mu c/cm^3$ (21·1 μc total radioactivity). A small 2 cm cube was filled with an I^{131} solution 5·0 times more concentrated (0·0610 $\mu c/cm^3$ and 0·488 μc total radioactivity). The seven-hole collimator was positioned 8·0 cm above the center of the large cube, and the counting rates were determined both with and without the small cube in position at the center of the large cube. The counting rate with the small cube in place (R_T) was 912 c.p.m. and 36 per cent higher than the counting rate with the cube removed ($R_{NT} = 672$ c.p.m.). These counting rates compare well with the calculated counting rates, 849 and 627 c.p.m.

Studies were also made with the other collimators. Calculated and experimental counting rates were determined in a similar manner for each, and the results are tabulated in Table 3. It is evident that the experimental results and calculations agree quite well in all cases. By comparing the percentage difference between the target and nontarget counting rates with the percentage standard error it is verified that the seven-hole collimator is the best collimator for detecting the 2 cm cube.

The cubes were scanned automatically with the seven-hole focusing, the nineteen-hole focusing, and the $\frac{3}{4} \times 3$ in. single-bore collimators. The counting rate obtained with the ninety-one-hole collimator was too low for the photo-scanning equipment. The photoscans shown in Fig. 10 demonstrate that the small 2 cm cube placed at the center

TABLE 3. Counting rates obtained with various collimators over a phantom. Collimators were positioned 2·0 cm above a 12 cm cube (0·0122 μc/cm^3 of I^{131}), both with and without a 2 cm cube (0·0610 μc/cm^3 of I^{131}) located at the center

Collimator	Calculated*					Experimental†			
	R_{NT} (c.p.m.)	R_T (c.p.m.)	ΔR (c.p.m.)	Percentage difference $\Delta R/R_{NT} \times 100$	Percentage‡ standard error in R_{NT}	R_{NT} (c.p.m.)	R_T (c.p.m.)	ΔR (c.p.m.)	Percentage difference $\Delta R/R_{NT} \times 100$
Ninety-one-hole focusing	177	228	51	28·8	21	170	215	45	26·5
Nineteen-hole focusing	266	368	102	38·8	17	281	383	102	36·3
Seven-hole focusing	627	849	222	35·4	11	672	912	240	35·8
$\frac{3}{4} \times 3$ in. single-bore	1553	1763	210	13·5	7	1865	2099	234	12·5

* Calculations are discussed in detail in the text. R_T is the counting rate with the 2 cm cube in place, and R_{NT} is the counting rate with it removed.

† These are net counting rates after a background of 50 c.p.m. was subtracted.

‡ Percentage standard error $= 100/\sqrt{R_{NT}t}$, where t is the pre-set time (8 sec).

of the large 12 cm cube was detected with both the 7 hole and the 19 hole collimators. The fluctuations over the nontarget regions are apparent in the scan obtained with the seven-hole collimator, but are not apparent in the scan obtained with the nineteen-hole collimator because more of the background was erased. The scan obtained with the $\frac{3}{4} \times 3$ in. single-bore collimator was badly distorted and is not shown.

Acknowledgements—Appreciation is expressed to Mr. E. BAILEY MOORE and Mr. CECIL JOHNSON for their ideas and interest in the construction of the collimators. The technical assistance of Mr. P. J. SIROTA and Miss J. C. CUNNINGHAM is also appreciated.

REFERENCES

1. VAN DER DOES DE BYE J. A. W. *Nucleonics* **14,** 128 (1956).
2. ALLEN H. C. and RISSER J. R. *Nucleonics* **13,** 28 (1955).
3. NEWELL R. R., SAUNDERS W. and MILLER E. *Nucleonics* **10,** 36 (1952).
4. MILLER E. R. and SCOFIELD N. E. *Radiology* **65,** 96 (1955).
5. BROWNELL G. L. *Int. J. Appl. Rad. Isotopes* **3,** 181, (1958).
6. KELLERSHOHN C. and PELLERIN P. *J. Phys. Rad.* **17,** Suppl. 6, 81A (1956).
7. COOK C. S. *Nucl. Instrum. Meth.* **4,** 103 (1959).
8. SIMONS H. A. B. and CHOMET S. *Phys. Med. Biol.* **3,** 233 (1959).
9. EVANS R. D. *The Atomic Nucleus* p. 714. McGraw-Hill, N.Y. (1955).
10. FOLICHON A. and GANDY A. *J. Radiol. Electr.* **37,** 334 (1956)
11. FLÜGGE S. *Nuclear Instrumentation–II: Encyclopedia of Physics XLV* p. 252. Springer–Verlag, Berlin (1958).
12. KRAMER S., BURTON L. K. and TROTT N. G. *Acta Radiol.* **46,** 415, (1956).

International Journal of Applied Radiation and Isotopes, 1961, Vol. 10, pp. 17 to 21. Pergamon Press Ltd. Printed in Northern Ireland

A Simple Method for the Differential Counting of Radioactive Iron (Fe^{59}) and Chromium–51 in Mixtures

L. A. WALKER, G. SPARLING and H. MERCER
The Mason Clinic, Seattle 1, Washington, U.S.A.

(*Received* 15 *June* 1960)

VOL. 10 1961

A method is described for the accurate counting of Cr^{51} and Fe^{59} in mixtures containing both isotopes. This method makes use of only a scintillation counter and associated scaler. Neither lead filters nor gamma-ray spectrometer is needed, and the accuracy is as good as that of either of the other two methods.

UNE METHODE SIMPLE POUR LE COMPTAGE DIFFERENTIEL DU FER RADIOACTIF (Fe^{59}) ET DU CHROMIUM-51 MELANGES

Une méthode est présentée pour compter exactement Cr^{51} et Fe^{59} dans des mélanges contenant les deux isotopes. La méthode emploit seulement un cristal scintillation et compteur associé. Pas les filtres de plomb, pas le spectrometer gamma sont necessaires, et l'accuracie était comparable que l'un ou l'autre de deux autres methodes.

ПРОСТОЙ МЕТОД РАЗДЕЛЬНОГО СЧЕТА РАДИОАКТИВНОГО ЖЕЛЕЗА (Fe^{59}) И ХРОМА-51 В СМЕСЯХ

Дано описание метода точного счета Cr^{51} и Fe^{59} в смесях содержащих оба изотопа. Этот метод использует только сцинтилляционный счетчик совместно с пересчетным устройством. Не требуется ни свинцовых фильтров, ни гамма-спектрометра, а точность измерений не ниже, чем при применении двух других методов.

EINE EINFACHE METHODE ZUR DIFFERENZIERTEN ZÄHLUNG VON Fe^{59} UND Cr^{51} IN GEMISCHEN

Eine Methode zur genauen Zählung von Cr^{51} und Fe^{59} in Mischungen von beiden Isotopen wird vorgestellt. Diese Methode bringt nur eine Szintillationsrohr und beilegende Zähler in Gebrauch. Weder Bleifilter noch Gammastrahl-spektrometer werden gebraucht, und die Genauigkeit scheint so gut zu sein als die beiden anderen Methoden.

It is frequently desirable or necessary to count the radioactivity in mixtures of two radioactive isotopes, and to calculate the amount of each isotope present in the mixture. Such a situation may pertain in studies involving hemodynamics, iron absorption or other situations, where radioactive iron (Fe^{59}) and radioactive chromium (Cr^{51}) are employed in the same subject at the same time.

The determination of the quantity of these two isotopes may be accomplished by means of gamma-ray spectrometry[1], or by the use of lead filters, as reported by Libby and Hand[2].

Gamma-ray spectrometry involves the use of special electronic circuitry which costs in the neighborhood of two thousand dollars. The method employing lead filters is much cheaper, but suffers from certain inaccuracies, in addition to which the lead filter, if used inside a well, seriously cuts down on the useful counting volume within the well.

The purpose of this communication is to

report on another method for the differential determination of Fe^{59} and Cr^{51} in mixtures. This method involves only a scintillation counter with scaling circuit, and no other special equipment. We have found this method as accurate as either of the other two methods, and it involves only simple algebraic calculations.

During the course of hemodynamic studies, we have evaluated all three methods. We found the method presented herein superior to the other two methods. It should be observed that these methods are valid only for gamma-emitting isotopes, the principal gamma rays of which are appreciably different in energy. Iron-59 (45·1 day half-life) has gamma photons of 1·10 and 1·29 MeV, while chromium-51 has gamma photons of 0·32 MeV. The lead filter method depends upon the fact that the attenuation of the higher energy radiation from the Fe^{59} is less than that of the Cr^{51}. Hence, if the sample is counted first without and then with a lead filter between the sample and the crystal of the scintillation counter, it is possible, knowing the attenuation factor for each isotope, to calculate the quantity of each which is present[2].

The gamma-ray spectrometry method depends on a special gamma-ray spectrometer circuit which can be adjusted to count only voltage pulses from the scintillation counter between certain magnitudes. By previous calibration of the dials, it is possible to count those voltage pulses which correspond to the principal gamma energies of a particular isotope. However, this method suffers from two main disadvantages, (a) because it does count only each "peak" (principal gamma photon) of a particular isotope; the sensitivity of the scintillator in counts per minute per microcurie is considerably less than it would be with an ordinary scaling circuit, because other peaks from the same isotope, as well as much of the scattered and "degraded" radiation from the principal peak which reaches the crystal, is not detected: (b) in a mixture of two isotopes, it is not possible to "zero out" the radiation from the higher energy peaks, as much of it is degraded and will be counted at the dial setting corresponding to the lower-energy gamma photon. (For a more complete discussion of these problems see Reference 3). For both of these reasons, the method described below is as good as the much more expensive gamma-ray spectrometer method.

METHOD

Using two samples of Cr^{51} and Fe^{59} of known arbitrary strength, counting rates are observed with a scintillation counter and associated scaling circuit over a series of voltage settings, about 100 V apart. Two voltages are then selected for the counting of the unknown mixtures. Those voltages are selected which give the maximum variation in the ratio of the net counting rates per microcurie for Cr^{51} and Fe^{59}. That is, one wishes to detect Cr^{51} at the greatest possible efficiency at the higher voltage, and Fe^{59} at the greatest possible efficiency at the lower voltage. The optimum voltages can be selected by a quick inspection of the net counting rates. This whole procedure takes less than 1 hr.

The second step is to calibrate the scintillation counter with accurately measured solutions of Fe^{59} and Cr^{51} at the two voltages. From the net counting rates, one calculates the sensitivities in counts per second (or per minute) per millimicrocurie of each isotope.

The counting rates at the two voltages are related by the equations:

$$R' = S'_{Cr}C_{Cr} + S'_{Fe}C_{Fe} \quad (1)$$

$$R'' = S''_{Cr}C_{Cr} + S''_{Fe}C_{Fe} \quad (2)$$

where

R' = the net counting rate observed at the lower voltage

S'_{Cr} = the sensitivity in counts per second per millimicrocurie Cr^{51} at the lower voltage

S'_{Fe} = the sensitivity in counts per second per millimicrocurie Fe^{59} at the lower voltage

C_{Cr} = the amount of Cr^{51} in the sample in millimicrocuries

C_{Fe} = the amount of Fe^{59} in the sample in millimicrocuries

R'' = the net counting rate observed at the higher voltage

S''_{Cr} = the sensitivity in counts per second per millimicrocurie Cr^{51} at the higher voltage

S''_{Fe} = the sensitivity in counts per second per millimicrocurie Fe^{59} at the higher voltage.

For our well counter, operating at 800 and 1150 V, we found the following values for the sensitivities:

S'_{Cr} = 0 net counts per second per millimicrocurie (800 V)

S''_{Cr} = 2·0 net counts per second per millimicrocurie (1150 V)

S'_{Fe} = 2·6 net counts per second per millimicrocurie (800 V)

S''_{Fe} = 6·5 net counts per second per millimicrocurie (1150 V)

(for 4·0 ml samples inside the well).

Thus equation (1) reduces to

$$R' = S'_{Fe}C_{Fe} = 2{\cdot}6\ C_{Fe}.$$

Solving for C_{Fe} we obtain:

$$C_{Fe} = \frac{R^1}{2{\cdot}6}. \qquad (3)$$

Solving equation (2) for C_{Fe} we obtain:

$$C_{Cr} = \frac{R''}{2{\cdot}0} - 3{\cdot}25\ C_{Fe}. \qquad (4)$$

Thus, by dividing R' (the net rate in counts per second at $V = 800$) by 2·6, we obtain C_{Fe}, the amount of Fe^{59} in millimicrocuries. The value of C_{Fe} is then substituted in equation (4), to give C_{Cr}, the amount of Cr^{51} in millimicrocuries. The following series of recovery experiments illustrate the accuracy which may be achieved by this method. The samples consist of a series of vials containing 4·0 ml each of mixtures of Cr^{51} and Fe^{59}. The quantities of Cr^{51} and Fe^{59} added are indicated, together with the quantities of Cr^{51} and Fe^{59} found, in millimicrocuries, and the percentage recovery of each isotope.

Repeated recovery on these and other samples on different days demonstrated comparable accuracy of recovery which indicates good voltage stability of the well counter.

The instrument used was a well-type scintillation counter made by Curtis Nuclear Corporation* and a Berkeley Decimal Scale, Model 2000.† Any well-engineered unit with a stable voltage supply can be used in this manner.

Although an exhaustive treatment of the accuracy of this method would be beyond the scope of this paper, a brief treatment of the subject seems appropriate.

It is obvious that, for two counting conditions, be they two discriminator settings on a gamma spectrometer, two counting rates with and without a lead filter or two counting rates at different voltage settings, equations (1) and (2) obtain. For either of the two counting conditions, we may write:

$$R = S_{Cr}C_{Cr} + S_{Fe}C_{Fe}. \qquad (5)$$

If $S_{Cr} = 0$, we have

$R = S_{Fe}C_{Fe}$ and for a fixed S_{Fe},

$$\Delta C_{Fe} = \frac{\Delta R}{S_{Fe}} \qquad (6)$$

where ΔC_{Fe} = a change in concentration of Fe, and

ΔR = the corresponding change in the net counting rate R.

If ΔC_{Fe} is considered to be the minimum change in iron concentration that we can detect, then ΔR is the corresponding minimum change in the counting rate that we can detect.

But if $S_{Cr} \neq 0$, then equation (5) will yield

$$\Delta C_{Fe} = \frac{\Delta R}{S_{Fe}} - \frac{S_{Cr}}{S_{Fe}}\Delta C_{Cr} \qquad (7)$$

so that, if ΔR is the minimum change in rate that we can observe, it is apparent, from a comparison of equations (6) and (7) that the

* 1645 W. 135th Street, Garden City, California (formerly Reed Curtis Scientific Company).

† Berkeley Scientific Company, Richmond, California.

VOL. 10 1961

TABLE 1. Recovery of added Fe^{59} and Cr^{51} from mixtures

Vial No.	Fe^{59} added (mc)	Fe^{59} recovered (mc)	Recovered (%)	Cr^{51} added (mc)	Cr^{51} recovered (mc)	Recovered (%)
1	0	0		70·8	71·0	100
2	2·28	2·5	110·0	62·0	61·0	98·5
3	4·57	5·0	109·0	53·0	52·7	99·5
4	9·14	9·65	106·0	35·4	32·6	92·0
5	11·4	11·5	101·0	26·6	26·1	98·0
6	13·7	14·0	102·0	17·7	17·0	96·0
7	16·0	16·2	101·0	8·85	8·8	99·5
8	17·3	17·6	102·0	3·54	3·2	90·5
9	18·2	18·1	99·5	0	0	
10	0·9	1·0	111·0	67·3	67·0	99·5
11	18·0	17·9	99·5	1·8	1·8	100

TABLE 2. Gamma-ray spectrometer with scintillation well counter. Operating voltage 850

Window setting	To count	Background (c/min)	Sensitivity (c/min/mc)
1–1·6 MeV	Fe^{59}	1·0	10·8 for Fe^{59}
1–1·6 MeV	Fe^{59}	1·0	0·0 for Cr^{51}
0·310–0·330 MeV	Cr^{51}	3·0	4·6 for Fe^{59}
0·310–0·330 MeV	Cr^{51}	3·0	6·0 for Cr^{51}
Lower level only			
1·0 MeV	Fe^{59}	29·0	77·5 for Fe^{59}
1·0 MeV	Fe^{59}	29	0·0 for Cr^{51}
0·31 MeV	Cr^{51}	3·0	307 for Fe^{59}
0·31 MeV	Cr^{51}	3·0	23·5 for Cr^{51}

Simple scaling circuit with scintillation well counter

Voltage setting	To count	Background (c/min)	Sensitivity (c/min/mc)
1150	Fe^{59} and Cr^{51}	310	405·0 for Fe^{59}
1150	Fe^{59} and Cr^{51}	310	120·0 for Cr^{51}
800	Fe^{59}	84	156·0 for Fe^{59}
800	Fe^{59}	84	0·0 for Cr^{51}

minimum change in concentration of the Fe, ΔC_{Fe} is less, hence the accuracy is less, when the Cr^{51} cannot be "zeroed out" ($S_{Cr} \neq 0$).

LIBBY and HAND[2] found, for their lead absorbers, an attenuation of only 67 per cent for Cr^{51}, that is, 33 per cent of the radiation from the Cr^{51} was still present. We evaluated the efficiency of detection of Fe^{59} and Cr^{51} in mixtures, using both the lead filter method and a gamma-ray spectrometer. The method presented herein gave much greater accuracy than either of the other two methods.

The gamma-ray spectrometer and well scintillation counter employed in these comparisons was that of a well-known manufacturer. Calibration, operation and sensitivity determination was carefully carried out and checked by technical representatives of the manufacturer. Sensitivities for Fe^{59} and Cr^{51} was comparable to those of other gamma-ray spectrometers on the market. In every case where sensitivity comparisons

between the gamma-ray spectrometer with well scintillation counter, and the well counter with simple scaling circuit were made, aliquots of the same radioactive solutions were tested in order to obviate errors in the absolute radioactive strength of the sample.

The following (Table 2) are our results for the sensitivities of the two methods.

Thus it is apparent that the sensitivities for Fe^{59} and Cr^{51} are much higher for the simple scaling circuit, although the backgrounds are higher. Sensitivity of the gamma-ray spectrometer can be increased only by widening the window, which then raises the background. Ratio of Fe^{59} sensitivities by the two methods is $156 \div 10{\cdot}8 = 14{\cdot}4$. Ratio of Cr^{51} sensitivities by the two methods is $120 \div 6 = 20$.

In order to achieve recoveries of Cr^{51} and Fe^{59} comparable to those indicated above for the simple scaling circuit, it is necessary, when the gamma-ray spectrometer is used, to count for prolonged periods of time. In repeat experiments using the simple scaling circuit method, it was possible to duplicate the efficient recoveries of Cr^{51} and Fe^{59} indicated in the Table 1.

VOL.
10
1961

CONCLUSION

A simple method for the differential counting of the two gamma-emitting isotopes, Fe^{59} and Cr^{51}, in the presence of each other has been presented. This method requires only a scintillation detector and associated scaling circuit with a stable voltage supply. It does not require any special filters and has proved more accurate than either methods employing lead filters or the expensive method of gamma-ray spectrometry.

Acknowledgement—The authors wish to express thanks to the Virginia Mason Foundation for Medical Research for support in carrying out this project.

REFERENCES

1. Mitchell T. G., Spencer R. P. and King R. E. *Amer. J. clin. Path.* **28,** 461 (1957).
2. Libby R. L. and Hand K. *J. Lab. clin. Med.* **48,** 289 (1956).
3. Curran S. C. *Luminescence and the Scintillation Counter*, Academic Press, New York (1953); Butterworths, London (1953).

International Journal of Applied Radiation and Isotopes, 1961, Vol. 10, pp. 22 to 29. Pergamon Press Ltd. Printed in Northern Ireland

Self-Absorption of Carbon-14 Samples on Thin Paper Planchets

E. R. POWSNER
Medical Research Department, Veterans Administration Hospital, Dearborn, and Department of Medicine, Wayne State University College of Medicine, Detroit, Michigan, U.S.A.

(*Received* 29 *April* 1960)

Using carbon-14 samples absorbed on thin paper discs, the apparent radioactivity was measured in a gas-flow counter over a wide range of specimen thickness. Results show that specimens ranging up to a thickness of 150 $\mu g/cm^2$ may be regarded as approximately infinitely thin. It is estimated that the count rate is decreased by approximately 20 per cent as a result of absorption of the radioactivity by the paper. To a considerable extent, the change in count rate due to self-absorption varies as the reciprocal of a linear function of the thickness of both the paper and the specimen.

L'AUTO-ABSORPTION DANS LES ECHANTILLONS DE CARBONE-14 SUR DES SUPPORTS DE PAPIER MINCE

Utilisant des échantillons de carbone-14 absorbé sur des disques de papier mince, on mesura la radioactivité apparente dans un compteur à écoulement de gaz à travers une grande gamme d'épaisseur d'échantillons. Les résultats montrent qu'on peut considérer les échantillons de jusqu' à 150 g/cm^2 comme étant à peu près infiniment minces. On juge que le taux de compte diminue d'environ 20 pour cent à cause de l'absorption de la radioactivité par le papier. En grande partie le changement du taux de compte produit par l'auto-absorption varie avec l'inverse d'une fonction linéaire de l'épaisseur à la fois du papier et de l'échantillon.

САМОПОГЛОЩЕНИЕ ОБРАЗЦОВ УГЛЕРОДА-14, НАНЕСЕННЫХ НА ТОНКИЕ БУМАЖНЫЕ ДИСКИ

Кажущаяся радиоактивность образцов C^{14}, абсорбированных тонкими бумажными дисками, измерялась газовым счетчиком в широких пределах толщины образца. Полученные результаты показывают, что обрацы толщиной до 150 $\mu г/см^2$ можно приближенно рассматривать как бесконечно тонкие. Установлено, что в результате абсорбции скорость счета уменьшается примерно на 20%. Обусловленное самопоглощением изменение скорости счета в значительной степени обратно пропорционально линейной функции толщины как бумаги, так и образца.

SELBSTABSORPTION VON C-14 PROBEN AUF DÜNNEN PAPIERSCHEIBEN

An C-14-Proben, die auf dünnen Papierscheiben absorobiert werden, wurde in einem Gas-Durchfluss-Zähler die scheinbare Aktivität in Abhängigkeit von der Probendicke innerhalb eines weiten Bereiches gemessen. Die Ergebnisse zeigen, dass Proben bis zu einer Dicke von 150 $\mu g/cm^2$ als annähernd unendlich dünn betrachtet werden dürfen. Infolge der Absorption der Radioaktivität durch das Papier nimmt die Zählrate schätzungsweise auf 20% ab.

Die Änderung der Zählrate infolge Selbstabsorption verläuft weitgehend reziprok einer linearen Funktion von sowohl Proben-wie Papierdicke.

VOL. 10 1961

INTRODUCTION

SELECTION of the counting method and the concomitant problem of sample preparation are major considerations in experiments requiring the use of radioactive carbon-14 and other moderately low-energy beta-emitting isotopes. Gas-flow counters with or without thin windows are used frequently because of their comparative simplicity and cost. The problems of sample preparation for these counters is complicated by the low energy of the beta particles and resultant absorptive losses in the specimen. Among the numerous methods devised to minimize and compensate for these losses is the use of very thin preparations. If the specimen is sufficiently thin, the self-absorption, i.e. the absorptive loss in the specimen itself, is reduced to the point where it is negligible. This is the so-called infinitely thin preparation. Not only do these preparations have negligible loss of radioactivity resulting from self-absorption, but they require a minimum of material.

Absorption on thin paper discs is a technique the advantages of which are well known.[3,7] In the use of the infinitely thin preparation this technique represents a comparatively simple method for rapidly preparing geometrically uniform samples. As used here the technique has proven to be not only as reproducible as direct plating, but also more rapid and more convenient. An additional advantage is the comparatively extensive useful range of specimen weight which may be considered infinitely thin. To ascertain this range, as well as to provide the necessary correction factors for specimens of greater thickness, it is necessary to know the manner in which the apparent activity varies with sample thickness. For comparison with data obtained by other methods and in particular for determining the efficiency of this technique, it is important to determine the absorption of radioactivity in the paper. This information has not been available previously.

It is the purpose of the present experiments to measure the effect of the self-absorption on the apparent activity of C^{14} specimens prepared on thin paper discs, and to determine separately the effect of variation of absorption resulting from variation in specimen thickness and paper thickness.

METHOD

The C^{14} compounds selected for these measurements were glycine and hemin. Both are readily available in this laboratory; the former has the advantages of high solubility in water and of availability with high specific activity, permitting a wide range of measurement, while the latter, containing iron, is sufficiently different in density to make comparison of interest.

A measured amount of commercially available glycine-C^{14} (0·228 mg) was dissolved in 10 ml of water. One-milliliter volumes of this solution were then transferred to six flasks containing 10 ml of six different concentrations of stable glycine ranging from zero to 150 mg/ml and to one flask containing 100 ml of water. A volume of solution, measured gravimetrically, was then placed on a lens paper disc (1·27 cm diameter punched from sheets weighing 1·2–1·3 mg/cm^2) on an aluminum foil planchet (1·6 cm squares of foil, approximately 0 02 mm thick). When the paper was dry, the corners of the foil were folded back over the extreme edge of the paper disc to retain the paper. About ten specimens were prepared from each of the seven solutions. The amount of glycine in each specimen was calculated from the volume and concentration. The preparation of the hemin samples was similar except that pyridine was used as the solvent, the least concentrated solutions were prepared by serial dilutions of the original active specimen without the addition of further carrier, and the amount of solution placed on a planchet was measured volumetrically because of the greater volatility of the pyridine. For the

determination of the effect of variation of paper thickness on the measured activity of the absorbed specimen, increasing numbers of discs containing approximately equal quantities of radioactive glycine were placed on top of one another in a stack on a single aluminum-foil planchet.

Apparent radioactivity was measured in both a windowless gas-flow counter, operated proportionally, with 2π geometry (Model PC-3A, Proportional Gas Flow Counter, Nuclear Measurements Corporation), and a thin-window gas-flow counter operated as a Geiger counter (Model D-47 Gas Flow Counter with window of less than 150 μgm/cm^2 Nuclear Chicago Corporation, Chicago, Illinois), In addition, the absolute radioactivity of a few of the specimens, following total combustion of both specimen and paper, was determined as CO_2 in a gas-phase counter[2] calibrated by means of a National Bureau of Standards sample of C^{14}.

RESULTS

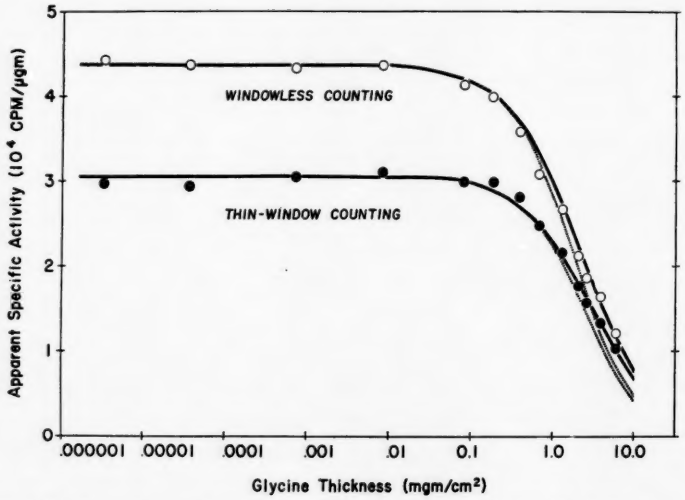

FIG. 1. Carbon-14 specimens absorbed on thin paper discs. Relationship between apparent specific activity and thickness of specimen. The activity of a series of specimens made of glycine-C^{14} diluted with various amounts of inactive glycine is shown as a function of the total glycine thickness (mass per unit area). Each experimental point represents the mean value of measurements at the indicated thickness. The measurements for both the windowless counter (open circles) and the thin-window counter (closed circles) were made on the same specimens.

The solid lines represent the specific activity (10^4 c.p.m./μg) calculated for each counter using the reciprocal relationship,

$$\text{specific activity} = 1/(am + b)$$

where m is the total glycine mass in milligrams, and a (=0·107 and 0·113 for upper and lower curves, respectively) and b (=0·229 and 0·327, respectively) are the constants of the equation for the respective straight line of Fig. 2.

The dotted lines represent the specific activity calculated using the negative exponential relationship,

$$\text{specific activity} = (1 - e^{-k_2 m})/k_1 m$$

where m is the total glycine mass, and k_1 (=0·213 and 0·226 for the upper and lower curves, respectively) and k_2(=0·930 and 0·691, respectively) are constants calculated most conveniently by use of the equations relating them to the constants a and b (see text).

The results of these experiments are presented in accompanying graphs. Fig. 1 shows the specific count-rate measurements and calculated curves over a wide range of glycine-C^{14} specimen thickness for thin-window and windowless counting. The same glycine specimens were counted in both counters. These results show that the measured specific activity is very nearly constant for specimen thickness ranging from

VOL. 10 1961

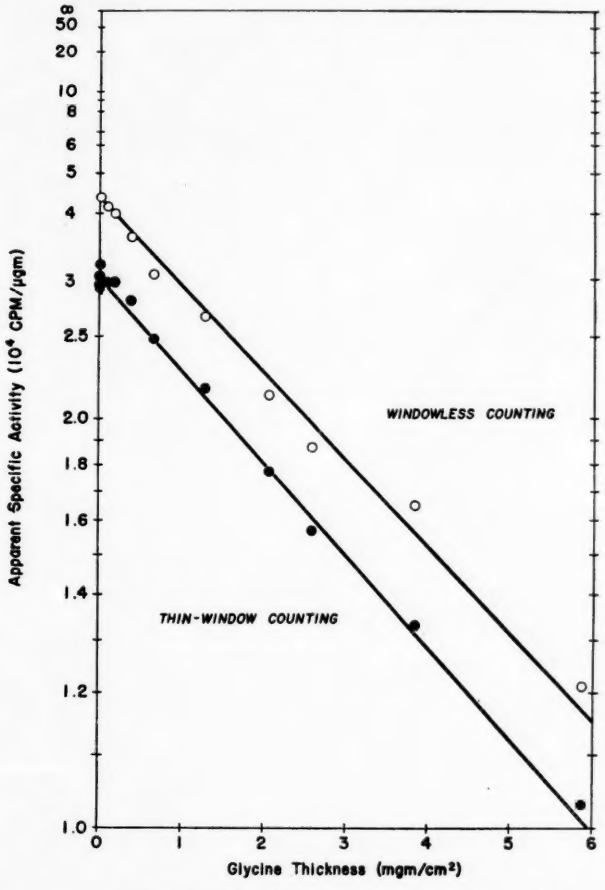

FIG. 2. Carbon-14 specimens absorbed on thin paper discs. Relationship between apparent specific activity and thickness of specimen. The experimental data is that of Fig. 1. Reciprocal ruling is used to show the extent to which the reciprocal of the specific activity is a linear function of the specimen thickness.

0·003 to 30 μg/cm^2 and that the decrease is less than 5 per cent up to about 150 μg/cm. No maxima or irregularities were observed in these curves. The curve for glycine counted in the thin-window counter differed from that in the windowless counter only in magnitude, a difference reasonably attributable to the effect of the window. Hemin specimens were counted only in the windowless counter, and very similar results were obtained. In Fig. 2, the reciprocals of the measured specific activities are presented for the same specimens. Here the reciprocal of the apparent specific activity may be seen to decrease approximately as a linear function of the specimen thickness. (The analysis of data of this type is facilitated by the use of commercially available graph paper with reciprocal ruling along one axis and linear ruling along the other.)

Fig. 3 shows the specific activity measurements obtained using various numbers of paper discs containing an average of 0·046 μg of glycine-C^{14} each. Similar results were

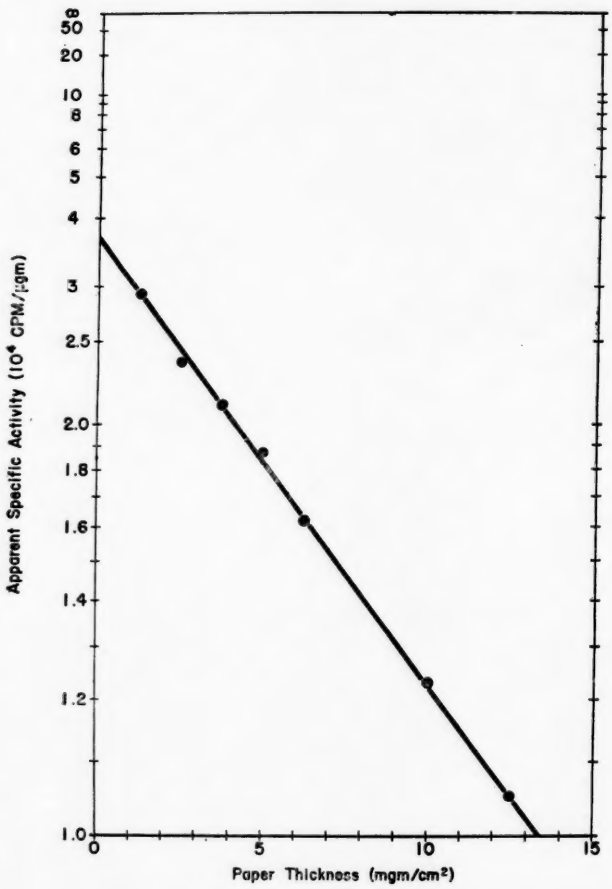

FIG. 3. Carbon-14 specimens absorbed on thin paper discs. Relationship between apparent specific activity (reciprocal ruling) and thickness of paper. Discs of lens paper (approximately 1·25 mg/cm², 1·27 cm diameter) each containing glycine-C^{14} (0·046 μg) were counted in a thin-window counter. Increased thickness was obtained by arranging the same set of discs in stacks of two to ten.

obtained using discs containing other small amounts of glycine. In every case, the reciprocal of the apparent specific activity decreased as linear function of the paper thickness. From the projection of this function, it may be estimated that the specific activity at zero paper thickness would be $3{\cdot}64 \times 10^4$ counts/min per μg compared with 2·94 for a single thickness of paper. This represents a loss of approximately 20 per cent of the activity in the single sheet of paper.

The measured activity of the glycine-C^{14} after combustion was $0{\cdot}89 \times 10^5$ decays/min per μg. Corrected for the calibrated 72 per cent efficiency of the gas-phase counter, this is equivalent to $1{\cdot}2 \times 10^5$ decays/min or 0·056 μc/μg of glycine.

VOL. 10 1961

DISCUSSION

The theoretical treatment of self-absorption has not been entirely satisfactory. A number of workers[1,3,5,8] assuming a constant rate of absorption for the beta particles traversing the specimen, have developed a negative exponential equation for specific activity as a function of specimen thickness. Experimental deviation from this simple exponential function has been commented on by many.[4,6,9–11] The explanations given include backscattering, forescattering or self-focusing, and various geometric considerations. Some of these workers[4,9–11] have observed maxima in the specific activity curves, and one group[4] has gone so far as to recommend avoiding thin films whenever possible. Recently, HENDLER[6] has shown that his experimental data are best described by a reciprocal relationship between specific activity and specimen thickness. From this he concludes that the beta particles traversing the specimen are not absorbed at a constant rate or, in other words, that the so-called self-absorption constant of the exponential treatment is not actually a constant.

In the case of samples absorbed on thin paper planchets, the application of the equations, either reciprocal or negative exponential, requires only the assumption that the paper and specimen masses are additive in constant proportion. It may then be shown that the dependence of specific activity on specimen thickness, for a constant paper thickness, is of the same general form whether or not paper is used, and that the constant thickness of the paper affects only the magnitude of the constant terms of the equation. Thus for HENDLER's reciprocal equation,[6] rewritten for convenience,

$$1/S = am + b$$

(where S is the apparent specific activity, a and b are constants and m is the mass of absorbing material) if thickness (or masses) are additive in constant proportion, i.e. if

$$am = a_s m_s + a_p m_p$$

where the subscripts s and p refer to specimen and paper, respectively, and a_s and a_p are constants which, among other things, depend on the relative density of the specimen and paper, then

$$1/S = a_s m_s + a_p m_p + b.$$

For constant paper thickness, this may be simplified to:

$$1/S = a_s m_s + b'$$

where b' is a new constant the value of which is defined by the last two equations. This last equation is clearly of the same form as the original one. A similar development may be applied to the exponential equation. Likewise the equations may be expected to apply equally well to variations in paper thickness, the specimen size being constant.

In the present experiments the apparent specific activity of a series of radioactive specimens has been measured over a wide range of specimen thickness and of paper thickness. Considering first the variation of measured specific activity with varying specimen thickness, the results show that variation in apparent specific activity of less than 5 per cent may be expected for specimens up to about 150 $\mu g/cm^2$. For practical purposes this is the range of specimen thickness which may be regarded as infinitely thin. In this laboratory, paper discs up to $2\frac{1}{2}$ cm in diameter, corresponding to about 700 μg for the upper limit of the infinitely thin region, have been used successfully without correction for self-absorption.

As may be seen in Fig. 1 the extent of this infinitely thin region corresponds well with that which might be predicted by the use of either the reciprocal or the exponential relationship. It is an advantage of the thin-paper plating method that this entire predicted range is useful. Because no maxima or irregularities are noted in the curves relating the specific activity and specimen thickness, there does not appear to be any reason to avoid the use of thin specimens, as has been suggested.[4] The probable reason for this lack of irregularity is the comparatively constant specimen distribution afforded by the use of the paper disc to absorb and support the specimen.

For this infinitely thin region and for values of specimen thickness up to about 1 mg/cm², it is not possible to distinguish with accuracy between the exponential and the reciprocal equations. This is well illustrated by the curves of Fig. 1. The reason for this is apparent when the two equations are expanded as an infinite series and the constants appropriately related. Thus the reciprocal equation, above, rewritten

$$S = 1/(am + b)$$

may be expanded to the following infinite series:

$$S = 1/b - (a/b^2)m + (a^2/b^3)m^2 - (a^3/b^4)m^3 + \ldots.$$

The usual negative exponential equation, may be written in the following form:

$$S = (1 - e^{-k_2 m})/k_1 m$$

where S is the apparent specific activity, e is the Napierian base, m is the mass of absorbing material, and k_1 and k_2 are constants. Substituting the usual expansion of e and performing the indicated operations,

$$S = k_2/k_1 - (k_2^2/2k_1)m + (k_2^3/6k_1)m^2 - (k_2^4/24k_1)m^3 + \ldots.$$

If the following relationships are assigned to the constants,

$$k_1 = 2a$$
$$k_2 = 2a/b$$

and these are substituted in the last expansion

$$S = 1/b - (a/b^2)m + 2/3(a^2/b^3)m^2 - 1/3(a^3/b^4)m^3 + \ldots,$$

then this expansion of the exponential equation may readily be compared with the expansion for the reciprocal equation. It is apparent that the two series differ only in the value of the constants of the second (squared) and higher-order terms, and therefore the magnitude of the difference between the reciprocal and exponential relationships diminishes rapidly with decreasing specimen thickness. Conversely, for the increasing specimen thickness the curves of apparent specific activity calculated using the reciprocal equation differ progressively from those calculated using the negative exponential. This is also illustrated by the curves of Fig. 1. It should be noted that in the uppermost range the experimental points fall somewhat more nearly along the curves of the reciprocal equation.

Considering next the variation of measured specific activity with variation of paper thickness (Fig. 3) it can be seen that the reciprocal of the specific activity is a linear function of the paper thickness within limits of experimental accuracy. From this graph, the effect of a single sheet of paper can be determined readily by comparison with the value of the intercept for zero paper thickness.

TABLE 1. Comparison of the relative predictive values of the reciprocal and the exponential relationships between apparent specific activity and thickness

Paper thickness	Apparent specific activity				
	Experimental	Calculated			
		Exponential		Reciprocal	
		Value	Apparent error	Value	Apparent error
(No. of sheets)	(10^4 c.p.m./μg)	(10^4 c.p.m./μg)		(10^4 c.p.m./μg)	
1	2·92	2·92	0·00	2·92	0·00
2	2·36	2·44	−0·08	2·44	−0·08
3	2·10	2·08	0·02	2·10	0·00
4	1·87	1·79	0·08	1·84	0·03
5	1·62	1·55	0·07	1·64	−0·02
8	1·23	1·08	0·15	1·23	0·00
10	1·05	0·89	0·16	1·06	−0·01

When appropriate this difference between the specific activity measured using a paper disc and that predicted for zero paper thickness can be expressed as a fraction of the measured value. This fraction may then be applied to correct the measured specific activity for absorption in the paper.

Because the maximum paper thickness employed is considerably greater than the maximum specimen thickness, there is in the case of the paper a much greater difference between the values of specific activity predicted by the two equations over the upper range of paper thickness. This difference and the relative predictive value of the reciprocal and exponential equations may be seen in Table 1. This is in full accord with the results presented by HENDLER[6] and serves to emphasize the value of reciprocal presentation when the magnitude of thickness involved is sufficiently great.

It may be concluded that the preparation of radioactive samples by absorption on thin paper is a simple and effective method for producing samples sufficiently uniform to facilitate the use of thin specimens, and that to a considerable extent, the change in count rate due to self-absorption varies as the reciprocal of a linear function of the thickness of both the paper and the specimen.

Acknowledgements—This investigation was supported in part by a grant from the National Institutes of Health USPHS (C-2149). The author wishes to thank Dr. I. BERNSTEIN, Departments of Dermatology and Biochemistry, University of Michigan, for his advice and for performing the measurements of absolute radioactivity in the gas-phase counter. Illustrations were made by the Medical Illustration Service, Veterans Administration Hospital, Dearborn, Michigan.

REFERENCES

1. ARONOFF S. *Techniques of Radiobiochemistry*, Iowa State College Press, Ames (1956).
2. BERNSTEIN W. and BALLENTINE R. *Rev. Sci. Instrum.* **21,** 158 (1950).
3. CALVIN M., HEIDELBERGER C., REID J. C., TOLBERT B. M. and YANKWICH P. F. *Isotopic Carbon*, Wiley, New York (1949).
4. COLLIE C. H., SHAW P. F. D. and GALE H. J. *Proc. Phys. Soc.* **63,** 282 (1950).
5. DODSON R. W. (quoted by HENRIQUES F. C. JR., KISTIAKOWSKY G. B., MARGNETTI C. and SCHNEIDER W. G.) *Industr. Engng. Chem.* (*Anal.*) **18,** 349 (1946).
6. HENDLER R. W. *Science* **130,** 772 (1959).
7. KAMEN M. D. *Radioactive Tracers in Biology*, Academic Press, New York (1951).
8. LIBBY W. F. *Analyt. Chem.* **19,** 2 (1947).
9. SAJI Y., SAKISAKA M. and MIYAKE K. *J. Phys. Soc. Japan* **8,** 580 (1953).
10. SCHWEITZER G. K. and NEHLS J. W. *J. Phys. Chem.* **56,** 541 (1952).
11. SOLOMON A. K., GOULD R. G. and ANFINSEN C. B. *Phys. Rev.* **72,** 1097 (1947).

VOL. 10 1961

International Journal of Applied Radiation and Isotopes, 1961, Vol. 10, pp. 30–37. Pergamon Press Ltd. Printed in Northern Ireland

Preparation and Testing of Low-Energy Radiation Sources

R. E. BLACK
Research Laboratories, General Motors Corporation,
Warren, Michigan, U.S.A.

(*Received* 15 *June* 1960)

Low energy radiation sources, to be of value in industrial and medical radiography, must emit essentially no high-energy photons. They must have high specific activity, good mechanical strength and small physical size. Sources having these characteristics can be made by standard powder metallurgical techniques from certain powdered rare-earth oxides and aluminum powder.

Tests designed to determine mechanical strengths and radioisotope retention abilities of sources of varying compositions formed at various pressures are described and the results reported.

LA PREPARATION ET L'EPREUVE DES SOURCES DE RAYONNEMENT DE PETITE ENERGIE

Afin que les sources de rayonnement de petite énergie servent à la radiographie industrielle et médicale, elles ne doivent émettre pour ainsi dire point de photons de grande énergie. Elles doivent être de forte activité spécifique, de bonne robustesse mécanique et de dimension minuscule. On peut fabriquer des sources ayant ces qualités, selon les techniques normales de la métallurgie de poudre, de certains oxydes poudrés des terresrares et de l'aluminium en poudre.

On décrit des épreuves, et on rend compte des résultats, où le but était de mesurer la robustesse et le pouvoir de retenir les radioisotopes de différentes sources dont la composition variait et dont la formation était achevée à des pressions variées.

ИЗГОТОВЛЕНИЕ И ИСПЫТАНИЕ РАДИОАКТИВНЫХ ИСТОЧНИКОВ НИЗКОЙ ЭНЕРГИИ

Применяемые в промышленности и медицинской радиографии источники низкой энергии не должны испускать фотоны высокой энергии. Они должны обладать высокой удельной активностью, достаточной механической прочностью и быть небольших размеров. Такого рода источники можно изготавливать при помощи стандартной порошковой методики из некоторых измельченных редкоземельных окислов и из порошка алюминия.

Дано описание опытов по испытанию механической прочности источников и их способности удерживать радиоизотопы. Рассматриваются источники различного состава, приготовленные под различными давлениями, а также изложены результаты испытаний.

HERSTELLUNG UND PRÜFUNG NIEDERENERGETISCHER STRAHLENQUELLEN

Niederenergetische Strahlenquellen für industrielle und medizinische Radiographie dürfen praktisch keine hochenergetischen Photonen emittieren. Sie müssen eine hohe spezifische Aktivität, gute mechanische Festigkeit und eine kleine Ausdehnung besitzen. Quellen mit diesen Eigenschaften können durch pulvermetallurgische Standardmethoden aus gewissen, gepulverten Seltenerdoxyden und Aluminium-Pulver hergestellt werden.

Testmethoden zur Bestimmung der mechanischen Festigkeit und der Verseuchungssicherheit von Quellen verschiedener Zusammensetzung, hergestellt bei verschiedenen Drucken, werden beschrieben und die Ergebnisse dieser Teste werden mitgeteilt.

VOL. 10 1961

INTRODUCTION

Work performed in this and other laboratories has shown that the low-energy X-ray and gamma radiations from certain rare-earth radioisotopes are useful for industrial radiography and gaging, and possibly for medical work.[1–4] The sources which we initially used for laboratory evaluation were fragile and unsuited for field use. It was necessary to develop more rugged radiation sources to permit field evaluation in other General Motors facilities and in hospitals.

A radiation source that is to be used outside of a radioisotope facility must possess sufficient mechanical strength to endure normal handling and forseeable accidents, and should retain most of the radioactive material when subjected to catastrophic accidents. For sources of low-energy radiation such as we are interested in, these properties must be obtained without the use of an excessively thick exterior housing.

Many radiographic applications require that the physical dimensions of the source be extremely small in order to secure good resolution, and that the source strength be large so that reasonable exposure times can be used.

The sources must be made of low-density low-atomic-number elements to minimize self-absorption of the radiations within the sources.

It was proposed to fabricate the sources from Calutron separated stable Sm^{144}, Sm^{152} and Gd^{152} and from Tm^{169}. The sources were then to be irradiated with thermal neutrons to produce the desired radioisotopes Sm^{145}, Sm^{153}, Gd^{153} and Tm^{170}. The stable isotopes were available as the oxides. For all except Tm^{169}, the delivery time is long and the cost is quite high. Therefore, the fabrication procedure must not waste the isotope. A literature search indicated that reducing the oxide to the pure metal would be wasteful of material. Sintering the pure oxide to form a solid mass was considered, and tried experimentally, but the equipment that is necessary reliably to produce a uniform sintered product was not available. The possibility remained of compressing and sintering a mixture of the rare-earth oxide and some binding material by powder metallurgical techniques.

Aluminum was found to be the best binding material because it has a very small thermal neutron activation cross-section and its daughter product has a very short half-life. Hence, no significant amounts of high-energy gamma radiation would be emitted from a source constructed with aluminum as the binder. Also, the aluminum is of low atomic number and low density so that self-absorption of the desired radiations would be small.

EXPERIMENTAL

General considerations

Of the many factors that influence the properties of the finished pellets, only the percentage composition of the mix and the forming pressure were investigated. The percentage composition was selected as one variable because one would like to have as much rare-earth oxide powder in a given volume as possible in order to make a radiation source with high specific activity.

Too high forming pressures soon damage the small punch and die, and make it difficult to remove the formed pellets. Hence, forming pressures should be no higher than is necessary to produce a sound product. Forming pressure was selected as the second variable.

All pellets that were broken in the strength tests were made from the same batch of powders, so particle size and particle size

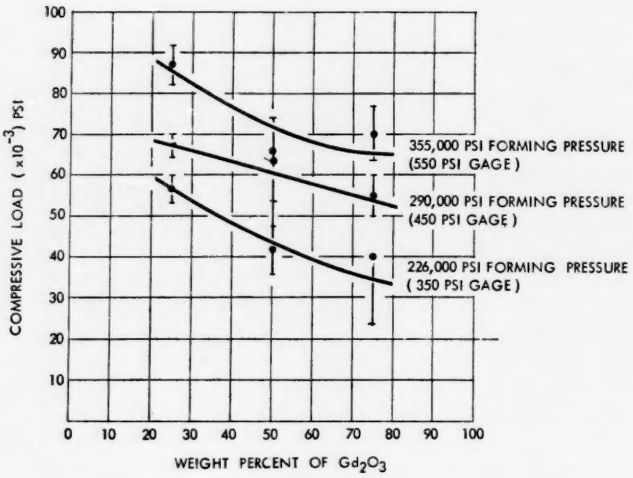

FIG. 1. Variation of compressive strength with composition and forming pressure.

distribution were constant. All pellets were subjected to the same sintering cycle.

Pellet fabrication technique

Unenriched reagent-grade rare-earth oxide powder and aluminum powder (−200 mesh) were mixed in the desired proportions on a glass plate, using a scalpel as a spatula.

A single acting die, made from a 0·078 in. I.D. drill bushing, was lubricated with a dilute solution of Johnson's 140 Metallurgical Wax in benzene and loaded with 20 or 30 mg of the powder mixture. The upper punch was inserted, and the die was placed in a small hydraulic laboratory press, which was equipped with a calibrated 0-500 PSI gage installed in the hydraulic system. The powder mixture was compressed until the desired pressure was indicated by the gage.

After compression, the green pellet (0·078 in. in diameter and 0·050–0·100 in. long) was pushed out of the die and sintered in air at a temperature of 1000°F for $\frac{1}{2}$ hr.[5]

The finished pellets were then ready for testing.

Longitudinal mechanical strength tests

A total of forty-five pellets was made for the longitudinal mechanical strength tests. After being formed and sintered, the pellets were examined visually and those which were chipped were discarded; for this reason some of the groups listed in the tables consist of only four pellets. The forty-three pellets remaining were weighed and measured before being destructively tested.

Each pellet was placed in a laboratory hydraulic press so that a compressive load could be applied along the longitudinal axis. One man slowly increased the compressive load while observing the pellet through a magnifier. When a fracture was observed, the man called out "Mark", and a second man recorded the reading of the hydraulic pressure gage. This reading was multiplied by the appropriate geometrical factors to calculate the load applied to the pellet in pounds per square inch. The pellets' composition, physical characteristics, forming pressures and breaking strengths are shown in Tables 1, 2 and 3. The statistical errors shown in all Tables are standard deviations. The data are plotted in Fig. 1.

Transverse mechanical strength tests

Seven pellets were crushed with the compressive load applied at right angles to the longitudinal axis. Other details of the testing procedure were as described above.

VOL.
10
1961

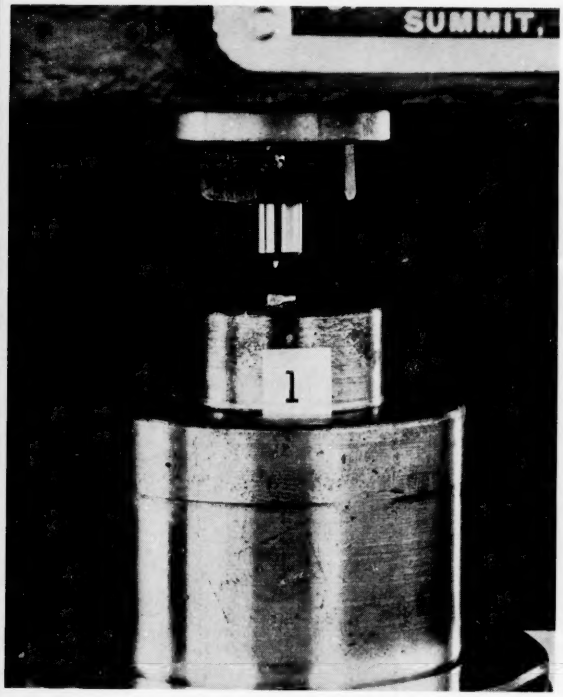

FIG. 2. Plastic deformation of a pure aluminum pellet to which a transverse load of 314 lb was applied.

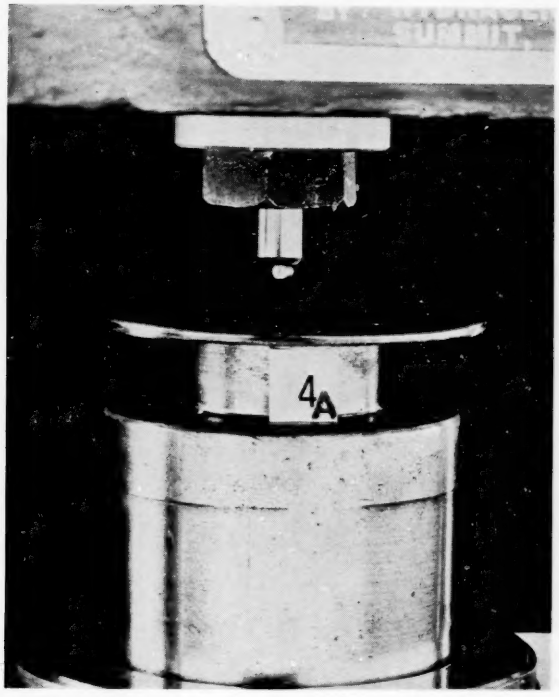

FIG. 3. Simple fracture of a 50% Sm_2O_3–50% Al pellet to which a transverse load of 148 lb was applied

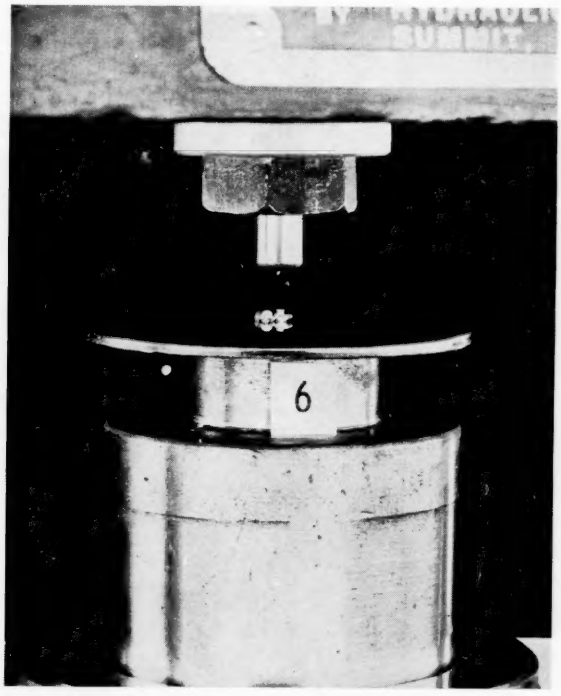

FIG. 4. Crumbling fracture of a 75% Sm_2O_3–25% Al pellet to which a transverse load of 63 lb was applied. Note the reflections on the bottom plate.

VO
1
19

VOL. 10 1961

TABLE 1. Longitudinal load fracture characteristics of 25% Gd_2O_3–75% Al pellets

(a) 226,000 PSI forming pressure

Pellet number	Density (gm/cm^3)	Longitudinal fracture load ($lb/in.^2$)
1	2·78	$5·17 \times 10^4$
2	2·79	$5·80 \times 10^4$
3	2·79	$5·49 \times 10^4$
4	2·79	$6·12 \times 10^4$

Mean specific longitudinal fracture load = $5·64 \pm 0·35 \times 10^4$ lb/in².

(b) 290,000 PSI forming pressure

Pellet number	Density (gm/cm^3)	Longitudinal fracture load ($lb/in.^2$)
1	2·79	$6·71 \times 10^4$
2	2·79	$6·71 \times 10^4$
3	2·79	$7·04 \times 10^4$
4	2·70	$6·06 \times 10^4$
5	2·81	$7·04 \times 10^4$

Mean specific longitudinal fracture load = $6·71 \pm 0·30 \times 10^4$ lb/in².

(c) 355,000 PSI forming pressure

Pellet number	Density gm/cm^3)	Longitudinal fracture load ($lb/in.^2$)
1	2·78	$7·98 \times 10^4$
2	2·84	$8·95 \times 10^4$
3	2·81	$8·95 \times 10^4$
4	2·81	$9·28 \times 10^4$
5	2·83	$8·30 \times 10^4$

Mean specific longitudinal fracture load = $8·69 \pm 0·48 \times 10^4$ lb/in².

TABLE 2. Longitudinal load fracture characteristics of 50% Gd_2O_3–50% Al pellets

(a) 226,000 PSI forming pressure

Pellet number	Density (gm/cm^3)	Longitudinal fracture load ($lb/in.^2$)
1	2·96	$3·19 \times 10^4$
2	3·01	$3·88 \times 10^4$
3	3·02	$4·52 \times 10^4$
4	3·05	$4·85 \times 10^4$
5	2·68	$4·19 \times 10^4$

Mean specific longitudinal fracture load = $4·13 \pm 0·59 \times 10^4$ lb/in².

(b) 290,000 PSI forming pressure

Pellet number	Density (gm/cm^3)	Longitudinal fracture load ($lb/in.^2$)
1	3·06	$6·06 \times 10^4$
2	3·11	$5·74 \times 10^4$
3	3·13	$8·38 \times 10^4$
4	3·13	$6·13 \times 10^4$
5	2·97	$5·49 \times 10^4$

Mean specific longitudinal fracture load = $6·36 \pm 1·04 \times 10^4$ lb/in².

(c) 355,000 PSI forming pressure

Pellet number	Density (gm/cm^3)	Longitudinal fracture load ($lb/in.^2$)
1	3·18	$6·71 \times 10^4$
2	3·22	$7·41 \times 10^4$
3	3·18	$7·41 \times 10^4$
4	3·15	$6·06 \times 10^4$
5	3·03	$5·18 \times 10^4$

Mean specific longitudinal fracture load = $6·55 \pm 0·84 \times 10^4$ lb/in².

The pellet characteristics and the transverse mechanical strength data are presented in Table 4.

The figure of merit that is used for comparing the transverse mechanical strengths is expressed in units of pounds per linear inch. It is calculated by dividing the compressive load (in pounds) by the length of the pellet (in inches). It is meaningless to measure the flattened area on the fractured pellet to which the load was applied and calculate a specific load in pounds per square inch. If the pellet crumbles, it is impossible to measure such an area. If the pellet does not crumble, it is often so deformed that the flattened area observed on the pellet after the test bears no relation to the area to which the compressive force was applied at the moment of fracture.

Type of fracture

When rare-earth oxide-aluminum pellets are subjected to excessive compressive loads, ideally they would undergo a plastic deformation and remain an integral mass. The

TABLE 3. Longitudinal load fracture characteristics of 75% Gd_2O_3–25% Al pellets

(a) 226,000 PSI forming pressure

Pellet number	Density (gm/cm³)	Longitudinal fracture load (lb/in.²)
1	3·35	$4·38 \times 10^4$
2	3·40	$5·28 \times 10^4$
3	3·21	$2·64 \times 10^4$
4	3·08	$2·31 \times 10^4$
5	3·39	$5·28 \times 10^4$

Mean specific longitudinal fracture load = 3·98 ± $1·65 \times 10^4$ lb/in².

(b) 290,000 PSI forming pressure

Pellet number	Density (gm/cm³)	Longitudinal fracture load (lb/in.²)
1	3·07	$4·95 \times 10^4$
2	3·49	$4·95 \times 10^4$
3	3·56	$5·93 \times 10^4$
4	3·56	$5·93 \times 10^4$
5	3·55	$5·60 \times 10^4$

Mean specific longitudinal fracture load = 5·47 ± $0·49 \times 10^4$ lb/in².

(c) 355,000 PSI forming pressure

Pellet number	Density (gm/cm³)	Longitudinal fracture load (lb/in.²)
1	3·75	$75·6 \times 10^4$
2	3·84	$59·3 \times 10^4$
3	3·69	$69·1 \times 10^4$
4	3·70	$75·6 \times 10^4$

Mean specific longitudinal fracture load = 6·99 ± $0·67 \times 10^4$ lb/in².

TABLE 4. Transverse load fracture characteristics of pellets (all formed at 355,000 PSI)

(a) 50% Sm_2O_3–50% Al

Pellet number	Density (gm/cm³)	Transverse fracture load (lb/in.)
1	3·32	1660
2	3·30	908
3	3·30	1950

Mean specific transverse fracture load = 1506 ± 439 lb/in.

(b) 75% Sm_2O_3–25% Al

Pellet number	Density (gm/cm³)	Transverse fracture load (lb/in.)
1	3·67	1120
2	3·51	1155
3	3·57	924
4	3·51	1210

Mean specific transverse fracture load = 1102 ± 108 lb/in.

least desirable type of fracture would be that in which the pellet crumbles into fine particles scattered throughout the surrounding environment.

Further destructive tests were performed (some with transverse loads, and some with longitudinal loads) to study the types of fractures from pellets of different compositions. These were placed in the press and slowly compressed. When signs of fracture were observed, the pressure was released. This method of fracturing the pellets is not meant to duplicate actual accidental breakage. It was selected as a means of obtaining data for comparing one type of pellet with another.

As the accompanying pictures show (Figs. 2, 3 and 4), samples with a low rare-earth oxide content approach the ideal of plastic deformability, while those with a high rare-earth content fracture into many small fragments.

Airborne contamination released from fractured pellets

When a pellet is subjected to excessive compressive loads, it fractures into two or more fragments (as shown above), and also releases a certain amount of radioactive dust into the air. The apparatus shown in Fig. 5 was designed so that nearly 100 per cent of the dust released by a test pellet as it is fractured could be collected.

(1) *Experimental procedure.* Non-radioactive pellets composed of europium oxide and aluminum were fractured. The airborne dust particles that were produced were collected on Millipore filter paper. The amounts were too small to be measured by weighing, so the amount of dust was measured by neutron activation. The samples were placed next to a paraffin moderated

VOL. 10 1961

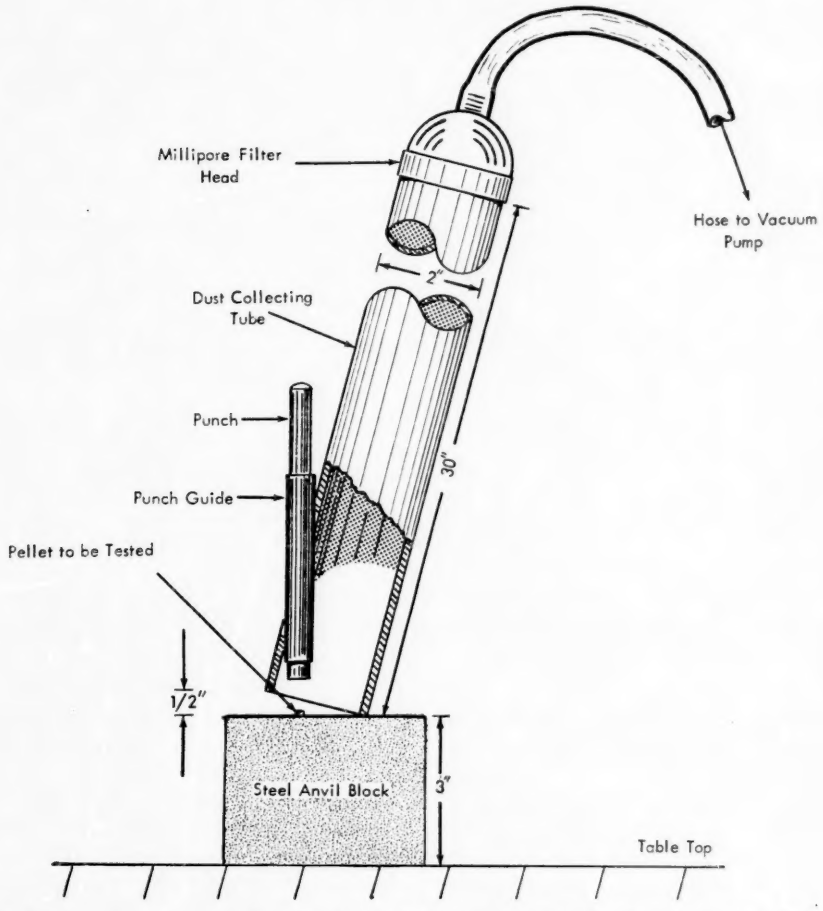

Fig. 5. Apparatus for measuring the release of airborne contamination from fractured pellets.

polonium–beryllium neutron source for 24 hr. There, radioactive Eu^{152} was formed by the nuclear reaction

$$Eu^{151}(n,\gamma)Eu^{152}.$$

Pellets containing 50 or 75 per cent by weight of Eu_2O_3 were placed on the iron block and beneath the punch of the apparatus shown in Fig. 5. The vacuum pump was started, drawing air up the tube and through the filter. The hammer was raised 12 in. above the top of the punch, and the punch was struck a single sharp blow. The punch was raised immediately after being struck so that its bottom was about one inch above the upper surface of the block. This allowed any pellet particles which were clinging to the punch bottom to be exposed to the air stream. This breaking procedure was intended to simulate the worst possible type of fracture that one might encounter.

To evaluate the amount of airborne contamination that would be produced from breaking the worst possible type of source, a lump of pure Eu_2O_3 powder was crushed in the above apparatus and the dust collected (Sample 5, Table 5). Before being crushed, the lump was dried at 200°F for 12 hr, so that its mechanical strength was very low.

A standard sample (Table 5) consisting of 0·93 mg of Eu_2O_3 deposited on a Millipore filter paper was also prepared. As a further

TABLE 5. Release of airborne contamination by fractured pellets

(a) Standards—All counts are for 10 min

Sample	Gross count	Net count	Time of count	Time after 10.00 a.m.	Time corrected net count
Blank air sample	296		11.35 a.m.	1·58 hr	296
Blank air sample	300	4	3.20 p.m.	5·33 hr	296
0·93 mg Eu_2O_3	2479	2188	11.25 a.m.	1·42 hr	2390 ± 55

The same blank air sample was counted twice, to detect any short-lived activity due to faulty experimental technique.

(b) Pellets—All counts are for 10 min

Pellet number	Pellet type	Pellet weight (mg)	Gross count	Net count	Time of count	Time after 10.00 a.m. (hr)	Time corrected net count	Wt. of Eu_2O_3 collected (mg)	% of sample Eu_2O_3 released
1	50% Eu_2O_3—U	15·9	583	287	1.30 p.m.	3·50	372 ± 31	0·145	1·8%
2	50% Eu_2O_3—C	18·2	294	24·3*	1.55 p.m.	3·92	33 ± 25	0·013	0·1%
3	75% Eu_2O_3—U	16·3	392	96	2.15 p.m.	4·25	132 ± 27	0·051	0·4%
4	75% Eu_2O_3—C	14·9	316	20	2.35 p.m.	4·58	28 ± 25	0·011	0·1%
5	100% Eu_2O_3—U	9·4	570	274	2.05 p.m.	4·08	371 ± 29	0·145	1·5%

C—indicates pellets with a coating of pure aluminum.

U—indicates pellets without a coating of pure aluminum.

* Since net count is 0, value given is the standard deviation of twice the background. Weight of Eu_2O_3 released is the maximum probable amount.

control check a blank filter paper was prepared by drawing laboratory air which was free from Eu_2O_3 through the apparatus for 5 min.

The filter papers from the breaking tests, the blank test and the Eu_2O_3 standard sample were carefully folded and placed inside individual glassine envelopes. All of the samples were neutron irradiated simultaneously for 24 hr. The radioactive Eu^{152} which was produced decayed with a 9·3 hr half-life.

After the samples were withdrawn from the neutron source, 1 hr elapsed before any of them were counted, to allow any short-lived radioisotopes to decay. Each sample was counted for 10 min with a thin window Geiger–Muller counter. The counts were corrected for decay losses, assuming that the only radioisotope present was the 9·3 hr Eu^{152}. The weight of Eu_2O_3 dust that was in each sample was calculated by comparing the corrected sample count with a count obtained from the 0·93 mg of Eu_2O_3 on the standard sample.

(2) *Results and interpretation.* Referring to Table 5, note that the amount of airborne Eu_2O_3 released by pellet no. 1 was equal to that released by the lump of pure Eu_2O_3. We find no ready explanation for this result. Precautions such as thorough apparatus cleaning between samples and sample isolation and protection were practiced at all times. This no. 1 pellet experiment was not repeated at this time because of scarcity of raw material.

The data show that the well-behaved pellets released only 5–10 per cent as much material as did the lump of pure Eu_2O_3.

Let us calculate the concentration of airborne radioactive material that might result if a typical well-behaved pellet were broken in still air in an enclosed space. We shall consider the air volume to be a hemisphere, the radius of which is equal to the height of a man's nose from the floor:

$$\text{Air volume} = \tfrac{2}{3}\pi r^3 = \tfrac{2}{3}\pi\ (60\text{ in.})^3$$

$$\text{Air volume} = \tfrac{2}{3}\pi(216 \times 10^3\text{ in.}^3)$$

$$= 4{\cdot}53 \times 10^5\text{ in.}^3$$

$$\text{Air volume} = 7{\cdot}43 \times 10^6\text{ ml.}$$

Tm^{170} is a typical radioisotope which might be used as a pellet. The maximum permissible concentration of Tm^{170} in air in a restricted area is $1{\cdot}5 \times 10^{-7}$ μc/ml based on a 40 hr week.[6]

Airborne activity $= 1{\cdot}5 \times 10^{-7}$ μc/ml $\times$ $7{\cdot}43 \times 10^{6}$ ml $= 1{\cdot}12$ μc. If the pellets release 0·1 per cent of their total activity to the air upon being fractured, the largest pellet one could "safely" fracture in a dead air volume would be

$$\frac{1{\cdot}12\ \mu\text{c released/fractured pellet}}{0{\cdot}1\%\ \text{released}} = 1{\cdot}12\ \text{mc/pellet}.$$

We see that a 1 mc pellet could be fractured with "little" danger, if no more than 0·1 per cent of its activity were released to the air. Larger pellets could be "safely" fractured in a volume in which the air is changed several times per hour or if occupancy time were limited.

Activity wipe-off

It has been observed in our Laboratory that measurable amounts of radioactive material can be transferred from the surface of this type of source pellet by contact. To date, all source pellets have been loaded into source holders while inside a glove box. The sealed holders can then be used without contaminating the environment.

A technique has been devised in our Laboratory by which it is possible to fabricate a pellet which has an integral coating of pure aluminum. Experimental data indicate that these coated pellets will transfer little or no radioactive material by contact.

REFERENCES

1. West R. *Nucleonics* **11,** 20 (1953).
2. Green F. L. and Cheek W. D. *Proceedings of the Second International Conference on the Peaceful Uses of Atomic Energy, Geneva,* **19,** pp. 169–175. United Nations, N.Y. (1958).
3. Robertson J. S. *Proceedings of the Second International Conference on the Peaceful Uses of Atomic Energy, Geneva,* **26,** pp. 268–271. United Nations, N.Y. (1958).
4. Rumyantsev S. V. and Matsyuk L. N. *Proceedings of the Second International Conference on the Peaceful Uses of Atomic Energy, Geneva,* **19,** pp. 120–126. United Nations, N.Y. (1958).
5. Baeza W. J. *A Course in Powder Metallurgy* pp. 122, 191. Reinhold, N.Y. (1943).
6. *Federal Register* **22,** 19, Title 10, Chap. 1, Part 20, App. B (29 January, 1957).

VOL. 10 1961

International Journal of Applied Radiation and Isotopes, 1961, Vol. 10, pp. 38–46. Pergamon Press Ltd. Printed in Northern Ireland

Radio-Tracer Techniques for the Study of Flow in Saturated Porous Materials*

H. E. SKIBITZKE, H. T. CHAPMAN,
G. M. ROBINSON and R. A. McCULLOUGH
U.S. Geological Survey, Phoenix, Arizona, U.S.A.

(*Received* 5 *February* 1960 *and in revised form* 6 *May* 1960)

An experiment was conducted by the U.S. Geological Survey to determine the feasibility of using a radioactive substance as a tracer in the study of microscopic flow in a saturated porous solid. A radioactive tracer was chosen in preference to dye or other chemical in order to eliminate effects of the tracer itself on the flow system such as those relating to density, viscosity and surface tension. The porous solid was artificial "sandstone" composed of uniform fine grains of sand bonded together with an epoxy adhesive. The sides of the block thus made were sealed with an epoxy coating compound to insure water-tightness. Because of the chemical inertness of the block it was possible to use radioactive phosphorus (P^{32}). Ion-exchange equilibrium was created between the block and nonradioactive phosphoric acid. Then a tracer tagged with P^{32} was injected into the block in the desired geometric configuration, in this case, a line source. After equilibrium in isotopic exchange was reached between the block and the line source, the block was rinsed, drained and sawn into slices. It was found that a quantitative analysis of the flow system may be made by assaying the dissected block.

LES TECHNIQUES RADIO-INDICATIVES A L'ETUDE DE L'ECOULEMENT DANS DES MATERIAUX POREUX SATURES

Une expérience fut entreprise par le Bureau d'Etude Géologique des E-U. afin d'observer la possibilité d'employer une matière radioactive comme indicateur pour étudier l'écoulement microscopique dans un solide poreux saturé. On choisit un indicateur radioactif plutôt qu'une teinture ou autre produit chimique pour éliminer les effets de l'indicateur même sur le systême d'écoulement, tels que ceux associés à la densité, à la viscosité et à la tension superficielle. Le solide poreux fut un "grès" artificiel fait de grains fins et uniformes de sable réunis avec un adhésif époxy. Les côtés de la masse ainsi formée furent scellés avec une couche d'époxy pour assurer l'étanchéité. Vu l'inertie chimique de la masse on put employer le phosphore radioactif (P^{32}). On acheva l'équilibre d'échange ionique entre la masse et de l'acide phosphorique non-radioactif. Alors on introduit un indicateur marqué de P^{32} dans la masse selon la forme géométrique désirée, en ce cas une source linéaire. Après l'atteinte de l'équilibre quant à l'échange isotopique entre la masse et la source linéaire, la masse fut lavée, laissée à égouter et puis coupée en tranches. On trouva possible de faire l'analyse quantitative du système d'écoulement en dosant la masse disséquée.

РАДИОИЗОТОПНАЯ МЕТОДИКА ИССЛЕДОВАНИЯ ПОТОКА В НАСЫЩЕННЫХ ПОРИСТЫХ ТЕЛАХ

Геологическим Управлением США был проведен ряд опытов для выяснения возможности применения радиоактивных индикаторов при исследовании микроскопических потоков в твердых пористых телах. С целью избежать влияния индикатора на такие свойства потока как плотность, вязкость и поверхностное натяжение, радиоактивным индикаторам было отдано предпочтение перед красителями или какими-либо другими химическими веществами. В качестве пористого тела был взят "песчаник", приготовленный из зерен песка одинакового размера, соединенных между собой эпоксидной смолой. Стороны приготовленного образца были покрыты эпоксидной пленкой для

* Publication authorized by the Director, U.S. Geological Survey.

обеспечения водонепроницаемости. Благодаря химической инертности образца можно было применить радиоактивный фосфор (P^{32}). После достижения ионно-обменного равновесия с нерадиоактивной фосфорной кислотой в образец вводился индикатор, меченый P^{32}, в желаемой геометрической конфигурации, в данном случае в виде линейного источника. Когда изотопный обмен между образцом и линейным источником достигал равновесия, образец промывался, сушился и разрезался на пластинки. Было установлено, что изучение этих пластинок дает возможность провести количественный анализ системы потока.

RADIOAKTIVE INDIKTOREN-METHODE FÜR DURCHFLUSS-UNTERSUCHUNGEN AN GESÄTTIGTEN, PORÖSEN MATERIALIEN

Vom U.S. Geological Survey wurde ein Versuch durchgeführt, welcher bezweckte, die Verwendbarkeit von Radioindikatoren für die Untersuchungen des Mikroflusses durch gesättigte, poröse, feste Körper zu bestimmen. Radioaktive Indikatoren wurden an Stelle von Farbstoffen oder anderen chemischen Indikatoren verwendet um dadurch Einflüsse des Indikators auf das fliessende System wie z.B. Veränderungen der Dichte, der Viskosität oder der Oberflächenspannung, zu vermeiden. Der Poröse feste Körper war ein künstlicher "Sandstein" der aus feinen Sandkörnern etwa gleicher Grösse bestand, die durch einen Epoxy-Kleber gebunden waren. Die Seiten des Blockes waren mittels des Klebers wasserdicht gemacht. Radioaktiver Phosphor konnte verwendet werden, da der Block davon chemisch nicht angegriffen wurde. Zwischen dem Block und nicht-radioactiver Phosphorsäure wurde Ionenaustauschgleichgewicht hergestellt. Hierauf wurde P^{32} in der gewünschten geometrischen Form, in diesem Fall in Form einer geraden Linie, in den Block injiziert. Nach Herstellung des Isotopenaustauschgleichgewichtes zwischen dem Block und der linienförmigen Quelle wurde der Block gewaschen, drainiert und in Scheiben gesagt. Es zeigte sich, dass die Untersuchungen des zerteilten Blockes eine quantitative Analyse des Flussystems möglich machte.

VOL. 10 1961

INTRODUCTION

This work, which was undertaken by the U.S. Geological Survey on behalf of the Division of Reactor Development of the Atomic Energy Commission, is important in the development of radio-tracer techniques for studying principles of ground-water movement as they may be applied to problems of radioactive waste disposal. Study of the physics of the flow of ground water in the earth's crust has been difficult because of the remoteness of the flow system and the extremely low velocities. Ground-water velocities in most places range from less than a foot a year to slightly more than a foot a day prior to disturbance by man. These velocities would be extremely difficult to measure by any metering instrument even if suitable instruments could be inserted into the porous space of the aquifer. Because engineers are unable to do this, the motions, and thereby the streamlines, are inferred by measuring the hydraulic potential field existing in the aquifer. The potential is then plotted on a map of the permeability for the region of interest. By use of Darcy's law, the velocity in this region may then be derived. The mapping of the permeability is a difficult task. Even when this is possible, very little is determined concerning the microscopic flow system. By "microscopic flow system" is meant the paths of motion of the individual water molecules.

Two problems of great importance to the ground-water hydrologist today are (1) the diffusion of atomic wastes if they should be injected into a ground-water reservoir, and (2) the diffusion of salt water into aquifers near the ocean front (Cooper[1]). In both problems the question of the movement of the molecules as compared to the paths of the streamlines is of prime concern: first, it is not known whether the streamlines always close back on one another as in two-dimensional planar flow; second, it is not known if the streamlines intermix and therefore form a diffusion system. Further, it is not known how much normal thermal diffusion is increased by interchange between

adjacent streamlines of molecules responding to thermal agitation. The streamlines determined by Darcy's law describe the velocities at any given point as a function of the force field due to the hydraulic gradient alone. There still remains a system of random molecular motion superimposed upon the motion due to the hydraulic force field. This microscopic flow system can alter the paths of molecules from those described by the streamlines, as the streamlines intertwine about the solid material of the aquifer. In addition to these effects, other force fields can be found causing motion in the aquifer—for example, the forces due to differences in density and surface tension resulting from material contained in solution within the liquid. A study of all these effects can be made if a portion of the flow system can be brought into the laboratory, where it is possible to make a quantitative analysis of the streamlines and the molecular motion and of how they are combined into the true particle path. This has been attempted often in the past by tracer experiments using either dye or electrochemical effects, but the experiments have not furnished observation of the interior of the flow system.

In addition, these past experiments have raised, and left unanswered, questions of the effects of the tracer itself on the flow system. The effects could relate to such properties as density, viscosity, or surface tension, as well as other factors. Because radio tracers gave promise of overcoming these obstacles they were chosen for use in the present experiment. It was hoped that by means of this method both a quantitative analysis and some observation of the interior of the aquifer could be obtained.

PRINCIPLES OF THE EXPERIMENT

Probably the largest single problem to be overcome during an experiment of this nature is the elimination of physicochemical effects. These effects, relating to density, viscosity and other physicochemical forces, can be obviated through isotopic exchange processes that require the use of an ion-exchange bed for the artificial aquifer material (BERAN,[2] MERRIAM *et al.*,[3] and MEYERS and PRESTWOOD[4]).

The method used here depends upon an artificial bed made of material having a slight ion-exchange capability. The bed must be artificial because it is necessary to keep conditions highly uniform as well as to have material that is relatively inert to the acids used in the flow system. The feature of inertness is important for safety reasons because it insures against accidental spillage due to block dissolution. The block was constructed of sand coated with an epoxy resin. After the block was cast the sides were coated with a compound of an epoxy resin and mica to make them watertight.

The finished block was flushed with distilled water for about a month. Two centigrams of potassium permanganate was added to each 5 gal of the distilled water to prevent growth of algae. After this preliminary flushing, a weak phosphoric acid solution replaced the distilled water circulating through the block. The acid was kept flowing through the block for several weeks until ion-exchange equilibrium was reached between the liquid and the interior surfaces of the porous solid. The system was then homogeneous with respect to the tracer that was to be introduced. A tracer having the same chemical nature as the liquid that had reached ion-exchange equilibrium in the block was then introduced in a needle-width stream at the upper end of the flow system. However, the phosphorus in the tracer was radioactive (P^{32}). The system was kept flowing until an equilibrium in the isotopic exchange between the radioactive and non-radioactive phosphorus had been reached. The guide to equilibrium is a constancy of radioactivity in the liquid leaving the block. This exchange occurred without chemical effects. After equilibrium was reached the flow through the block was changed to distilled water to rinse the acids out of the pore space of the block.

The block was then rapidly drained and dried out. The block was then cut into

slabs 1 in. and 2 in. in thickness. The surfaces of the slabs were sandblasted clean and a radio assay across each of them was made by film and counter. The results could then be used to make a quantitative analysis of the diffusion of the tracer by examining the spread of the contaminated band. The actual methods and useful data for completing such experiments are given in the following paragraphs.

LABORATORY METHODS

Sand-block construction

The "sandstone" aquifer in this experiment was designed as an even-grained, permeable block of fine sand of a desired size and shape. The block was composed of No. 30 commercially bagged washed silica sand bonded together with an epoxy adhesive. Thirty-two pounds of the sand thoroughly mixed with 26½ oz of Epocast No. 202 (manufactured by Furane Plastics), to which 3 oz of Epocast No. 951 Hardener had been added, produced the desired block or column measuring 6 × 6 × 19 in. (see Fig. 1). The block was cast by placing the mixture of sand and epoxy in a wooden mold which had been coated previously with ceresin wax to permit subsequent removal from the mold. A technique found most suitable for applying the wax was to melt it on with a heat lamp. The heat not only kept the wax coat uniform but caused the wax to penetrate into the wood of the mold to form a stable base. To prevent the block from being layered into several different strata the sand was poured into the mold without hammering. After the mold was filled a sliding top was installed and lateral pressure exerted by "C" clamps equally spaced along the length of the mold. The mixture in the mold was allowed to set for a period of 72 hr before the mold was removed. A mechanical analysis of the sand is given in Fig. 2. The resulting "sandstone" column had a permeability of 850 meinzers (gallons per day per square foot under unit hydraulic gradient at 60°F).

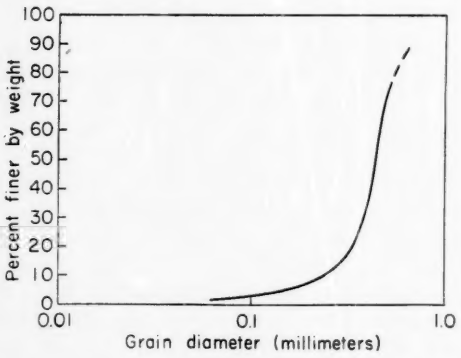

FIG. 2. Grain-size distribution curve of sand used to make sandstone block.

The sides of the column were sealed, leaving the ends unsealed to permit water to enter at the top and leave at the bottom. The seal was formed by coating each side with four layers of a mixture of Epocast No. H591-B Dipping Compound Resin and Epocast No. 951 Hardener in a proportion of 100 to 12 by weight.

Hydraulic installation

The model aquifer was placed in a glove box (Fig. 3) which was shielded with ⅛ in. of lead on the sides, back and top and 1 in. of lucite on the front. The box was installed on a stainless-steel sink-like table.

In order to maintain a constant flow of fluid through the model aquifer, tanks were connected to the upper and lower ends of the sandstone column. The tanks, prior to assembly, are shown in Figure 1. They were constructed of glass cloth impregnated with the same epoxy resin used to bond the sandstone column and sealed with the same resin dipping compound. A third tank, referred to as the "hot tank" because it held the supply of radioactive tracer, was made of lucite. From it extended a hollow needle with an outside diameter of 0·047 in. The hot tank was placed in the upper or head tank in such a manner that the needle was inserted ¼ in. into the block. The radioactive phosphoric acid was stored in a lead-shielded bottle, pumped to the hot tank, and introduced into the block through the needle.

VOL. 10 1961

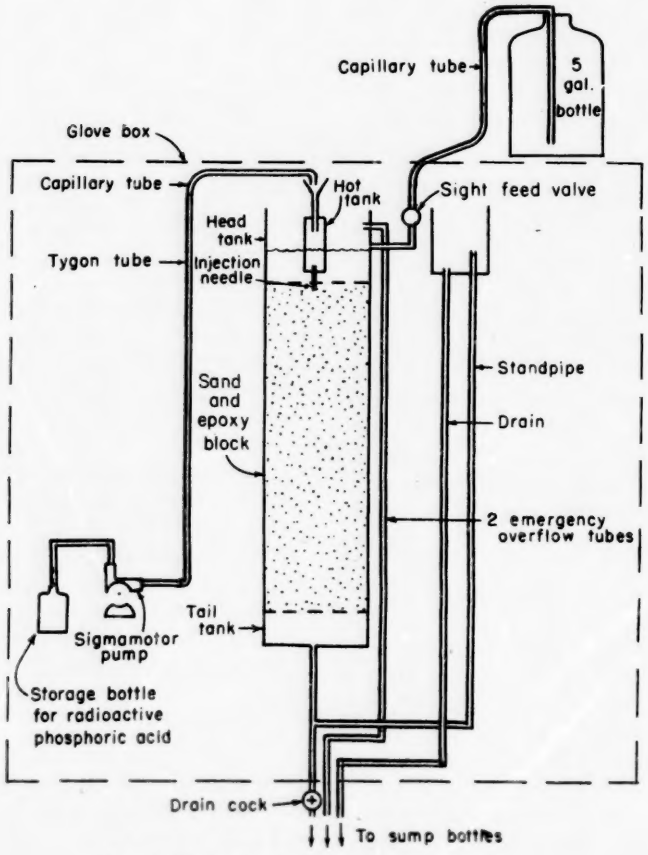

FIG. 4. Hydraulic diagram of the experiment.

The flow of solution through the model aquifer was regulated by means of an elevated 5 gal. bottle as a supply source, siphoning the solution from there into the head tank through a capillary tube. A constant fluid level was maintained in the head tank by use of a standpipe outside the model, as shown in Fig. 4. The hydraulic gradient was such that fluid flowed through the model aquifer prior to and during the experiment at the rate of approximately 4 l./day, or about 38 drops/min, through a cross-section of 36 sq. in. Two overflow pipes were installed on the head tank as a precaution against possible excessive contamination of the interior of the glove box in the event of a stoppage. The overflow pipes are shown on the right side of the model in Fig. 5.

Because the ratio of the cross-sectional area of the model aquifer to the inside cross-sectional area of the tracer-injection needle was 21,000:1, and because 38 drops/min was the rate of flow through the model, one drop of tracer was pumped into the hot tank every 9 hr to produce a proportionality of about 21,000 to 1 between the two rates of flow.

The radioactive phosphoric acid was transferred from the lead-shielded storage bottle to the hot tank through a tygon tube in series with a capillary tube (Fig. 4). An electric-powered Sigmamotor pump proved very satisfactory in accomplishing the transfer because it could control flow at the rate of one drop at a time.

Two alternative methods were devised for

VOL.
10
1961

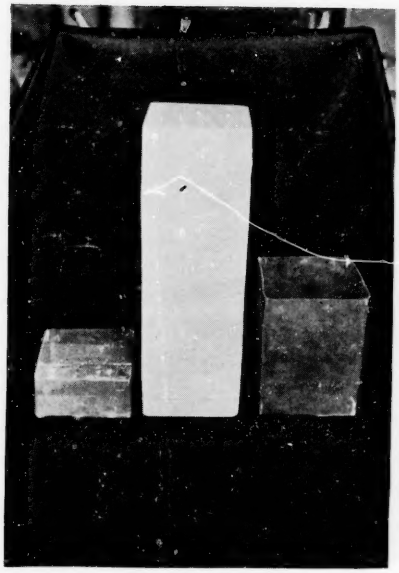

FIG. 1. The sand and epoxy block is pictured with the head tank at the right and the tail tank at the left prior to assembly.

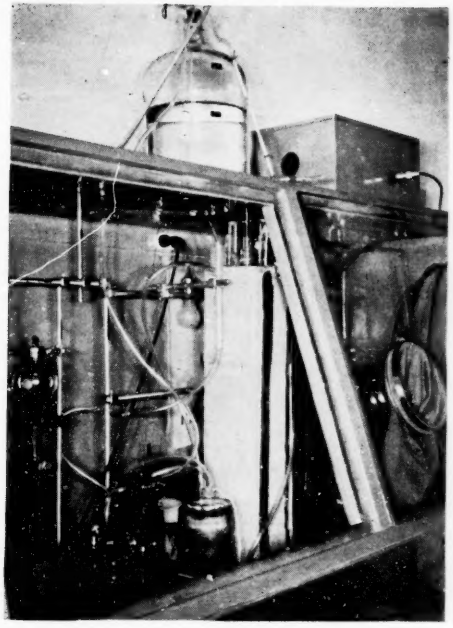

FIG. 3. A view of the model aquifer at the beginning of the experiment.

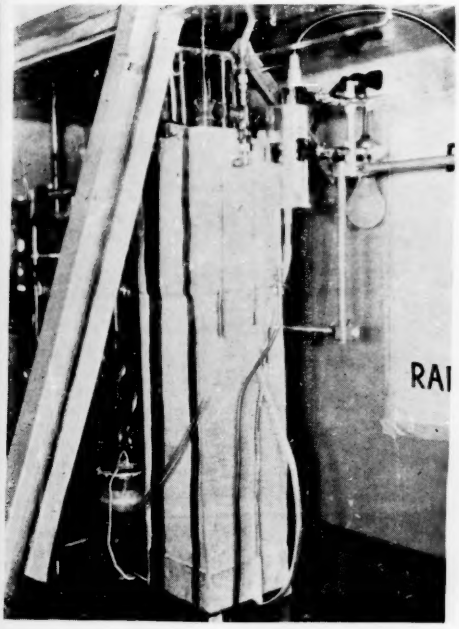

FIG. 5. Right side of the experimental block showing standpipe and overflow tubes.

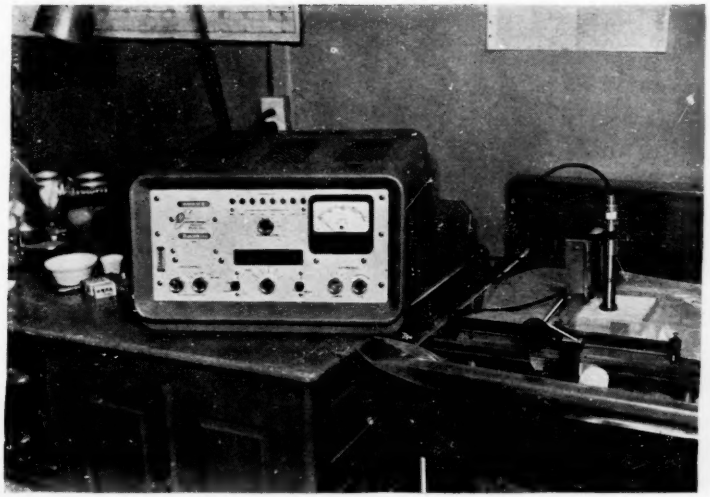

FIG. 9. Comparator used for making radioactivity measurements.

given a dose of 1320 r in a 1 day period, with a new group of plants being irradiated each day.

It was found that abundant endosperm changes in corn could be induced by radiating plants for 1 day with 1320 r rather than by use of prolonged chronic radiation. Hence it is not necessary to have a large field where many plants could be grown to maturity. With a limited time exposure of plants, a much smaller field is adequate. Even a small field can accommodate a comparatively large number of plants for 1 day, and a new lot of plants can be treated on each subsequent day, if desired. Further, since the plants are grown in soil in pails rather than in the ground, the field can be paved, thus facilitating the movement and care of experimental plants.

BLANDY RADIATION FIELD

With these facts in mind, the radiation facility at the Blandy Experimental Farm was designed. It consists of a circular pit 30 ft in diameter with a 6 ft retaining wall, behind which an earthen embankment rises to a height of 12 ft (Fig. 2). Entrance to the radiation area is through a 10 ft wide alley. Sixty feet from the center of the pit, across the end of the entrance alley is a 12 ft high earthen embankment to intercept the horizontal beam of radiation that emerges through the entryway. A sky-shine shield intercepts the vertical beam of radiation. This shield consists of an oak table 80 in. square, holding three tons of solid concrete blocks, erected over the radiation machine as is shown in Figs. 1 and 4.

The entire radiation field (approximately 1 acre) is enclosed by a 7 ft security fence. The control house is located in the fence at one corner of the field, 100 ft from the radiation machine. Entrance to the radiation facility is through the control house. Also there is a padlocked vehicle gate, in the security fence, which can be opened only from the inside.

Drawings of the radiation area show contour lines of the earthen embankment (Fig. 2), a close-up of the center of the field (Fig. 3) and a cross-section of the field (Fig. 4).

The radiation machine is patterned after the one in operation at Brookhaven National Laboratory. Basically it consists of a 2 ton lead pig (shipping container), 19 in. in diameter by 28 in. high, on which is bolted a 9 ft long stainless-steel mast of four inches inside diameter in which the source is raised and lowered. The stainless-steel in the mast screens out all the beta rays but not the gamma rays. At present the machine is designed to take $1\frac{1}{4}$ in. O.D. $\times$ 9/16 in. I.D. cobalt ring sources. An 8 in. source can be loaded. If necessary the source holder and shielding plug could be adapted to use a cesium-137 source.

The source holder and shield plug are lifted by an electromagnet which is connected to the stainless-steel cable. Since this electromagnetic type of connection is considered "fail safe" it is not necessary to add a mechanical cable cutter to lower the source in case of mechanical failure.

The lifting cable runs from the electromagnet, out of the top of the mast, and then down to a pulley mounted on the top of the sky-line shield, from there to a pole set at the edge of the pit, and then overhead to a windlass in the control house. A microswitch, to indicate that the source is in the down position, is mounted on the top of the mast where it is actuated by a "mole" clamped to the cable. The up position of the source is indicated by markings on the cable where it enters the control house.

The electrical controls of the machine are simple in design. As the electromagnet operates on 12 V d.c., this voltage is used for all controls and interlocks. A battery eliminator keeps the 12 V 100 A/hr batteries charged. Thus, if there should be an interruption of line power the machine would continue to operate for some 50 hr.

The electrical controls consist of a microswitch on the door from the control house into the radiation field and one on the vehicle gate. These two switches are connected

VOL. 10 1961

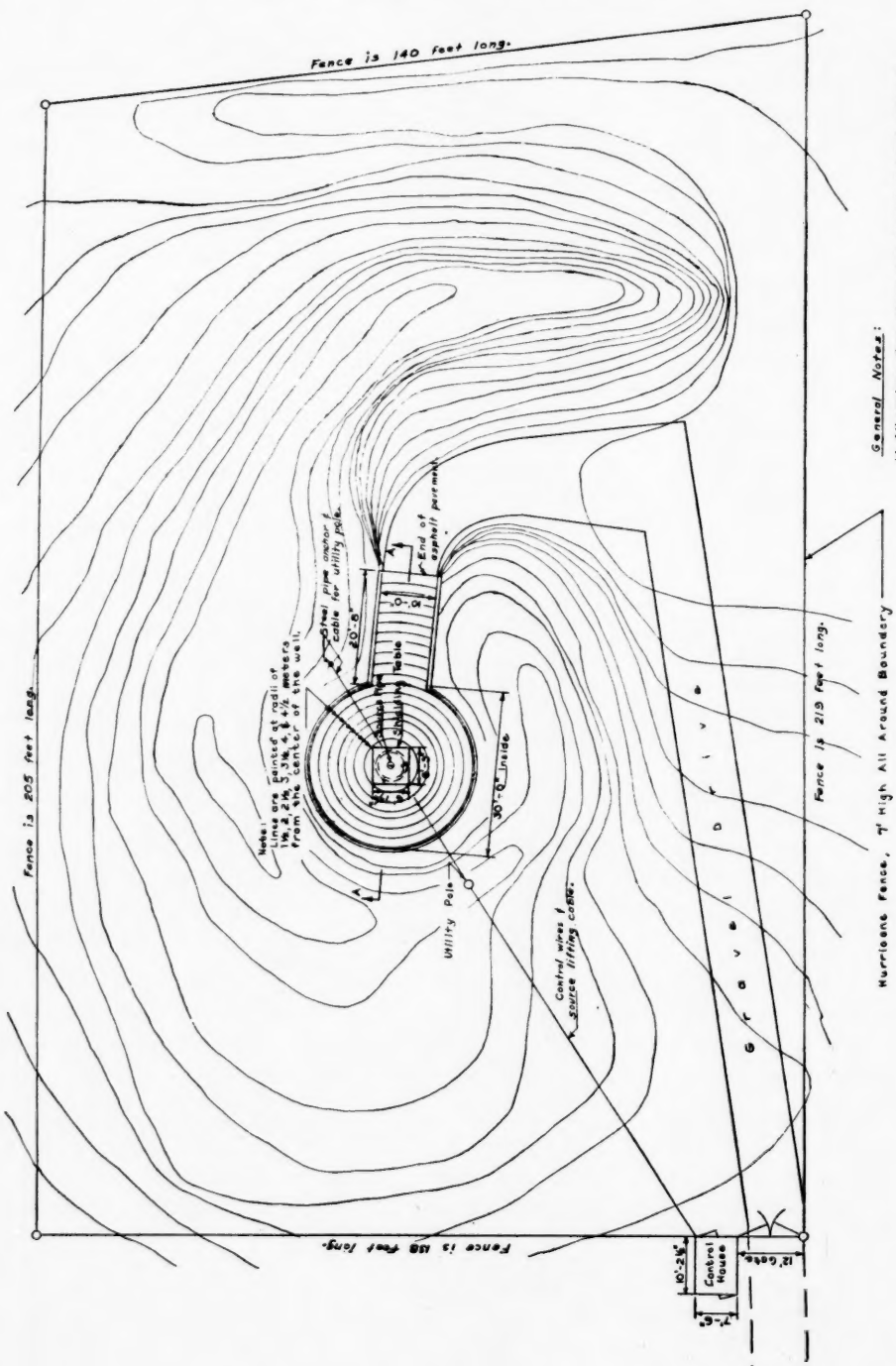
Fence is 140 feet long.
Fence is 205 feet long.
Fence is 150 feet long.
Fence is 213 feet long.
Hurricane Fence, 7' High All Around Boundary
General Notes:
1. All contour lines shown are spaced at 1 foot intervals.
2. Floor of pit and entry ramp are paved with asphalt.
Steel pipe anchor & Cable for utility pole.
End of asphalt pavement
Utility Pole
Control wires & source lifting cable.
Control House
Grade Level
Notes: Lines are numbered at radii of 5, 10, 15, 20, 25 & 30 feet from the center of the well.

FIG. 2. Drawing of Blandy Radiation Field, showing location of Co^{60} machine, radiation area with concentric circles at one-half meter intervals, control house and entryway to radiation pit. Contour lines at 1 ft intervals show earthen embankments to intercept radiation.

VOL. 10 1961

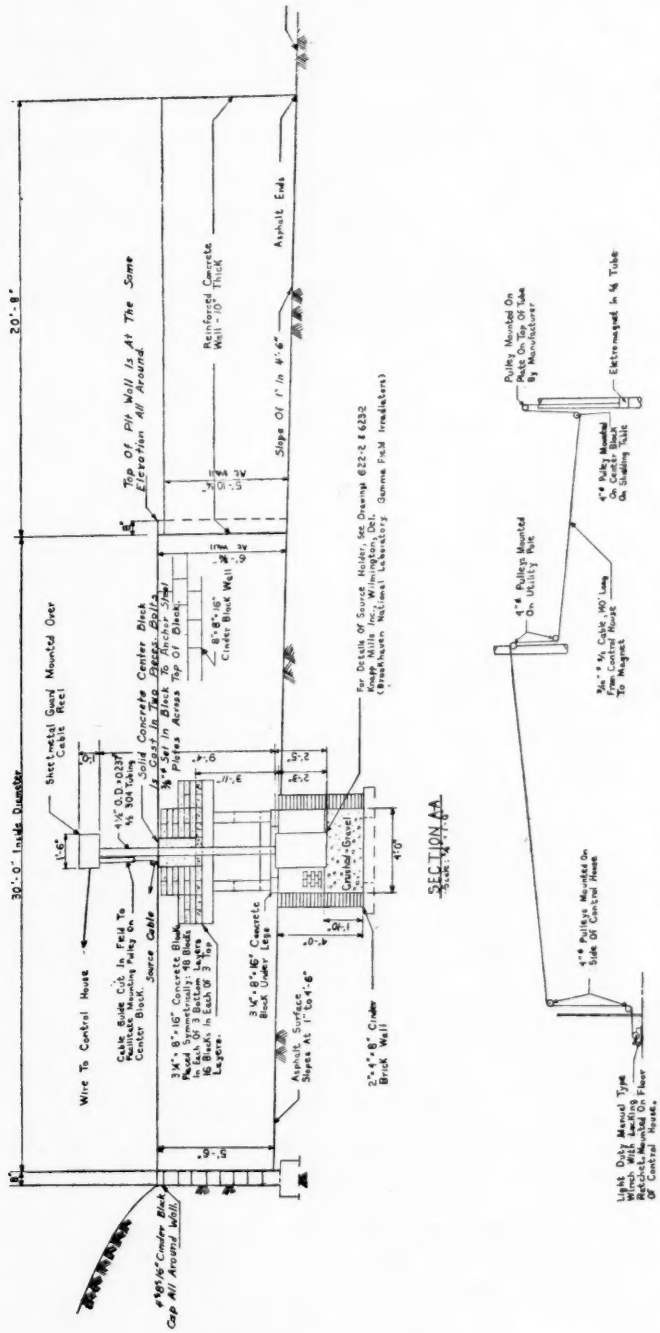
30'-0" Inside Diameter
20'-8"
Top Of Pit Wall Is At The Same Elevation All Around
Reinforced Concrete Wall - 10" Thick
Asphalt Ends
Slope Of 1" In 4'-6"
Wire To Control House
Sheet-metal Guard Mounted Over Cable Reel
Cable Built Up In Field To Facilitate Mounting Pulley On Center Block. Source Cable
1/4" O.D. 0.023" Wall 304 Tubing
Solid Concrete Center Block Is Cast In Two Parts Over Top Of Block
3/8" Set In Block Plates Across
8"-8"-16" Cinder Block Wall
For Details Of Source Holder, See Drawings 622-2 E 6232 Hood Nuclear Corporation, Inc. (Brookhaven National Laboratory Gamma Field Irradiators)
3'4"-8"-16" Concrete Block Placed Symmetrically: 48 Blocks In Each Of 3 Bottom Layers. 16 Blocks In Each Of 3 Top Layers.
3'4"-8"-16" Concrete Block Under Legs
Asphalt Surface Slopes At 1" To 4'-6"
2'-4"-8" Cinder Brick Wall
Crushed Gravel
4'6"
SECTION AA
Scale: 1/4" = 1'-0"
#8 5/16" Cinder Block Cap All Around Wall
Light Duty Manual Type Winch With Locking Ratchet, Mounted On Floor Of Control House.
4"-8" Pulley Mounted On Side Of Control House
4"-8" Pulley Mounted On Utility Pole
3/16" 7x7 Cable, 140' Long From Control House To Magnet
Pulley Mounted On Plate On Top Of Tube By Manufacturer
Extravasyed In 1/4 Tube
4" Pulley Mounted On Center Block On Shielding Table

FIG. 3. Details of center of radiation pit showing location of Co^{60} machine, construction of dry well and also "sky-shine" shield.

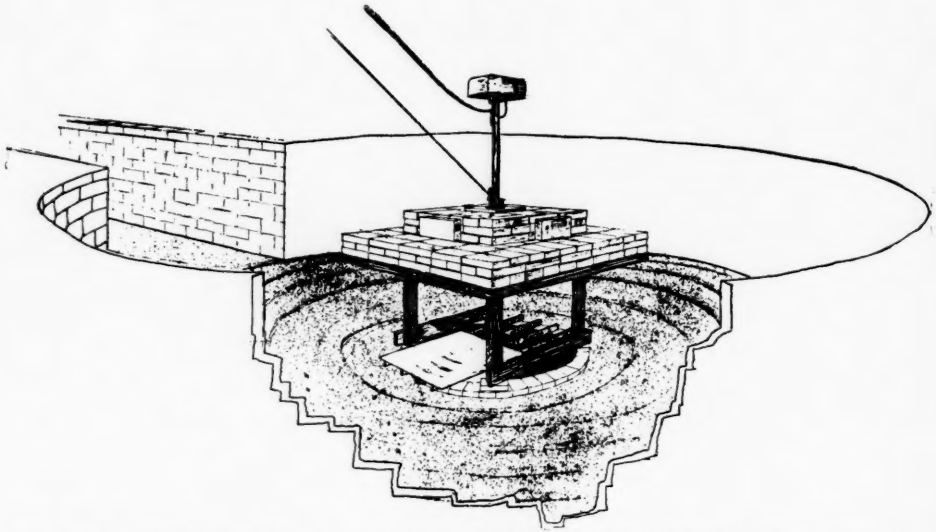

FIG. 4. Cutaway schematic drawing of center of radiation field, showing sky-shine shield, dry well and entry way. Circles on masonite board surrounding mast are used in placing small samples to receive intense radiation.

in series with the operating coil of the relay which sends power to the electromagnet when the door and gate are both shut. Indicator lights are connected to contact points of the relay to indicate if the door and gate are open or closed. The microswitch at the top of the mast is connected to an indicator light and a push switch which operates the electric door latch. Thus the door into the radiation facility cannot be opened until the source is down. The handle of the windlass is provided with a padlock; also a fuse in the 12 V line may be removed to prevent operation of the machine when anyone is in the radiation area.

In operation the source is raised to a height of 25 in. which is about half-way between the top of the pig and the bottom of the sky-shine shield. In this position the direct gamma rays from the source are intercepted by either the sky-shine shield or the earthen embankments so that comparatively little radiation escapes. At the control house, with the 200 c source in operation, the level of radiation is approximately 2 mr/hr. The facility has been used for three summers, and film badges worn for personnel monitoring have always shown zero readings.

OPERATING PROCEDURE

The control house is locked at all times. This is especially important when radiation is present. To enter the field, after unlocking the control house, the operator proceeds first to take a reading on the survey meter and record the amount of radiation present while the source is in the raised position. This usually does not exceed 2 mr/hr.

The next operation is to unlock the winch and turn it to lower the source into the lead shield in the center of the field. Two diagonal green lights on the control panel indicate that the source is down. In addition, a zero reading on the survey meter will show no radiation present.

It is then possible to open the door leading into the radiation field. As the operator goes into the field he carries a survey meter in a complete circle around the radiation machine to make sure that no

radiation is present. During 3 years of operation the mechanism has worked perfectly so that no measurable radiation was apparent while the source was in the down position.

Once the inner door of the control house is opened the vehicle gate may be opened from the inside, since the padlock on the gate is not accessible outside the fence.

Plants are carried into the radiation field by truck and are placed at the desired distances from the radiation machine. Plants that have just been irradiated are, of course, removed at the same time. Normally the field is in operation 23½ hr/day, with ½ hr being taken out for changing and watering plants. An accurate record is kept of the amount of time the source is down, also of the readings of the survey meter when the radiation source is in operation and when the source is in a down position.

VOL. 10 1961

COST OF THE BLANDY RADIATION FIELD

TABLE 1. Expenses involved in construction of radiation field at the Blandy Experimental Farm (in dollars)

Bulldozing, building hills, grading, etc., at pit		552
Retaining walls, pit and entryway materials and labor		1012
Dry well for source—digging and walling		194
Paving—pit and entryway		271
Control house, 7 ft 6 in. × 10 ft 2½ in.		
Excavating and concrete base	123	
Building	230	353
Sky-shield		
Construction	95	
Engineering advice and aid	137	232
Gravel and shale—around pit for drainage and for entryway and road		150
Electric setup		
Wiring in control house, line to control house, control house to pit, etc. (complete)		555
Fence—7 ft woven fencing, with gate (692 ft)		2012
Signs		51
Labor around pit		40
Expenses in connection with Co^{60} machine		
Shipping	111	
Placing in dry well	10	121
Miscellaneous		11
Total		5554

The cobalt-60 machine is the property of the Atomic Energy Commission which generously loaned it to the Blandy Experimental Farm for use in studying the effects of irradiation on growing plants. Aside from the cost of the machine itself, the other costs involved in the construction of the field amounted to $5554. The biggest single item in this was $2012 for 692 ft of 7 ft woven wire security fencing with a vehicle gate.

TABLE 2. Radiation levels at different distances from 200 c cobalt-60 source. Measurements made November 1959

Distance from source	Radiation (approximate) (r/hr)
20 cm	7000
30 cm	3300
40 cm	1900
50 cm	1250
60 cm	880
70 cm	650
80 cm	500
90 cm	400
100 cm (1 m)	310
1·5 m	150
2·0 m	81
2·5 m	54
3·0 m	37
3·5 m	28
4·0 m	21
4·5 m	17
5·0 m	14
6 m	9·5
7 m	7·0
10 m	3·5
14 m	1·8
20 m (last available row)	0·9

Although the costs will vary in different locations it may be helpful to list the various items of expense involved (Table 1).

The Co^{60} machine in the Blandy Radiation Field is used primarily to provide radiation for growing plants in an attempt to learn more about the sensitivity of various stages to radiation; also to learn more about the nature of induced changes. Long-time chronic radiation at a low level of intensity is not practical since the field is small in area and the radiation area is paved. Plants must be grown in their own containers, an entirely satisfactory procedure. As good corn plants can be produced in these pails as in the field, provided they are watered and fertilized adequately.

Nursery stock has been radiated while growing in 12 quart pails and later set in the field. Included here have been several ornamentals, as well as apple trees. Preliminary observations revealed that gymnosperms are less tolerant of radiation than angiosperms (Flory and Singleton).[10]

It is possible to irradiate nursery stock as it comes from the nursery by placing it in an "upside down" position around the shielding table which will shield the roots while radiating the tops. By this method a large amount of material can be treated before transplanting to a permanent location.

In addition to plants, seeds have been irradiated by placing them within a few centimeters of the stainless-steel mast, where they receive a rather high dose over a short period of time. Seeds of the American chestnut, *Castanea dentata*, have been irradiated with the hope of producing a strain resistant to the chestnut blight.

Table 2 shows the doses received by plants placed at different distances from the stainless-steel mast housing the Co^{60} source, also doses received by smaller samples (of seed) placed at intervals of a few centimeters from the source.

CONCLUDING REMARKS

This paper describes a simple, economical and effective radiation facility, using Co^{60} as a source. The combination of a natural hill and of artificial earthen bunkers adequately contain radiation within a 1 acre field. The facility is proving satisfactory for its intended purpose of studying the radiation effects on growing plants. In addition to genetic studies of corn, it has also been used for experimental treatments of fruit and nut trees, several bulbous plants and a variety of woody ornamental nursery materials.

The cost of the field, exclusive of the machine, was $5554. The total cost would probably not exceed $12,000. Such a radiation source will be useful for several years, since at the end of 5 years it will still be operating at approximately one-half of original strength.

Blueprints of the radiation field are available.

REFERENCES

1. Stadler L. J. *J. Hered.* **21,** 3 (1930).
2. Muller H. J. *Science* **66,** 84 (1927).
3. Stadler L. J. *Proc. Nat. Acad. Sci., Wash.* **14,** 69 (1928).
4. Stadler L. J. *Science* **68,** 186 (1928).
5. Gustafsson A. *Hereditas* **27,** 225 (1941).
6. Gustafsson A. *Hereditas* **33,** 1 (1947).
7. Singleton W. *Seed World* **86,** No. 2, 4–9 (1960); continued in No. 4, 6–10 (1960).
8. Sparrow A. H. and Singleton W. R. *Amer. Nat.* **87,** 29 (1953).
9. Sparrow A. H., Binnington J. P. and Pond V. *Bibliography on Effects of Ionizing Radiation on Plants,* 1896–1955. *Biology and Medicine.* BNL 504 (L103) (1958).
10. Flory W. S. and Singleton W. R. *Va. Jour. Sci.* **10**(N.S.), 258 (1959).

technical notes

VOL. 10 1961

Method for Autoradiography Using Individually Packaged X-Ray Film*

(*First received* 27 *May* 1960 *and in revised form* 24 *June* 1960)

Recently X-ray film has been marketed in packages in which each sheet of film is individually wrapped in light-tight envelopes.† Packaged in this manner, X-ray films are contained one in an envelope in a heavy craft-like paper sandwiched between sheets of black paper and backed with a piece of cardboard. The packages come sealed and are quite convenient for making macro-autoradiographs of plant materials.

Several procedures have been recommended for making macroautoradiographs of plants. The simplest is perhaps just to place the plant material flat against a sheet of X-ray film[1] with a piece of thin plastic material between the plant and the film to prevent plant juices from oozing onto the film and causing artifacts.[2] The plant is pressed into close contact with the film, both are wrapped in black paper, and exposure permitted. This procedure may be improved somewhat by placing the plant material between layers of "Saran wrap" which has the advantage of electrostatically adhering to itself, insuring a tight seal. The plant material in "Saran wrap" may be placed in contact with X-ray film in an X-ray film holder. The X-ray film holders allow more freedom of movement since they may be loaded in the dark and brought out of the darkroom for exposure. The "Saran wrap" will prevent liquids from oozing onto the film and if the film is exposed in the freezer, biological activity will be arrested.

Bakelite X-ray film holders are quite expensive and the inexpensive cardboard X-ray film holders that have been used repeatedly to expose film in the freezer become warped. With the new individually packaged film all operations can be performed in the light. Plant materials are sandwiched as previously in "Saran wrap" and this plastic envelope containing the plant may be fastened directly onto the surface of the film package. The film plus plant material must still be exposed in the freezer. However, the plant material being autographed is constantly visible and information relating to type of isotope, length of exposure and date placed in the freezer, etc., may be written directly onto the surface of the film package. When the film is developed the film envelope may also serve as a storage container for the exposed film. Individually packaged films are obtainable in the same sizes as other X-ray films, that is, sheets 8 × 10 in. and 14 × 17 in.

Since this method introduces several additional layers of paper between the plant materials and the X-ray film, it is unsuitable for autoradiography with weak alpha or beta emitters. Isotopes with hard betas, such as phosphorus-32 and strontium-89, or gamma emitters, such as iron-59 and zinc-65, however, may be used with little reduction in the clarity of the resultant image. Paper absorbs very little of the beta rays from P^{32} and the exposure time using the individually packaged film is the same as when the plant specimen is placed directly on the surface of the film. Care must be taken to have the plant material flat and in close contact with the film package. With reasonable care and correct exposure, macro-autoradiographs having good resolution, will result from this method. Fig. 1 shows the Saran wrapped specimen, placed on the surface of the individually packaged film, and the resultant autoradiograph.

Dept. of Plant Pathology and Botany T. W. Sudia
Institute of Agriculture A. J. Linck
University of Minnesota
St. Paul 1, *Minnesota*

References

1. Boyd A. *Autoradiography in Biology and Medicine*, Academic Press, New York (1955).
2. Chase G. D. *Principles of Radioisotope Methodology*, Burgess, Minneapolis (1959).

* Paper No. 4389, Miscellaneous Journal Series, Minnesota Agricultural Experiment Station. Research supported in part by A.E.C. Contract AT (11-1)-783.

† Individually packaged film described is manufactured by Ansco Company and Eastman Kodak Company.

Efficiencies and Photofractions of Some Commonly Used NaI(Tl) Well Crystals

(*First received* 29 *February* 1960 *and in revised form* 21 *July* 1960)

The use of thallium-activated sodium-iodide crystals of the "cylindrical well" configuration for the assay

TABLE 1. Crystal specifications

Crystal size (in.)	Well diameter (in.)	Well depth (in.)	Model No.	Crystal No.	Al wall thickness (in.)
1·75 × 2·0	0·630	1·50	SW–2*	*A*	0·015
1·75 × 2·0	0·656	1·50	7F8†	*B*	0·032
2·0 × 2·0	1·00	1·50	8F8†	*C*	0·032
3·0 × 3·0	1·00	2·25	AW†	*D*	0·032

* National Radiac, Newark, New Jersey.
† Harshaw Chemical Company, Cleveland, Ohio.

TABLE 2. Spectrometer efficiencies and photofractions

Quantum energy	Isotope	Crystal *A*		Crystal *B*		Crystal *C*			Crystal *D*		
		$\varepsilon(E)$	$p(E)$	$\varepsilon(E)$	$p(E)$	$\varepsilon(E)$	$p(E)$	$R(E)$	$p(E)$	$p(E)$	$R(E)$
0·080	Ho^{166}	0·96	1·00	0·97	1·00	0·98	1·00	0·22	0·95	1·00	0·34
0·142	Ce^{141}	0·95	0·91	0·94	0·94	0·93	0·97	0·17	0·98	0·98	0·19
0·279	Hg^{203}	0·61	0·78	0·61	0·80	0·59	0·72	0·14	0·80	0·87	0·17
0·321	Cr^{51}	0·50	0·70	0·51	0·70	0·49	0·65	0·14	0·73	0·80	0·16
0·364	I^{131}	0·47	0·63	0·48	0·64	0·45	0·62	0·13	0·68	0·74	0·15
0·411	Au^{198}	0·42	0·55	0·43	0·56	0·41	0·56	0·13	0·61	0·67	0·14
0·662	Cs^{137}	0·32	0·37	0·32	0·36	0·32	0·35	0·11	0·51	0·49	0·13
0·835	Mn^{54}	0·28	0·33	0·30	0·31	0·27	0·31	0·11	0·47	0·46	0·12
1·114	Zn^{65}	0·27	0·25	0·28	0·24	0·25	0·24	0·11	0·45	0·37	0·11
1·332	Co^{60}	0·24	0·24	0·25	0·24	0·24	0·22	0·10	0·41	0·35	0·11

of low-level activity solutions has become widespread in medical and biological tracer work. Since a large choice of crystal sizes is now available commercially in this geometry, a problem usually arises in any given application in selecting the crystal size and well dimensions that provide the best compromise between cost and efficiency. Many problems now involve multitracer techniques in which the investigator is interested in a quantitative study of the characteristic radiations of different tracer isotopes whose energies may embrace a fairly broad region (e.g. 0·05–2·75 MeV). Hence, a knowledge of the ratio of the number of gamma rays that are completely absorbed in the crystal to the total number of gamma rays that interact at least once is necessary in evaluating a detector for applications involving selective pulse-height analysis. A calculation of this ratio, called the photofraction, $p(E)$, is complicated by the variable source volumes encountered in practice, and, as a result, an empirical study of $p(E)$ as a function of crystal and sample geometry has been made.

Spectrometer system

In this investigation, four different scintillation spectrometers were used which are probably representative of the types of well-systems in most common usage today. The crystal specifications are shown in Table 1. The transducers consisted of these NaI(Tl) crystals mounted on either RCA 6655 or DuMont 6363 photomultipliers which, in turn, were used in conjunction with a suitable dynode voltage divider network and cathode follower. Pulses from these units were delivered to a type A-61 linear amplifier and an Argonne-type 256-channel analyzer which recorded spectral data in either digital or chart form. The counting rate was monitored at the output of the linear amplifier in order to obtain a total efficiency determination of each system for the gamma-ray energy under study. These efficiency measurements were also made with the use of the integrated spectrum and the known time of collection on the analyzer. The former was in each case complemented for the contribution due to the laboratory background, while the latter was automatically corrected for the analysis dead-time of the system.

Sample preparation

The efficiencies and photofractions of the four crystals were studied at gamma energies of from 0·080 to 1·33 MeV by use of liquid samples prepared from aliquots of calibrated standard solutions. These solutions were either obtained commercially or prepared and calibrated in our laboratory with standard (4π, β–γ coincidence, or scintillation) counter techniques. The gamma-ray activity was known in each case to an accuracy of ± 3 per cent.

VOL.
10
1961

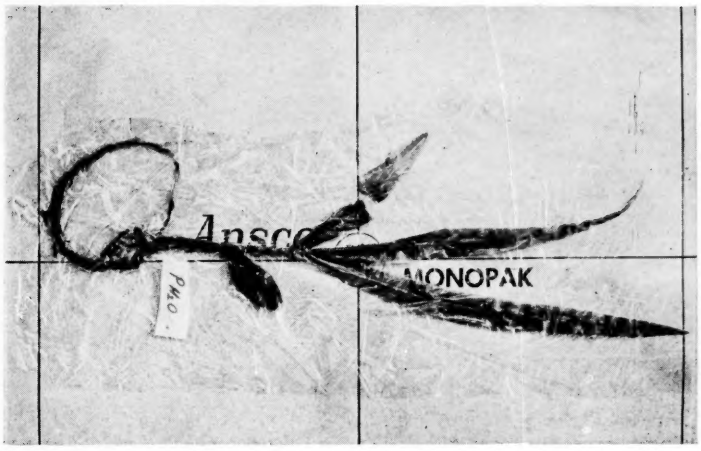

FIG. 1(a).

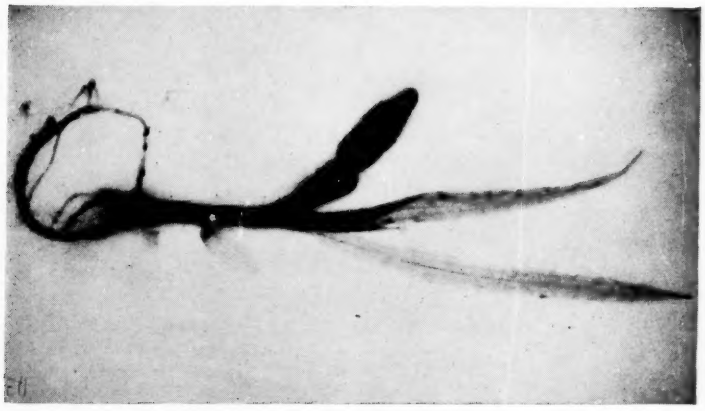

FIG. 1(b).

FIG. 1(a,b). Autoradiography using individually packaged X-ray film. At the top (Fig. 1(a)) is the plant material positioned and taped onto the surface of the film package. A corn seedling has been supplied with P^{32} to the youngest leaf. Before autoradiography the plant was wrapped in "Saran wrap". Below (Fig. 1(b)) is the autoradiograph

[See p. 55

VOL. 10 1961

At least two determinations were made at each energy for the values shown in Table 2.

Experimental

Due to the variation in the crystal-well diameters and the need for measuring these parameters under reproducible geometries, an attempt was made to use sample containers normally employed for such applications. Suitable absorbing liners were used where necessary to ensure that the detection in the crystal of beta particles emitted from the source did not affect these data. No corrections for bremsstrahlung production were required, as only low Z materials surrounded the sample volume. In all cases shown, quantum radiation absorption in the test tube or liner could be ignored. Crystal A was studied with a standard 10 ml Lusteroid* centrifuge tube (0·018 in. wall-thickness) having a protective polyethylene liner inside the crystal well. Crystal B was studied with a 20 ml Lusteroid* centrifuge tube. Standard 14 ml polyethylene containers, 0·875 in. in diameter with 0·031 in. wall thickness† and of varying depth, were used with the 1 in. diameter wells of crystals C and D. Since this investigation was originally initiated to permit the quantitative analysis of complex spectra involving fission-product activities emitting quantum radiation of widely differing energies, the efficiencies quoted in Table 2 are given in terms of the quantum-detection efficiency, $\varepsilon(E)$, and not in terms of the "isotope" efficiency that has been used as a criterion in earlier papers on this subject.[1–4] The isotopes used in this study are listed in column 2 of Table 2 and represent a useful list of sources that provide a good range of uncomplicated spectra for such a study. In the cases of the complex emitters used, i.e. I^{131} and Co^{60}, the spectra of the radiations of interest were deduced from the gross spectra with the use of response functions obtained or interpolated from sources demonstrating unique spectra. All of the measured efficiencies shown are on the basis of a 1 ml total sample volume. The experimental data were corrected for any pulse-resolution losses in the spectrometer system by the use of the automatic dead-time correction features of the multichannel analyzer. Effects arising from the summation of cascade gamma rays in the complex emitters were corrected by the usual subtraction method.

The experimental photofraction, i.e. the ratio of the number of events leading to counts under the peak to the total number of interactions, was found at each energy using the spectrum plotted from the digital information obtained from the analyzer. For the purpose of improving the applicability of these data, the total spectrum is considered here as the sum of the areas under the photoelectric peak, its associated iodine X-ray escape peak, the Compton distribution and the backscatter peak. It does not, however, include any contribution from the characteristic X-rays present in several of these sources arising from either K-capture or internal conversion accompanying the decay under study, or from the lead fluorescent X-rays originating in the surrounding shield. It should be noted that for quantum energies below 150 keV, where the corrections for iodine X-ray escape become significant, the effects of escape in the well geometry are very much less than those encountered for the solid right-cylindrical geometry.[5,6] Due to the "low" resolution of the NaI(Tl) spectrometers considered, the effect of X-ray escape is no longer significant at higher energies and, in fact, may be ignored in most counting applications. The area under the photopeak was determined by extrapolation of the low-energy edge of the photopeak, treated as a Gaussian distribution, to the underlying Compton distribution. The experimental values of $\varepsilon(E)$ listed in Table 2 are given with errors of ± 3 per cent, while the photofraction figures are quoted to ± 1 per cent for these crystals. The resolution figures, $R(E)$, quoted for crystals C and D are indicative of the performance to be expected from such scintillators. It is known, of course, that these will vary appreciably with the quality of the crystal-photomultiplier combination used.

Volume effects

Since a wide range of sample volumes is usually encountered in applications involving the use of these high-sensitivity scintillation spectrometers, a study of the variation of both $\varepsilon(E)$ and $p(E)$ with volume was made for all four crystals at various energies. As one would expect, the diminution of efficiency with volume is only slightly energy-dependent. The curves of Fig. 1 show the relative efficiency for quantum detection with a variation in volume of 1–10 ml with crystal A, 1–18 ml with crystal B, and 1–25 ml with crystals C and D. Aliquots of standard solutions of Cs^{137} and Zn^{65} were used to obtain these curves.

The variation of photofraction with volume, at a gamma energy of 0·662 MeV, is presented for all four crystals in Fig. 2. Curves C* and D* represent the same variation at an energy of 1·114 MeV for crystals C and D. This variation is quite energy-dependent, as $p(E)$ represents the probability for total absorption of the gamma ray in the crystal. This probability for the cylindrical source geometry normally encountered demonstrates only a small volume dependence for sample volumes very much larger than that of the crystal well. The curves of

* International centrifuge tube Nos. 655 and 657.

† Nalge Co. Inc., No. 45.

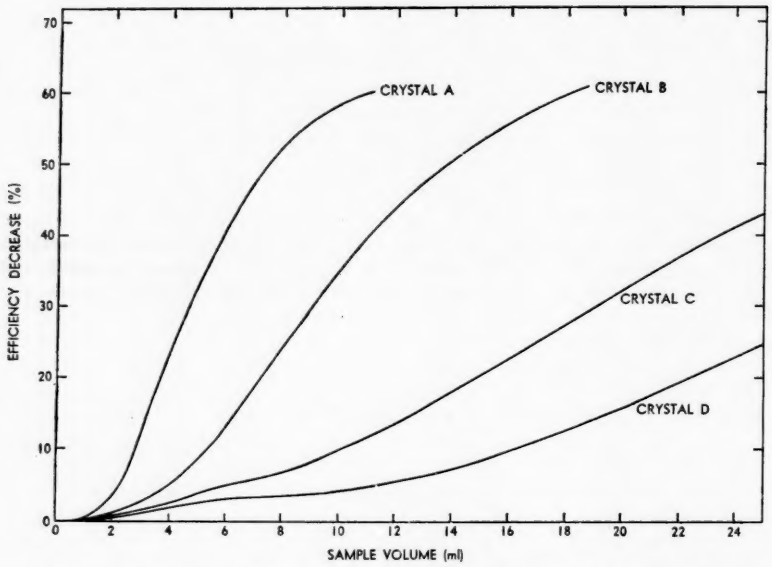

FIG. 1. Variation in efficiency of four NaI(Tl) well crystals with sample volume.

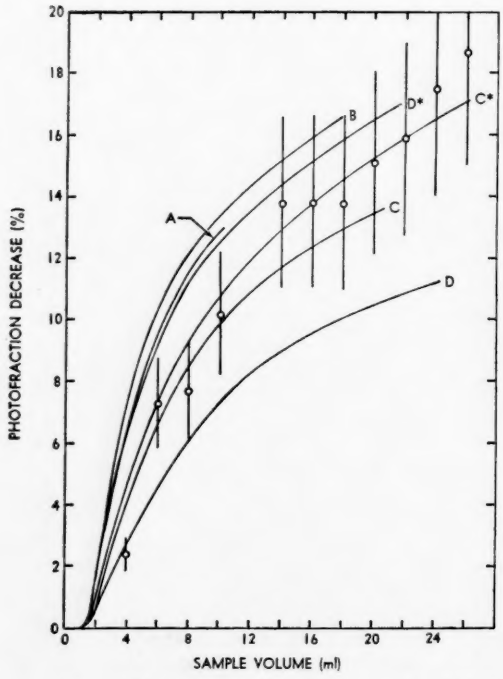

FIG. 2. Variation of photofraction with volume.

Fig. 2 are not accurate enough to use in correcting spectra for variation of sample volume; they are included to show a trend only. Precise measurements of this small effect are difficult to make as indicated by the error bars on the data points plotted for case *C**.

Efficiencies for I^{131}

Most applications of these spectrometers will routinely involve the assay of the radiations from I^{131}. Hence, the four crystals, when used in conjunction with a conventional single-channel analyzer accepting only the pulses within a window embracing the 364 keV peak, have been compared with respect to their over-all detection efficiencies. The window width was 20 per cent of the voltage corresponding to the peak. The results are shown in Table 3 below, and the values of V_w listed in column 2 represent the fraction of the 364 keV photopeak actually included within the discriminator window. These measurements were conducted with a 4 in. thick lead (4π) shield around the counters in order

TABLE 3. Spectrometer efficiencies for I^{131}. Sample vol. = 1 ml

Crystal	V_w	Efficiency	A_{min}
A	0·66	16·4 %	60 $\mu\mu$c
B	0·88	20·8 %	42 $\mu\mu$c
C	0·92	18·7 %	55 $\mu\mu$c
D	0·75	13·7 %	113 $\mu\mu$c

VOL. 10 1961

that A_{min} (the minimum detectable activity), arbitrarily defined as that for which the signal to background ratio is unity, for each spectrometer system with the same "window" width could be evaluated in a "normal laboratory" radiation environment. Minimum tracer isotopes for other energies and sample volumes may be ascertained in a similar manner using the data of Tables 2 and 3 and Fig. 1. The geometries used with these 1 ml liquid samples were, of course, quite unfavorable for obtaining optimum efficiencies with crystals *C* and *D* because of their large well diameters. (Crystals having smaller-diameter wells are obviously more efficient.)

Light losses in large well-type crystals

The resolution of a scintillation-type detector is known to vary approximately inversely as the square root of the number of photoelectrons in the pulse arising at the photocathode of the photomultiplier. The number of light quanta incident upon the photocathode that arise from the detection of a particle of given energy will depend upon the point of interaction of the incoming gamma ray in the scintillator as well as the reflectivity of the coating (MgO or Al_2O_3) surrounding the peripheral surfaces of the crystal. Caution should be used in the interpretation of the energy measurements and spectra obtained with large bored NaI(Tl) crystals, as exemplified by crystal *D*. The high probability of the summation of pulses arising from cascade gammas which, due to the approximately 4π detector geometry, are "simultaneous" in time has been used to advantage in some applications.[7] In most cases, however, this perturbation of the spectra, as well as that photopeak degradation arising from variable light loss in the scintillator, render "deep" well crystals of limited usefulness in assay work where the spectrum analysis of complex samples is necessary. The deleterious effect of this smearing is demonstrated by the low-efficiency figure shown for the 3 in. crystal in Table 3.

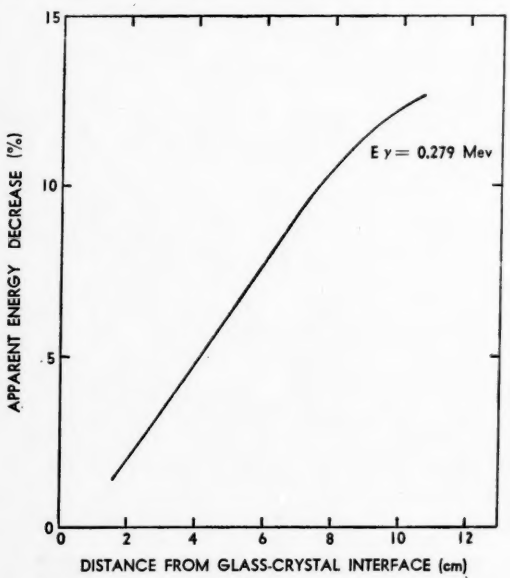

FIG. 3. Apparent energy decrement as a function of source position in crystal *D*.

The magnitude of this latter effect was demonstrated in the case of the large 3 in. diameter crystal through illumination with a finely collimated beam of 0·279 MeV (Hg^{203}) gamma rays placed (1) along its longitudinal axis of symmetry at varying distances from the bottom of the well and (2) outside the well at varying distances between the planes defined by the bottom of the well and the glass–crystal interface. Fig. 3 demonstrates the apparent energy decrease as a function of source position measured from the glass-crystal interface. This energy decrement arises from the increased light losses suffered by scintillations subjected to reflection in the annular portion of the crystal. These results indicate that the annular geometry of a "through-type" well would yield photopeaks of greater symmetry and uniqueness than the "deep-well" geometry (represented in crystal *D*) without a serious loss in the total counting efficiency of the system.

The same effect can lead to apparent nonlinearities of as much as 10 per cent in similar well-type spectrometer systems in the low energy region (<0·50 MeV) most useful for tracer studies. In the worst cases, monoergic gamma rays will give rise to two unresolved photopeaks, the least prominent of which will appear on the high energy side of the main photopeak and represent interactions occurring at sites favorable to efficient light collection at the photocathode. The lower lying peak then consists of those events resulting from interactions at less favorable sites, particularly at some distance in the crystal above the plane defined by the bottom of the well. Similar results have been observed in crystals having through-holes bored in the side—a geometry most commonly used in wire scanners. In this case, almost completely resolved dual photopeaks are observed corresponding to events occurring in the upper and lower portions of the cylindrical crystal. It is felt that an awareness of this behavior of bored crystals is important, if a realistic interpretation of such spectra is to be made.

Conclusion

If the investigator possesses a knowledge of the complexity of the gamma-ray spectrum present in

the sample to be assayed, and employs good techniques[8,9] in a determination of the peak area (or total count in a pulse-height analyzer window embracing a known fraction of the photopeak of interest), then quantum intensities may be determined by use of the spectrometers described here with excellent accuracy over a wide range of sample volumes and quantum energies. The quantum intensity, $N(\gamma)$, may be expressed as

$$N(\gamma) = \frac{A(E)}{p(E)\varepsilon(E)\alpha},$$

where $A(E)$ is the peak area in the units of $N(\gamma)$, $p(E)$ and $\varepsilon(E)$ are the photofractions and efficiencies, respectively, and α is the correction factor for gamma-ray absorption in the source, vial, and crystal container. The photofraction and efficiency values may be interpolated from the data of Table 2 and Figs. 1 and 2. Fig. 2 is applicable only if small volumes are used; for volumes larger than a few milliliters, the $p(E)$ for that particular geometry must be measured. The total activity present may then be determined from a knowledge of the role played by that particular radiation in the isotope of interest.

Acknowledgements—The authors would like to acknowledge the assistance of the Health Physics Group of Convair-Fort Worth for their loan of the large well crystal. This work was supported by the U.S. Air Force.

Convair, S. V. NABLO*
A Division of General Dynamics Corp., T. C. MARTIN
Fort Worth, Texas, U.S.A.

References

1. BORKOWSKI C. J. ORNL 1160 (April 1952).
2. BASKIN R., DEMOREST H. L. and SANDHAUS S. *Nucleonics* **12,** 46 (1954).
3. MACINTYRE W. J. and CHRISTIE J. H. *J. Lab. clin. Med.* **50,** 653 (1957).
4. HINE G. J., BURROWS B. A., APT L., POLLYCOVE M., ROSS J. F. and SARKES L. A. *Nucleonics* **13,** 23 (1955).
5. HETTINGER G. and STARFELT N. *Nucl. Instrum.* **3,** 25 (1958).
6. AXEL P. *Escape Peak Correction to Gamma-ray Intensity Measurements Made with Sodium Iodide Crystals.* BNL 271, (September 1953).
7. SHAPIRO P. and HIGGS R. W. *Rev. Sci. Instrum.* **28,** 939 (1957).
8. HEATH R. L. and SCHROEDER F. *The Quantitative Techniques of Scintillation Spectrometry as Applied to the Calibration of Standard Sources.* IDO-16149, (25 April, 1955).
9. *Measurements and Standards of Radioactivity.* Nat. Res. Council No. 573 (1958).

* Present address: High Voltage Engineering Corp., Burlington, Mass.

VOL. 10 1961

E. BRODA: **Radioaktive Isotope in der Biochemie.** Franz Deuticke, Vienna, 1958. viii + 326 pp., 86*s* 6*d* (49 DM).

THIS is a scholarly work which should be indispensable to biochemists who are interested in using radioactive tracers in their research. It summarizes the immense amount of published work in this field in a critical fashion, and demonstrates how labelled compounds have become one of the most important research tools in biochemistry. Dr. Broda has a good grasp of his subject, and gives a clear exposition of both the techniques and their exploitation.

The first third of the book (Chapters 1–9) is devoted to a discussion of principles, methods and techniques. Isotope effects, radiochemical syntheses, activation and isotope dilution analysis are among the many subjects treated. A thorough survey of methods of measuring radioactivity, particularly weak beta radiation from C^{14} and tritium, is included to aid those unfamiliar with counting techniques. Methods for determining the stable isotopes H^2, N^{15} and O^{18} are not described, though the results obtained with these tracers are extensively used in later chapters. Chapters 6 and 7, on radiation chemistry and radiation biology respectively, are the least satisfactory in this section, as they fail to provide an adequate picture of these two rapidly developing subjects. For example, the difference in ion density produced by alpha and gamma rays is nowhere mentioned. The omission of these two chapters would not harm this work, as they are only referred to once in the sequel.

In the remainder of the book, Dr. Broda has ranged far and wide over topical problems in biochemistry. Inorganic biochemistry is dismissed in twenty eight pages, while organic biochemistry is allotted one hundred and fifty. This seems a little unbalanced in view of the number of tracers available for the former subject compared with H^3, C^{14}, P^{32} and S^{35} for the latter, but probably corresponds with the current allocation of research interests. In particular, the reviewer missed any reference to the problem of the function of metals in enzymes, where tracers have played an important part, as in establishing that molybdenum is essential for nitrate reductase.

Chapters 11–16, on organic biochemistry, cover all the main subjects in this field, and include important summaries of recent work on photosynthesis and on biosynthesis of nucleic acids. Both these topics have experienced phenomenal new developments since the introduction of tracers. One cannot but admire Dr. Broda's skill in reviewing so much data in so many varied fields. A minor criticism is that Chapter 13 (on fats) might precede Chapter 11, (on phosphorylation and photosynthesis), as its subject matter involves less advanced biochemistry and fewer tracer species.

The quality of both paper and illustrations is good, and the type is a model of what it should be. Dr. Broda keeps his sentences short so that his German is easy for a foreigner to read. One final criticism involves the footnotes. References are given on each page, which wastes some space through repetition, and the system of numbering is occasionally confusing. There is an author index and a subject index, and the book is good value for its price.

H. J. M. BOWEN

A. GERLOF HOMAN and RICHARD R. TARRICE: **Radioisotopes at Work for Agriculture.** Stanford Research Institute, California, 1959. 200 pp., $3.50.

THIS volume is the result of a request from the United States Atomic Energy Commission that the Stanford Research Institute should prepare a report on the application of radioisotopes in agriculture. The most interesting parts of the report are statements, prepared by a number of eminent consultants, which occupy three quarters of the volume. Present achievements and possible future application of radioisotopes in a wide range of agricultural studies are discussed. Together, these papers provide a comprehensive review of the very numerous uses of radioactive tracers which have caused them to become standard procedures in virtually all major laboratories concerned with the physiology of plants or animals, with the problems of soil and with protection from disease.

The Stanford Research Institute did not, however, let the matter rest on this impressive qualitative assessment. It attempted also to estimate "the probable economic benefits", that is to say the profit in dollars. The reader may feel that at this point the Institute attempted a journey into territory which angels would very reasonably fear to tread. No one, to the reviewer's knowledge, has attempted an evaluation of the economic benefit in biological research which has so far accrued from the use of

partition chromatography; earlier generations do not appear to have attempted any such calculation for the microscope.

The Stanford Research Institute, however, has concluded that, during the next 20 years, a minimum estimated saving of 180 million dollars a year will be attained through the use of radioisotopes in agriculture. The credentials of part of the data on which this estimate rests are indicated by the statement, "if, as a result of knowledge gained (by tracer investigations) the phosphate fertiliser bill has been reduced by 10 per cent, a not unlikely figure, then this item alone has resulted in a saving of 15 million dollars a year for at least the last five years." No one with knowledge of this subject can doubt the value of tracer methods; but, equally, it cannot be disputed that many of the basic concepts on which progress has depended had been enunciated and were already giving rise to considerable benefit before the research worker's task was eased by tracers. The dollar credit given to tracers in this report implies, however, the unstated assumption that had tracers not become available there would have been no progress in fields where they are now of use. The spectacular progress of agricultural research in the United States in the half-century before the first large tracer experiment was undertaken, shows the ineptness of any such premise.

Thus, while grateful to Stanford Research Institute for bringing together so much information of the types of research in which tracers are now employed, the reader may regret that the Institute did not call a halt when it could show that radioactive isotopes had become an almost universal tool in nearly all the main branches of agricultural research. This conclusion would surely have been both sufficient and amply justified.

R. Scott Russell

Richard R. Tarrice and Mark S. Blumberg: **Radioisotopes in Medicine.** US. AEC Research and Development Report SRIA-13, Office of Technical Services, Department of Commerce, Washington D.C., 1959. 180 pp., $3.

During 1958, the value of radioisotope shipments from production centres in North America and the United Kingdom alone was about $5,000,000 and a high proportion of these were used in medicine. The immediate purpose of the present study was to obtain data which would indicate the overall pattern of utilization of radioisotopes in medical research, diagnosis and treatment in the United States of America. The results obtained have provided the basis for some tentative predictions, for example that the current investment in isotope equipment by United States hospitals of some $13,000,000 can be expected to exceed $40,000,000 by 1965, but the authors strongly emphasize that reliable estimates of future tends require further surveys of this type at suitable intervals.

The report relies on shipment figures provided by the major isotope production centres as well as information relating to licensed medical users provided by the U.S. AEC. The main feature of the document, however, is the detailed analysis of the answers to a comprehensive questionnaire sent to over thirteen hundred doctors and institutes who between them reported on over five thousand isotope administrations given during a one-week sample period. The analysis indicates the isotopes most used, dosage; whether for diagnosis, therapy or research, the nature of the diseases being studied or treated and so on—in fact there are sixty-seven tables including those dealing with the use of teletherapy units.

In some cases the data provide authoritative confirmation of the impressions which an individual worker might form on the basis of personal experience. Thus, I^{131} accounted for 85 per cent of the clinical administrations and 67 per cent were for thyroid diagnosis. Even so, of the I^{131} purchased, only 28 per cent is actually administered to patients, the remainder being lost by radioactive decay. (This figure is probably very different in those countries where the user can obtain the isotope on the day he requires it and is only charged for the amount received as distinct from the amount shipped.) On the other hand, it may come as a surprise to many readers to learn that some 30 per cent of the isotopes used clinically in the United States of America are imported from other countries.

It is possible that an economist or statistician might regard this document as good light reading. Most others will find it heavy going. Nevertheless it contains the sort of information which is essential to those who are concerned with future plans relating to any aspect, including finance, of medical isotope services; either on a national scale or in a single hospital.

It is clear from the marked geographical variations in the level of medical isotope services within the United States of America itself that the data in this report can be of little quantitative significance to other countries, particularly if one takes into account sociological factors and variations in the pattern of endemic disease, especially thyroid disorders. There is a strong case for the carrying out of regular surveys of a similar nature in countries other than the United States of America; and the present report is a particularly valuable one in that it shows how the necessary data can be obtained and interpreted.

N. Veall

books received

ROBERT HERMAN and ROBERT HOFSTADTER: **High-Energy Electron Scattering Tables.** Stanford University Press, 1960. 278pp., $8.50.

VOL.
10
1961

international news

The Isotopes and Radiation Division of the *American Nuclear Society* is actively soliciting well-qualified members from abroad. The Division, with over 600 members is the largest in the ANS. Primary areas of interest in nuclear science and engineering are: radioisotope research, production and use; radiation applications; and associated equipment. Member disciplines include: industry, education, biology and medicine and health physics. Information on the Society and membership details may be obtained from Mr. OCTAVE J. DU TEMPLE, *American Nuclear Society*, 86 East Randolph Street, Chicago 1, Illinois, U.S.A.

VC
1
19

International Journal of Applied Radiation and Isotopes, 1961, Vol. 10, pp. 65–71. Pergamon Press Ltd. Printed in Northern Ireland

A Beta–Gamma Ionization Chamber for Substandards of Radioactivity—I

Uses and Calibration

J. W. G. DALE, W. E. PERRY* and R. F. PULFER†
National Physical Laboratory, Teddington, Middx.

(*First received* 5 *May* 1960 *and in final form* 20 *October* 1960)

VOL. 10 1961

The paper gives information on the construction, characteristics and calibration of the type 1383A chamber for the guidance of users. This instrument is a combination of a re-entrant cylinder (well-type) gamma-ray chamber with an approximately "2π" beta-ray chamber which in conjunction with a d.c. amplifier or electrometer, is suitable for the measurement of samples of γ-emitting and β-emitting isotopes. The γ-ray and β-ray ionization currents and the background are of the order of 10^{-11}, 10^{-10} and 10^{-14} A/mc, respectively. The calibration figures for standard Na^{24}, P^{32}, K^{42}, Fe^{59}, Co^{60}, Br^{82}, Y^{90}, Au^{198} and Ra^{226} sources and the correction factors applicable to measurements of solutions in 2 ml and 5 ml ampoules, and 10 ml bottles are given.

UNE CHAMBRE A IONISATION BETA-GAMMA POUR DES ETALONS SECONDAIRES DE RADIOACTIVITE—I

UTILISATIONS ET ETALONNAGE

Cette communication donne des renseignements sur la construction, les caractéristiques et l'étalonnage de la chambre type 1383A, pour la direction des usagers. Cet instrument réunit une chambre à rayons gamma, faite d'un cylindre rentrant sur luimême, avec une chambre à rayons béta de caractéristique à peu près "2π", lequel en combinaison avec un amplificateur à courant direct ou avec un électromètre sert à la mesure des échantillons d'isotopes émetteurs de γ et de β. Les courants d'ionisation des rayons γ et β et le courant de base sont de l'ordre de 10^{-11}, 10^{-10} et 10^{-14} A/mc, respectivement. Les chiffres d'étalonnage pour des sources normales de Na^{24}, P^{32}, K^{42}, Fe^{59}, Co^{60}, Br^{82}, Y^{90}, Au^{198} et Ra^{226} sont présentés, ainsi que les facteurs correctifs applicables aux mesures des solutions dans des ampoules de 2 ml et de 5 ml et dans des bouteilles de 10 ml.

ИОНИЗАЦИОННАЯ КАМЕРА ДЛЯ ИЗМЕРЕНИЯ БЕТА- И ГАММА-ИЗЛУЧЕНИЯ СТАНДАРТНЫХ РАДИОАКТИВНЫХ ПРЕПАРАТОВ—I

ВОЗМОЖНОСТИ ПРИМЕНЕНИЯ И ГРАДУИРОВКА

В статье приводятся данные по конструкции, характеристикам и градуировке камеры типа 1383А. Установка представляет собой комбинированное устройство из цилиндрической камеры для измерения гамма-излучения и камеры для бетаизлучения с телесным углом около 2π. При применении совместно с усилителем постоянного тока или электрометром это устройство пригодно для измерения γ- и β-излучателей. Ионизационные токи γ и β излучения и фон составляют, соответственно, величины порядка 10^{-11}, 10^{-10} и 10^{-14} А/милликюри. Приведены градуировочные данные для стандатных источников Na^{24}, P^{32}, K^{42}, Fe^{59}, Co^{60}, Br^{82}, Y^{90}, Au^{198}, и Ra^{226}, а также поправочные коэфициенты, которые следует учитывать при измерениях растворов в 2-ти, 5-ти и 10-ти миллилитровых ампулах.

* Deceased.

† Radiation Counter Laboratories, Skokie, Illinois, U.S.A.

EINE β-γ-IONISATIONSKAMMER FÜR RADIOAKTIVE SUBSTANDARDS—I ANWENDUNG UND KALIBRIERUNG

Die vorliegende Arbeit gibt eine Anleitung für den Benützer bezüglich Konstruktion, Charakteristik und Kalibrierung der Kammer 1383A. Das Gerät ist eine Zisternenkammer für γ-Strahlen und eine nahezu 2π-Kammer für β-Strahlen in Verbindung mit einem Gleichstromverstärker oder einem Elektrometer und eignet sich zur Messung von β- und γ-strahlenden Isotopen. Der Ionisationsstrom für γ- und β-Strahlung und für den Leereffekt beträgt 10^{-11}, 10^{-10} bzw. 10^{-14} A/mc. Die Kalibrierung für Na^{24}, P^{32}, K^{42}, Fe^{59}, Co^{60}, Br^{82}, Y^{90}, Au^{196} und Ra^{226} Standards, ebenso wie die Korrekturfaktoren für Messungen von Lösungen in 2 ml und 5 ml Ampullen und in 10 ml Flaschen werden angegeben.

INTRODUCTION

THE use of radioactive isotopes has led to the production of a wide variety of equipment for comparing the activities of samples. In many instances relative measurements only are required. Very often, however, it is desirable to check the activity in millicuries or microcuries at some stage in an investigation, and it is then necessary to use equipment which has been calibrated with standardized samples having known disintegration rates.

In general, the calibration must be made with a standardized sample of each of the radioactive isotopes used in an investigation. The preparation of such radioactivity standards is a specialized task which most users of radioactive isotopes do not wish to undertake and they prefer to purchase them from a recognized standardizing laboratory. The recurrent expense involved, particularly when the radioisotopes are short-lived, is reduced when the equipment retains its calibration, and for this reason d.c. ionization chamber equipment has been set up by many organizations.[1–5] Such chambers differ in design and construction, depending on the particular requirements of the user; they have to be calibrated individually, and there is little correlation of calibration data.

The ionization chamber type 1383A has been designed with the above considerations in mind and is being manufactured by General Radiological Limited, London. Used with a d.c. amplifier or electrometer, it is suitable for relative measurements of samples of β-emitting and γ-emitting isotopes. The ionization current per millicurie is of the order of 10^{-11}A for γ-emitters and 10^{-10}A for β-emitters. The background current is between 1×10^{-14} and 2×10^{-14}A, which is about the same as the γ-ray ionization current produced in the chamber by 0·3 μc of Ra^{226} (in equilibrium with its decay products), or the β-ray ionization current produced by 1 ml of solution containing 0·05 μc of P^{32}.

The specifications to which type 1383A chambers are manufactured was drawn up in collaboration with the National Physical Laboratory Advisory Committee on Radioactivity Standards and the Atomic Energy Research Establishment, Harwell, and it has been shown by tests at the N.P.L. with standard γ-ray sources (Na^{24}, Co^{60}, I^{131}, Au^{198} and Ra^{226}) that chambers have the same calibration characteristics within about ± 1 per cent, the corresponding limits for β-ray sources (P^{32}, S^{35}, Co^{60} and $Sr^{90} + Y^{90}$) being about ± 3 per cent.

Results obtained with one chamber are thus applicable to other chambers of this type provided a uniform procedure for source preparation and ionization measurement is adopted. Thus organizations working with the same radioactive isotopes can compare the activities of their samples without necessarily having to interchange samples. This may have particular advantages when the radioactive isotopes are short-lived.

Chambers are tested by the manufacturers to ascertain that they have a uniform response (within ± 1 per cent) to a Co^{60} γ-ray reference source, and a uniform response (within ± 3 per cent) to a $Sr^{90} + Y^{90}$ β-ray reference source. The National Physical Laboratory will, on request, test individual chambers by comparing them with the reference chamber of this type maintained at the Laboratory.

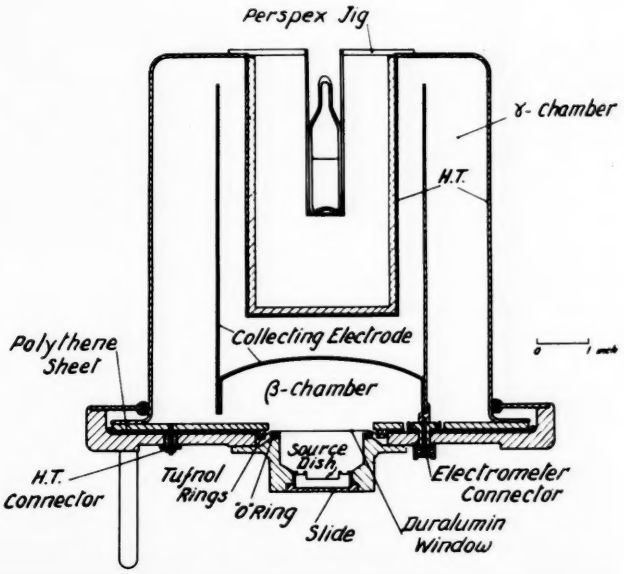

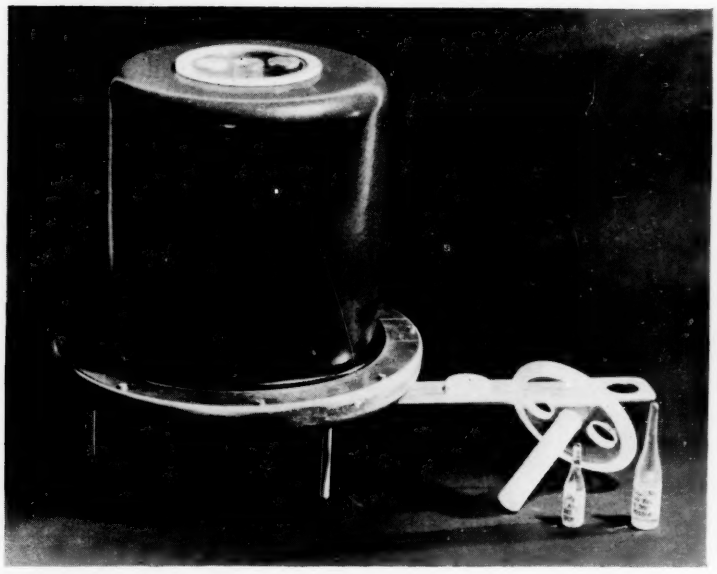

FIG. 1. Ionization chamber for secondary standardization of β- and γ-ray sources.

VO
1
19

VOL. 10 1961

This reference chamber has been calibrated at the National Physical Laboratory with N.P.L. standards of a number of radioactive isotopes, thereby providing data for the derivation of the activities of samples in millicuries from measurements of ionization current in amperes.

(1) *Description of chamber*

The following description of the chamber and its characteristics has been prepared for the guidance of users.

The chamber (Fig. 1) is a combination of a re-entrant cylinder chamber for γ-ray measurements and a "parallel plate" chamber for β-ray measurements. The inner and outer cylinders form one component which, with the circular aluminium plate and the duralumin window, comprise the h.t. electrode system. The circular plate is insulated from the aluminium base plate by the polythene sheet. The exterior surface of the outer cylinder is coated with plastic insulating material. The intermediate cylinder is the collecting electrode which is insulated from the base plate by polystyrene bushes. The re-entrant cavity for γ-ray sources, is 5 in. (12·7 cm) deep and 2·6 in. (6·6 cm) internal diameter, and has a brass lining*, which is $\frac{1}{8}$ in. (3·2 mm) thick, to absorb β-particles. The β-chamber is defined by the brass dome, the lower portion of the intermediate cylinder and the circular plate; the β-particles enter the chamber through the central circular aperture after passing through the duralumin window (0·68 mg/cm^2 thick). The window is in electrical contact with the circular plate and insulated from the base plate; it is mounted between two insulating washers, the one which touches the circular plate having been coated with Aquadag, and is kept under tension by a rubber "O" ring. The window and washers form one component which is easily replaceable in the event of damage to the window. The chamber is not sealed and contains air at atmospheric pressure. Its overall dimensions are height 10 in. (25 cm), diameter 9 in. (23 cm). A terminal is provided on the underside of the base plate for connecting the h.t. electrode system to a polarizing battery, and a screened concentric cable is provided for connecting the collecting electrode to a current measuring instrument, e.g. a d.c. amplifier.

(2) *Polarizing voltage*

Saturation within a few parts in a thousand is obtained with a polarizing voltage of 100 V when the ionization currrent is of the order of 10^{-10}A; such a current is produced by a γ-ray source containing a few milligrams of radium or by a β-ray source containing a few millicuries of P^{32}. The voltage normally used in measurements at the N.P.L. is 300 V which produces saturation within 0·3 per cent for currents of the order of 5×10^{-9}A, corresponding to a γ-ray source of about 100 mc Co^{60}. The γ-ray ionization current under near-saturation conditions is numerically the same for negative and positive collecting voltages. With low-energy β-emitters the current is numerically slightly greater for positive ion collection (h.t. positive) than for negative.

(3) *Background current*

The normal background current is between 1×10^{-14}A and 2×10^{-14}A. The background should be checked for a period of about $\frac{1}{2}$hr after the chamber has been connected to the battery, and at appropriate times when measurements are being made.

(4) *Environment and shielding*

The response of the chamber is not independent of its environment; shielding the chamber (e.g. by a lead cylinder to reduce the effect of extraneous radiation) causes an increase in the γ-ray ionization current. Thus with a radium source in the cavity, scattering from lead cylinders surrounding the outer cylinder of the chamber and having total thicknesses 2, 4, 6 and 8·5 mm increased the ionization by 1·6, 1·8, 1·9 and 2·1 per cent, respectively. With Au^{198} the increase in γ-ray ionization current was 2·5 per cent for 2 mm lead and 2·7 per cent for 8·5 mm

* The lining is at h.t.

lead. The calibration data (Table 3) apply to an unshielded chamber standing on a wooden table, the chamber being not less than 2 ft from the nearest wall.

(5) *Correction for pressure and temperature*

Correction of the observed γ-ray ionization current is made in the usual way, the correction factor (to 760 mm and 22°C) being $760\ (273 + T)/295.P$ where T is the temperature in degrees centigrade and P is the atmospheric pressure in millimetres of mercury. For the β-ray chamber, the factor so calculated leads to over-correction by an amount which is greater the lower the energy of the β-particles. Table 6 gives the experimentally determined correction factors corresponding to calculated factors ranging from 0·9 to 1·20.

(6) *Measurement of γ-ray sources*

The γ-ray ionization current varies with the position of the source in the cavity, displacement of a source downwards causing an increase in the ionization current. For γ-ray sources of small dimensions and for 2 ml and 5 ml ampoules containing respectively 1 ml and 4 ml of solution, the change in ionization current is about 3 per cent/cm of vertical displacement in the middle region of the cavity, so that, to avoid errors greater than $\pm$0·5 per cent due to this, adjustment of the position of the source to within $\pm$1·5 mm is necessary. When a source is displaced 1 cm from the axis towards the wall of the cavity, the increase in ionization current is about 1 per cent. Measurements of sources of different lengths and diameters have not been made; the dependence of ionization current on length up to about 5 cm, and on diameter up to 2 cm is expected to be small, provided the sources are symmetrically placed with respect to the mid-point of the cavity.

The two perspex holders supplied with the chamber are for use with 2 ml and 5 ml ampoules (Table 2) such as those in which the 1 g and 4 g N.P.L. standard solutions are issued. The reference chamber of this type maintained at the N.P.L. has been calibrated with these standards in the appropriate holders (Table 3). Calibration data for a solid Co^{60} source and for radium in a platinum tube are also given in Table 3.

Owing to unavoidable variations in dimensions of ampoules and holders, the depth of the mid-point of the solution in the cavity, when the ampoules contain 1 ml and 4 ml respectively, can vary by about $\pm$1·5 mm for the 2 ml and $\pm$2·5 mm for the 5 ml ampoules. Measurements of Na^{24}, Co^{60} and I^{131} solutions have shown that the corresponding variations in ionization current are about $\pm$0·15 and $\pm$0·5 per cent, respectively. To correct for differences in height of liquid arising from excess or deficiency of solution in ampoules, the measured values of ionization current should be multiplied by the factors given in Table 4 before applying the calibration data.

The large holder referred to in Table 2 is intended for use with the chamber for measurements of solutions in bottles, beakers, etc. One application is the checking of the activities of solutions of radioactive isotopes in the bottles in which they are received from the suppliers. Such bottles commonly have a capacity of about 10 ml, an external diameter of about 22 mm. and wall thickness about 1 mm. The γ-ray calibration data in Table 3 can be applied to such bottles when they contain about 10·5 ml of solution, and are measured in the large holder. For bottles containing more or less than 10·5 ml, the measured ionization currents should be multiplied by the correcting factors given in Table 5.

(7) *Measurement of β-ray sources*

A spring controlled slide is provided for the insertion of β-ray sources to a position beneath the window of the β-chamber. The centre of the circular depression in this slide is vertically below the centre of the window when the inner end of the slot in the slide is in contact with the leg of the chamber. The polythene dishes (Table 2) supplied hold 1 ml of liquid and fit into the circular depression on the slide. The groove in the upper edge of each dish is intended to limit the

effects (e.g. contamination of the chamber) of a small accidental overflow of solution. Calibration data for solutions in the dishes are given in Table 3.

The ionization produced by a β-ray source is critically dependent on the distance of the source from the window and it is essential that the polythene dish should be correctly placed in the recess of the slide. It is also important that the volume of liquid transferred to the dish should not differ appreciably from 1 ml. A deficiency in the volume of liquid reduces the ionization current; for a P^{32} solution the reduction is about 1 per cent for a deficiency in volume of 0·02 ml.

(8) *Accuracy of standardization of samples by means of chamber*

The solutions used for the calibrations referred to in Table 3 were standardized by $4\pi\beta$ proportional counting or by $4\pi\beta\gamma$ coincidence counting, and the ionization currents were measured with an induction balance and Lindemann electrometer. Measurements of ionization current per millicurie were reproducible to within ± 1 per cent, part of this spread being due to relative errors in the disintegration-rate values of different standard solutions of the same nuclide prepared at different times. Assuming that the user is able to measure the absolute value of the ionization currents to an accuracy of ± 1 per cent, and that the maximum differences between the γ-ray and β-ray responses of the chambers are ± 1 per cent and ± 3 per cent, respectively, the accuracy of standardization of solutions (in terms of N.P.L. standards)by means of a chamber of this type is about ± 2 per cent for the γ-emitters listed in Table 3, and about $\pm 3{\cdot}5$ per cent for the β-emitters. Reduction of these limits is possible by calibration of individual chambers.

It should be noted that the errors in the standards themselves have not been included in the above limits. The accuracy claimed for N.P.L. standards is ± 3 per cent, i.e. it is believed that the disintegration-rate value ascribed to them following direct methods of measurement do not differ from the true values by more than ± 3 per cent. Intercomparisons of standards of the radioactive isotopes listed in Table 3 by different organizations have generally shown agreement to within these limits.

(9) *Reference sources*

It is desirable that the long-term stability of an ionization chamber together with its associated current measuring equipment should be checked from time to time. This can most conveniently be done by making use of a reference source of long half-life. If the reference source is included during each measurement made with the chamber it also affords a ready means of verifying the accuracy of the pressure–temperature correction. The choice of reference source is best made by the user. At the N.P.L., radium, in a platinum tube having walls 0·5 mm thick and a radium content of 250 μg, is used. Radium in solution is not entirely satisfactory mainly because it is difficult to avoid variations in the distribution of radon and active deposit between the solution and the air above it in the ampoule. Cobalt-60, either in solid form or in solution, is suitable. A low-activity $Sr^{90} + Y^{90}$ foil (Radiochemical Centre SIM3) mounted in a brass holder, which fits the recess on the slide, serves as a convenient reference source for the β-ray chamber. Particulars of the construction of such a source may be obtained, on request, from the N.P.L.

Acknowledgement—The work described above has been carried out as part of the research programme of the National Physical Laboratory and this paper is published by permission of the Director of the Laboratory.

TABLE 1

Cylinder	Material	Internal height (cm)	Internal diameter (cm)	Thickness (cm)
Outer	Aluminium	17·8	16·8	0·16
Inner	Aluminium	13·3	7·3	0·12
Intermediate	Brass	16·2	10·2	0·07
Cavity liner	Brass	12·4	6·7	0·31

The distance between the centre of the dome and the duralumin window is 3·9 cm and that between the surface of the liquid in the β-ray source dish and the window is 2·0 cm. The diameter of the window is 4·2 cm.

VOL. 10 1961

TABLE 2. Dimensions of ampoules and source holders

	Overall height	Diameter		Wall thickness	Height of liquid in ampoule
		Internal	External		
		*Ampoules**			
	(mm)	(mm)	(mm)	(mm)	(mm)
2 ml	55	10·3	12·0 ± 0·5	0·85 ± 0·1	12 (1 g)
5 ml	85	13·8	15·5 ± 0·5	0·85 ± 0·1	26 (4 g)
		γ-ray source holders			
For 2 ml ampoules	73	14·3	17·3	1·5 ± 0·1	
For 5 ml ampoules	80	16·7	19·7	1·5 ± 0·1	
For bottles† beakers, etc.		57·1	63·5	3·2	
		β-ray source dishes (1 ml capacity)			
				Internal depth	Overall depth
Polythene dishes		19	28·6	3·5	8

* The ampoules are made to B.S.I. specification except that the wall thickness is 0·85 mm instead of 0·5 mm.
† This holder is for supporting bottles, beakers etc., containing radioactive solutions.

TABLE 3. Mean values of ionization currents (corrected to 760 mm and 22°C) in chamber type 1383A, serial number 14.
(a) 1 g of solution in a 2 ml ampoule
(b) 4 g of solution in a 5 ml ampoule
(each supported in the source cavity in the appropriate perspex holder)
(c) 1 ml of solution in a polythene dish
(d) Co^{60} in an AERE Birmabright capsule, in the holder used for 2 ml ampoules; flat end of capsule on base of holder; long axis of capsule vertical
(e) Radium source (active length 3 mm, in platinum tube 6 mm long having walls 0·5 mm thick); flat end of tube on base of 2 ml holder; long axis of tube vertical

Radioactive isotope	Ionization current		Radioactive isotope	Ionization current	
	γ-Ray chamber (A × 10^{-12}/mc)	β-Ray chamber (A × 10^{-12} per mc/ml)		γ-Ray chamber (A × 10^{-12}/mc)	β-Ray chamber (A × 10^{-12} per mc/ml)
		—	Br^{82}	(a) 63	(c) 103
				(b) 62	
Na^{24}	(b) 75·6	—	Y^{90}	—	(c) 335
P^{32}	(b) 0·079*	(c) 268	I^{131}	(a) 10·6	(c) 73
K^{42}	(b) 6·0	(c) 433		(b) 10·5	
Fe^{59}	(a) 27·1	—	Au^{198}	(b) 10·8	(c) 137
Co^{60}	(a) 53·2	—		(A × 10^{-12}/mg)	
	(b) 53·2		Ra^{226} + decay products	(b) 35·6	
	(d) 53·2			(e) 34·5	—

* Bremsstrahlung.

TABLE 4. Correction factors for partially filled 2 ml and 4 ml ampoules

Height of liquid in ampoule (mm)	2 ml ampoules		5 ml ampoules	
	Volume of liquid (ml)	Correction factor	Volume of liquid (ml)	Correction factor
5	0·4	0·99	—	
10	0·8	1·00	1·5	0·97
15	1·3	$1·00_5$	2·3	0·98
20	1·7	$1·01_0$	3·1	0·99
25	—	—	3·9	1·00
30	—	—	4·7	1·01

TABLE 5. Correction factors for γ-ray measurements of solution contained in 10 ml bottles which are supported in the source cavity in the appropriate perspex holder

Height of liquid in bottle (mm)	Volume of liquid (ml)	Correction factor
10	3·2	0·96
20	6·4	0·98
30	9·5	0·99
35	11·1	1·00
40	12·7	1·01

TABLE 6. Corrections to 760 mm 22°C for β-ray sources

Calculated correction factor	K^{42}	Y^{90}	P^{32}	Au^{198}	Br^{82}	Co^{60}	S^{35}
0·90	$0{\cdot}90_4$	$0{\cdot}91_0$	$0{\cdot}90_7$	$0{\cdot}91_4$	$0{\cdot}93_9$	$0{\cdot}96_8$	$1{\cdot}03_0$
0·95	$0{\cdot}95_2$	$0{\cdot}95_4$	$0{\cdot}95_2$	$0{\cdot}95_8$	$0{\cdot}96_6$	$0{\cdot}98_3$	$1{\cdot}00_7$
1·00	1·000	1·000	1·000	1·000	1·000	1·000	1·000
1·05	$1{\cdot}04_7$	$1{\cdot}04_6$	$1{\cdot}04_6$	$1{\cdot}04_2$	$1{\cdot}03_2$	$1{\cdot}02_7$	$0{\cdot}99_8$
1·10	$1{\cdot}09_4$	$1{\cdot}09_1$	$1{\cdot}09_2$	$1{\cdot}08_2$	$1{\cdot}06_4$	$1{\cdot}05_1$	$0{\cdot}99_8$
1·20	$1{\cdot}19_0$	$1{\cdot}18_2$	$1{\cdot}18_6$	$1{\cdot}16_4$	$1{\cdot}13_0$	$1{\cdot}09_9$	$1{\cdot}02_2$

REFERENCES

1. BULLEN M. A. *Nucleonics* **11,** No. 12, 15 (1953).
2. KEENE J. P., MACKENZIE L. A. and GILBERT C. W. *Physics in Medicine and Biology* Vol. 2, p. 360. (1958).
3. SELIGER H. H. and SCHWEBEL A. *Nucleonics* **12,** No. 7, 54 (1954).
4. SINCLAIR W. K. and NEWBERY S. P. *J. Sci. Instrum.* **28,** 234 (1951).
5. SINCLAIR W. K., TROTT N. G. and BELCHER E. H. *Brit. J. Radiol.* **27,** 565 (1954).

VOL. 10 1961

International Journal of Applied Radiation and Isotopes, 1961, Vol. 10, pp. 72–78. Pergamon Press Ltd. Printed in Northern Ireland

A Beta–Gamma Ionization Chamber for Substandards of Radioactivity—II

Instrument Response to Gamma Radiation

J. W. G. DALE
National Physical Laboratory, Teddington, Middx.

(*First received* 5 *May* 1960 *and in final form* 20 *October* 1960)

The paper describes a method of calculating the response to gamma radiation of the Type 1383A chamber for those isotopes whose gamma energies lie within the range 0·2–3·0 MeV. The instrument response is expressed as current per millicurie for each isotope. An allowance is made for the effect on response, especially at lower energies, of the materials with which the instrument is constructed. Estimates of current per millicurie produced by this method have been shown by subsequent experimental calibrations to lie, with few exceptions, within ±3 per cent of the experimental values. Activity estimates may therefore be made with reasonable precision where no absolute method (such as 4π proportional counting) is available or a very short half-life precludes its use.

UNE CHAMBRE A IONISATION BETA-GAMMA POUR DES ETALONS SECONDAIRES DE RADIOACTIVITE—II

RESPONSE DE L'INSTRUMENT AU RAYONNEMENT GAMMA

Cette communication décrit une méthode de calculer la réponse de la chambre type 1383A au rayonnement gamma de ceux des isotopes dont les énergies gamma tombent dans la rangée 0,2–3,0 MeV. On précise la réponse de l'instrument en courant par millicurie pour chaque isotope. On fait un ajustement pour l'effet sur la réponse, surtout aux énergies inférieures, donné par les matériaux de construction de l'instrument. Des étalonnages expérimentaux subséquemment achevés ont montré que les estimations du courant par millicurie que donne cette méthode reviennent, avec peu d'exceptions, à ±3 pour cent des valeurs expérimentales. Aussi peut-on faire des estimations d'activité avec une précision raisonnable où on ne dispose d'aucune méthode absolue (telle que le comptage proportionnel 4π) ou lorsqu'une période de demi-valeur très brève empêche son emploi.

ИОНИЗАЦИОННАЯ КАМЕРА ДЛЯ ИЗМЕРЕНИЯ БЕТА- И ГАММА-ИЗЛУЧЕНИЯ СТАНДАРТНЫХ РАДИОАКТИВНЫХ ПРЕПАРАТОВ—II

РЕАКЧИЯ ПРИБОРА НА ГАММА-ИЗЛУЧЕНИЕ

Дано описание метода расчета чувствительности камеры типа 1383А для изотопов, гамма-энергии которых лежат в пределах 0,2–0,3 мэв. Чувствительность выражается величиной тока на милликюри для каждого изотопа. Учитывается влияние материалов, из которых сделана камера, на ее чувствительность, особенно в случае низких энергий. Последующая градуировка показала, что определенная этим методом чувствительность совпадает с экспериментальной с точностью до ±3%. Поэтому в отсутствии абсолютного метода измерений (например, при помощи счетчика с телесным углом 4π) или при периоде полураспада слишком коротком для применения такого счетчика удовлетворительные результаты могут быть получены с помощью данного расчетного метода.

EINE β-γ-IONISATIONSKAMMER FÜR RADIOAKTIVE SUBSTANDARDS—II
γ-ANZEIGE DES GERÄTES

Die vorliegende Arbeit beschreibt eine Methode zur Berechnung der γ-Anzeige der Kammer Type 1383A für jene Isotope, deren γ-Energien zwischen 0,2 und 3,0 MeV liegen. Die Anzeige des Gerätes ist dabei in Ampere pro mc für jedes Isotop angeben. Dabei werden besonders bei niedrigen Energien die Effekte, hervorgerufen durch das Material der Kammer selbst, berücksichtigt. Experimentelle Kalibrierung zeigte, dass die nach dieser Methode errechneten Daten mit wenigen Ausnahmen innerhalb $\pm 3\%$ der experimentellen Werte liegen. Aktivitätsbestimmungen können daher mit ausreichender Genauigkeit durchgeführt werden, wenn keine Absolutbestimmungsmethode (z.B. 4π Proportionalzählung) angewendet werden kann oder wenn eine sehr kurze Halbwertszeit eine Absolutbestimmung unmöglich macht.

VOL. 10 1961

INTRODUCTION

THE type 1383A β–γ ionization chamber is routinely used to check the activities of radioactive solutions once the instrument has been calibrated in terms of current per millicurie for the isotope in question. Occasionally, however, it may be required to know the activity of an isotope for which calibration data is not yet available or on which, by reason of a very short half-life, it is impracticable to made absolute measurements at all.

As far as gamma ray-emitting isotopes are concerned, these notes attempt to show that such a prediction may be carried out within reasonably close limits of accuracy (± 3 per cent).

(1) *Routine calibration of chamber*

The instrument consists insofar as γ-ray measurements are concerned of a re-entrant cavity chamber of cylindrical form, in which the source to be measured is placed in a perspex jig within the cavity. The source consists of a sealed glass ampoule containing a specified quantity of solution and use of the perspex jig ensures that the mid-point of the liquid always occupies the same position in the cavity.

Measurements are made via a Lindemann electrometer system and Townsend balance of the observed current per millicurie of isotope present in the ampoule, the activity having first been determined by an absolute counting method such as a 4π-proportional counter.

It has been found that for any particular isotope the value of current per millicurie remains constant, although differing greatly from isotope to isotope. This variation in response is very nearly in direct proportion to the "k-value" or specific γ-emission of the isotope.

(2) *Ideal case. "Airwall" response*

The "*k*-value" of an isotope is the dose rate in röntgen per hour which 1 mc of isotope would produce at a distance of 1 cm in 1 ml of dry air at NTP. If an ionization chamber were to be constructed of such materials that the assemblies forming the sensitive volume boundaries and collecting electrode systems behaved exactly as air so far as incident gamma radiation is concerned, then a curve of current per millicurie against *k*-value would result in a straight line passing through the origin. It would also be a simple matter to predict accurately the response of any isotope whose *k*-value was sufficiently well known.

(3) *Practical limitations*

In a commercially produced instrument such as the Type 1383A chamber, it is not usually possible to construct to airwall conditions, so that some deviations in response are to be expected, and in fact a plot of experimental current per millicurie against *k*-value, although almost straight, does not pass through the origin (Fig. 1). If current per millicurie divided by *k*-value is plotted against *k*-value (Fig. 2), the deviation is exaggerated and shows that, for isotopes whose *k*-value lies below 10, there is a tendency for the measured current per millicurie to be too high. This is not so, however, for K^{42}, which has a low *k*-value, but produces a current response lower than this latter curve would lead one to expect. Since K^{42} has a branching ratio of 4 : 1 and

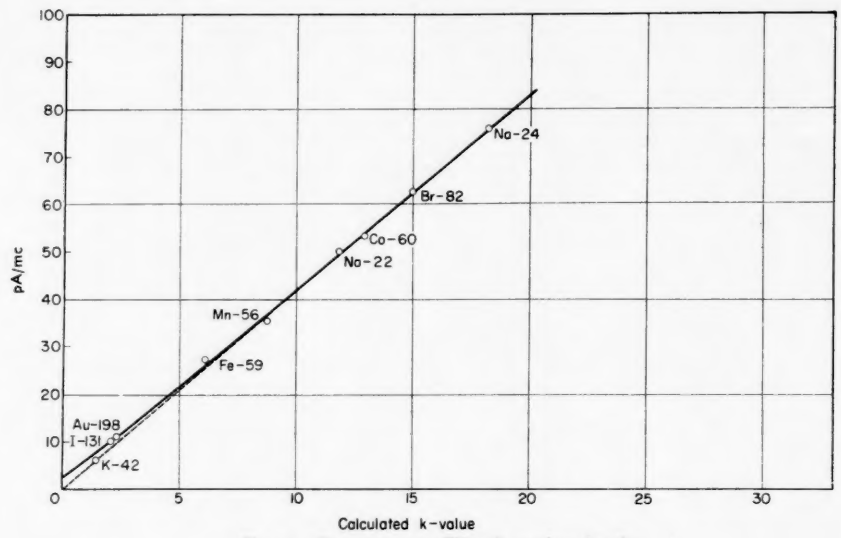

FIG. 1. Current per millicurie against k-value.

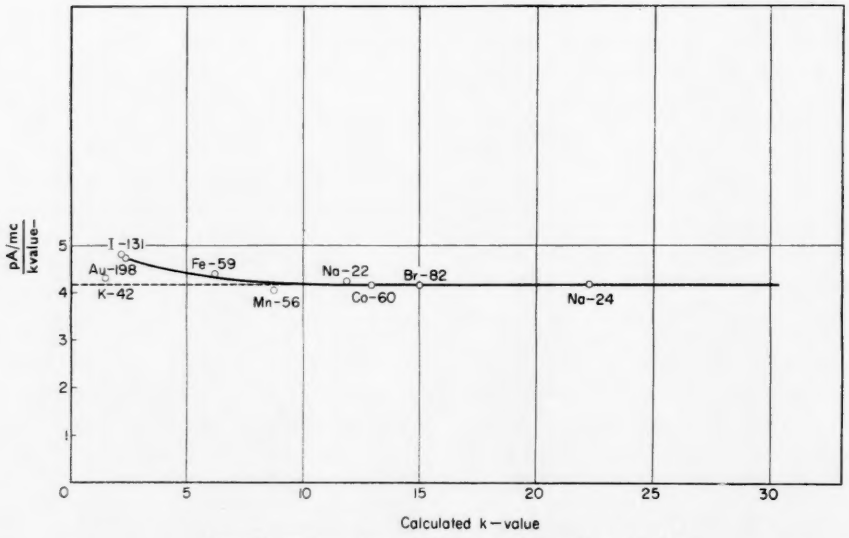

FIG. 2. Current per millicurie/k-value against k-value.

therefore, since only one γ-quanta is produced every five disintegrations, its low k-value is no indication of its γ-energy which is quite high. It is evidently the lower-energy γ-radiations which produce abnormally high chamber responses in terms of observed current.

(4) *Gamma ray scattering*

If a block of material is placed in the path of a beam of incident γ-radiation, the rays are scattered by three processes, two of which result in the production of secondary electrons.

At all energies of the incident radiation there are electrons produced by Compton scatter and this production is proportional to Z (the atomic number of the absorbing material).

At lower energies photoelectric scattering

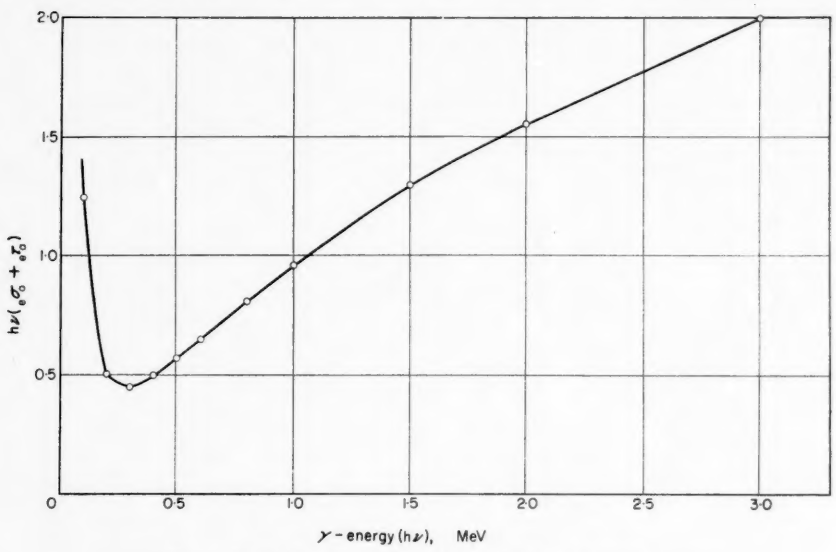

FIG. 3. Secondary electron production in brass against γ-energy

predominates when the secondary electron production is approximately proportional to Z^5.

At high energies pair production occurs.

Reverting now to the practical case of the ionization chamber, only the first two processes are of immediate interest, since the energies of the γ-radiation of all isotopes normally used lie between 200 keV and 3 MeV, so that pair production may be neglected. As the instrument has a brass collecting electrode assembly and is of aluminium construction otherwise, the effect of photo-electric scatter becomes very important as Z is now much higher than that of air.

An attempt to assess the relative contributions of the brass electrode, aluminium wall, and the air space between, on secondary electron production results in the estimation that with the air at NTP, it is the brass of the collecting electrode system which predominates in the production of secondary electrons (This has been partly confirmed by experiments in which 0·002 in. plating was carried out on the electrodes of two chambers with quite large variation in response.)

(5) *Theoretical curve of chamber response*

A curve of $h\nu(e^{\sigma}a + e^{\tau}a)$ against $h\nu$ for brass was plotted (Fig. 3),

where

$h\nu$ = incident γ-ray energy
$e^{\sigma}a$ = Compton scatter coefficient for brass
$e^{\tau}a$ = photo-electric absorption coefficient for brass.

The values were taken from *Beta and Gamma Ray Spectroscopy* (Siegbahn).

The resulting curve showed a decrease of electron production with energy down to about 300 KeV followed by a rapid increase at energies below this value.

(6) *Practical adaptation of response curve*

Since the chamber has an inner liner of $\frac{1}{8}$ in. brass which attenuates the γ-radiation before it reaches the ionizing volume, the curve was modified to allow for this and then replotted (Figs. 4, 5).

The Y ordinate now represents in arbitrary units chamber response in current for γ-radiation of various energies.

Two isotopes were selected, namely, Co^{60} and Na^{24}, from which it was hoped to normalize the curve so as to read directly in current per γ-ray quanta against γ-energy.

These two isotopes were selected since they had been accurately standardized by means of 4π proportional and $4\pi\beta\gamma$ methods. The

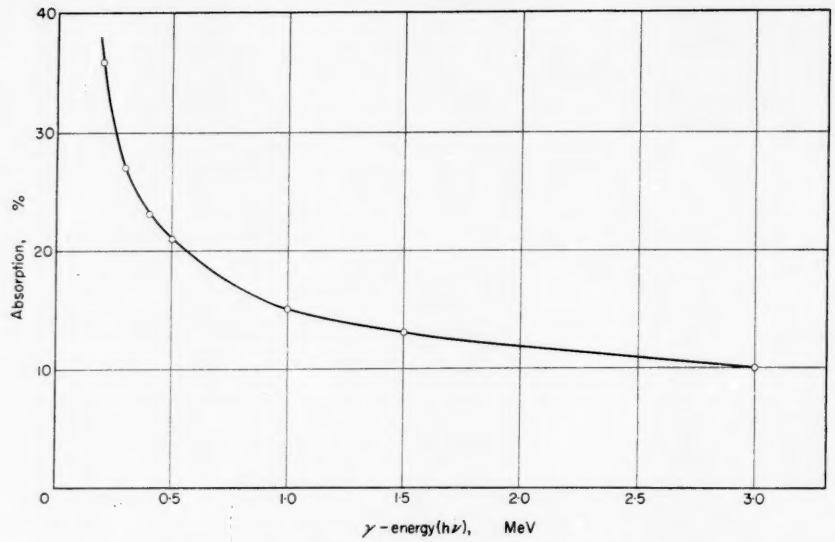

FIG. 4. Absorption of γ-radiation in brass liner of cavity.

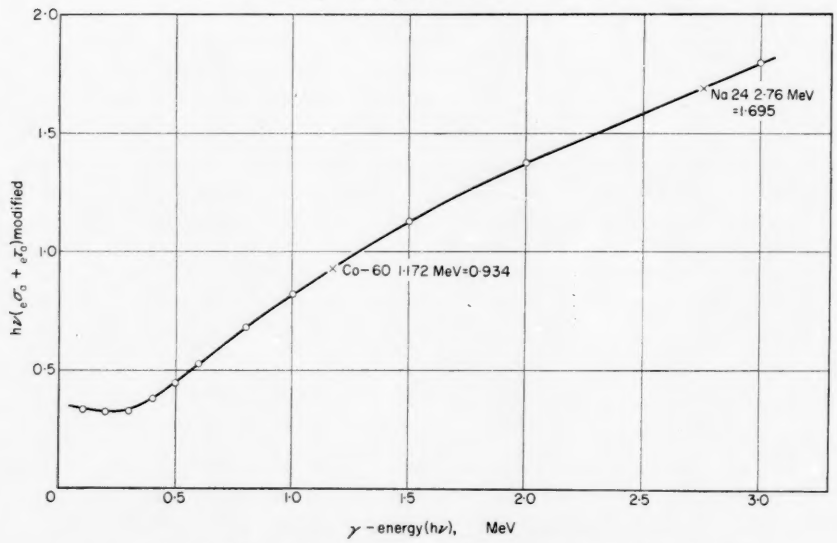

FIG. 5. Secondary electron production in brass against γ-energy.
(Modified for absorption in brass liner of cavity.)

values of current per millicurie for each isotope were taken as measured in the γ-chamber and the relative contributions from each γ-ray were calculated from Klein Nishina coefficients. As the energy of each ray was above 1 MeV, it was assumed that the percentage of the total current per millicurie due to each γ-energy was in the same proportion as the percentage of the total k-value. (In other words, only Compton scattering need be considered.) See Table 1.

The reason that the final column in the table expresses the current as pA/3·7 $\times$ 10^7 quanta/sec is so that simple summing of the contributions of the constituent γ-rays of an

TABLE 1

Isotope	Current/mc	γ-Energy	% per disintegration	% of total K	Current (pA) per $3{\cdot}7 \times 10^7$ quanta/sec
Na^{24}	75·65	2·760	100%	61·3%	46·37
		1·380	100%	38·7%	29·28
Co^{60}	53·24	1·332	100%	52·5%	27·95
		1·172	100%	47·5%	25·29

isotope via the curve gives current per millicurie ($3{\cdot}7 \times 10^7$ d.p.s.) directly.

For the purpose of producing a curve normalized to the two selected isotopes, a table was produced (Table 2) which related the arbitrary scale of $h\nu(e^{\sigma}a + e^{\tau}a)$ to the current in pA from the 1·172 MeV γ-ray of Co^{60} and the 2·760 MeV γ-ray of Na^{24}.

The values given in the final column of the Table were plotted against $h\nu$ in mega-electron volts to give a curve reading directly in current vs. γ-energy (Fig. 6).

This curve was then used to calculate chamber response per millicurie for several other γ-emitting isotopes, most of which had already been measured and for which, therefore, calibrations already existed which could be compared with the predicted values.

Two worked examples are given below which explain the method of calculation, and which also give the experimental values for comparison (Table 3).

TABLE 2

Isotope	$h\nu$ (MeV)	$h\nu$ $(e^{\sigma}a + e^{\tau}a)$	pA	pA	Mean pA
	0·1	0·3379	9·15	9·24	9·20
	0·2	0·3207	8·68	8·77	8·73
	0·3	0·3260	8·83	8·92	8·88
	0·4	0·3793	10·27	10·38	10·33
	0·5	0·4465	12·09	12·21	12·15
	0·6	0·5224	14·15	14·29	14·22
	0·8	0·6775	18·34	18·53	18·44
	1·0	0·8150	22·07	22·30	22·19
	1·5	1·1279	30·54	30·86	30·70
	2·0	1·3720	37·15	37·53	37·34
	3·0	1·7973	48·67	49·17	48·92
Co^{60}	1·172	0·934	25·29	—	—
Na^{24}	2·76	1·695	—	46·37	—

Table 4 gives a more complete table of

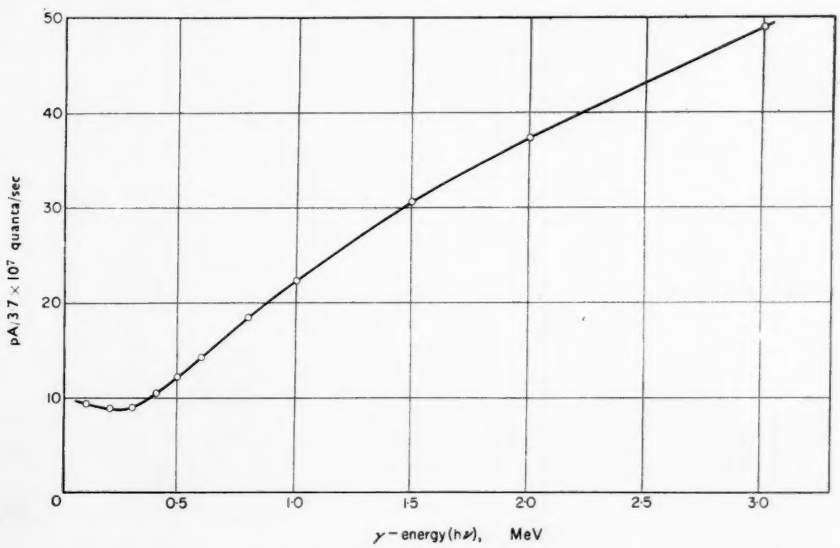

FIG. 6. Chamber response to γ-radiation (pA/$3{\cdot}7 \times 10^7$ quanta/sec).

TABLE 3

Isotope	γ-Energy (MeV) (from decay (scheme)	% per disintegration (from decay (scheme)	Curve pA (per $3{\cdot}7 \times 10^7$ quanta/sec)	Corrected pA (for % per disintegration)	Total pA (per mC)	Experimental pA/mc
K^{42}	1·51	20%	30·75	6·15	6·15	6·00
Na^{22}	1·277	100%	27·10	27·10	49·42	49·9
	0·51	90%	12·40	11·16		
	0·51	90%	12·40	11·16		

TABLE 4

Isotope	pA/mc (energy curve)	pA/mc (experimental)	% difference (experimental/ curve)
Na^{24}	75·0	75·65	—
Co^{60}	53·3	53·24	—
Fe^{59}	25·7	27·1	+5·4%
K^{42}	6·15	6·0	−2·5%
Au^{198}	10·64	10·82	+1·7%
I^{131}	10·23	10·42	+1·9%
Br^{82}	59·6	62·3	+4·5%
Na^{22}	49·4	49·9	+1·0%
Mn^{56}	36·2	35·2	−2·8%
Cs^{137}	14·8	—	—
I^{132}	48·3	—	—

results in which predicted values are compared where possible with experimentally obtained results. It can be seen that for most isotopes the agreement is within ± 3 per cent and in the case of Fe^{59} it may be worth pointing out that the disagreement of 5 per cent is close to that found between $4\pi\beta\gamma$ measurements of Fe^{59} and Co^{60} and a consideration of their decay schemes. It is probable that with more precise information as to the decay scheme of Fe^{59} this difference will disappear.

Acknowledgement—The work described above has been carried out as part of the research programme of the National Physical Laboratory, and this paper is published by permission of the Director of the Laboratory.

International Journal of Applied Radiation and Isotopes, 1961, Vol. 10, pp. 79–85. Pergamon Press Ltd. Printed in Northern Ireland

Determination of the Specific Activity of Tritiated Compounds on Paper Chromatograms using an Automatic Scanning Device

F. J. CARLETON* and H. R. ROBERTS†
Research and Development Division, National Dairy Products Corporation,
Oakdale, Long Island, New York, U.S.A.

(*Received* 31 *March* 1960)

VOL.
10
1961

The specific counting of low-energy beta emitters has heretofore involved complex radiochemical procedures. Paper chromatography offers a simpler means of separating components of complex mixtures. An automatic scanning device allows radiochemical counting procedures to be done directly from the paper chromatograms. Quantitative assays of specific tritiated compounds are made directly from paper chromatograms. The method of calibration is described.

LA CARACTERISATION DE L'ACTIVITE SPECIFIQUE DES COMPOSES TRITIES SUR LES CHROMATOGRAMMES DE PAPIER EN EMPLOYANT UN APPAREIL EXPLORATEUR AUTOMATIQUE

Le comptage spécifique des émetteurs béta de petite énergie a entraîné, jusqu'ici, des procédés radiochimiques compliqués. La chromatographie sur papier donne un moyen plus simple pour la séparation des composants dans des mélanges complexes. Un appareil explorateur automatique permet l'achèvement des procédés de comptage radiochimiques directement des chromatogrammes de papier. Des essais quantitatifs de certains composés tritiés se font directement des chromatogrammes de papier. On décrit le système d'étalonnage.

ОПРЕДЕЛЕНИЕ ПРИ ПОМОЩИ АВТОМАТИЧЕСКОГО СЛЕДЯЩЕГО УСТРОЙСТВА УДЕЛЬНОЙ АКТИВНОСТИ МЕЧЕНЫХ ТРИТИЕМ СОЕДИНЕНИЙ НА БУМАЖНЫХ ХРОМАТОГРАММАХ

Определение удельной активности при помощи бетаизлучателей низкой энергии было до настоящего времени связано со сложной химической методикой. Бумажная хроматография дает возможность более простого разделения компонентов сложных смесей. Автоматическое следящее устройство позволяет производить необходимые радиохимические измерения и количественный анализ отдельных, меченых тритием, соединений непосредственно на бумажных хроматограммах. Дано описание метода градуировки.

BESTIMMUNG DER SPEZIFISCHEN AKTIVITAT VON TRITIUM-HALTIGEN VERBINDUNGEN AUF PAPIERCHROMATOGRAMMEN UNTER VERWENDUNG EINES AUTOMATISCHEN SCANNERS

Die spezifische Zählung von niederenergetischen β-Strahlern benötigte bisher komplexe radiochemische Prozeduren. Papierchromatographie bietet ein einfaches Mittel zur Trennung von Komponenten komplexer Gemische. Ein automatischer Scanner gestattet die Messung direkt an dem Papierchromatogramm. Quantitative Analysen von spezifischen, Tritium-hältigen Verbindungen wurden direkt am Papierchromatogramm gemacht. Die Kalibrierungsmethode wird beschrieben.

* Present address: Chas. Pfizer and Co. Inc., Maywood, N. J.
† E. R. Squibb, New Brunswick, N. J.

INTRODUCTION

THE increasing use of tritium and other low-energy beta emitters has indicated a need for a method whereby these radioactive components in complex mixtures can be separated both rapidly and simply for radiochemical measurements. Since paper chromatography offers a means of separating components in complex mixtures, a method of measuring the activity of separated tritiated compounds directly on paper is advantageous in that it eliminates physical isolation of these products. The development of such a method for determining the quantitative distribution of C^{14}-labeled compounds on paper chromatograms[1] indicated that the procedure might well be extended to include tritiated compounds. This paper describes a method for quantitatively assaying tritiated compounds on paper chromatograms using an automatic scanning device.

EXPERIMENTAL

The procedure was developed using glycine-H^3* and glucose-H^3.† The technique is basically the same as that developed for assaying radiochromatograms containing C^{14}-labeled sugars.[1]

The automatic windowless chromatogram scanner (Fig. 1), which has previously been described,[1] has been modified by eliminating the variable speed-ratio-changer and replacing it with a gear box and set of gears identical with those mounted in the recorder. In this manner the drum speed can be adjusted either to equal the chart speed or to any exact ratio. The detector has also been modified by the manufacturers‡ so that the center wire loop is easily replaced and the detector housing is easily removed for decontamination purposes.

The sensitivity of the technique as affected by various factors was determined by using glycine-H^3 in 10% isopropanol with a specific activity of 16.5×10^{-4} $\mu c/\mu l$ and glucose-H^3 with a specific activity of 27.0×10^{-4} $\mu c/\mu l$. The tritiated compounds were assayed using the procedure of WILZBACH[2] as modified by CHRISTMAN[3].

PROCEDURE

Seven glycine-H^3 solutions in 10% isopropanol (four standards and three dilutions of the sample) are spotted on a 20×55 cm strip of Whatman No. 1 filter paper buffered at pH 12.0.[4] The seven spots are introduced along a line 7.5 cm from one end of the strip in 1 μl applications using a Gilmont ultramicroburet. The four standard glycine solutions (0.103, 0.206, 0.309 and 0.412 $\mu c/\mu l$) were alternately spotted with the three dilutions of the glycine sample. Spotting the known and unknown in this manner compensate for any change variation in the homogeniety of the paper and chromatographic development conditions across the width of the paper. The filter paper strip is developed for 24 hr in phenol–pH 12.0 buffer (1–1).[4] After solvent development, the chromatogram is dried for 30 min at 60°C, dipped in a solution containing 0.4% ninhydrin plus 4% acetic acid, and then heated for 15 min at 60°C in order to make the glycine spots visible.

A 3.5 cm strip containing the seven glycine-H^3 spots is cut out, taped to the revolving drum of the scanner and then scanned using a 2.0 mm slit width. A typical scanning record is shown in Fig. 2. The heights of the scanning curves of the standards are measured (the record chart contains fifty divisions and each division is assigned an arbitrary value of one) and a straight-line standard curve is prepared by plotting the activity of the known standards against the height of the scanning curves corresponding to these activities (Fig. 3). The heights of

* Glycine-H^3 was purchased from the New England Nuclear Corporation.

† Glucose-H^3 was labeled by exposing it to tritium gas for 5 days at room temperature and purified by recrystallization techniques.

‡ Manufactured by Atomic Accessories, Valley Stream, New York

VOL.
10
1961

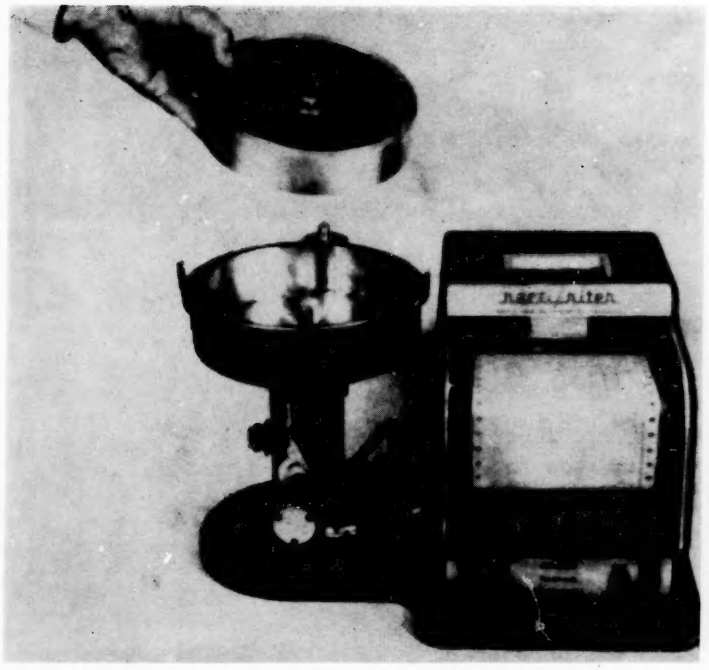

FIG. 1. Automatic windowless chromatogram scanner.

VO
1
19

VOL. 10 1961

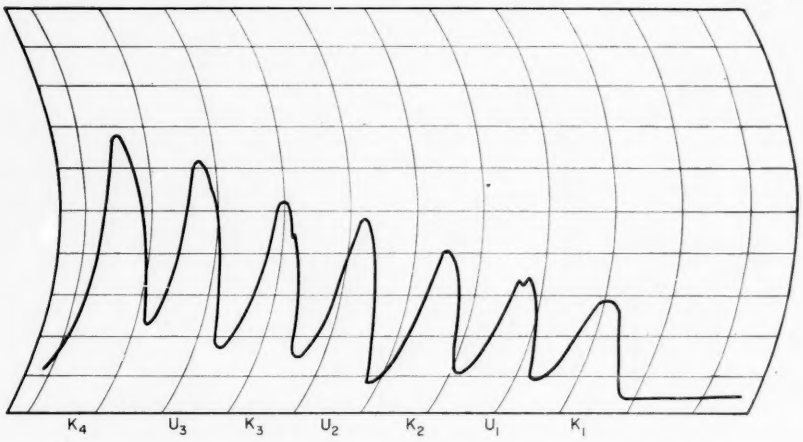

FIG. 2. Typical scanning record using known standards for determining specific activity of glycine-H^3 sample.
Source: glycine-H^3 Count rate setting: 2500 c.p.m. Slit width: 2 mm
$K_1K_2K_3K_4$ = 0.103, 0.206, 0.309, 0.412 μc respectively. Solutions applied to the chromatogram in 1 μl applications. $U_1U_2U_3$ = three dilutions of glycine-H^3 samples being assayed.

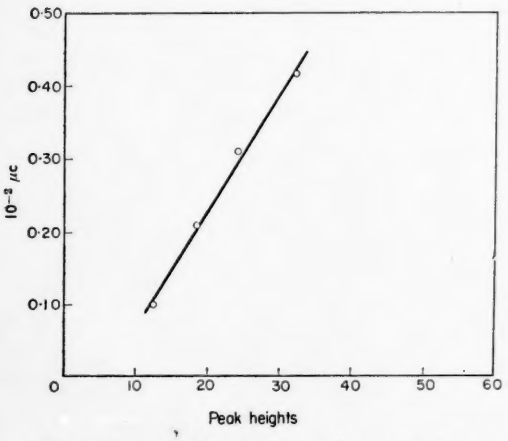

FIG. 3. Relationship of peak height to activity.
Source: glycine-H^3
Count rate setting: 25,000 c.p.m.
Slit width: 2 mm.

the scanning curves of the unknowns are then measured and their specific activities calculated from the standard curve. This procedure did not require the measurement of the areas under the curves, since the height of the curves showed a linear relationship. The activity of the known tritiated compounds used as standards varies depending on the source available. The four glycine-H^3 standards used in this phase were 0.103, 0.206, 0.309 and 0.412 μc/μl, respectively.

The sensitivity of the technique was determined initially as follows.

(1) Both components were applied as 1 μl spots to Whatman No. 1 paper and the strip scanned.

(2) The procedure was repeated and the paper treated with color reagents. The strip containing the glycine was dipped in 0.4% ninhydrin and was then heated at 60°C in a mechanical convection oven for 15 min. The strip containing the glucose was dipped into a solution composed of 3 parts of 0.14% benzidine in butanol plus 1 part of 50% aqueous citric acid, and was heated at 105°C for 5 min.

(3) Glycine was treated as described in the 24 hr solvent development and staining procedure. Glucose was spotted on Schleicher and Schuell No. 589 White Ribbon filter paper and developed for 16 hr in ethyl acetate–pyridine–water (2.5–1.0–3.5) and air-dried for 1 hr. For color development, the chromatogram was dipped into a solution containing 930 mg of aniline and 1.6 g of

phthalic acid (made to 100 ml with water-saturated butanol) and then heated for 20 min at 80°C.

(4) The final scans were obtained by chromatographing the components following which guide strips were cut out and treated with color reagents. The unreacted portions of the chromatograms were cut out and scanned.

RESULTS AND DISCUSSION

Fig. 4(a) is a scan of glycine and glucose applied directly to the paper strip and scanned as such. A minimum of 16.5×10^{-4} μc is detected. When the strips are treated with color reagents as in Fig. 4(b), there is almost a two-fold absorption of the radiation, 33×10^{-4} μc being reliably detected. With solvent and color development, 99×10^{-4} μc can be analyzed with certainty (Fig. 4c). Employing the guide strip technique (1), unreacted portions of the solvent developed chromatogram can be quantitatively scanned when the minimum activity is 33×10^{-4} μc (Fig. 4d).

Table 1 lists the results and error in determining the specific activity of a known solution of glycine-H^3 used as an unknown. Following the chromatographic resolution, the 3.5×20 cm strip containing the ninhydrin-treated glycine-H^3 spots were scanned seven times at a count rate setting of 2500 counts/min using a slit width of 2 mm, P-10 gas as the counting gas, and a drum speed of 15 cm/hr.

The data in Table 1 show that of the seven scans, only one scan resulted in a calculated value of glycine-H^3 which deviated from the theoretical value by as much as

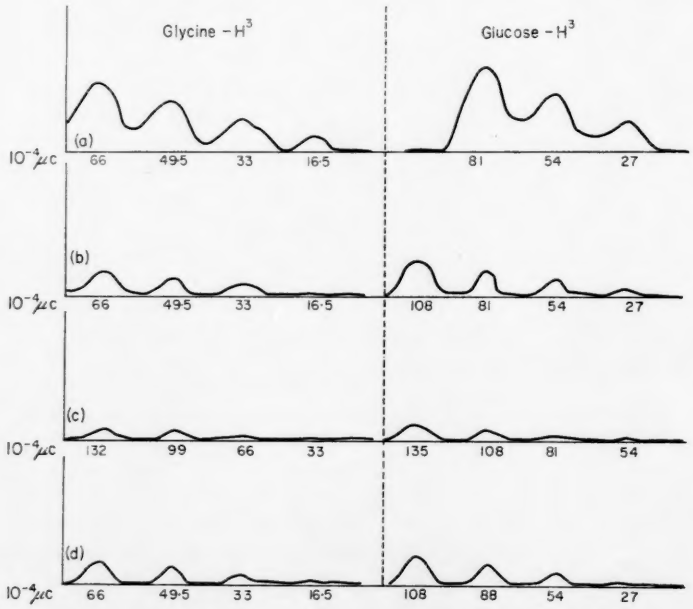

FIG. 4. Effect of solvent development and chromogenic agents on scanning radiochromatograms. (a) Direct application of radiosolutions to paper and scanned as such. (b) Same as (a) except strips are treated with color reagents prior to scanning. (c) Solvent and color development of strips prior to scanning. (d) Solvent development only prior to scanning, using guide strip technique.

VOL. 10 1961

TABLE 1. Calculation of specific activity of glycine-H^3 from scanning curve peak heights using known standards. Descending paper chromatography

	Peak heights*						
	Scan No. 1	No. 2	No. 3	No. 4	No. 5	No. 6	No. 7
Standards 10.3×10^{-2} μc	15.0	15.0	15.3	15.7	15.0	14.5	15.0
20.6×10^{-2} μc	21.0	21.2	20.0	21.0	22.0	20.0	20.0
30.9×10^{-2} μc	25.2	25.5	25.3	26.0	27.3	26.0	26.0
41.2×10^{-2} μc	36.5	34.0	34.5	34.0	35.0	34.0	34.6
Sample 3 μl	18.0	17.8	17.8	18.0	17.3	17.0	17.8
5 μl	23.7	23.7	24.3	25.0	24.3	24.0	23.4
7 μl	30.0	30.5	30.8	31.2	32.7	31.0	31.5
Calculated specific activity (1×10^{-2} μc/μl)	5.3	5.2	5.3	5.3	5.0	5.2	5.3
Percentage deviation from theoretical value (5.2×10^{-2} μc/μl)	2	0	2	2	4	0	2
Average of seven scans	5.2×10^{-2} μc/μl						
Percentage deviation from theory	0						
Standard deviation	1.1×10^{-3} μc/μl						
Coefficient of variation	2.1%						

* Count rate setting = 2500 counts/min; slit width = 2 mm; 1.34 μg of unlabeled glycine superimposed on each spot prior to solvent development.

TABLE 2. Comparison of peak heights of glycine-H^3 before and after treatment of the paper chromatogram with ninhydrin

Activity ($\times 10^{-2}$ μc)†	No ninhydrin peak heights*				Ninhydrin peak heights*			
	2.1	4.2	6.3	8.4	2.1	4.2	6.3	8.4
Scan No. 1	4.3	8.0	11.4	16.0	3.3	5.3	7.0	8.5
Scan No. 2	5.0	9.0	11.0	16.5	3.0	4.9	7.8	8.8
Scan No. 3	4.8	7.3	9.5	15.2	3.7	4.8	7.0	8.0
Scan No. 4	5.0	8.0	11.3	14.5	3.2	5.3	7.0	9.0
Scan No. 5	5.0	8.0	11.3	16.5	3.8	5.2	7.0	8.0
Scan No. 6	4.5	8.5	12.5	16.5	3.0	5.0	7.5	8.3
Average	4.8	8.1	11.2	15.9	3.3	5.1	7.2	8.4

* Scanned at a count rate setting of 1000 c.p.m.; 2.0 mm slit width; P-10 counting gas. Each division of chart assigned an arbitrary value of one.

† Activity applied to the paper in 1 μl applications.

4 per cent. The average value of the seven determinations were equivalent to the theoretical value of 5.2×10^{-2} μc/μl of glycine-H^3. The reproducibility was excellent, a standard deviation calculation gave a value of 1.1×10^{-3} μc/μl.

When the specific activity of the glycine-H^3 solution is high, it is necessary to superimpose an unlabeled glycine solution (1 μl application) on both the standard and unknown spots in order to provide a concentration of glycine which will produce visible spots when the chromatogram is treated with the ninhydrin color reagent. While the color development of glycine-H^3 with ninhydrin introduces an absorption factor which reduces the peak heights by a factor of approximately 1.6 (Table 2), it is

TABLE 3. Calculation of specific activity of glycine-H^3 from scanning peak heights using known standards. Horizontal paper chromatography

	Peak heights*					
	Chromatogram No. 1			Chromatogram No. 2		
	Scan No. 1	No. 2	No. 3	Scan No. 1	No. 2	No. 3
Standards 5.1×10^{-2} μc	8.5	9.6	11.3	10.0	10.2	11.5
Standards 10.3×10^{-2} μc	18.5	22.5	23.2	19.0	22.2	21.5
Standards 15.4×10^{-2} μc	34.3	35.8	35.0	30.7	31.4	32.3
Standards 20.6×10^{-2} μc	43.0	45.0	43.5	44.0	45.0	44.0
Sample 1.5 μl	15.0	16.6	16.4	15.5	16.6	17.3
Sample 2.5 μl	28.0	28.3	29.5	26.0	29.5	29.0
Sample 3.5 μl	39.2	39.5	38.8	36.5	37.6	37.5
Calculated specific activity (1×10^{-2} μc/μl)	5.7	5.2	5.3	5.2	5.3	5.3
Percentage deviation from theoretical value (5.2×10^{-2} μc/μl)	10	0	2	0	2	2
Average of three scans	$5.\_ \times 10^{-2}$ μc/μl			5.3×10^{-2} μc/μl		
Percentage deviation from theory	4			2		

* Scanned at a count rate setting of 1000 counts/min, 2.0 mm slit width.

necessary to make the spots visible so that the 3.5 cm wide strip contains all of the separated glycine-H^3. This is critical if an accurate scan is to be obtained.

The standard curves obtained from known activities are not reproducible from one paper strip to another. Standards are applied each time on the same chromatogram with the unknowns. The necessity for doing this is illustrated by the data contained in Table 1 and Table 3. The data in Table 1 show that even for repeated scans on the same chromatogram the peak heights for identical activities varied for each scan. This may be in part attributed to the effect of residual solvent contributing to the absorption of the weak beta particles and in part attributed to the statistics of counting.

The specific activity of the standards used are governed by the specific activity of the tritiated compounds available for this purpose and also by the specific activity of the sample being analyzed. It is important that the sample is spotted on the filter paper so that the peak heights fall within the same range as the unknowns. This condition is established by preliminary scans.

The error of the assay is lessened by taking the average of three or more determinations. This is easily accomplished by scanning a strip three or more times, calculating the specific activities for each scan, and then averaging the results.

The important step prior to scanning is the separation of the tritiated compounds on the paper chromatograms. The choice of the chromatographic system will determine the amount of labeled compounds placed on the filter paper.

In reference to glycine-H^3, two paper chromatographic systems are available in this laboratory for separating this amino acid in a protein hydrolysate. In addition to the descending paper chromatographic procedure already described in detail, the horizontal paper chromatographic procedure also provides a chromatographic pattern which lends itself to scanning.

When using the horizontal paper technique for the separation of glycine (see Reference[5] for the detailed procedure), the tritiated amino acid is spotted in 0.5 μl applications. Following the 2 hr solvent development at 60°C and color development

VOL. 10 1961

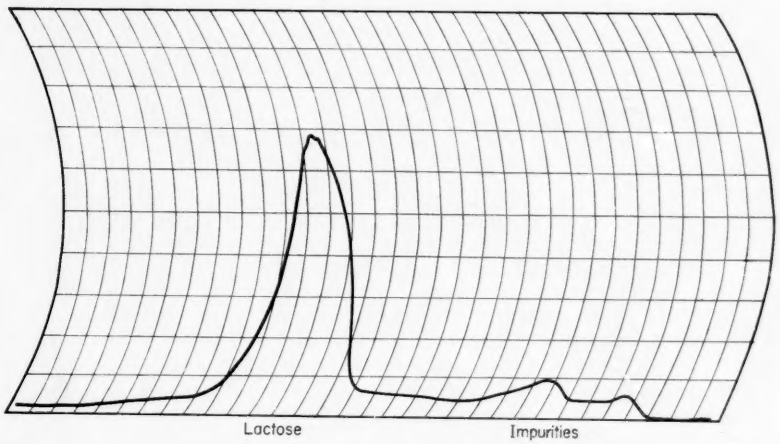

FIG. 5. A scan of a chromatogram of lactose-H^3 (2.92 μc) revealing the presence of radioactive impurities. Count rate setting = 25,000 c.p.m. Slit width = 2 mm. Lactose was exposed to 30 c of tritium gas for 14 days at room temperature and 0.39 atm.

with ninhydrin, the strip is ready for scanning. The width of the filter paper used in horizontal paper chromatography, 12 cm, enables more strips to be scanned at one setting than when the descending chromatograms are used since the latter measure 20 cm in width.

Table 3 lists the results obtained when two separate horizontal paper chromatograms were scanned three times each. In only one out of six scans was the answer completely out of line, resulting in an error of 10 per cent. The other five scans gave results having an error of 2 per cent or less. The average value of the three scans of the first chromatogram gave a value of 5.4×10^{-2} μc/μl which deviated from the theoretical value of 5.2×10^{-2} μc/μl by 4 per cent. The average value of the three scans of the second chromatogram, 5.3×10^{-2} μc/μl, varied by 2 per cent from the theoretical value.

The scanner has been utilized for determining the purity (Fig. 5) of various compounds labeled by the WILZBACH technique. In addition, this radiochromatographic scanning technique has found application in studying transport and metabolism of specific substances.

REFERENCES

1. ROBERTS H. R. and CARLETON F. J. *Analyt. Chem.* **28,** 11 (1956).
2. WILZBACH C. E., KAPLAN L. and BROWN W. G. *Science* **118,** 522 (1953).
3. CHRISTMAN D. R. *Chem. Anal.* **46,** 5 (1957).
4. MCFARREN E. F. and MILLS J. A. *Analyt. Chem.* **24,** 650 (1952).
5. ROBERTS H. R. and KOLOR M. G. *Nature, Lond.* **180,** 384 (1957).

International Journal of Applied Radiation and Isotopes, 1961, Vol. 10, pp. 86–93. Pergamon Press Ltd. Printed in Northern Ireland

Solid Angle Calculations

G. ROWLANDS*
Atomic Energy Research Establishment, Harwell, Berks.

(*First received* 11 *May* 1960 *and in final form* 28 *July* 1960)

An analogy between the calculation of the total solid angle subtended by an aperture at a point or extended source and the calculation of certain electrostatic forces and energies is discussed. It is shown that such solid angle calculations reduce to the evaluation of the electrostatic energies of uniformly charged surfaces.

A collection of formulae for the calculation of the electrostatic energy of uniformly charged surfaces for a range of different shapes is given.

The general method is illustrated by considering the solid angle subtended by circular and rectangular apertures at point, surface and volume sources. In the case of rectangular apertures and for a range of source distributions, the value of the solid angle may be expressed analytically in closed form.

LE CALCUL DES ANGLES SOLIDES

On discute une analogie entre le calcul de l'angle solide total sous-tendu par une ouverture à un point ou à une source étendue et le calcul de certaines forces et énergies électrostatiques. On montre que tels calculs d'angle solide se réduisent à l'évaluation des énergies électrostatiques des surfaces uniformément chargées.

On présente un recueil de formules pour calculer l'énergie électrostatique des surfaces uniformément chargées pour une série de différentes formes.

On exemplifie la méthode générale en considérant l'angle solide sous-tendu par des ouvertures circulaires et rectangulaires à des sources en point, en surface et en volume. Dans le cas des ouvertures rectangulaires et pour une variété de distributions de source, la valeur de l'angle solide peut être exprimée analytiquement en forme fermée.

РАСЧЕТ ТЕЛЕСНОГО УГЛА

Обсуждается аналогия между расчетом общего телесного угла, отвечающего апертуре точечного или не-точечного источника, и расчетом некоторых электростатических сил и энергий. Показано, что такие расчеты телесного угла аналогичны оценке электростатической энергии равномерно заряженных поверхностей.

Приводится ряд формул для расчета электростатической энергии равномерно заряженных поверхностей различной формы.

В качестве иллюстрации общего метода рассматривается телесный угол, отвечающий круглым и прямоугольным апертурам точечных, плоских и объемных источников. В случае прямоугольных апертур, в пределах некоторой области распределения источников, значение телесного угла получает точное аналитическое выражение.

RAUMWINKELBERECHNUNGEN

Eine Analogie zwischen der Berechnung des Raumwinkels begrenzt durch eine Apertur für eine Punktquelle oder eine ausgedehnte Quelle und der Berechnung von gewissen elektrostatischen Kräften und Energien wird diskutiert. Es wird gezeigt, dass diese Raumwinkelberechnungen sich zu einer Bestimmung von elektrostatischen Energien einer aufgeladenen Fläche reduzieren.

Eine Formelsammlung für die Berechnung der elektrostatischen Energie einer gleirhföcmig aufgeladenen Fläche verschiedener Gestalt wird gegeben.

* Harwell Junior Research Fellow.

Die allgemeine Methode wird erläutert durch Betrachtung des Raumwinkels bei kreisförmiger und rechtwinkeliger Apertur für Punkt-, Flächen- und Volumsquellen. Für rechtwinkelige Apertur und für eine Reihe von Quellenverteilungen kann der Wert für den Raumwinkel analytisch in geschlossener Form dargestellt werden.

VOL. 10 1961

1. INTRODUCTION

In a number of distinct problems in the field of radiation physics, for example the calculations of the efficiency of counters, the fraction of the total radiation emitted from a source which passes through an aperture system is required. In this paper we shall neglect any absorption of the radiation as it passes from the source to the aperture system. Then the fraction emitted from a point source, emitting isotropically, which passes through any surface is simply the solid angle Ω subtended by this surface at the source point divided by the total solid angle, namely 4π. This fraction, which is called the geometry G, is, for a point source at the point r_2 and any aperture, given by

$$G_p(r_2) = \frac{1}{4\pi}\int_{S_1}\frac{r_{12}\cdot dS_1}{|r_{12}|^3}, \qquad (1.1)$$

where r_{12} is the vector distance from the point source to an element of area dS_1 of the aperture. The integration is over the surface of the aperture. The geometry G_S for a surface distribution which emits isotropically is given by

$$G_S = \frac{1}{4\pi S_2}\int_{S_1}\int_{S_2}\frac{r_{12}\cdot dS_1}{|r_{12}|^3}\,dS_2, \qquad (1.2)$$

while the geometry G_V for a volume distribution of such sources takes the form

$$G_V = \frac{1}{4\pi V_2}\int_{S_1}\int_{V_1}\frac{r_{12}\cdot dS_1}{|r_{12}|^3}\,dV_2. \qquad (1.3)$$

It is shown in the next section that the calculation of these G factors is related quite simply to the calculation of the electrostatic energy of uniformly charged surfaces.

The author[7] has shown that the calculation of coefficients of inductances may also be reduced to the calculation of electrostatic energies of uniformly charged surfaces. By making use of this analogy and also by direct calculation quite a large amount of information has been accumulated for the calculation of electrostatic energies, and this is discussed in Section 3.

This information may be used in conjunction with the results obtained in Section 2 to obtain formula for the calculation of G_Ss and G_Vs for a range of geometric shapes, and a number of illustrative examples are considered in Section 4.

Garrett[2] has independently pointed out the analogy between inductance calculations and the calculation of G factors. However, the full advantages of using these analogies is only obtained by expressing the G factors in terms of electrostatic energies. Of course inductance calculations can be used and in fact have been used to obtain the electrostatic energies.[7]

2. GENERAL METHOD

The geometry G_p for a point source is given by equation (1.1). Using the identity

$$\text{grad}\,(1/|r_{12}|) = \frac{r_{12}}{|r_{12}|^3}, \qquad (2.1)$$

and by changing the order of integration and differentiation, (1.1) may be transformed into the form

$$G_p(r_2) = \frac{1}{4\pi}\left|\frac{d}{dn}\int\frac{dS_1}{|r_{12}|}\right|. \qquad (2.2)$$

n is the perpendicular distance of the point r_2 from the surface S_1. The straight brackets denote the modulus. (In later equations these will be omitted. This should cause no confusion if it is remembered that G factors are always positive.) The integral term is equal to the electrostatic energy of a uniformly charged surface S_1 of unit charge density and a unit point charge at r_2; G_p is thus proportional to the magnitude of the

force acting between these charge distributions.

This result may be obtained in a more physical manner in the following way. As is well known, the magnetic potential at any point due to a current-carrying loop is proportional to the solid angle subtended by the loop at that point. Further, the potential due to such a loop is proportional to the potential due to a sheet of magnetic dipoles (see for example COULSON[1], Chap. 6). Thus the solid angle subtended by any aperture is proportional to the magnetic potential due to a dipole sheet of the same cross-sectional area as the aperture.

Now the dipole sheet may be considered as two uniformly charged sheets of opposite sign which are very close together. Thus if we denote by $q\phi_p(r)$ the potential at r due to a uniformly charged sheet of charged density q, then the potential due to two adjacent sheets of opposite charge, a perpendicular distance dl apart, is given by

$$q\phi_p(r) - q\phi_p(r - dl).$$

For small values of dl we may expand the second term in a Taylor's series to obtain

$$\frac{d\phi(r)}{dn}\, q\, dl + \text{higher terms},$$

where n is the normal to the charge sheet. In the limit as $dl \to 0$, $q\, dl$ equals the dipole moment, m, and the higher terms in the above go to zero, so that the potential due to a dipole sheet is given by

$$m \frac{d\phi_p}{dn}(r).$$

Combining the above results, we see that the solid angle subtended at a point by any aperture is proportional to the gradient of the potential at that point due to a uniformly charged surface of the same cross-section as the aperture. This result is expressed mathematically by (2.2).

In a similar manner, the geometry G_S for a surface distribution of radiation, which is defined by (1.2), may be expressed in the form

$$G_S = \frac{1}{4\pi S_2} \frac{d}{dn} \int_{S_1} \int_{S_2} \frac{dS_1\, dS_2}{|r_{12}|}. \qquad (2.3)$$

Here n is the perpendicular distance from the aperture to any representative point on the surface of the source. The integral term is proportional to the electrostatic energy of two uniformly charged surfaces, and thus G_S is proportional to the magnitude of the force between these two surfaces.

Here, as above, we may consider the aperture as a dipole sheet and the source as a uniformly charged surface. Then the G_S factor is proportional to the potential energy of such a system which itself is proportional to the gradient of the potential energy (that is the force) due to two uniformly charged surfaces, one replacing the aperture and the other replacing the source. This is expressed mathematically by (2.3).

The geometry G_V for a volume distribution of sources is given by (1.3). Using the identity

$$dS_1 . \text{grad}_2\left(\frac{1}{|r_{12}|}\right) = \text{div}_2\left(\frac{dS_1}{|r_{12}|}\right), \qquad (2.4)$$

where the suffix on the operators denotes the set of co-ordinates on which they act, and the identity given by (2.1), (1.3) may be transformed, on applying Gauss's theorem, to the form

$$G_V = \frac{1}{4\pi V_2} \int_{S_1} \int_{S_2} \frac{dS_1 \mathbf{n} \,.\, dS_2}{|r_{12}|}, \qquad (2.5)$$

where $\mathbf{n}$ is a unit vector perpendicular to the surface S_1. G_V is thus proportional to the electrostatic energy of a uniformly charged surface S_1 and a surface distribution of density $\mathbf{n} \,.\, dS_2$ over the surface enclosing the source. In a number of cases of practical interest, the above integration reduces to the sum of terms each proportional to the electrostatic energy of uniformly charged surfaces. This result may also be obtained by using the physical arguments given above and used to derive (2.2) and (2.3).

The above method of calculating G factors may be summarized as follows: (1) we replace the aperture by a uniformly charged surface and the source distribution by a charge distribution; that is, a point source by a point charge and a surface source by a surface distribution of charge; (2) we then calculate the potential energy of such a

charge distribution; and finally (3) find the gradient of this potential with respect to the normal to the aperture surface, that is, calculate the force between these two charge distributions. This latter quantity is then proportional to the G factor.

Thus the calculation of the geometric factors G_p, G_S and G_V reduces to the calculation of the electrostatic force or electrostatic energy of uniformly charged surfaces. Formulae for the calculation of such energies are discussed in the next section. The calculation of the force degenerates to a simple differentiation of the energy expression.

3. ELECTROSTATIC ENERGIES

Rectangular surfaces

The mutual energy of uniformly charged similarly orientated parallel rectangular surfaces has been discussed in detail by RHODES and the author[6]. It is found that the mutual energy of any two such surfaces may be expressed in terms of a single function $F(p,q)$ where

$$\begin{aligned} F(p,q) = {} & (p^2 - q^2)\phi\{1/(p^2 + q^2)^{1/2}\} \\ & + p(1 - q^2)\phi\{p/(1 + q^2)^{1/2}\} \\ & + pq^2\phi(p/q) + q^2\phi(1/q) \\ & + 2pq \tan^{-1}\{q(1 + p^2 + q^2)^{1/2}/p\} \\ & - \pi pq - \tfrac{1}{3}(1 + p^2 - 2q^2) \\ & \times (1 + p^2 + q^2)^{1/2} + \tfrac{2}{3}q^3 \\ & + \tfrac{1}{3}(1 - 2q^2)(1 + q^2)^{1/2} \\ & + \tfrac{1}{3}(p^2 - 2q^2)(p^2 + q^2)^{1/2} \end{aligned} \tag{3.1}$$

where $\phi(x) = \sinh^{-1} x$.

Numerical values for $F(p,q)$ are given in[6] for $p = 0$ (0·1) 1·1 and $q = 0$ (0·1) 1·6. Series expressions are also given which may be used to calculate values of $F(p,q)$ for values of p and q outside this range.

In terms of $F(p,q)$, the mutual energy of two identical equally charged rectangles with sides of length a and b lying opposite each other in parallel planes a distance c apart is given by

$$E_m = 2a^3F(p,q), \tag{3.2}$$

where $p = b/a$ and $q = c/a$. The mutual energy of two similarly orientated strips of length a and widths b_1 and b_2 separated by a distance d_{12} in a direction perpendicular to the edge of length a and lying in parallel planes a distance c apart is

$$\begin{aligned} E_m = {} & a^3\{F(p_1 + p_2 + r,q) + F(r,q) \\ & - F(p_1 + r,q) - F(p_2 + r,q)\}, \end{aligned} \tag{3.3}$$

where

$$p = b/a, \quad q = c/a \quad \text{and} \quad r = d_{12}/a.$$

Similar expressions may be obtained for the mutual energy of the more general charge distributions mentioned above. These may be obtained from the more detailed discussion given elsewhere.[6]

The mutual energy of uniformly rectangular surfaces which are parallel along one edge only has been discussed by the author[7] but the formula are quite complicated and will not be reproduced here.

Circular surfaces

The electrostatic energy of two uniformly charged circular surfaces in various geometric positions has been obtained by using the analogy with certain inductance calculations.[7] Only the final results will be given here.

We define the mutual energy, E_m, of two parallel coaxial uniformly charged disks, each with unit charge density, by

$$E_m = R(r_1,r_2,d), \tag{3.4}$$

where r_1 and r_2 are the radii of the disks and d the perpendicular distance between them. Then

$$R(r,r,d) = 4\pi r^3\left[\frac{4}{3} - \pi\beta\{1 - K(\beta)\}\right], \tag{3.5}$$

where $\beta = d/2r$ and $K(\beta)$ is a function of β only. NAGAOKA and SAKURAI[5] have tabulated $K(\beta)$ and $\ln\{K(\beta)\pi^2\}$ for $\beta = 0{\cdot}0$ (0·001) 1, $1/\beta = 0{\cdot}0$ (0·001) 1 and for $k^2 = 1/(1 + \beta^2) = 0{\cdot}0$ (0·001)1, correct to six decimal places. An abridged version of these tables is given by GROVER[3] with values

VOL. 10 1961

for $\beta = 0{\cdot}0\ (0{\cdot}01)1$ and $1/\beta = 0{\cdot}0\ (0{\cdot}01)1$. For $\beta \to 0$

$$\frac{R(r,r,d)}{4\pi r^3} = \frac{4}{3} - 4\pi\beta + 2\beta^2 \times \{\ln(4/\beta) - 1/2\} + \ldots \quad (3.6)$$

and for $1/\beta \to 0$

$$= \pi \sum_{n=0} \frac{(-1)^n(2n)!(2n+2)!}{n!\{(n+1)!\}^2(n+2)!} \frac{1}{2^{4n+3}} \frac{1}{\beta^{2n+1}} \quad (3.7)$$

For disks of unequal radii

$$R(r_1,r_2,d) = 2\pi\alpha^2 r_1^3 \left\{\frac{1}{p}\beta(\alpha,p^2) - 2\beta\right\}, \quad (3.8)$$

where

$$\alpha = r_2/r_1,\ \beta = d/2r_1,$$

and

$$p^2 = 1/(1 + 4\beta^2).$$

The function $B(\alpha,p^2)$ is tabulated by GROVER[3] for $\alpha = 0{\cdot}0\ (0{\cdot}05)1$ and $p^2 = 0{\cdot}0\ (0{\cdot}05)1$ to six decimal places. By far the more important is a series expression for $B(\alpha,p^2)$ which converges for all values of α and d.

$$B(\alpha,p^2) = \sum_{n=0}^{\infty} B_{2n}(p^2) \cdot (\alpha p)^{2n}, \quad (3.9)$$

where

$$B_0 = 1,\ B_2 = p^2/8,\ B_4 = p^2(5p^2 - 4)/64,$$

and

$$B_6 = 5p^2(21p^4 - 28p^2 + 8)/1024.$$

For parallel non-coaxial circular disks with their axes displaced a distance t,

$$E_m = \pi^2\alpha r_1^3 \sum_{n=0} \times \frac{(-1)^n F(-n-1, -n, 2, \alpha^2) S^{2n}(2n)!\, P_{2n}(qs)}{(n+1)!\, n!\, 2^{2n}}; \quad (3.10)$$

where $s^2 = r_1^2/(d^2 + t^2)$, $q = d/r_1$, $F(\ldots)$ is a hypergeometric function and P_n, a Legendre polynomial.

Series expression for E_m for non-parallel circular disks have been obtained[7] but are complicated and will not be reproduced here.

Other shapes

Closed expressions may be obtained for parallel polygonal surfaces of any numbers of sides by a method described by the author.[7] These expressions, which in general are complicated, are however all expressable in terms of a single function of three variables.

The author is unaware of any results that may be used to obtain electrostatic energies of uniformly charged surfaces of shapes other than those discussed above.

4. EXAMPLES

In this section a few examples are discussed to illustrate the general methods developed above.

Point sources

The G factor for a point source and circular aperture has been discussed in detail by JAFFEY[4] and GARRETT[2].

The potential due to a uniformly charged rectangular surface has been discussed.[6] Using some of the results given in[6] and equation (2.2), it may be shown that for such a surface

$$4\pi G_p(x,y,z) = \Psi(x,y,z) + \Psi(x,b-y,z) + \Psi(a-x,y,z) + \Psi(a-x,b-y,z), \quad (4.1)$$

where x, y, z are the co-ordinates of the point source relative to an origin at one corner of the rectangular surface with z the perpendicular distance from the point to the plane of

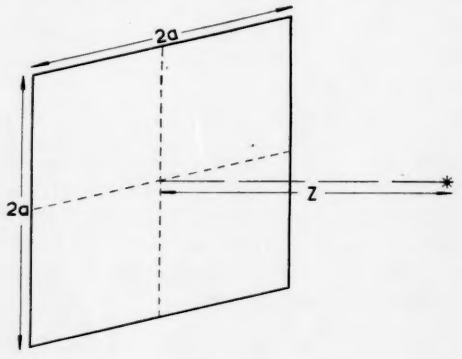

FIG. 1.

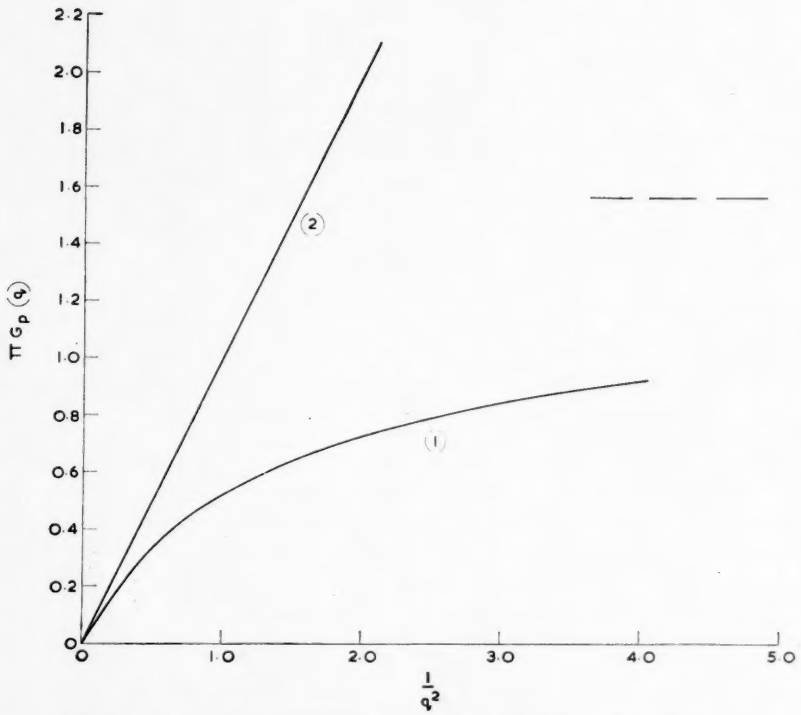

FIG. 2. The geometry G_p for a square rectangular aperture of side $2a$ and a point source a perpendicular distance z ($= aq$) from the centre of the aperture. (1) gives $\pi G_p(q)$ as a function of $1/q^2$; the broken line shows the limiting value for $q = 0$, namely $\pi/2$; (2) corresponds to the approximation $\pi G_p(q) = 1/q^2$.

the surface. a and b are the dimensions of the aperture in the x and y directions respectively.

The function $\Psi(x,y,z)$ is given by

$$\Psi(x,y,z) = \tan^{-1}\left\{\frac{xy}{z\sqrt{x^2+y^2+z^2}}\right\}. \tag{4.2}$$

It is readily seen that the above result may be used to obtain the G_p factor for a point source and any aperture which may be decomposed into a finite number of non-overlapping rectangular apertures.

For example, suppose we need to calculate the G_p factor appropriate to a point source a perpendicular distance z above the centre of a square aperture of side $2a$ (Fig. 1). Then, from above, the G_p factor is the sum of the G_p factors appropriate to the four square surfaces of sides a whose corners meet immediately below the source point. The G_p factor for each of these surfaces is given by (4.1) with $x = 0$, $y = 0$, $a = b$, so that the total G_p factor is given by

$$G_p = \frac{1}{\pi}\Psi(a,a,z)$$

which from (4.2) may be written in the form

$$G_p(z) = \frac{1}{\pi}\tan^{-1}\left(\frac{1}{q\sqrt{2+q^2}}\right),$$

where $q = z/a$. This function is shown graphically in Fig. 2.

Plane sources

The G factor for a circular source, coaxial and parallel with a circular aperture, is obtained by applying equation (2.3) to the particular form for the equivalent electrostatic energy given by (3.8). In this way we find

$$G_S(r_1,r_2,d) = \tfrac{1}{2} - \beta p C(\beta,p) \tag{4.3}$$

where

$$C(\beta,p) = \sum_{n=0}^{\infty} (\alpha p)^{2n} C_{2n}(p^2), \qquad (4.4)$$

and

$$C_0 = 1, \quad C_2 = -3p^2/8,$$
$$C_4 = -p^2(35p^2 - 20)/64,$$
$$C_6 = \frac{-5p^2}{1024}(231p^4 - 212p^2 + 56). \qquad (4.5)$$

This series converges for all values of the perpendicular distance d between the source and aperture. Where the source and aperture are of equal radii, formula (3.5), (3.6) or (3.7) may be used instead of (3.8) to obtain expressions for G_S.

Consider a circular source of radius 1 cm a perpendicular distance of 1·5 cm from a parallel coaxial aperture of radius 2 cm. In the above notation $r_1 = 1$, $r_2 = 2$, $d = 1{\cdot}5$ so that $\alpha = 2$, $\beta = 0{\cdot}75$ and $p^2 = 4/13$. Substitution of these values for α, β and p^2 in (4.3), (4.4) and (4.5) gives the appropriate G_S factor to be equal to 0·1298.

For a rectangular source and a similarly orientated rectangular aperture lying in a parallel plane, the G_S factor may, by analogy with the results given in Section 3, particularly equations (3.3) and (3.2), be expressed in terms of $\partial F(p, q)/q\partial$. It is readily shown from (3.1) that

$$\frac{\partial F(p, q)}{\partial q} = H(p, q) = 2q\phi\{1/(p^2 + q^2)^{1/2}\} + 2pq\phi\{p/(1 + q^2)^{1/2}\} - 2pq\phi(p/q) - 2q\phi(1/q) + \pi p - 2q^2 - 2p\tan^{-1}\{q(1 + p^2 + q^2)^{1/2}/p\} + 2q(p^2 + q^2)^{1/2} + 2q(1 + q^2)^{1/2} - 2q(1 + p^2 + q^2)^{1/2}. \qquad (4.6)$$

The exact form for the G factor may be obtained by replacing $a^3F(p, q)$ by $a^2H(p,q)$ in the expression for the equivalent electrostatic energy and then dividing by $4\pi S_2$.

For example, consider a rectangular aperture of side a_1 and b_1 a perpendicular distance c from a similarly orientated rectangular source of side a_2 and b_2 with the centres of both rectangular surfaces lying on the perpendicular drawn between their centres. From the results given in[6] it may be shown that the equivalent electrostatic energy E_m is given by

$$E_m = 2\bar{a}^3\{F(\bar{b}/\bar{a}, c/\bar{a}) - F(b'/\bar{a}, c/\bar{a})\} - 2(a')^3\{F(\bar{b}/a', c/a') - F(b'/a', c/a')\}, \qquad (4.7)$$

where $\bar{a} = |a_1 + a_2|/2$, $a' = |a_1 - a_2|/2$ and similarly for the bs. If this result is used in conjunction with (2.3) with c replacing n, we find that

$$4\pi G_S = \frac{2\bar{a}^2}{a_2 b_2}[H(\bar{b}/\bar{a}, c/\bar{a}) - H(b'/\bar{a}, c/\bar{a})] - \frac{2(a')^2}{a_2 b_2}[H(\bar{b}/a', c/a') - H(b'/a', c/a')]. \qquad (4.8)$$

For example, consider a source of 1 cm square and an aperture 2 cm square a perpendicular distance 1·5 cm apart. In the above notation the bs equal the as and $a_1 = 1$, $a_2 = 2$ and $c = 1{\cdot}5$ so that $\bar{a} = 1{\cdot}5$, and $a' = 0{\cdot}5$. From (4.8) we then have

$$4\pi G_S = \frac{9}{8}\left\{H(1, 1) - H\left(\frac{1}{3}, 1\right)\right\} - \frac{1}{8}\{H(3, 3) - H(1, 3)\}.$$

Using (4.6) to evaluate the Hs we find that in this particular case $G_S = 0{\cdot}02358$.

Volume sources

We consider a source in the shape of a rectangular parallelepiped of length c and cross-sectional area $a \times b$, and an aperture of the same shape as this cross-section, lying coaxial with the source and in a plane parallel to the end planes of the source. The perpendicular distance between the aperture and the nearest end we take as d, so that the perpendicular distance between the aperture and furthest end is $d + c$. The G_V factor is given by (2.5) and in this particular case the surface integral over S_2 degenerates into a contribution of opposite sign from each end of the source. The equivalent electrostatic energy is readily obtained from (3.2). In this manner we find

$$4\pi G_V = \frac{2a^2}{bc}\{F(b/a, d/a) - F(b/a, (d + c)/a)\}. \qquad (4.9)$$

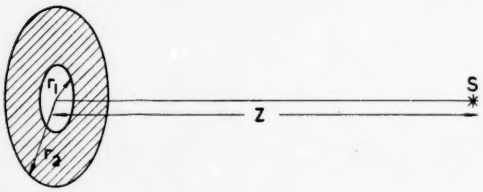

FIG. 3. The shaded area represents the aperture, whilst S denotes the source.

Other aperture shapes

So far we have only discussed circular and rectangular apertures. However the above results may be used to obtain the G factors for apertures of other shapes. These other shapes are best discussed with reference to a particular example.

Consider an aperture in the form of a circular disk of outer radius r_2 and inner radius r_1. The G factor is simply the difference between the G factor for a circular surface of radius r_2 and one of radius r_1. This result is seen directly from the form of the expressions for the G factors. The integration over the surface S_1 may be rearranged to be the difference of two terms, one being an integration over a circular surface of radius r_2 and the other over a similar surface of radius r_1.

For example consider a point source lying on the axis of such an aperture a distance z from the centre (Fig. 3). Now the G_p factor for a point source on the axis of a circular disk of radius r and a perpendicular distance z from the centre is given by the well-known formula

$$G_p(r, z) = \frac{z}{2}\left\{\frac{1}{z} - \frac{1}{\sqrt{r^2 + z^2}}\right\}.$$

Hence the G_p factor appropriate to the aperture shown in Fig. 3 is given by

$$\begin{aligned} G_p &= G_p(r_2, z) - G_p(r_1, z) \\ &= \frac{z}{2}\left\{\frac{1}{\sqrt{r_1^2 + z^2}} - \frac{1}{\sqrt{r_2^2 + z^2}}\right\}. \end{aligned}$$

REFERENCES

1. COULSON C. A. *Electricity*, Oliver and Boyd, London (1951).
2. GARRETT M. M. *Rev. Sci. Instrum.* **25,** 1208 (1954).
3. GROVER F. W. *Inductance Calculations*, Van Nostrand, New York (1947).
4. JAFFEY A. H. *Rev. Sci. Instrum.* **25,** 349 (1954).
5. NAGAOKA H. and SAKURAI S. *Scientific Papers of Tokyo Institute of Physics* Table II, pp. 69–180 (1927).
6. RHODES R. and ROWLANDS G. *Proc. Leeds Phil. Lit. Soc.* **6,** 191 (1954).
7. ROWLANDS G. Thesis, Leeds (1956).

VOL. 10 1961

International Journal of Applied Radiation and Isotopes, 1961, Vol. 10, pp. 94–98. Pergamon Press Ltd. Printed in Northern Ireland

Proteolysis of I^{131}-Labelled Gamma-Globulin

V. Bocci
National Institute for Medical Research, Mill Hill, London

(*First received* 7 *July* 1960 *and in final form* 1 *September* 1960)

The proportion of iodide in a papain digest of I^{131}-labelled denatured γ-globulin is negligible whilst after acid hydrolysis it is more than 85 per cent.

On the basis of this observation the measurement of TCA-soluble radioactivity as a procedure for estimating enzymic proteolysis of labelled globulins is justified. Using double labelling, the rates of digestion of native and altered γ-globulins are compared.

LA PROTEOLYSE DE LA GAMMA-GLOBULINE MARQUEE D'I^{131}

La proportion d'iode dans un digeste en papaïne de la γ-globuline dénaturée et marquée d'I^{131} est négligeable, mais après l'hydrolyse acidique elle revient à plus de 85 pour cent.

Vu cette observation on justifie la mesure de la radioactivité soluble en TCA comme procédé pour le dosage de la protéolyse des globulines marquées. En employant les marques doubles, on compare les taux de digestion des γ-globulines naturelles et altérées.

ПРОТЕОЛИЗ γ-ГЛОБУЛИНА, МЕЧЕНОГО I^{131}

В продуктах протеолиза папаином денатурированного γ-глобулина, меченого I^{131}, обнаруживается незначительное количество иодида, в то время как при кислотном гидролизе количество иодида доходит до 85%.

Это наблюдение подтверждает правильность метода измерений радиоактивности в ТХУ-растворимой фракции для оценки глубины протеолиза меченых глобулинов. Скорости переваривания нативного и модифицированного γ-глобулинов сравниваются при помощи двойной метки.

PROTOLYSE VON I-131-MARKIERTEM γ-GLOBULIN

Der Jodanteil bei Papain-Aufspaltung von I-131-markiertem, denaturiertem γ-Globulin ist vernachlässigbar klein, während er nach Säurehydrolyse mehr als 85% beträgt.

Auf Grund dieser Erkenntnisse erscheint die Messung der TCA-löslichen Aktivität als Methode zur Bestimmung der enzymatischen Protolyse von markierten Globulinen gerechtfertigt. Unter Verwendung von doppelter Markierung wurde die Geschwindigkeit der Aufspaltung von nativen und veränderten Globulinen miteinander verglichen.

It is well known that denatured proteins are readily digested by enzymes in conditions in which native proteins are partially resistant or are only slowly hydrolysed.[1,2,3] While investigating the biological behaviour of heat-denatured I^{131} rabbit γ-globulins, we have tried to obtain a relative measure of their degrees of denaturation by comparing their rates of hydrolysis with papain.

The progress of proteolysis has been followed in different ways, among which are the following: measurement of acid-soluble non-protein nitrogen[4], alkalimetric titration of charged ammonium groups of amino acids and peptides[5], determination of tyrosine[6], and estimation of the proportion of acid-insoluble protein by various methods.

Arising out of an interest in I^{131}-labelled γ-globulin, the possibility that different degrees of hydrolysis can be estimated correctly by measuring the progressive increase of TCA-soluble radioactivity has been examined with results which are reported here.

VOL. 10 1961

EXPERIMENTAL

Rabbit gamma-globulin was prepared by chromatography using D.E.A.E. cellulose according to SOBER *et al.*[7,8]. Only the slower fraction of γ-globulin was used in these experiments. Iodination was performed with I^{131} or with I^{125} using MCFARLANE's method[9]. Denaturation of the I^{131} γ-globulin was effected by heating within a wide range of temperatures (60–100°C) in a water bath thermostatically regulated to within $\pm 0{\cdot}1$°C with continuous shaking. Unless otherwise indicated the γ-globulin was dissolved in 0·1 M phosphate buffer pH 7, the concentration of the protein being 0·1–0·5 per cent.

Papain digestion of native or denatured γ-globulin was carried out according to KIMMEL and SMITH[10]. Crystalline papain (Worthington Biochemical Corp., New Jersey) was used in a ratio of 0·5—1 mg/100 mg γ-globulin. To 1 ml of the substrate was added 1 ml phosphate buffer pH 7 containing 0·02 M cysteine and 4 mM ethylenediamine tetra-acetate and the enzyme. Toluene (0·1 ml) was then added with traces of NaI, mono-iodotyrosine and di-iodotyrosine. The solutions were incubated, some at 7°C and the others at 37°C up to a maximum of 136 hr, and samples of 0·1 ml or less were removed at intervals and diluted with 0·5 ml of 10% carrier albumin (Lister) and saline to a final volume of 2 ml. Traces of NaI, MIT and DIT were again present. The samples were measured for total radioactivity in a well-type scintillation counter and then precipitated by adding 1 ml 30% trichloroacetic acid. After shaking and, if necessary, repeated centrifugation, 2 ml of perfectly clear supernatant was measured for TCA-soluble radioactivity.

Heat denaturation in the temperature range 60–100°C releases only 0·1–2·5 per cent of the radioactivity from I^{131} γ-globulin. Also the increase in TCA-soluble radioactivity in the samples incubated at 37°C without papain is very small, reaching a maximum of 2·4 per cent after 95 hr. In any case, blank determinations on solutions without papain were carried out at the same time and corrections for TCA-soluble radioactivity applied to the data. Duplicate determinations were generally made.

In other experiments the increase of TCA-soluble radioactivity was measured only at the end of the enzymatic reaction. Residual protein was precipitated with 30% TCA and measured according to GORNALL *et al.*[11]. To estimate the distribution of radioactivity after papain digestion, or after hydrolysis of the rabbit I^{131} γ-globulin with 6 N HCl, the digests were subjected to filter paper (Whatman No. 3) chromatographic analysis. The descending, one-dimensional chromatograms were developed at room temperature with n-butanol, acetic acid, water (vol/vol/vol = 4:1:5)[12], and for two-dimensional chromatography the second solvent used was phenol in the presence of NaCN and NH_3.[13] The papers were sprayed with ninhydrin reagent or with α-nitroso-β-naphthol according to ACHER and CROCKER[14]. Location of I^{131} and of added carrier was determined using 1% palladium chloride.[15] Radioactive spots were localized by scanning or by autoradiography and, for quantitative estimations, the papers were cut in small segments (1×2 cm), put in counting tubes with 2 ml of 3% NaOH and their radioactivity measured in a scintillation counter. The proportion of free I^{131} is expressed as a percentage of the total radioactivity found on each chromatogram. When two isotopes were used, their radiations were measured separately with the help of a pulse analyser.

RESULTS AND DISCUSSION

The main aim of this work was to study the radioactivity distribution after cleavage of I^{131} γ-globulin with papain, but it was interesting at the same time to compare the distribution of radioactivity in acid (HCl) hydrolysate of the same material. Because deiodinase can dehalogenate mono-iodotyrosine and di-iodotyrosine[16], it was important

to ascertain if papain has any deiodinating activity since, in such a case, the measurement of TCA-soluble radioactivity would be valueless.

The percentage distribution of radioactivity corresponding to the Rf is given in Fig. 1, the pictures being completely different after enzymatic and acid proteolysis. In the acid hydrolysate the spot of I^{131}-iodide is elongated due to oxidation of iodide to iodine with a much greater Rf, and about 90 per cent of the radioactivity appears in this area. In the enzyme-digested material only about 3 per cent of the radioactivity is free. No upward displacement of the iodide spot was seen in this case. About 73 per cent of the radioactivity is within Rf 0·70–0·84 and from ACHER's reaction it seems linked to small peptides containing I^{131}-tyrosine. No attempts at further identification were made.

To avoid the possibility of overlapping, two-dimensional chromatograms were carried out. In fact the iodide spot in the two-dimensional chromatograms of the enzymatic digest contained less than 0·4 per cent of the total radioactivity, while the same spot on the acid hydrolysate chromatogram contained more than 85 per cent.

Therefore we conclude that papain in the course of hydrolysing heat-denatured I^{131} γ-globulin causes the proportion of radioactive acid-soluble split products to increase progressively without having any deiodinating action.

On these findings it is reasonable to use the amount of TCA-soluble radioactivity as a measure of proteolysis. This is more evident from Tables 1 and 2 in which it will also be noted that the rate of hydrolysis is quite different when papain is added to normal or to denatured I^{131} γ-globulin. The results obtained with this technique agree well

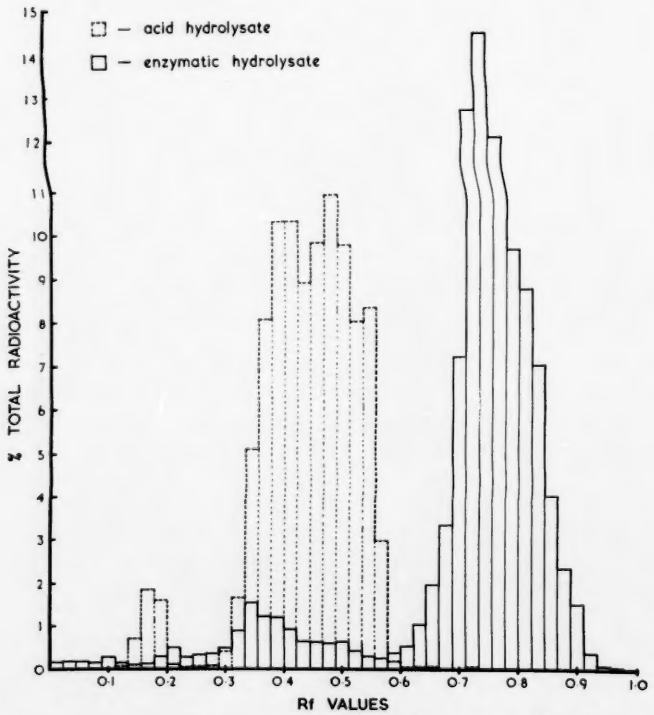

FIG. 1. Distribution of I^{131} in a paper chromatogram of an enzymatic hydrolysate and of an acid hydrolysate of heat-denatured rabbit I^{131} γ-globulin (100°C—5 min).

TABLE 1. Percentage TCA-soluble radioactivity in supernatant after hydrolysis of γ-globulin (1·1 mg/ml) with papain. Incubation at 7°C

Rabbit I^{131} γ-globulin		Time (hr)				
		0	14	24	48	136
Normal		0	0·7	0·9	1·1	1·6
Denatured by heat	60°C—30 min	0	2·0	2·3	2·8	3·6
	70°C—10 min	0	4·4	5·0	5·2	5·9
	70°C—30 min	0	6·7	7·7	8·4	9·6

TABLE 2. Percentage TCA-soluble radioactivity in supernatant after hydrolysis of γ-globulin (1·8 mg/ml) with papain—*a* and *b* incubated at 7°C, *c* and *d* incubated at 37°C

Rabbit I^{131} γ-globulin	Time (hr)					
	0	*1·5*	*3*	*7*	*24*	*95*
(a) Normal	0	—	—	0·50	0·90	1·40
(b) Heat denatured (70°C—30 min)	0	—	—	4·3	6·2	8·1
(c) Normal	0	1·1	1·9	2·9	6·5	9·4
(d) Heat denatured (70°C—30 min)	0	6·7	8·7	11·7	18·5	24·9

TABLE 3. Percentage TCA-soluble radioactivity in supernatant, after 60 hr incubation at 37°C, of normal and heat denatured rabbit I^{131} γ-globulin (1·2 mg/ml) with papain. The value for normal γ-globulin was 8·3 per cent

Heat-denaturation period (min)	2·5	5	10	20	40	80	120
Heat denatured at 65°C	—	10·5	11·2	11·4	11·6	11·3	11·6
Heat denatured at 71°C	—	13·1	16·6	19·2	24·7	29·7	33·7
Heat denatured at 75°C	16·9	23·3	29·9	37·8	45·9	—	—
Heat denatured at 85°C	58·5	70·5	70·2	74·4	—	—	—

with the findings of PETERMANN[17] and of PORTER[18] concerning the limited splitting of normal γ-globulin with consequent small increase in non-protein nitrogen. It is also noticeable that a significant increase in TCA-soluble radioactivity is obtained using denatured γ-globulin if the enzymatic reaction is carried out at 7°C.

Numerous samples of I^{131}-labelled normal γ-globulin, after incubation at 37°C with papain for 24 hr, gave from 2–7 per cent acid-soluble radioactivity. In two samples of normal γ-globulin, one labelled with I^{131} and the other with I^{125} digested in the same test-tube, the amounts of acid-soluble radioactivity differed by only 0·8 per cent, and this could be accounted for by differences in the iodination procedures.

Table 3 shows a progressive increase in TCA-soluble radioactivity with different degrees of heat denaturation. Values obtained by measuring the amount of undigested protein at the end of the reaction, agree with the data shown in Table 3 to within an average difference of ± 1 per cent.

In comparing the susceptibility of two proteins to denaturation in identical circumstances, a double labelling technique was used. Digestion of the mixed proteins with papain was carried out and the results are given in Fig. 2 where the rates of proteolysis of normal I^{125} and denatured I^{131}

VOL. 10 1961

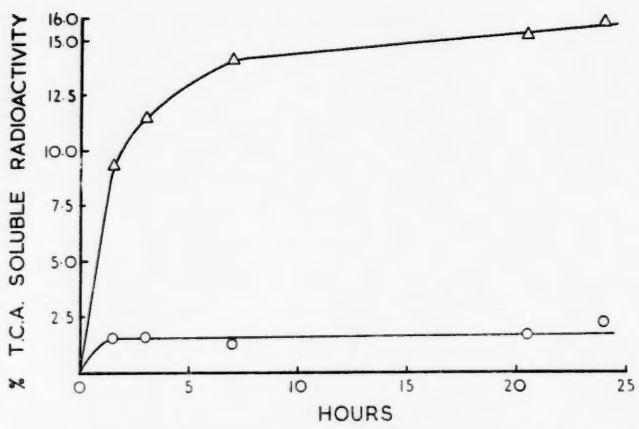

FIG. 2. The kinetics of digestion of I^{125} normal γ-globulin (○) and of heat-denatured (70°C for 1 hr) I^{131} γ-globulin (△) with papain (37°C). Gamma-globulin concentration 0·4 per cent.

γ-globulin are compared with one another. The native γ-globulin is hydrolysed much more slowly than the heated material.

This procedure is simple and quick to perform and is very sensitive. Since only a small amount of the radioactive substrate is necessary for each determination, accurate analyses are possible.

Acknowledgements—The author is indebted to Dr. A. S. McFARLANE for his interest and criticism in this study. Thanks are due to Miss J. WILCOX for skilled technical assistance.

REFERENCES

1. LINDERSTROM-LANG K., HOTCHKISS R. D. and JOHANSEN G. *Nature, Lond.* **142,** 996 (1938).
2. LINEWEAVER H. and HOOVER S. R. *J. biol. Chem.* **137,** 325 (1941).
3. BERNHEIM F., NEURATH H. and ERICKSON J. O. *J. biol. Chem.* **144,** 259 (1942).
4. KUNITZ M. *J. gen. Physiol.* **30,** 291 (1947).
5. FRENCH D. and EDSALL J. T. *Advanc. protein Chem.* **2,** 277 (1945).
6. FOLIN O. and CIOCALTEU V. *J. biol. Chem.* **73,** 627 (1927).
7. SOBER H. A., GUTTER F. J. WYCKOFF M. M. and PETERSON E. A. *J. Amer. Chem. Soc.* **78,** 756 (1956).
8. SOBER H. A. and PETERSON E. A. *Fed. Proc.* **17,** 1116 (1958).
9. MCFARLANE A. S. *Nature, Lond.* **182,** 53 (1958).
10. KIMMEL J. R. and SMITH E. L. *J. biol. Chem.* **207,** 515 (1954).
11. GORNALL A. G., BARDAWILL C. J. and DAVID M. M. *J. biol. Chem.* **177,** 751 (1949).
12. SLOTTA K. H. and PRIMOSIGH J. *Nature, Lond.* **168,** 696 (1951).
13. DENT C. E. *Biochem. J.* **43,** 169 (1948).
14. ACHER R. and CROCKER C. *Biochim. Biophys. Acta* **9,** 704 (1952).
15. GROSS J. and LEBLOND C. P. *Endocrinology* **48,** 714 (1951).
16. TATA J. R. *Biochem. J.* **73,** 36P (1959).
17. PETERMANN M. L. *J. Amer. Chem. Soc.* **68,** 106 (1946).
18. PORTER R. R. *Biochem. J.* **73,** 119 (1959).

International Journal of Applied Radiation and Isotopes, 1961, Vol. 10, pp. 99–105. Pergamon Press Ltd. Printed in Northern Ireland

A Total-Body Irradiator

M. BRUCER*
The Medical Division, Oak Ridge Institute of Nuclear Studies, Oak Ridge, Tennessee, U.S.A.

(*Received* 8 *August* 1960)

VOL. 10 1961

A total-body irradiation room has been built with eight cesium-137 sources. One 500 c source is near each corner of an 8 ft cubical room. An open maze, closed only with a gate, allows the patient and nurse to appear, through mirrors, to be in the same room. The patient is supported in the center of the 2 × 2 × 6 ft irradiation volume on a rigid aluminum bed. The exposure rate to the patient can be changed from 280 to 1·8 r/hr. The exposure rate outside the room is less than 0·01 mr/hr. Clinical dosimetry is defined in terms of minutes. Physical dosimetry includes classical, chemical and phantom studies.

UN IRRADIATEUR A CORPS ENTIER

On a bâti une salle à rayonnement du corps entier avec huit sources de césium-137. Une source de 500c est située près de chaque coin d'une pièce cubique de 8 pieds (2m.44). Un labyrinthe ouvert, fermé seulement d'une barrière, permet au malade et à l'infirmière de se croire, grâce à des miroirs, être dans la même pièce. Le malade est supporté au centre de l'espace à irradiation qui mesure 2 × 2 × 6 pieds (0,61 × 0,61 × 1,83 mètres), sur un lit rigide en aluminium. Le taux de pose au malade peut varier de 280 à 1,8 r/hr. Le taux de pose au dehors de la pièce est moins de 0,01 mr/hr. La dosimétrie clinique se précise en minutes. La dosimétrie physique comporte des études classiques, chimiques et fantomatiques.

ОБЛУЧАТЕЛЬ ДЛЯ ТОТАЛЬНОГО ОБЛУЧЕНИЯ

Комната, предназначенная для тотального облучения, была снабжена восемью источниками цезий-137. В каждом углу 8-футовой комнаты кубической формы расположено по одному источнику мощностью 500 кюри. Вход в комнату сделан из прозрачной сетки, закрывающейся только дверцей. Благодаря этой сетке пациент и медицинский работник отражаются в зеркалах так, как если бы они были в одной комнате. Пациента помещают на алюминиевой тележке в центре облучаемого объема размером 2 × 2 × 6 футов. Дозу облучения можно менять в пределах от 280 до 1,8 р/час. Доза за пределами комнаты меньше 0,01 мр/час. Клиническая дозиметрия выражается в минутах и основана на классических, химических и модельных исследованиях.

EINE GESAMT-KORPER-BESTRAHLUNGSANLAGE

Ein Gesamt-Körper-Bestrahlungsraum mit 8 Cs-137 Quellen wurde errichtet. Je eine 500 c Quelle ist in den Ecken eines kubischen Raumes von 8 ft Kantenlänge angebracht. Ein offenes Labyrinth, das nur durch eine Schranke verschlossen ist, lässt mit Hilfe von Spiegeln Patient und Schwester im gleichen Raume erscheinen. Der Patient wird im Zentrum des 2 × 2 × 6 ft Bestrahlungsraumes durch ein fixes Aluminiumbett festgehalten. Die Expositionsrate für den Patienten kann zwischen 280 und 1,8 r/hr variiert werden. Die Expositionsrate ausserhalb des Raumes beträgt weniger als 0,01 mr/hr. Die klinische Dosis wird nach Minuten gerechnet, die physikalische Dosis wird durch klassische und chemische Methoden, sowie durch Studium am Phantom bestimmt.

* Under contract with the United States Atomic Energy Commission.

THE earliest workers with Crookes tubes received an unknown amount of total-body irradiation. From early descriptions of the instruments, methods and of the local damage, mainly to the hands, it seems obvious that the danger was in the close approach to a low-energy source. The first good word about total-body irradiation was said by Nicholas Tesla who stated that, after working for a considerable time measuring Roentgen's new light with an unshielded Crookes tube, he noticed that his chronic cough disappeared and he seemed to be in much better health. The idea of total-body irradiation is not new. From the *Archives of the Roentgen Ray* (Vol. 13, p. 2, June 1908):

> "Holzknecht has recently drawn attention to a method of applying Roentgen irradiation to internal organs . . . for this so-called homogeneous irradiation he uses a battery of Roentgen tubes, thus bathing the patient on all sides with X-rays of great penetration."

During the next quarter century, as ideas of physical and biological dosimetry developed, some physicians felt that there was a difference between port irradiation (already in vogue) and irradiation of the entire organism. HEUBLEIN was one of the first modern physicians to implement a total-body irradiation facility.[1] He irradiated a number of patients at Memorial Hospital, New York, in 1930 with an exposure rate of about 1 r/hr. The patients were in the field of irradiation for about 20 hr/day for as long as a whole week. HEUBLEIN's results were not startlingly good, but since this was an experimental program, neither were his patients startlingly fortunate selections. The main idea behind the work seemed to be that surgeons may cut just so far. They are ultimately stopped, if by nothing else, just by the extent of surgical intervention. The radiotherapists of HEUBLEIN's day were also restrained: they could point their beams to specific volumes of tissue, but ultimately were stopped by the appalling speed with which different areas had to be covered.

It is interesting that during this same era Coutard was demonstrating the desirability of slow cumulative radiation and Mayneord was formulating his ideas of integral dose. The ideas of "dose" were changing rapidly. Point-exposure measurements were different from integral dose. The factor of volume caused difference in biological effect. The factor of time, long known to make a difference became an important item in the radiation prescription.

No one suggested that the price of mutilating surgical intervention was too great if surgical intervention was feasible. No one suggested that port therapy had too great a price if it were feasible. Patients unacceptable to surgeons or radiotherapists still remained. One approach was more astute diagnosis and earlier therapy. No one argues with this position, but patients with generalized disease still remain.

In a note to the *Archives of the Roentgen Ray* in 1903 (Vol. 7, p. 67, January 1903) Dr. W. B. Coley of New York pointed out:

> "In one case, coincidentally with the tumor that was being X-rayed, other tumors which had not been exposed to the rays also diminished in size."

The work of JACOBSON and others[2] ultimately led to a verification that total-body irradiation did something more than just treat a tumor; it might or might not destroy the immune mechanism. If we can alter the immune mechanism with radiation (or any other drug) we might be able to develop methods of control. With controlled destruction a new field of repair is open to the surgeon. The technical competence of modern surgery allows almost any kind of repair to the body, but the body's competence to accept this repair is not so great. It has been known for a long time that the biological effect of radiation is not "just local." There is also a diffuse biological effect.

With all these ideas reaching a boiling point after the Second World War, and with a newly available source of radiation energy in relatively inexpensive form, the idea of total-body irradiation was revived. Our ideas of attenuation by the end of the Second World War demanded something akin to supervoltage. As a first step in dosimetry we demanded something akin to uniform exposure throughout the total volume of the body.

At first, in this revival, total-body irradiation was done with ordinary therapy machines. The patient was moved a long distance from the source of energy and the problem of inverse-square attenuation was thus corrected. The problem of absorptive attenuation was corrected by using rotation or super-voltage equipment. These makeshift arrangements were unsatisfactory because the primary problem is still "dose rate." This has been described in a thousand different articles, but the problem of total-body irradiation is still a problem of time, tissue and energy.

Three devices have been specifically made with the demands of total-body irradiation foremost in their design. One is the total-body irradiator at the U.S. Naval Medical Research Hospital in Bethesda, Maryland; this device uses cobalt very close to the body. A second device is the total-body irradiator at the City of Hope Medical Center, Duarte, California; this device uses cesium-137 relatively close to the body.[3] The third device is the ORINS Medical Division total-body irradiator, described in this article.

VOL. 10 1961

Design criteria

In designing the ORINS total-body irradiator a number of criteria were paramount.

(1) The design must permit any of the historical methods (or any new method) of investigating the dosimetry problem. It was originally designed to meet a maximum requirement for 200 r/hr exposure. The final device has exceeded the requirement; we have achieved approximately 300 r/hr. Auxiliary phantoms are part of this problem, but are explained elsewhere.[4]

(2) Patients of various sizes must be exposed uniformly. To meet this requirement the design was centered around a $2 \times 2 \times 6$ ft volume supported in the middle of the room by a bed that has sufficient structural strength, but as little absorption as possible. Patients on this bed will receive the same exposures to any part of their bodies; however, different-dimensioned patients will not necessarily receive the same dose.

(3) The irradiation room must be open to patients and nurses. Since many of the patients that will be treated are not ambulatory, there must be no question of the immediate availability of nurses. Since the patients might be children or physically handicapped, there must be no question of claustrophobia. Since the patients might be irradiated for long periods of time, the irradiation bed must be comfortable.

(4) The irradiation facility must be safe. The safety criterion of a maximum of 1 mr/hr was placed as a restriction on the design. To implement radiation safety, we built into a hill available in the area; however, shielding would have done just as well.

(5) The facility must allow for shielding parts of the body. This has not yet been done, but is easy with movable lead shields.

The design

Fig. 1 shows a cutaway model of the total-body irradiation room. A $2 \times 2 \times 6$ ft virtual volume was suspended over a bed by four posts that are out of the exposure field. The bed was made of two sheets of 1/32 in. aluminum separated by approximately an inch and a half of honeycomb cardboard. The material is usually used for the extreme strength necessary in airplane fuselage construction and has no sag when a patient is placed on the bed. The bed is slightly trough-shaped so that patients cannot easily roll off. A nylon net surrounds the bed (Fig. 2). A television set with remote controls is placed so that a patient lying on the bed can view television. This might or might not, depending upon the televison programs available, help to pass the hours necessary for the exposure of the patient.

The room is constructed of poured concrete, but the inside wall is covered with an acoustic tile, which has no effect on the radiation characteristics. The floor is of vinyl tiles. Ventilation is arranged so that the air enters through the maze and leaves through a ventilator funnel on the wall opposite. Heating is done with electric wall heaters. In summer, air is drawn through a louvered door from an air-conditioned corridor. Two steel rails at the ceiling over the bed support an instrument trolley. The instrument cables go through a conduit in the ceiling. Preliminary investigations

showed no appreciable scatter from the accessories.

The bed is placed in the center of an 8 ft (plus entry) cubical room. Eight teletherapy machines (four each side of the therapy space, near the corners) all point toward the center of the irradiation volume. Each source contains 500 $\pm$ 0·5 c of cesium-137. With all sources "ON" the exposure to the 2 $\times$2$\times$ 6 ft irradiation volume ranges from 308 to 318 r/hr without the final filter covers in place. The exposure rate drops off slowly (about 8 r/hr) at the very head and foot ends of the bed, but more quickly outside the irradiation volume.

The room is approached through a semispiral maze (Fig. 3). At the end of this maze is a wrought-iron gate that must be closed for the machine to be turned on. Opening the gate automatically shuts off the machine. Any person going through the gate will shut off the machine before he can receive a significant exposure. The maze is sufficiently wide for patients' beds to be wheeled through, but patients are usually carried on a travelling cart.

Each of the sources can be turned on separately (Fig. 3). While this might be of value in later treatment problems, its primary purpose was to allow for dosimetry testing. These separate controls will be covered and the only control necessary for the clinician is a clock and the master control button.

Treatment procedure

The master control button is connected with the clock and treatments are done in terms of minutes. When the gate is closed and the key is turned in the control panel, the sources go "ON" and a red light shines indicating irradiation. When the gate is opened or a large thumb button is pushed, the sources turn "OFF" and a green light shines indicating that the source is in full safe position. The red and green lights indicate either full "ON" or full "OFF" positions. A set of chimes clatters whenever any source is not in either the full "ON" or the full "OFF" position.

Beam-shaping lens

Since eight sources pointed at one point in space would result in a high dose in the middle of the irradiation volume and a low dose at the ends, a series of beam-shaping devices was made out of thin sheets of aluminum and brass. By shifting the thicknesses of aluminum and brass, a gamma-ray lens was made that reduced the exposure in the center of the bed. Thus the exposure over the entire 2 $\times$ 2 $\times$ 6 ft irradiation volume was kept reasonably uniform. It will also be possible, as more dosimetry information becomes available, to shift these beam shaping gamma-ray lenses to produce either higher or lower proportionate irradiation exposure to any large segment of the body. Increasing or decreasing the proportionate irradiation to small segments of the body must be done with movable shielding.

The dose-rate filters

With all the sources "ON" and no filters in place, the exposure rate is at a maximum of approximately 300 r/hr. Since one of the primary problems is longer-term irradiation, it was necessary to install filters so that the dose rates could be changed. The filtration mechanism consists of five filters labeled 1, 2, 4, 8 and 16. Each of these filters represents a calculated number of tenths of a tenth-value layer. For example, the No. 4 filter is 4/10 of a tenth-value layer. The No. 16 filter is 16/10 of a tenth-value layer. Each time a layer of the attenuating filter is added, the radiation intensity falls to about 80 per cent of the preceding level; the exposure rate can thus be changed from 0 to 31 different exposure rates. With any of these filters in place, the spectrum changes. This spectral change is not a minor one; it will be determined by future measurements.

Special sources for spectrometry

No clinical gamma-ray spectrometer will operate in a field as intense as this one. Therefore, a series of mock sources has been manufactured. Before these sources were loaded, a number of experiments were run

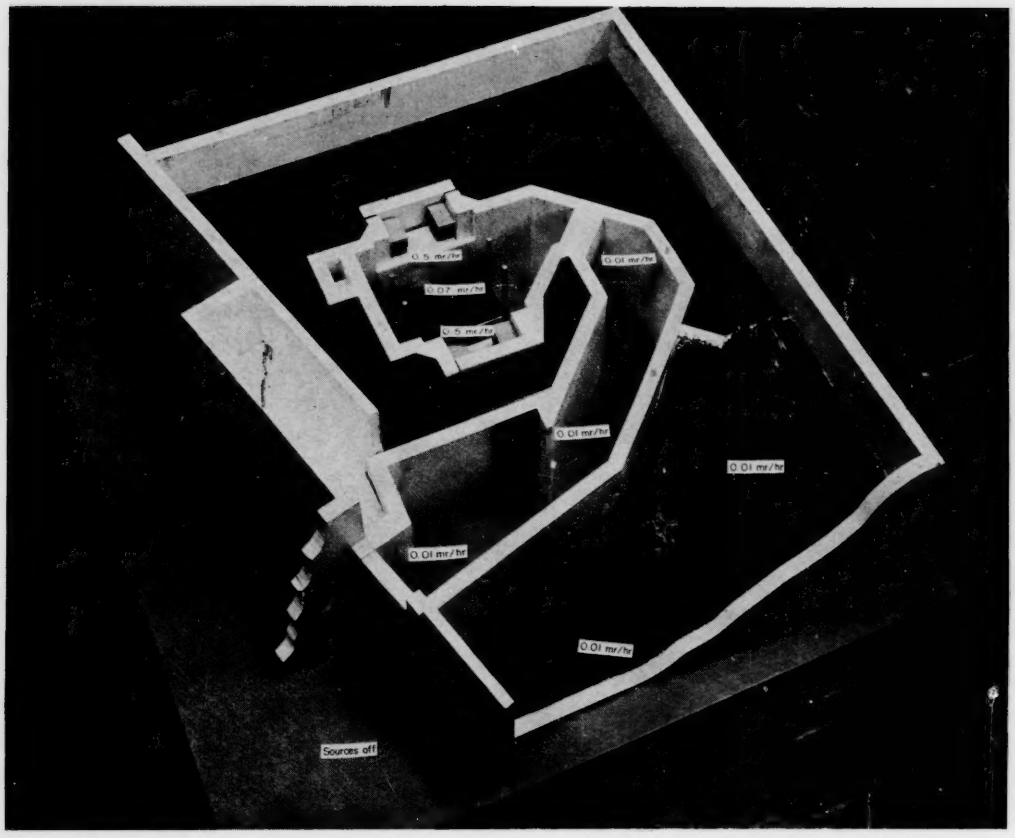

FIG. 1. Cutaway model of the ORINS total-body irradiation facility. "Radiation-safety" measurements with all sources "OFF."

FIG. 2. View, through mirror, of the ORINS total-body irradiation room.

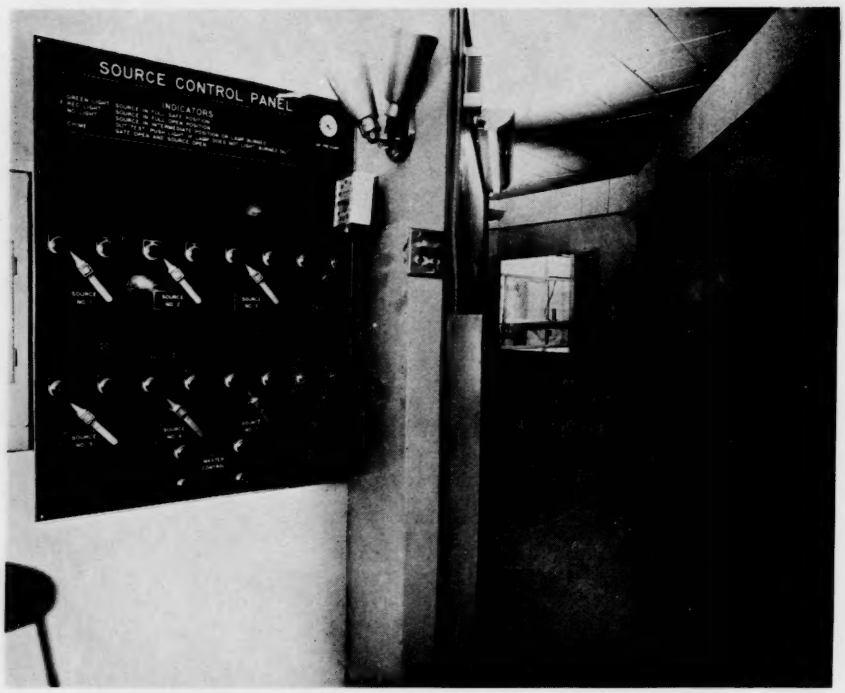

FIG. 3. Entrance to maze into ORINS total-body irradiation room.

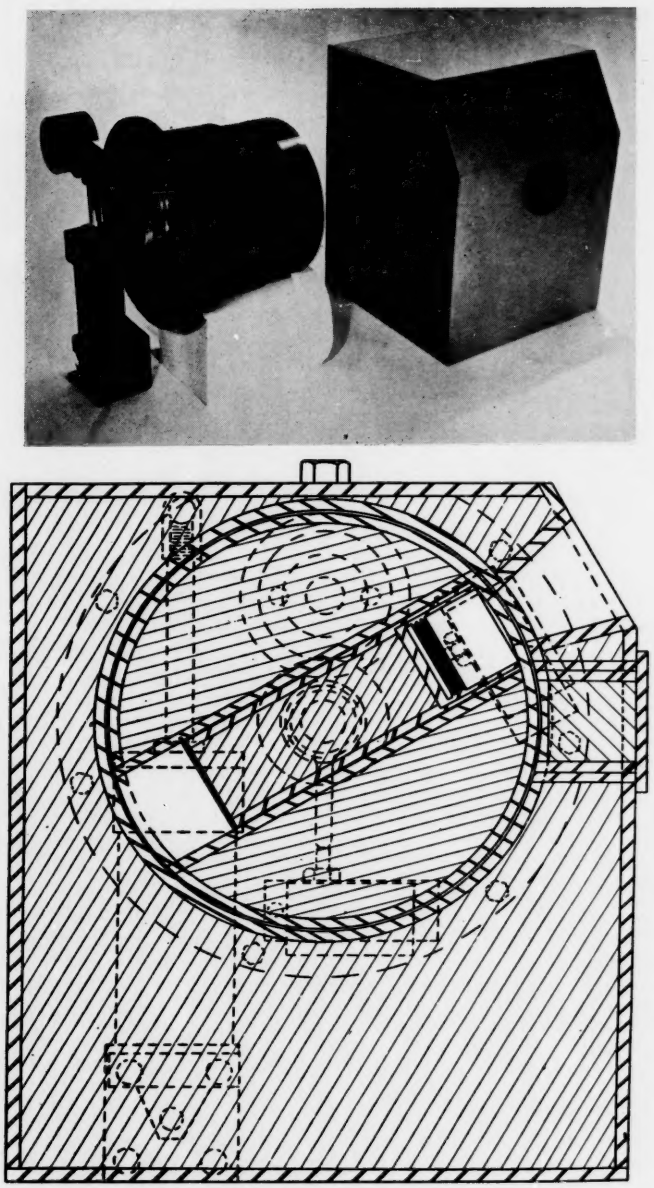

FIG. 4. Construction details of the ORINS total-body irradiator.
(a) One of the eight therapy machines.

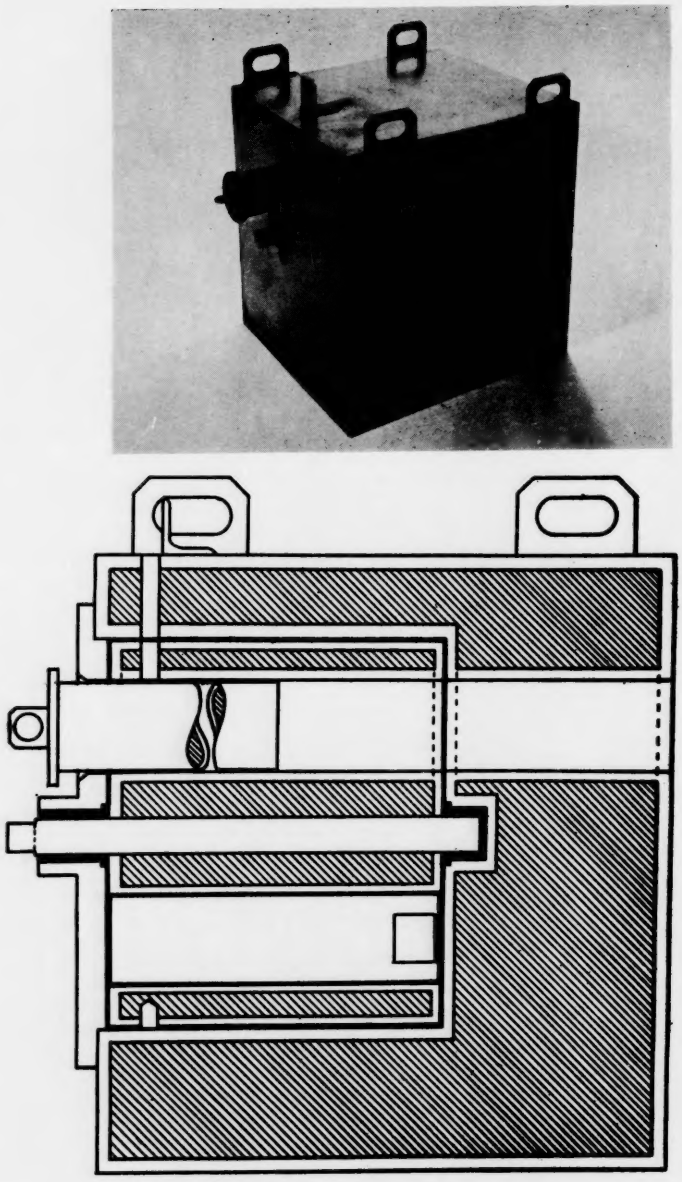

FIG. 4(b). Special device for loading large cesium sources.

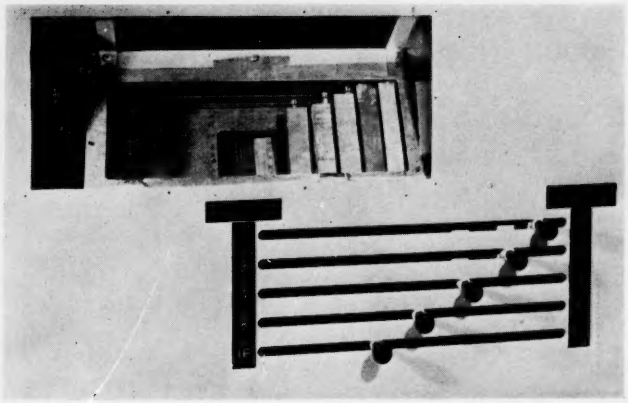

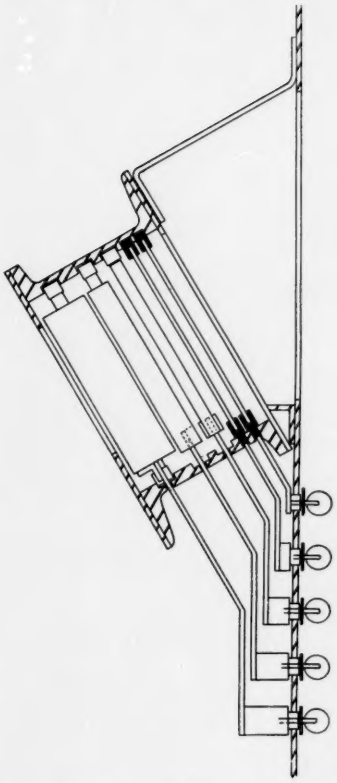

FIG. 4(c). One of the eight filter mechanisms.

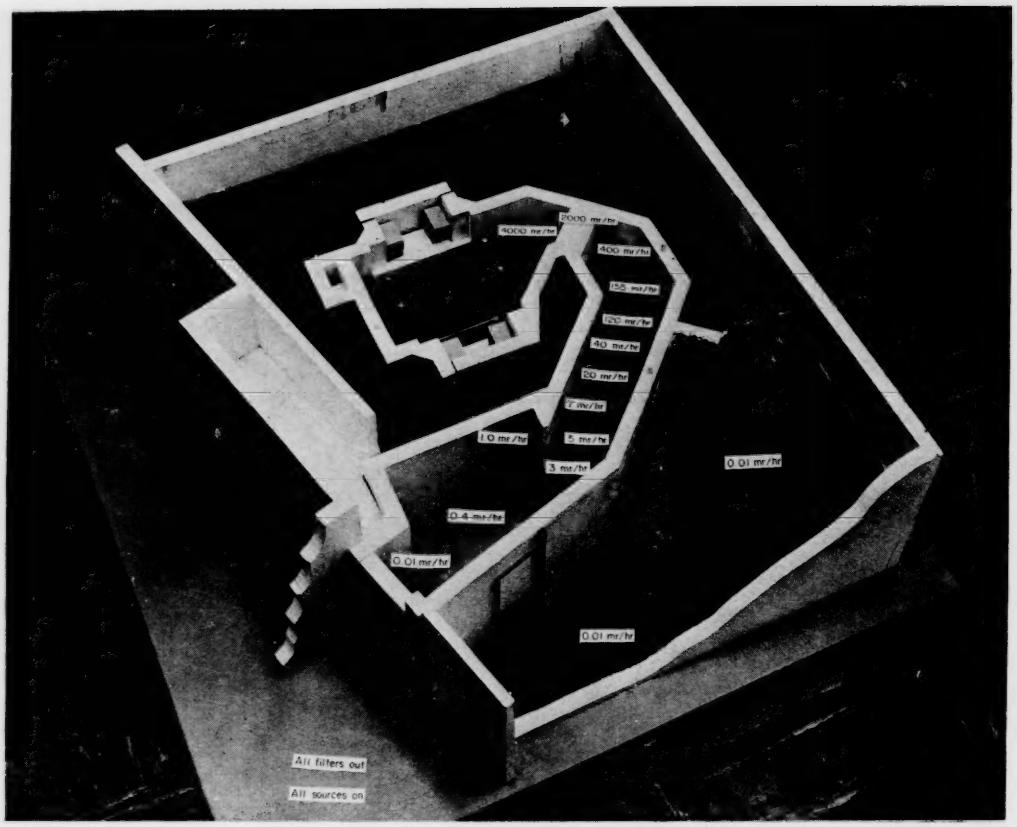

FIG. 5. Cutaway model of the ORINS total-body irradiation facility. "Radiation-safety" measurements with all sources "ON".

with a small source of cesium-137. This was placed in various positions and the spectrum was matched to the position that simulated the actual source in its actual position. A 2 mc (small) source was made from the same batch of cesium-137 as the 500 c (large) sources. The small source was placed in the container for the large source and its spectrum was determined. This same small source was then placed in a recess in the source wheel (with the wheel in the "OFF" position). The recess was redesigned until the two spectra matched. Thus spectrometry studies can be done with varying intensities of mock sources without again going through the time and trouble necessary to remove the high-intensity sources.

Construction and loading of the individual teletherapy machines

Since this device had to be as foolproof as possible, it was necessary to design an "ON–OFF" mechanism with gravity used as the final source of energy for the "OFF" position (Fig. 4). A rotating wheel was used that would bring the source into the "ON" position by applying pneumatic pressure to a counterweight. When pressure or power is cut off, the counterweight sinks to a lower position and the source is rotated back to the "OFF" position. In the "OFF" position the cesium-137 source is surrounded by approximately 10 tenth-value layers of lead. The only things that can go wrong in this closing device are for the pneumatic cylinder or the gears to jam.

The standard operating procedure for an accident in which the chime is ringing is for someone to use a long-handled device to close the No. 16 filter in each source and then to remove the patient from the irradiation room. Since this can be done in less than 1 min, the exposure to a person who follows instructions will be in the millirad range.

Loading eight 500 c sources of cesium-137 has a hazard all its own. Each therapy device has a special plug for loading. When the source opening is locked in position for loading and the source plug is removed, a loading box is pushed into place. This conforms in size to the source chamber and exact positioning is achieved by means of a long rod.

The loading box (Fig. 4) contains a rotating wheel similar in construction to that of a six-shooter, only this is a two-shooter. The empty hole is used for positioning the loading container. When this is properly located, the source is rotated into position and simply pushed into each teletherapy machine. The safety of the device is proved by the lack of readable exposure on the film badges of the men who loaded all eight machines.

Radiation safety

One of the primary problems of such a high-level room is that the radiation safety measurement must be less than 2 mr/hr around the complete device. Since in the Medical Division we have instruments that are far more sensitive to radiation than human beings, we increased this requirement to a necessity for an outside source reading of less than 0·1 mr/hr. The total-body irradiation facility was over-protected purposely so that other counting instruments could be used in the immediate area.

Figure 5 shows the final measurements with all sources "ON" superimposed on the cutaway model. With one exception, at all points around the outside of the facility, the readings were less than 0·01 mr/hr. (Our radiation safety monitors would not read less than 0·01 mr/hr.) In one place, directly over the ventilator, there was a narrow vertical leak of approximately 0·1 mr/hr.

With the sources "OFF" (Fig. 1) the exposure rate is less than 0·01 mr/hr all the way through the maze into the room itself. The exposure rates very close to the individual teletherapy machines increase to 0·5 mr/hr. Therefore, this machine is completely safe in the "OFF" position for everything except fine measuring devices. During the study of background radiation, the crystal used in the spectrometer was affected by 0·07 mr/hr. Spectrometry is a special situation in which background spectra must be subtracted from irradiation spectra.

The worst possible safety situation occurs when no filters are in use and all sources are

"ON". In such circumstances the exposure rate where the maze enters the treatment room is 4000 mr/hr (Fig. 5). This is a tremendous drop from the radiation to the patient himself. The exposure rate continues to drop rapidly as one goes from the room to the gate, where it is only 3 mr/hr. The exposure rate at the control panel, where a technician might be working, is 1 mr/hr; where technicians and nurses sit during an irradiation, it has fallen to 0·01 mr/hr. Therefore, the machine is safe to use, provided the machinery is always in either operating or in non-operating condition.

Costs

The cost breaks down as follows.

Construction of the room	$24,624
Finishing the room	2,743
The eight teletherapy machines	7,965
Eight filters	5,500
Cesium-137 (4000 c)	12,528
Total cost	$53,360

If exposure rates exceeding 300 r/hr are needed, the sources must be replaced with a more expensive source material. From other studies[5] we already know that the irradiation spectrum for cobalt and cesium in this kind of application is about the same. This and other teletherapy units are "scatter machines", therefore the problem of replacing sources with cobalt will never come up, nor will there be a change in the shielding for the room itself. Since only a small fraction of the total volume of the source capsule is used for the source, it will be easily possible to double the exposure rate with 1000 c cesium-137 sources. It will probably be possible to triple the dose rate to 900 r/hr with 12,000 c of cesium-137. If this is done in the future, it will change the radiation safety measurements, but even at three times the present rate, the facility is still a thoroughly safe one.

Dosage considerations

Throughout the last quarter century of discussions concerning dosage, and especially since the biological radiation-effects problem has become foremost in our thinking, questions of radiation dosimetry have inevitably been confused by a lack of definition of what is meant by dose. For this reason we have divided the dosimetry problem into two entirely separate problems. One is the "dose rates" used by clinicians who need not be trained in dosimetry. These clinicians will give a "nominal dose." Nevertheless, this nominal dose has nothing whatever to do (except that it can be reproduced and followed by physicists) with the dosage questions that will come up to biophysicists. The physical dosimetry is a separate problem from the clinical dosimetry and a long series of measurements must be made. The problems in physical dosimetry will be (1) the point dosimetry of background, (2) the spectral point dosimetry, (3) point dosimetry in phantoms, (4) spectral dosimetry in phantoms, (5) isodose curves within phantoms, (6) iso-ergic–isodose curves within phantoms, (7) compartmented direct rad dosage with chemical dosimeters, (8) organ specific rad dosimetry with chemical dosimeters, (9) mathematical computations of dose from geometric models, and (10) mathematical computations of dose from human models.

These are not all the physical dosimetry studies necessary, nor will this problem be completed or even solved in our lifetime; however, this physical dosimetry has very little immediate relationship to the equally important problems of biological dosimetry and the treatment of patients.

Clinical dosimetry

Because so many scientists will be using this irradiator for so many different kinds of treatments on so many different kinds of patients, a simplified clinical dosimetry has been set up. The "dose" is measured with a clock and is based upon an exposure time. This "dose" is called the "nominal dose" for the particular object being irradiated. A particular Victoreen high-energy chamber was placed at the center of the beam from all eight machines, somewhat above the center of the bed, but approximately above the center of any patient put into an irradiation

TABLE 1. Exposure in the ORINS total-b

(1) Select the desired exposure; (2) choose the lowest filter number to approximate the desired time. Time is
studies. (Ion chamber—Victoreen #605—NBS ca

r/min	4·77	4·00	2·86	2·34	2·13	1·78	1·36	1·13	0·90	0·74	0·57	0·49	0·46	0·39	0·314	0·271	0·174
Filters "in" r Exposure	0	1	2	3	4	5	6	7	8	9	10	11	12	13	14	15	16
25	00:05	00:06	00:09	00:11	00:12	00:14	00:18	00:22	00:28	00:34	00:44	00:51	00:54	01:04	01:20	01:32	02:24
50	00:10	00:12	00:17	00:21	00:23	00:28	00:37	00:44	00:56	01:08	01:28	01:42	01:49	02:08	02:39	03:04	04:47
75	00:16	00:19	00:26	00:32	00:35	00:42	00:55	01:06	01:23	01:41	02:12	02:33	02:43	03:12	03:59	04:37	07:11
100	00:21	00:25	00:35	00:43	00:47	00:56	01:14	01:28	01:51	02:15	02:55	03:24	03:37	04:16	05:18	06:09	09:35
150	00:31	00:38	00:52	01:04	01:10	01:24	01:50	02:13	02:47	03:23	04:23	05:06	05:26	06:25	07:58	09:14	14:22
200	00:42	00:50	01:10	01:25	01:34	01:52	02:27	02:57	03:42	04:30	05:51	06:48	07:15	08:33	10:37	12:18	19:09
250	00:52	01:02	01:27	01:47	01:57	02:20	03:04	03:41	04:38	05:38	07:19	08:30	09:03	10:41	13:16	15:22	23:57
300	01:03	01:15	01:45	02:08	02:21	02:49	03:41	04:25	05:33	06:45	08:46	10:12	10:52	12:49	15:55	18:27	28:44
350	01:13	01:28	02:02	02:30	02:44	03:17	04:17	05:10	06:29	07:53	10:14	11:54	12:41	14:57	18:35	21:32	33:31
400	01:24	01:40	02:20	02:51	03:08	03:45	04:54	05:54	07:24	09:01	11:42	13:36	14:30	17:06	21:14	24:36	38:19
450	01:34	01:52	02:37	03:12	03:31	04:13	05:31	06:38	08:20	10:08	13:09	15:18	16:18	19:14	23:53	27:40	43:06
500	01:45	02:05	02:55	03:34	03:55	04:41	06:08	07:22	09:16	11:16	14:37	17:00	18:07	21:22	26:32	30:45	47:54
550	01:55	02:18	03:12	03:55	04:18	05:09	06:44	08:07	10:11	12:23	16:05	18:42	19:56	23:30	29:12	33:50	52:41
600	02:06	02:30	03:30	04:16	04:42	05:37	07:21	08:51	11:07	13:31	17:33	20:24	21:44	25:38	31:51	36:54	57:28
650	02:16	02:42	03:47	04:38	05:05	06:05	07:58	09:35	12:02	14:38	19:00	22:07	23:33	27:47	34:30	39:58	62:16
700	02:27	02:55	04:05	04:59	05:29	06:33	08:35	10:19	12:58	15:46	20:28	23:49	25:22	29:55	37:09	43:03	67:03
750	02:37	03:08	04:22	05:21	05:52	07:01	09:11	11:04	13:53	16:54	21:56	25:31	27:10	32:03	39:49	46:08	71:50
800	02:48	03:20	04:40	05:42	06:16	07:29	09:48	11:48	14:49	18:01	23:24	27:13	28:59	34:11	42:28	49:12	76:38
850	02:58	03:32	04:57	06:03	06:39	07:58	10:25	12:32	15:44	19:09	24:51	28:55	30:48	36:19	45:07	52:16	81:25
900	03:09	03:45	05:15	06:25	07:03	08:26	11:02	13:16	16:40	20:16	26:19	30:37	32:37	38:28	47:46	55:21	86:12
950	03:19	03:58	05:32	06:46	07:26	08:54	11:39	14:01	17:36	21:24	27:47	32:19	34:25	40:36	50:25	58:26	91:00
1000	03:30	04:10	05:50	07:07	07:49	09:22	12:15	14:45	18:31	22:31	29:14	34:01	36:14	42:44	53:05	61:30	95:47

1 2

otal-body irradiator (1960–1961).
ime is read as *xx*:*yy*, when *xx* = hours and *yy* = minutes. This is the "nominal dose" for all clinical
3S calibration, 22° C, 760 mm pressure)

174	0·147	0·115	0·099	0·094	0·081	0·067	0·059	0·053	0·049	0·041	0·037	0·036	0·034	0·032	0·030
16	17	18	19	20	21	22	23	24	25	26	27	28	29	30	31
2:24	02:50	03:37	04:12	04:26	05:09	06:13	07:04	07:52	08:30	10:10	11:16	11:34	12:15	13:01	13:53
4:47	05:40	07:15	08:25	08:52	10:17	12:26	14:07	15:43	17:00	20:20	22:31	23:09	24:30	26:02	27:47
7:11	08:30	10:52	12:38	13:18	15:26	18:39	21:11	23:35	25:31	30:29	33:47	34:43	36:46	39:04	41:40
9:35	11:20	14:30	16:50	17:44	20:34	24:52	28:15	31:27	34:01	40:39	45:03	46:18	49:01	52:05	55:33
4:22	17:00	21:44	25:15	26:36	30:52	37:19	42:22	47:10	51:01	60:58	67:34	69:27	73:32	78:08	83:20
9:09	22:40	28:59	33:40	35:28	41:09	49:45	56:30	62:54	68:02	81:18	90:05	92:36	98:02	104:10	111:07
3:57	28:21	36:14	42:05	44:20	51:26	62:11	70:37	78:37	85:02	101:38	112:37	115:44	122:33		
8:44	34:01	43:29	50:30	53:11	61:44	74:38	84:45	94:20	102:02						
3:31	39:41	50:43	58:55	62:03	72:01	87:04	98:52	110:04							
8:19	45:21	57:58	67:20	70:55	82:18	99:30	113:00								
3:06	51:01	65:13	75:45	79:47	92:36	111:56									
7:54	56:41	72:28	84:10	88:39	102:53										
2:41	62:21	79:43	92:36	97:31											
7:28	68:02	86:57	101:01	106:23											
2:16	73:42	94:12													
7:03	79:22	101:27													
1:50	85:02														
6:38	90:42														
1:25	96:22														
6:12	102:02														
1:00															
5:47															555:56

2

3

position. The exposure to this chamber was measured with each of the filters in place. The amount of time necessary to deliver any exposure to this chamber from 25 to 1000 r is given in terms of rads in minutes. Table 1 lists the exposures available to the clinician. The clinician therefore, by definition, gives an irradiation measured in terms of minutes. In fractionated exposures he will have to give both a description of the fractionation and the total exposure.

There are reasons for this very autocratic decree:

(1) We must be able to repeat our exposures. The roentgen is the only available unit that is reproducible. Even the roentgen is dependent upon the source-detector geometry, but this is an argument in physical dosimetry and the clinician has more important things to worry about.

(2) We must be able to repeat our measurements. Only with the roentgen and a definition of the placement of the detector can we repeat the exposure many times under one set of circumstances.

(3) We must have a calibration with some standard. Only the roentgen now has a standardized calibration through the various national bureaus of standards. Presumably any other method can be calibrated back to this one necessarily arbitrary method.

(4) Our exposures must be capable of being transferred to any other irradiator. If a new system of dosimetry becomes available, we can always go back and cross-calibrate with the new system. This has not been true of any other system we have tried.

(5) The dosimetry must be exceedingly simple and adequately accurate. A treatment by minutes appears to be adequately accurate by any clinical standard. Any physician can give treatment in terms of minutes; possible errors are fewer in a clock than in any radiation–detection instrument.

(6) Cross-calibration must be adaptable to treatment with other forms of radiation; for example, neutrons. This is not yet available, but when it does become available we will be able to fall back on our original definition and accomplish cross-calibrations.

(7) The record-keeping must be exceedingly simple or it will not be done. Our present experience is that more complex systems are not being fully defined.

CONCLUSION

A new total-body irradiator is in a self-contained room designed to allow any patient to lie on a bed suspended in the middle of eight cesium-137 teletherapy machines. The $2 \times 2 \times 6$ ft volume over this bed receives a reasonably uniform maximum exposure of 280 r/hr. This exposure can be reduced with filters to approximately 1·8 r/hr. The "radiation safety" exposure around the room measures less than 0·01 mr/hr.

A specific "nominal dose" is defined for clinical use as the exposure in the center of the irradiation volume in terms of minutes. Physical dosimetry will include all classical, chemical and phantom dosimetry and its accompanying spectrometry.

REFERENCES

1. Heublein A. C. *Radiology* **18,** 1051 (1932).
2. Jacobson L. O. *Cancer Res.* **12,** 315 (1952).
3. Jacobs M. L. and Pape L. *Int. J. Appl. Rad. Isotopes* **8,** 141 (1960).
4. Hayes R. L. *Standard-Man Phantoms.* United States Atomic Energy Commission Report ORINS-35. Office of Technical Services, Department of Commerce, Washington (1960).
5. Brucer M. and Umegaki Y. *Radiation Measurements and the Spectrum.* United States Atomic Energy Commission Report ORINS-35. Offices of Technical Services, Department of Commerce, Washington (1959).

International Journal of Applied Radiation and Isotopes, 1961, Vol. 10, pp. 106–111. Pergamon Press Ltd. Printed in Northern Ireland

Design Studies for a Cs-137 Irradiator

D. O. Cummins and C. F. G. Delaney
Physical Laboratory, Trinity College, Dublin, Ireland

(*Received* 22 *July* 1960)

Design studies for a 600 c caesium irradiator for genetic experiments are described. The six source rods, arranged in a cylinder around the sample, can be moved in and out on an iris diaphragm arrangement so as to give varying intensities at the sample. The distribution of the discrete sources contained in the rods is discussed in detail, with a view to providing the maximum flux uniformity throughout the sample to be irradiated. A low-activity mock-up was used to arrive at an arrangement which was appreciably better than a uniform distribution of sources along the rods. A twelve rod system is also briefly discussed.

ETUDES DE DESSIN POUR UN IRRADIATEUR A Cs-137

On décrit des études de dessin pour un irradiateur à césium de 600 c pour des expériences génétiques. Les six tiges-sources, arrangées autour de l'échantillon dans un cylindre, peuvent être déplacées par un système comparable à un diaphrame iris afin de rendre variable l'intensité à l'échantillon. On discute en détail la distribution des sources discrètes contenues dans les tiges, ayant pour but la provenance de la plus haute uniformité du flux à travers le sujet soumis au rayonnement. On utilisa un modèle à activité faible pour atteindre une disposition qui était en quelque façon supérieure à une distribution uniforme des sources le long des tiges. Aussi discute-t-on brièvement un système à douze tiges.

ИССЛЕДОВАНИЕ КОНСТРУКЦИИ ОБЛУЧАТЕЛЯ Cs-137

Дано описание конструкции цезиевого источника в 600 кюри для опытов по генетике. Шесть стержней с источниками, расположенные вокруг образца по окружности цилиндра, можно передвигать с помощью ирисовой диафрагмы для обеспечения переменной интенсивности облучения образца. Подробно рассматривается распределение отдельных источников внутри стержней, обеспечивающее максимальную равномерность облучения. Исследования, проводившиеся с низкой активностью, позволили подобрать распределение источников, обеспечивающее значительно большую эффективность, чем равномерное распределение. Дается также краткое описание системы с 12 стержнями.

ENTWURF EINER Cs-137 BESTRAHLUNGSANLAGE

Der Entwurf einer Bestrahlungsanlage für 600 c Cs-137 für genetische Versuche wir dbeschrieben. Einzelne Quellen in insgesamt 6 stabförmigen Bestrahlungseinheiten werden zylindrisch rund um die Probe auf einer Irisblende angeordnet, sodass durch Bewegung der einzelnen Quellen von und zu der Probe verschieden grosse Bestrahlungsintensitäten am Ort der Probe erreicht werden. Die Verteilung der einzelnen Quellen in den Bestrahlungsstäben wird im Detail besprochen, im Hinblick darauf, dass ein möglichst hoher Fluss gleichförmig am Ort der Probe erzeilt wird. Ein Modell niederer Aktivität wurde zur experimentellen Bestimmung einer Verteilung der Quelle verwendet, welche bedeutend günstiger ist, als die gleichmässige Verteilung der Quellen innerhalb der Stäbe. Ein System mit 12 Stäben wird kurz diskutiert.

The 600 c caesium irradiator discussed in this paper is intended for genetic experiments on plants and must be capable of giving a wide range of dose rates from a maximum of about 100,000 rad/hr down to a small fraction of this value. To achieve this most economically the six source rods which surround the specimen will be attached to an iris diaphragm arrangement so that the radius of the cylinder on which they lie can

be altered from 1 in. to 3 in. Lead absorbers can then further reduce the dose to the plant.

The rods will be of length 6 in. and will each contain a set of discrete sources.

It is clear that in general in an irradiator of this type the flux may vary considerably from one part of the interior to another. For example with a uniform distribution of caesium sources in the rods, one would normally expect a fall off of flux on moving out along the axis of the irradiator from the centre. This paper is concerned with the possibility of suitably choosing the distribution of discrete sources in the rods so as to produce a fairly large region of approximately constant flux. The problem is obviously complicated by the requirement that a region of uniform flux must exist, not just for one, but for all values of the radius of the ring of source rods as they are moved in or out by the iris diaphragm.

GHORMLEY and HOCHANADEL[1] have given details of a distribution of sources such that the intensity along the axis of their irradiator was uniform within a few per cent, but do not give details for non-axial points. Since for these points, calculations of intensity are obviously very laborious, it was decided in the present instance to solve the problem by constructing a low-activity mock-up. This was made four times larger than the actual irradiator so that conventional sized detectors could be used. It is shown in Fig. 1. Six glass tubes of internal diameter $\frac{3}{4}$ in. simulated the source rods, and small sample bottles, which slid into these tubes and contained 1 ml of Cs-137 solution in a thin layer, simulated the sources. These bottles were $1\frac{1}{3}$ in. in height and thus nineteen sources could be contained in the 24 in. height of the rods. The radius of the ring of source rods could be made 4 in., 8 in. or 12 in.

It was first planned simply to set up a given arrangement of sources in the rods (using empty bottles as spacers where necessary) and quickly map the gamma field produced using a Geiger or scintillation counter. It was soon realized that such a method was impractiable due to the fact that the response, both of a Geiger and scintillation counter, depends strongly on the direction of the incoming radiation, i.e. the polar diagram of their sensitivity is far from spherical. However, a piece of plastic scintillator (1 in. long and 1 in. in diameter) on the end of a 6 in. light pipe and surrounded merely by a thin paper light shield proved to have a uniform sensitivity with direction in the upper half-plane, and this

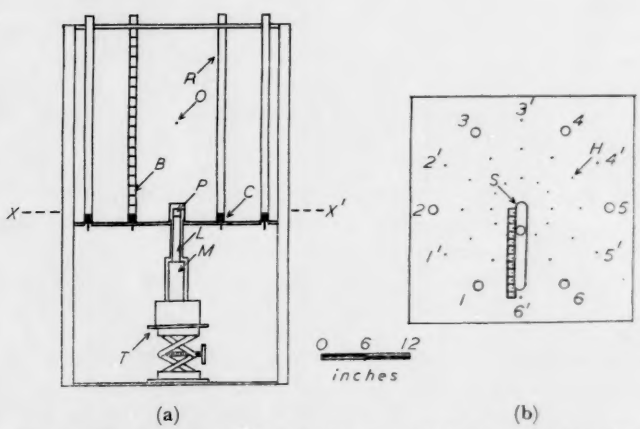

FIG. 1. The irradiator mock-up. (a) Vertical section; (b) horizontal section through *xx'*. (R) Source rod; (B) source bottle; (C) cork with locating pin; (H) locating hole; (P) plastic scintillator; (L) light pipe; (M) photomultiplier; (T) adjustable table for initial adjustment of heights; (S) slot for radial movement of detector; (O) origin of co-ordinates.

was made the basis of the final method of measurements, as described below.

Using cylindrical polar co-ordinates, r,θ,z, with the centre of symmetry of the irradiator (O) as the origin, the scintillation detector was kept permanently in the plane $Z = -12$ in. (Fig. 1). Thus all sources would always be in the upper half-plane of the detector and be detected with the same efficiency.

Suppose the source rods were at a radius of $R = 12$ in. and information is required about the flux along say the line $r = 3$ in. The detector was first placed at $r = 3$ in. in the plane $Z = -12$ in. A source bottle was placed in the top-most position in each rod (i.e. at $Z = 12$ in.), with empty bottles in all other positions, and a count taken for a suitable time. The Cs–137 activity was such that this was around 6000/min. The active bottles were then moved down one position in each rod, i.e. $1\frac{1}{3}$ in., and the count again taken. This process was repeated until the active bottles arrived at the lowest position, $Z = -12$ in. From the data thus obtained one can calculate the flux for any value of Z (at $r = 3$ in.) and for any arrangement of sources, as follows.

It will be easiest to take a concrete case, and so let us assume we are dealing with a source arrangement having sources in the first, third, fifth, . . . seventeenth, and nineteenth bottles (counting from the tops of the rods) with extra sources in the second and eighteenth positions. We might say, in another notation, that sources are at $Z = \pm 1, \pm 3, \pm 5, \pm 7, \pm 8$ and ± 9 units, where 1 unit = 1 bottle height = $1\frac{1}{3}$ in. (This particular arrangement was in fact quite a successful one.) Let us further call the count per minute, obtained experimentally as described previously, c_1, c_2, $c_3 \ldots c_{19}$, where c_1 is the count with the sources in the topmost position. Then the flux in the plane of symmetry, i.e. at $Z = 0$, $r = 3$ with the above source arrangements is given by:

$$2(c_{18} + c_{16} + c_{14} + c_{12} + c_{11} + c_{10}).$$

The flux at the bottom of the irradiator, i.e. at $Z = -12$ in., $r = 3$ in., is similarly given by

$$c_{19} + c_{18} + c_{17} + c_{15} + c_{13} + c_{11} + c_9 + c_7 + c_5 + c_3 + c_2 + c_1$$

while the flux at five "bottle" units from the plane of symmetry, i.e. at $Z = -6\frac{2}{3}$ in. is

$$c_{19} + 2c_{17} + c_{16} + 2c_{15} + c_{13} + c_{11} + c_9 + c_7 + c_6 + c_5.$$

By putting the detector at various values of r and θ, the flux over the whole region with the source rods at $R = 12$ in. can be mapped. Similar mapping can be carried out with the rods at other values of R.

In practice, flux determinations were made as follows:

with the rods at $R = 12$ in., at $r = 0$, 3, 6 and 9 in.
with the rods at $R = 8$ in., at $r = 0$, 3 and 6 in.
with the rods at $R = 4$ in., at $r = 0$ and 2 in.

Two θ positions were measured in each case, one with the detector opposite a source rod and the other with the detector mid-way (as regards angle) between two source rods. As it was impossible to move the detector except in a radial direction along a slot this was achieved by taking readings first with the six rods placed in the positions marked 1, 2, 3, 4, 5, 6, in Fig. 1, and then with them in the positions marked 1′, 2′, 3′, 4′, 5′ and 6′.

(The results for $R = 12$ in. at $r = 9$ in. and $r = 6$ in. as well as those for $R = 8$ in. at $r = 6$ in. are not of much interest, both because, unlike the rest, they were strongly dependent on θ, and also because it is obvious anyhow that it is not going to be possible to produce near uniformity of flux over such a large fraction of the volume.)

From previous discussion, it is obvious that flux determinations in the vertical direction were possible at ten points from 0 to 12 in., i.e. at a spacing of 12/9 in. = $1\frac{1}{3}$ in. (negative values of Z were symmetrical with the positive ones). Readings were made at a

FIGS 2–7. Flux in different parts of the irradiator for various rod positions.
Source arrangement (a) denoted by ○ Source arrangement (b) denoted by ●
Source arrangement (c) denoted by ⊗ Source arrangement (d) denoted by □
Source arrangement (e) denoted by △.
In each case the vertical dashed line shows the limit of sample volume proposed, and the horizontal dashed lines the ±10 per cent variation allowed in the flux.

FIG. 2. Source rods at $R = 12$ in., detector at $r = 0$.

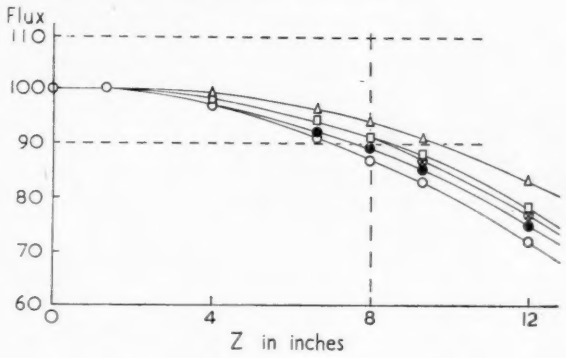

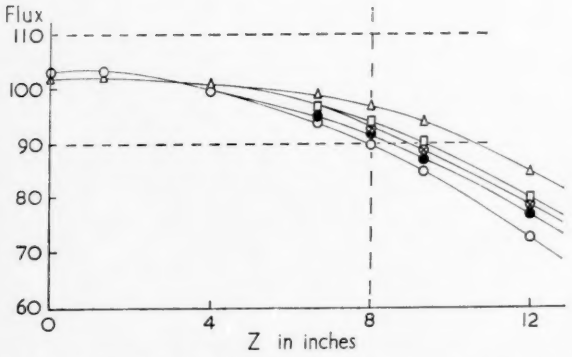

FIG. 3. Source rods at $R = 12$ in., detector at $r = 3$ in.

selected number of these; i.e. for all values of r readings were made at:

$Z = 0$, $1\frac{1}{3}$, 4, $6\frac{2}{3}$, 8, $9\frac{1}{3}$ and 12 in. that is at $Z = 0$, 1, 3, 5, 6, 7 and 9 "bottle" units of $1\frac{1}{3}$ in.

We must now discuss the actual source arrangements which were investigated. In all cases the arrangements in all the rods were identical. There was also symmetry with respect to the plane $Z = 0$.

Five arrangements were examined as follows.

(a) Sources at $Z = 0$, ±1, ±2, ±3, ±4, ±5, ±6, ±7, ±8 and ±9 units—a quasi-uniform arrangement (1 unit = $1\frac{1}{3}$ in.).

(b) Sources at $Z = 0$, ±1, ±2, ±3, ±4, ±5, ±6, ±7, ±8 and a double strength source at ±9 units.

(c) Sources at $Z = \pm1$, ±2, ±3, ±4, ±5, ±6, ±7, ±8 and a double strength source at ±9 units.

(d) Sources at $Z = \pm1$, ±3, ±5, ±7, ±8 and ±9 units.

(e) Sources at $Z = \pm1$, ±3, ±5, ±7, ±8 and a double strength source at ±9 units.

Graphs of the variation of flux at various points for the five arrangements above are shown in Figs. 2–7. For both the graphs with $R = 12$ in., the flux at $Z = 0$, $r = 0$ is taken as 100. For both the graphs with $R = 8$ in., the flux at $Z = 0$, $r = 0$ when $R = 8$ in. is taken as 100. Similarly, for both the graphs with $R = 4$ in. the flux at $Z = 0$, $r = 0$ when $R = 4$ in. is taken as 100.

For the present application, it was decided that a sample volume of $\frac{1}{2}$ in. radius by 4 in. high would be sufficient. This corresponds to $r = 2$ in., $Z = \pm8$ in. in the 4 to 1 mock-up.

VOL. 10 1961

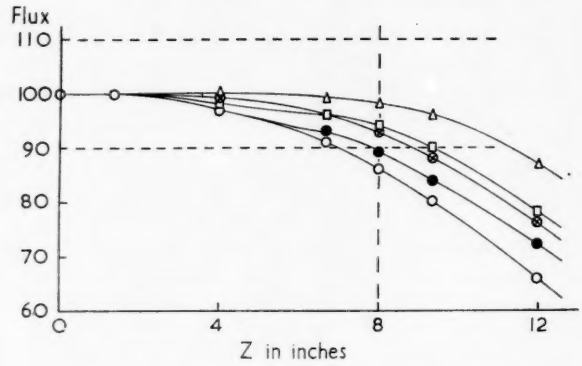

FIG. 4. Source rods at $R = 8$ in., detector at $r = 0$.

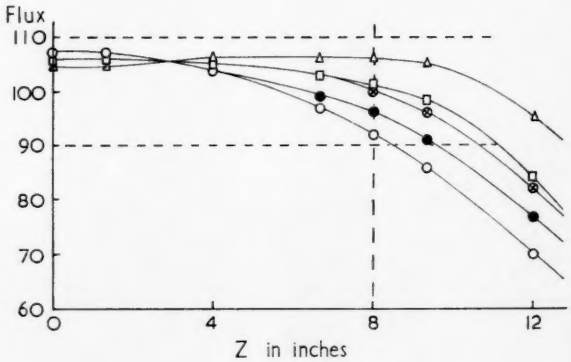

FIG. 5. Source rods at $R = 8$ in., detector at $r = 3$ in.

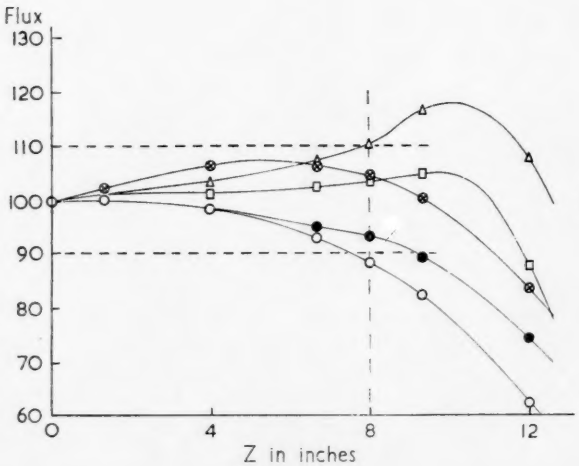

FIG. 6. Source rods at $R = 4$ in., detector at $r = 0$.

Suppose a constancy of flux to ± 10 per cent over this region is arbitrarily demanded. From the graphs it is clear that only arrangement (d) will satisfy this requirement. Arrangements (e) and (c) fail with the rods close in, i.e. at $R = 4$ in. and $r = 2$ in. Arrangements (a) and (b) fail both at $R = 12$ in., $r = 0$, and at $R = 8$ in., $r = 0$. It may be argued that arrangement (a) is not a true uniform distribution but a row of discrete sources. However, if one calculates the axial flux for a truly uniform distribution for $R = 12$ in. and $R = 8$ in.,

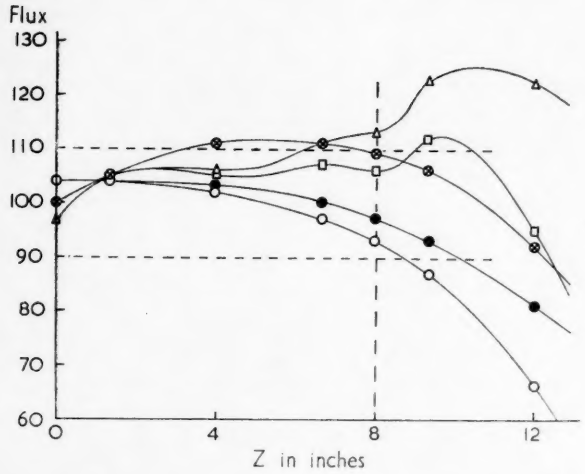

FIG. 7. Source rods at $R = 4$ in., detector at $r = 2$ in.

VOL. 10 1961

it gives a result very close to arrangement (a) and failing in the same way.

There are however other subsidiary points which must be taken into consideration before finally choosing arrangement (d). One is the ratio of intensities available at the centre of the sample when the source ring is moved from its fully closed ($R = 4$ in.) to its fully open position ($R = 12$ in.). This is 4·5, 4·4, 4·1, 4·1 and 3·9 for arrangements (a), (b), (c), (d) and (e) respectively.

Another very relevant consideration is the absolute value of the flux at the centre with the rods in their closest in position. If this is calculated for 600 c arranged in six-rods at a minimum radius of 1 in. (real, not mock-up), values are obtained (in thousands of radians per hour) of 115, 107, 98, 98 and 88 for arrangements (a) to (e) respectively. In both of these later considerations, arrangement (d) is obviously not the optimum one but, as uniformity of flux was the overriding factor, it was felt that it performed sufficiently well under these minor heads to be selected.

Before it was clear that six was the maximum number of rods which could be accommodated on the iris diaphragm, a twelve rod arrangement was investigated. In this case each rod contained only five sources and the distribution was not symmetrical with respect to the plane $Z = 0$, for any particular rod. Alternate rods however had a distribution which was the mirror image in the plane $Z = 0$ of the others. With a particular arrangement of this kind it was possible to hold the flux constant to ± 7 per cent over the region discussed previously, where with the six rod arrangement a variation of ± 10 per cent occurred. For the reason stated above, however, this improved performance is not of practical interest here.

Acknowledgements—The authors are indebted to the staff of Radiation Applications Incorporated (who are manufacturing the irradiator) for helpful discussions and also to Dr. J. H. J. POOLE of Trinity College for his advice and help. The irradiator itself is part of a generous gift of nuclear equipment to Trinity College from the United States Government.

REFERENCE

1. GHORMLEY J. A. and HOCHANADEL C. é. *Rev. Sci. Instrum.* **22,** 473 (1951).

International Journal of Applied Radiation and Isotopes, 1961, Vol. 10, pp 112 to 115. Pergamon Press Ltd. Printed in Northern Ireland

Greffage Radiochimique par Irradiation à Basses Temperatures

J. R. PUIG et J. DOBÓ*
Centre d'Etudes Nucléaires de Saclay, Gif-sur-Yvette (S. et O.), France

(*Received* 20 *June* 1960)

Le greffage radiochimique du styrolène sur du polyéthylène a été réalisé par irradiation simultanée du polymère et du monomère à basse température. Le greffage a lieu presqu'entièrement après l'irradiation lorsque l'échantillon s'est réchauffé jusqu'à la température ambiante. Il se fait d'autant mieux que le polymère est dépourvu d'antioxydant. La présence d'oxygène moléculaire semble empêcher l'homopolymérisation et favoriser la copolymérisation. Les échantillons obtenus sont exempts d'occlusion d'homopolymère comme ceux qu'on obtient par préirradiation sous vide. Les conditions nécessaires à une distribution homogène des greffons dans l'épaisseur du polymère sont discutées.

RADIOCHEMICAL GRAFTING BY MEANS OF LOW TEMPERATURE IRRADIATION

Radiochemical grafting of styrolene onto polyethylene has been achieved by the simultaneous irradiation of the polymer and the monomer at low temperature. Grafting takes place almost entirely after the irradiation when the specimen has warmed up to room temperature. The reaction is all the more efficient if the polymer is free of reducing agent. The presence of molecular oxygen appears to hinder homopolymerisation and to favour copolymerisation. The samples produced are free from homopolymer occlusion like those obtained by preirradiation in a vacuum. The conditions required for a homogeneous distribution of grafts in the thickness of the polymer are discussed.

РАДИАЦИОННО-ХИМИЧЕСКАЯ ПРИВИВКА ПОД ДЕЙСТВИЕМ ОБЛУЧЕНИЯ ПРИ НИЗКИХ ТЕМПЕРАТУРАХ

Радиационно-химическая прививка стиролена к полиэтилену осуществлялась путем одновременного облучения полимера и мономера при низкой температуре. Прививка происходит в основном после облучения, когда образец нагревается до комнатной температуры. Отсутствие антиокислителя способствует прививке. Присутствие молекулярного кислорода, повидимому, препятствует гомополимеризации и способствует сополимеризации. Полученные образцы не содержат блоков гомополимера, в отличие от образцов, получаемых при облучении в вакууме. Обсуждаются условия, при которых сшивки равномерно распределяются в массе мономера.

STRAHLENCHEMISCHE PFROPFUNG DURCH BESTRAHLUNG BEI NIEDRIGEN TEMPERATUREN

Die strahlenchemische Pfropfung von Styrol und Polyäthylen wurde durch gleichzeitige Bestrahlung des Polymers und des Monomers bei tiefen Temperaturen durchgeführt. Die Pfropfung findet fast gänzlich nach der Bestrahlung statt, wenn die Probe sich wieder auf die Temperatur der Umgebung erwärmt hat. Sie ist umso besser, je mehr aus dem Polymer die antioxydierenden Stoffe entfernt wurden. Die Gegenwart von molekularem Sauerstoff scheint die Homopolymerisation zu verhindern und die Copolymerisation zu fördern. Die erhaltenen Proben sind frei von homopolymeren Einschlüssen in gleicher Weise, wie Proben, die im Vakuum vorbestrahlt wurden. Die für die gleichmässige Verteilung im Inneren des Polymers nötigen Bedingungen werden diskutiert.

* Adresse actuelle: Institut de Recherches de l'Institut des Matières Plastiques de Budapest.

VOL. 10 1961

Le greffage radiochimique a fait l'objet de plusieurs recherches au cours des dernières années en raison, d'une part, de l'intérêt théorique incontestable présenté par les nouveaux matériaux ainsi formés et, de l'autre, en vue des possibilités d'applications industrielles.[1–18]

En ce qui concerne le greffage des monomères sur les polymères préformés, par exemple sur des films, trois méthodes sont en principe adoptées:

(1) irradiation simultanée du polymère et du monomère;

(2) préirradiation du polymère sous vide poussé et addition postérieure du monomère qui polymérise à partir des radicaux libres gelés;

(3) préirradiation du polymère à l'air et addition postérieure du monomère qui polymérise par suite de la décomposition des péroxydes initialement formés.

Les différentes méthodes ont chacune leurs avantages et leurs inconvénients. La dose d'irradiation exigée est la plus petite dans le cas de l'irradiation simultanée. Elle est la plus grande probablement dans le cas de la préirradiation sous vide; d'autre part les techniques de préirradiation ne donnent que très peu d'homopolymère et les films obtenus ont un aspect plus homogène par suite de l'absence d'homopolymérisation dans l'intérieur des films. Selon Ballantine[15], la préirradiation sous vide serait de ce point de vue la plus avantageuse.

Dans le présent travail, nous nous sommes proposés d'irradier simultanément le monomère et le polymère, mais à une température suffisamment basse pour que le polymère ne soit pratiquement pas gonflé par le monomère, en espérant qu'il en résulterait une certaine combinaison des caractères de l'irradiation simultanée et de la préirradiation, à savoir:

(1) qu'il ne se formerait pas d'homopolymère dans les films;

(2) qu'il ne se formerait que très peu d'homopolymère dans le monomère environnant, par suite des basses températures d'irradiation;

(3) que les exigences du point de vue désoxygénation seraient moins rigoureuses que dans les techniques de préirradiation.

Nous avons étudié le système polyéthylène–styrolène.

CONDITIONS EXPERIMENTALES

Deux types de polyéthylène-haute-pression en film ont été employés: (a) film préparé à partir d'une poudre ne contenant pas d'antioxydant d'environ 0,45 mm d'épaisseur; (b) film commercial de 0,03 mm d'épaisseur.

Le styrolène était distillé sous vide.

On s'est servi d'ampoules de 10 mm de diamètre intérieur. Le remplissage était fait par deux méthodes différentes correspondant à différentes qualités de désoxygénation:

(A) Le monomère était désoxygéné par congélation et évacuation et les films de polymère par 3 heures de dégazage dans un vide secondaire. Le styrolène était ensuite distillé sur le polyéthylène maintenu à la température de l'azote liquide et les ampoules étaient scellées.

(B) Le styrolène refroidi à $-30°$ C était ajouté aux films de polyéthylène. Après un barbotage rapide d'azote à froid, les ampoules étaient placées dans l'azote liquide et scellées.

Dans une des expériences, de l'air était admis avant irradiation.

Les ampoules étaient ensuite irradiées avec un accélérateur linéaire Massiot fournissant un faisceau d'électrons pulsés et balayés de 4 MeV avec une intensité de 30 μA. Après une irradiation de 45 sec correspondant à la dose totale de 25 Mrad environ, les ampoules initialement à la température de l'azote liquide s'étaient échauffées jusqu'à une température voisine de 0°C, le styrolène étant partiellement ou totalement fondu. Dans l'une des expériences, l'ampoule s'est échauffée pendant l'irradiation jusqu'à ce que sa surface atteigne une température de 40–50°C environ.

Une partie des ampoules était ouverte 10 à

15 minutes après l'irradiation, l'autre partie était gardée pendant deux jours à la température ambiante avant ouverture. Les films étaient lavés, séchés et pesés, l'homopolymère était précipité, séché et pesé comme à l'ordinaire.

RESULTATS EXPERIMENTAUX

Les résultats expérimentaux sont résumés dans le Tableau 1.

L'examen du Tableau 1 permet les constatations suivantes.

(1) En l'absence de post-effet prolongé le taux de greffage atteint seulement 2 à 3 % et l'homopolymérisation 3 à 5 % (Expériences 1, 3, 5).

(2) Après un post-effet de 2 jours à température ambiante l'homopolymérisation augmente d'environ 1, 5 à 2 fois, tandis que le greffage augmente, selon les conditions, de 3 à 20 fois. (Expériences 1, 3, 5, vs. 2, 4, 6).

(3) Le greffage sur du polyéthylène ne comportant pas d'antioxydant est beaucoup plus efficace que sur les films commerciaux (Expériences 2, 6, vs. 4, 7).

(4) Une désoxygénation plus efficace a pour effet d'augmenter la vitesse d'homopolymérisation et de diminuer la vitesse de greffage (Expériences 2, 4 vs. 6, 7).

(5) Un échauffement pendant l'irradiation a pour conséquence une augmentation de la vitesse d'homopolymérisation. Le taux de greffage est très petit, bien qu'une petite partie du film soit fortement (et très inégalement) greffée. La plupart des radicaux gelés est sans doute détruite par l'échauffement.

TABLEAU 1

No. d'essai	Type de film	Mode de désoxygénation	Post effet (heure)	Greffe‡ (%)	Homopolymérysation§ (%)
1	a	A	~0,25	3,1	5,2
2	a	A	48,0	19,9	6,69
3	b	A	~0,25	2,8	3,32
4	b	A	48,0	7,7	8,3
5	a	B	~0,25	2,1	3,085
6	a	B	48,0	45,8	6,27
7	b	*	48,0	15,9	5,76
8	b	B	48,0†	0,8	16,05

* Oxygène admis avant l'irradiation.
† Tube échauffé à 40–50°C pendant l'irradiation.
‡ $\frac{\text{Augmentation du poids du film}}{\text{Poids initial du film}} \times 100.$
§ $\frac{\text{Poids de l'homopolymère}}{\text{Poids du monomère}} \times 100.$

REMARQUES SUR L'HOMOGENEITE DU POLYMERE GREFFE

Par homogénéïté du polymère greffé on peut entendre l'absence plus ou moins complète d'occlusions d'homopolymère. Ballantine a étudié de ce point de vue les copolymères préparés par préirradiation sous vide, par préirradiation dans l'air et par irradiation simultanée et a trouvé que l'homogénéïté des films décroit dans l'ordre indiqué, d'où on pourrait tirer la conclusion que les copolymères greffés obtenus par préirradiation sous vide sont d'une qualité supérieure aux autres.

Les films obtenus par la méthode que nous proposons ont un aspect semblable à celui des produits obtenus par préirradiation sous vide tel que Ballantine l'a décrit.

Mais il existe aussi une autre sorte d' "homogénéïté" qui n'est pas, du point de vue pratique, de moindre importance, à savoir l'homogénéite *de la distribution des greffons* dans l'épaisseur du film. La condition d'une distribution homogène est que la vitesse de diffusion monomère soit beaucoup plus grande que la vitesse de destruction des centres formés dans les films. Or, d'après les résultats de Ballantine qui sont confirmés par nos expériences, l'augmentation de la température d'irradiation ou de la température de greffage au-dessus de 0°C aboutit dans la méthode de préirradiation sous vide à une chute de la vitesse de greffage, ce qui peut être expliqué par une destruction mutuelle des centres initiateurs potentiels. D'autre part, à une température de 0°C, par

VOL. 10 1961

exemple, la destruction mutuelle des centres est sans doute plus lente, mais la diffusion du monomère est elle aussi très lente. Ainsi, la condition ci-dessus mentionnée semble ne pas être satisfaite et cela d'autant moins que le film est plus épais.

En ce qui concerne la méthode par irradiation simultanée, on peut considérer que sous certaines conditions le greffage se déroule partiellement comme un greffage par préirradiation, le monomère qui diffuse pendant ou après l'irradiation atteignant des centres préalablement formés. Mais cette "préirradiation" est du point de vue utilisation de l'énergie absorbée beaucoup moins efficace, ce qui entraine un plus faible greffage dans les régions affectées. Si par contre on exécute l'irradiation après un fort gonflement du polymère dans le monomère, on obtient des inhomogénéïtés résultant de l'homopolymérisation dans l'épaisseur du film.

Dans le cas de la préirradiation en présence d'air, la décomposition des péroxydes et par conséquent la destruction des centres actifs exige des températures beaucoup plus élevées pour lesquelles la diffusion est déjà très rapide. Par conséquent, on peut obtenir une distribution plus homogène des greffons, sans avoir une quantité élevée d'homopolymère dans les films.

Pour étudier la distribution des greffons, nous proposons de greffer sur le polyéthylène un polymère de teinture facile.[18]

Nous pouvons conclure en disant que la méthode proposée présente la plupart des avantages de la préirradiation sous vide en particulier en ce qui concerne l'absence d'inclusions d'homopolymère. En outre cette méthode nécessite des conditions de désoxygénation peu rigoureuses. D'autre part, on ne peut éviter la formation d'une certaine quantité d'homopolymères dans le monomère environnant.

En ce qui concerne l'homogénéïté suivant l'épaisseur, les échantillons préparés par la méthode proposée ont, comme les échantillons obtenus par préirradiation sous vide, une distribution des greffons moins homogène que dans les méthodes de préirradiation dans l'air et d'irradiation simultanée.

Remerciements—Ce travail fait partie d'un stage effectué au Service de Physico-Chimie Appliquée du C. E. N. Saclay par M. J. Dobó sous les auspices de l'Agence Internationale de l'Energie Atomique.

Nous tenons à remercier M. Sack des Houillères du Nord et du Pas-de-Calais qui nous a obligeamment fourni du polyéthylène en poudre exempt d'antioxydant.

REFERENCES

1. Bouby L., Chapiro A., Magat M., Migirdicyan E., Prevot-Bernas A., Reinisch L. et Sebban J. *Actes de la Conférence Internationale sur l'Utilisation de l'Energie Atomique à des fins Pacifiques, Genève* 1955, **7,** 612 (1955).
2. Bern J., Mesrobian R., Restaino A., Ballantine D., Glines A. et Metz D. *J. Polym. Sci.* **19,** 219 (1956).
3. Chapiro A. *Industr. Plast. mod.* **9,** No. 2, 34 (1957).
4. Ballantine D. *Mod. Plast.* **35,** No. 1, 171 (1957).
5. Chen W., Mesrobian R., Ballantine D., Metz D. et Glines A. *J. Polym. Sci.* **23,** 903 (1957).
6. Pinner S. et Wycherley V. *Plastics* **22,** 243, 504 (1957); **23,** 244 (1958).
7. Charlesby A. et Pinner S. *Industr. Plast. mod.* **9,** No. 9, 30 (1957); **9,** No. 10, 43 (1957).
8. Henglein A. et Schnabel W. *Makromol. Chem.* **25,** 119 (1957).
9. Seban-Danon J. *J. Polym. Sci.* **29,** 367 (1958).
10. Henglein A., Schnabel W. et Heine K. *Z. Angew. Chem.* **70.** 461 (1958).
11. Chapiro A. *J. Polym. Sci.* **29,** 321 (1958).
12. Chapiro A. *J. Polym. Sci.* **34,** 439 (1959).
13. Chapiro A. *J. Polym. Sci.* **34,** 481 (1959).
14. Hoffman A. S., Gilliland E. R., Merrill E. W. et Stockmayer W. A. *J. Polym. Sci.* **34,** 461 (1959).
15. Ballantine D., Glines A., Adler G. et Metz D. Z. *J. Polym. Sci.* **34,** 419 (1959).
16. Dobó J. et Somogyi A. *J. Chim. Phys.* **56,** 863 (1959).
17. Restaino A. J. et Reed W. N. *J. Polym. Sci.* **36,** 499 (1959).
18. Dobó J., Somogyi A. et Lakmer E. *Plaste und Kantschuk,* **7,** 393 (1960).

International Journal of Applied Radiation and Isotopes, 1961, Vol. 10, pp. 116–127. Pergamon Press Ltd. Printed in Northern Ireland

Total Ionization in Gases by High-Energy Particles: An Appraisal of Our Understanding*

R. L. PLATZMAN†
Laboratoire de Chimie Physique, Faculté des Science, Université de Paris, France

(*Received* 2 *November* 1960)

This paper is dedicated with admiration and affection to Dr. WILLIAM P. JESSE, on the occasion of his seventieth birthday. To his remarkable experiments, more than to any other factor, we owe the new promise of developing a quantitative interpretation of the phenomena to be described.

Recent years have seen substantial progress in the reliability and accuracy of the experimental measurement of W, the mean energy required to form an ion pair by the absorption of high-energy radiations (such as α-particles or β-particles) in gases. In many cases—and especially, but not exclusively, in contaminated gases or in gaseous mixtures—the experiments do not determine the number of ions produced directly by the incident radiation and the secondary electrons which it generates, because ion collection is slower than many varieties of secondary process. Thus the total ionization may be augmented by ion-producing collisions of excited atoms (particularly atoms in metastable excited states) or subexcitation electrons. Use of high-energy radiations therefore affords valuable opportunities for the study of such processes. When the various artifacts have been disentangled from the "direct" ionization, the true value of W is available for theoretical analysis. Three different methods for theoretical calculation of W are outlined, and all are applied to the case of helium. Application of the theories together with experimental data to other gases and to gaseous mixtures yields new information on cross-sections for inelastic collisions of charged particles with atoms and molecules, and even on an important optical property of the medium. The theories also provide the first trustworthy information on the total numbers of various products formed in the absorption of high-energy radiations.

L'IONISATION TOTALE PRODUITE DANS LES GAZ PAR LES PARTICULES DE HAUTE ENERGIE: UNE EVALUATION DE NOTRE INTELLIGENCE (EN CE SUJET)

Depuis quelques années on a fait du progrès considérable dans la mesure expérimentale de W, l'énergie moyenne de formation d'une paire d'ions par les rayonnements de haute énergie dans les gaz. Souvent les expériences ne mesurent pas le nombre d'ions donné directement par le rayonnement incident et par ses électrons secondaires: l'ionization totale peut être augmentée, par exemple, par des rencontres d'atomes excités ou par des électrons en sous-excitation. Les

* This paper is based upon a lecture given at the *Conference on Penetration of Charged Particles in Matter*, organized by the Subcommittee on Penetration of Charged Particles in Matter, Committee on Nuclear Science, U.S. National Research Council, and held at Gatlinburg, Tennessee between 15–18 September 1958. Part of it is included in the *Proceedings* of that Conference, National Research Council Publication 752, Washington, D.C. (1960).

† Fulbright Professor, 1959–1960. On leave from Argonne National Laboratory, Argonne, Illinois, U.S.A.

rayonnements de haute énergie sont de valeur à l'étude de tels procédés. Lorsqu'on a dégagé les produits artificiels de l'ionization "directe", la valeur correcte de W reste pour servir à l'analyse théorique. On indique trois méthodes différentes de calculer W théoriquement, et toutes sont appliquées au cas de l'hélium. L'application des théories avec des données expérimentales à des autres gaz donne de nouveaux renseignements sur les sections transversales pour les rencontres inélastiques des particules chargées avec les atomes et les molécules, même sur une propriété optique importante. Les théories donnent aussi pour la premiére fois une indication valable du nombre total des différents produits formés au cours de l'absorption des rayonnements de haute énergie.

ПОЛНАЯ ИОНИЗАЦИЯ В ГАЗАХ ВЫСОКОЭНЕРГЕТИЧЕСКИМИ ЧАСТИЦАМИ; РАЗЦЕНКА НАШЕГО ПОНИМАНИЯ

За последние годы был сделан значительный прогресс в установлении надёжности и точности экспериментального измерения W—среднего коэффициента энергии, требующегося для образования ионной пары посредством поглощения высоко-энергичных излучений частиц /вроде частиц и частиц/ в газах. Во многих случаях, и в частности /но не исключительно/ в заражённых радиоактивностью газах или же газовых смесях, экспериментами не дается определения количеества ионов, которые непосредственно производятся, благодаря падающему излучению и вырабатываемых им вторичных электронов, т.к. ионы скопляются медленнее, чем другие разновидности вторичного процесса. Таким образом, полная ионизация может быть усилена ионо-производящими столкновениями возбуждённых атомов /особенно атомов, находящихся в состоянии метастабельного возбуждения/, или же посредством субвозбуждения электронов. Поэтому, использование высокоэнергичных излучений открывает ценные возможности в деле изучения таких процессов. После того как "непосредственная" ионизация освобождена от всех привходящих искусственных факторов, истинное значение W становится доступным для теоретического анализа. В общих чертах, было обнаружено три способа вычисления W, и все они приложимы в отношении гелия. Применение теорий, совместно с экспериментальными данными, к другим газам и газообразным смесям, выявляет новую информацию относительно неупругих столкновений заряженных частиц с атомами и молекулами взятых в целом, и даже относительно одного важного оптического свойства среды. В то же самое время, этими теориями снабжается первая надёжная сводка касательно общей суммы различных продуктов, образующихся в абсорпции высокоэнергичных излучений.

TOTALE IONISIERUNG VON GASEN DURCH TEILCHEN HOHER ENERGIE: EINE ABSCHÄTZUNG UNSERER VERSTÄNDNISSE

In den letzten Jahren sind wesentliche Fortschritte in der Verlässlichkeit sowie Genauigkeit der experimentellen Messung von W gemacht worden, wo W der Mittelwert der Energie ist, die zur Erzeugung eines Ionenpaares durch Absorption von Strahlen hoher Energie (z.B. α oder β Teilchen) in Gasen aufgewendet werden muss.

In vielen Fällen und besonders (aber nicht ausschliesslich) in unreinen Gasen oder Gasmischungen, bestimmen die Versuche nicht unmittelbar die durch die einfallende Strahlung sowie durch die sekundaren Elektronen erzeugte Anzahl von Ionen, weil die Ionensammlung langsamer erfolgt als viele Arten sekundarer Prozesse. Die totale Ionisation kann demzufolge durch Stösse erregter Atome, die Ionen bilden, vergrössert werden (besonders durch Atome in metastabilen erregtem Zustand) oder durch erregte Elektronen.

Der Gebrauch von Strahlen hoher Energie gibt deshalb wertvolle Gelegenheit für das Studium solcher Vorgänge.

Wenn die verschiedenen Nebenerscheinungen von der unmittelbaren Ionisation getrennt worden sind, wird der wirkliche Wert von W für die theoretische Analyse verfügbar. Drei verschiedene Methoden von W werden umrissen und werden alle drei für den Fall He angewendet. Die Anwendung der Theorien sowie der Versuchsergebnisse an anderen Gasen und Gasmischungen geben neue Erkenntnisse über den Wirkungsquerschnitt unelastischer Zusammenstösse von geladenen Teilchen mit Atomen und Molekülen, und sogar Aufschlüsse über eine wichtige Eigenschaft des Mediums.

Die Theorien geben auch die erste vertrauenswürdige Auskunft über die Gesamtzahl der verschiedenen Produkte die entstehen wenn Strahlen hoher Energie absorbiert werden.

VOL. 10 1961

1. INTRODUCTION

THE efficiency of ionization of gases by swiftly moving charged particles is generally measured by W, the mean energy expended per ion pair produced. (Quantities analogous to W can be determined in many solids,[1] but they will not be considered here. Section 2.15, Chap. 2[1] offers a brief review on the subject of ionization in gases, and includes many references to the recent literature.) For complete absorption, the most common case is $W = T_0/N_i$, where T_0 is the initial kinetic energy of the particle and N_i is the average total number of ion pairs formed. (More accurately, $\pm N_i e$ is the total electric charge of either sign; this allows for the formation of multiply-charged positive ions.)

Measurements of W have been made with abundance since the earliest days of radioactivity. The pre-eminent pioneer in this field was Sir William H. Bragg, whose 1912 book is still a valuable source of information and insight. The voluminous literature that has accumulated since then attests to the unfortunate fact that experimental determination of W is often very easy, but *accurate* determination is not. This literature abounds in disparities and contradictions, and even the greatly augmented activity of the past decade has failed to resolve many of them. It is a pity that published tables of experimental data do not bear a symbol indicating whether or not the data are correct.

Experimental values of W for α-particles or for β-particles in most gases lie in the range of 20–40 eV/ion-pair, and may vary with the nature and the energy of the particle. This dependence is in many cases slight, but in some it is marked, and in still others it is apparently absent. The magnitudes of W are important in a variety of ways. They are particularly vital for many types of nuclear-radiation detectors; with the evolution of these devices the pertinence of W to certain of them has risen or fallen, but the total interest in W has never declined. And W-values have much theoretical significance, in part because they are the simplest and most accessible measure of an aggregate effect of high-energy radiation. There is a great deal of physics involved in the absorption of an α-particle in a gas—and usually a great deal of chemistry as well.

This lecture attempts an assessment of contemporary understanding of the phenomena which determine the value of W. Because of limitation of time, many interesting aspects must be omitted; among them are the ionization by fission fragments and, by "slow" ions, the fluctuations in N_i for a fixed value of T_0, and the ionization in gaseous mixtures.

The problems that arise in the theoretical interpretation of W may be classified into three distinct categories.

(i) *Individual inelastic collision cross-sections.* Of chief interest are the total excitation and the total and differential ionization cross-sections for charged particles (electrons, and such positively charged particles as may be present). In the case of positive ions, the electron-capture and electron-loss cross-sections are also involved; the latter very definitely include the differential loss cross-section (i.e. ejected-electron distribution). Angular distributions are not ordinarily relevant, nor are elastic-scattering cross-sections.

(ii) "*Bookkeeping*" *problems.* The absorption of a single α-particle, for example, involves some half-million primary elementary processes of great variety. Thus $1/W$ is, in effect, an average of the ionization cross-section over the entire *degradation spectrum*, that is, the spectrum of positively charged particles and electrons actually present in the medium. (SPENCER and FANO, who pioneered in treating these spectra for electron sources,[2] called them "slowing-down spectra".) The bookkeeping problems have not yet been fully explored.

(iii) *Distractions.* These are of two kinds, trivial ones which cause errors in the experimental determination of W and may or may not be elucidated, and non-trivial ones, which are due to interesting and important physical processes that may alter the apparent value of W. Only the latter, of course, are germane here. They will be discussed next.

VOL. 10 1961

2. ARTIFACTS IN THE MEASUREMENTS OF *W*

(A) *Those that increase the apparent value of* W

Partial recombination of positive ions with negative ions (and perhaps electrons) is the offender here. It is generally believed that recombination is a hazard only in so-called "electronegative" gases (e.g. O_2, NO, H_2O), and then particularly for densely ionizing particles, like α-particles. Such columnar recombination is only imperfectly understood. With non-electronegative gases (e.g. noble gases, N_2, hydrocarbons), an ordinary saturation curve is attainable and is believed to ensure against ion loss, although criteria for saturation are by no means unequivocal.

(B) *Those that decrease the apparent value of* W

Three types are known, but others may well exist!

(i) *Ionization of impurities by excited atoms (or molecules?).* This is the well-known Jesse effect. It has been identified and studied quantitatively only in He and Ne (Jesse), and A (Hurst). For these gases the pertinent excited atoms are long-lived (metastable) and the effect takes over at impurity concentrations greater than about 0·1 mole per cent.

In the case of argon, the phenomena are somewhat complicated because of the following circumstance (PLATZMAN[1] p. 48): since the metastable states of (A) have comparatively low energy, only contaminate with low ionization potential are effective, and these are most conveniently polyatomic molecules; but transfer of energy not vastly in excess of the ionization potential to a polyatomic molecule does not invariably lead to ionization—excitation, followed by dissociation, can compete. (It is well known that a molecule may sustain excitation energy in excess of its ionization potential without losing an electron, the excitation energy ultimately causing dissociation or even, in a large molecule, being partially converted into heat. Direct information on this effect is provided by measurement of the ionization current resulting from absorption of ultraviolet light.[3] There is, as yet, no quantitative theoretical interpretation of this phenomenon in terms of properties of the excited states involved, but it has been possible to correlate the results of the optical measurements with those of Hurst, Jesse and others on energy transfer from metastable states of argon, neon and helium, deduced from data on *W* for noble gases contaminated with molecular gases.[4]) It would be anticipated that argon should show a normal Jesse effect if atomic vapours were used as contaminants, but such experiments have not been performed.

Existence of the Jesse effect in *molecular* gases is a remote but most interesting possibility. The effect in cases of short-lived (non-metastable) excited states has not been identified with certainty; the "impurity" concentration here would have to be a few per cent, at the least, and the complications experienced with gaseous mixtures, which stem from distortion of the degradation spectrum, must then ensue and becloud the interpretation.

(ii) *Ionization of impurities by subexcitation electrons.* That portion of the electron degradation spectrum having kinetic energy lower than the lowest excitation potential of the parent gas, will have a comparatively protracted existence, and such electrons may therefore ionize impurities with sufficiently low ionization potential.[5] Like many other aspects of inelastic electron collisions in gases, this phenomenon is poorly understood in the case of molecular gases, owing in part to the complications arising from low-lying electronic states of molecules.

(iii) *Ion production by formation of dimeric molecular ions.* An example is the reaction $He + He \rightarrow He_2^+ + \varepsilon^-$, which occurs with large cross-section for all excited states of helium having principal quantum number $\geqslant 4$ (and possibly also for $n = 3$). Since this process must compete with allowed radiation* of the excitation energy, it suggests[6] an increase in the apparent *W* for *pure* He by some 7 per cent at low pressures (probably in the range of 1–10 cm Hg);

* Radiation to lower excited states. Transitions to the ground state are, in effect, forbidden because of imprisonment.

this has not yet been investigated. The process is well known in monatomic gases (noble gases, alkali-metal vapours) but unexplored in molecular gases. It might be important for small molecules, but is less likely to be so for large ones because of the rapid internal dissipation of electronic excitation energy.

There are other latent sources of excess ionization. Among them may be mentioned the collision-induced dissociation of an excited molecule into ionic fragments rather than, in the absence of a collision, uncharged fragments. This possibility, like the processes discussed previously, points to the importance of measuring W over as great a pressure range as possible—a task that has scarcely been begun.

3. MAGNITUDES OF W IN PURE GASES

Let us momentarily pass over the variation of W with type and energy of particle, and consider the numerical values for total absorption of α- and β-particles which are never very different and are a useful standard for discussing those instances in which the W-value does deviate substantially.

(A) *Noble gases*

These are the only monatomic gases for which W has been determined. (Measurements on metal vapours would be of great interest.) The magnitude of W is most suggestively appraised as the ratio to the corresponding ionization potential, I, and for all five noble gases W/I is equal to 1·7 with at most a few per cent divergence. This value may be understood in terms of the energy balance of absorbed energy T_0:

$$T_0 = N_i\bar{E}_i + N_{ex}\bar{E}_{ex} + N_i\bar{\varepsilon}.$$

There are produced N_i (ultimately) singly charged atomic ions at an average energy expenditure of $\bar{E}_i$, N_{ex} excited atoms at an average expenditure of $\bar{E}_{ex}$, and N_i subexcitation electrons having average kinetic energy $\bar{\varepsilon}$.
Then

$$W = T_0/N_i = \bar{E}_i + \bar{E}_{ex}(N_{ex}/N_i) + \bar{\varepsilon} \quad (1)$$

and therefore

$$W/I = (\bar{E}_i/I) + (\bar{E}_{ex}/I)(N_{ex}/N_i) + (\bar{\varepsilon}/I).$$

In the case of helium, all of the quantities appearing on the right-hand side of this equation can be evaluated from information that is independent of the absolute measurement of W, and completeness of the energy balance can therefore be verified.[5] The numbers corresponding to these algebraic quantities are found to be

$$1{\cdot}72 \approx 1{\cdot}06 + (0{\cdot}85)(0{\cdot}40) + 0{\cdot}31.$$

Evidence for the other noble gases is incomplete, but the corresponding numbers appear to be at least roughly the same as those for helium. The quantity 1·06 exceeds unity because of the energy "wasted" in producing excited ions and multiply charged ions. The quantity 0·85 is an average excitation energy relative to I; it can be estimated successfully because, for the noble gases, all levels lie fairly close to the ionization limit. The quantity 0·40 is the ratio of total number of excited to total number of (singly) ionized atoms produced, and is equal to the ratio of corresponding *average* cross-sections, these being averaged over the degradation spectrum of particle energies. It is small because of the well-known characteristic of noble gases that an unusually great proportion of the total oscillator strength resides in the continuum. (The ratio for He of total matrix-element-squared for discrete excited states to that for continuum states is 0·55.) The quantity 0·31 I is the mean energy per ion pair left in the subexcitation electrons, and is therefore, in the pure gases, dissipated directly as heat. About 18 per cent of the absorbed energy takes this form.

(B) *Molecular gases*

For all molecular gases, including hydrogen, W/I is much greater than for the noble gases; it lies between 2·1 and 2·6 in most cases. Table 1 shows a few selected data. We are not able to interpret these values with anything like the detail possible for the noble

VOL. 10 1961

TABLE 1. Selected values for gases of W_β and W_β/I* (Uncertainties are approximately 1–2 per cent)

Gas	W_β (beta rays)	W_β/I
He	42·3	1·72
Ne	36·6	1·70
A	26·4	1·68
Kr	24·1	1·72
Xe	21·9	1·80
H_2	36·3	2·35
N_2	34·9	2·24
O_2	30·8	2·55
NO	—	3·3(?)(W_α/I)
Air	33·9	—
CO_2	32·8	2·38
CH_4	27·3	2·10
C_2H_6	24·5	2·10
C_2H_4	26·1	2·48
C_2H_2	25·7	2·25

* I is the ionization potential. This table is adapted from Reference 1, p. 50.

gases. The greater magnitude of W/I has contributions from all of *three* different factors.

(i) *Energy transferred to molecular potential energy*. There are two categories here. One, pertinent to stable excited and ionized states, is the extra energy transferred by virtue of the demands of the Franck–Condon principle. For example, the extra energy is small for N_2, but greater for O_2, for which (in contrast to N_2) the upper states have equilibrium nuclear separations markedly different from that of the ground state. The second, which is much more important, stems from transitions to "repulsive" potential curves (surfaces) for excited and ionized states. Since the ionization potential refers, by definition, to the lowest electronic state of the molecular ion, inclusion, in the averaging, of transitions to repulsive states increases the values of both $\bar{E}_{ex}/I$ and $\bar{E}_i/I$.

(ii) "*Multiple*" *electron transitions*. With the noble gases, most of the transitions involve promotion of a single electron; occasionally, however, two or more are excited (as in the case of multiple ionization). Little is known quantitatively about such transitions, especially in the case of molecules. However, there is good reason to believe them to be more common for molecules; this is particularly so for excitation by electrons having kinetic energy below about several hundred electron-volts, for which excitation cross-sections may be comparable to geometrical cross-sections. Indeed, results from chemical mass-spectrometry have been interpreted as indicating ion formation predominantly in electronically excited states at the bombarding energies commonly used (ca. 70 eV which is an important, although by no means "typical", portion of the degradation spectrum). In the case of certain hydrocarbons, for example, the average excitation energy of the ions has been estimated to lie in the neighbourhood of 5 eV.[7]

This effect obviously increases both $\bar{E}_{ex}/I$ and $\bar{E}_i/I$.

(iii) *Relative importance of the continuum*. It is well known that other substances have a smaller proportion of their total oscillator strength in the continuum than the noble gases have. This would lead to values of N_{ex}/N_i greater than the one (0·40) found for the latter. Table 2 shows the results of an attempt[8] to compute this ratio for several molecules from experimental values of W/I, on the basis of estimated contributions from the other quantities in equation (1). It is found that N_{ex}/N_i is about unity for most molecules, but the calculation is very rough.

Attention should be directed to interesting regularities in the W/I-values. For example, CH_4, which in some respects is akin to a noble-gas atom, has the small value of 2·10, and for other small alkanes it is about the same; adding a double bond in these hydrocarbons markedly increases the value of W/I. The "hard" molecule N_2 has an intermediate value, 2·24; the "softer" O_2 has a much greater one, 2·55. One does not know how to apportion these variations between changes in $\bar{E}/I$ on the one hand and changes in N_{ex}/N_i on the other, but the latter is probably the major factor. It is evident that interesting and hitherto unknown optical properties can be revealed by these studies.

The value of W/I quoted for NO, an odd-electron molecule which is, in fact, a

TABLE 2. Application of equation (1) to various gases

Gas	W_β/I	$\bar{E}_i/I$	$\bar{\epsilon}/I$	$\bar{E}_{ex}/I$	N_{ex}/N_i	W/I calculated	N_{ex}/N_i calculated
He	1·72	1·06	0·31	0·85	0·40	1·71	—
Ne	1·70	1·06	0·3	0·85	0·4	1·7	—
A	1·68	1·1	0·3	0·85	0·4	1·7	—
H_2	2·35	1·2	0·2	0·9	—	—	1·1
N_2	2·24	1·2	0·2	0·9	—	—	0·9
O_2	2·55	1·2	0·2	0·9	—	—	1·3
CO_2	2·38	1·2	0·2	0·9	—	—	1·1
CH_4	2·10	1·2	0·2	0·9	—	—	0·8
C_2H_2	2·25	1·2	0·2	0·9	—	—	0·9

stable free radical, is very high (3·3). (This should be re-studied, for NO exhibits very strong electron attachment.) Another odd-electron molecule, NO_2, also has a high value (2·7). Apparently these molecules are similar to atomic hydrogen, for which the ratio of total matrix-element-squared to discrete and to continuum states is 2·53 (compared to 0·55 for helium, as mentioned above).

In Table 3 the author has estimated values of N_{ex}/N_i for three central cases: atomic helium, molecular hydrogen and atomic hydrogen. One might surmise that these are typical, respectively, of the noble gases, normal molecules and "free radicals" (molecules containing an odd number of electrons*). In the case of helium, M_{ex}^2 and M_i^2, the total matrix-element-squared to discrete states and to continuum states, are known accurately.[9,10] The value of N_{ex}/N_i inferred from experiment is 0·50, greater than the number 0·40 mentioned earlier because correction has been made for the formation of He_2^+. This value is slightly smaller than $M_{ex}^2/M_i^2 = 0{\cdot}55$ because the probability of excitation is slightly smaller than the asymptotic value (1/1·55) for electrons of all kinetic energies greater than about 100 eV. In the case of H_2, the values of M_{ex}^2 and M_i^2 are not known as accurately, and the author has calculated them from certain experimental data as suggested by FANO[11]. Here again the value of N_{ex}/N_i inferred from W/I is slightly smaller than M_{ex}^2/M_i^2. For atomic hydrogen, in contrast, the matrix elements are known exactly from theory, but W cannot be measured; the author has used a theoretical calculation of W (cf. Section 5(B) below) which is admittedly not very trustworthy. Altogether, however, the data in the Table appear to be consistent and are probably a useful first approach. They suggest that N_{ex}/N_i is, respectively, approximately $\frac{1}{2}$, 1 and 2 for the three classes of molecules.

TABLE 3. Importance of the continuum

	He	H_2	H
M_i^2	0·49	0·71	0·283
M_{ex}^2	0·27	0·94	0·717
M_{ex}^2/M_i^2	0·55	1·32	2·53
N_{ex}^2/N_i	0·50	1·1	(1·8)
W/I	1·72	2·35	(2·65)

Note: Each of these three substances appears to be typical of a class of molecules.

4. DEPENDENCE OF W UPON ENERGY AND TYPE OF PARTICLE

(A) *Electrons*

Experiments with β-rays in several gases, both atomic and molecular, have failed clearly to disclose a measurable dependence of W upon β-ray energy; the experiments span the range from 5 to 60 keV *mean* β-ray energy, and the lack of energy dependence is established to about ± 2 per cent. Measurements on the specific ionization at relativistic energies are likewise insufficiently

* But excluding the alkali-metal atoms which would have even greater values of N_{ex}/N_i.

VOL. 10 1961

accurate to establish the magnitude of the energy dependence. This is understandable because so much of the measured ionization is caused by the low-energy portion of the degradation electron-spectrum, which is comparatively insensitive to the initial electron energy.

It would nevertheless be valuable to have measurements sufficiently accurate to reveal and assess the energy dependence in both atomic and molecular gases. This energy dependence must exist, for the relative probability of excitation and ionization in a single electron collision continues to vary up to the greatest energies; but since the effect is so strongly mediated by the degradation spectrum, very great experimental accuracy will be required. Experiments with monoenergetic electrons would be ideal, but they are not imminent; W-measurements with electrons are very difficult, as is evident from Dr. Jesse's description of his painstaking experiments.

The theory of W for electrons in helium has been developed in detail by MILLER[9,12]. It predicts an energy dependence for monoenergetic electrons in the range from 1 to about 2 or 3 keV, the value of W declining with increasing energy and reaching approximate constancy above that region. (The numerical results appear as Figs. 2–15 in Reference 1.) How molecular gases may behave in this respect is quite unknown.

(B) *Alpha particles*

In the case of α-particles, it is important to distinguish between phenomena occurring near the end of the track, where the particle carries one or two orbital electrons, and those occurring at energies greater than several MeV, where it is certainly a bare nucleus. The most remarkable experimental fact, discovered by Jesse and not yet understood, is that W_α/W_β (W here refers to the total ionization resulting from complete absorption of the particles) is close to unity (± 1 or 2 per cent) for the noble gases and hydrogen, but about 1·05–1·07 for all molecular gases that have been studied, except hydrogen. (Notice that H_2 falls with the noble gases, whereas with respect to the magnitude of its W/I value it falls with the molecular gases!) Most, but perhaps not all, of this striking difference, stems from the end of the track. It is well known that W for "slow" high-energy ions (e.g. α-particle recoil atoms) is much greater than W_α or W_β, because of the substantial proportion of the particle energy that is transferred to atoms *in toto*, which then dissipate their energy largely in non-ionizing quasi-adiabatic "elastic" collisions. However, this non-ionizing fraction* should, according to simple theory, depend principally upon the atomic numbers of particle and gas; thus no light is thrown on the cause of the two categories of behaviour in the case of α-particles.

Two possible explanations, both conjectural, are as follows.

(i) The W-value in the capture–loss region, W_{cl}, is significantly smaller than W_β for a gas in the first category†, but $W_{cl} \approx W_\beta$ for one in the second (molecules). Thus, in the case of the first group, the energy "wasted" in elastic nuclear collisions would be compensated, at least in part, by more efficient ion production in the capture–loss region. In favourable cases W_{cl} might be as small as I_{gas}. For an understanding of this question it will be necessary to know not only the pertinent capture and loss cross-sections, but also the specific states of the

* The fact that W/W_β exceeds unity for heavy charged particles and ions is often represented in the literature by an "ionization defect" T_d, defined by $W = W_\beta T_0/(T_0 - T_d)$. This term has come to be identified with a naive separation of the total energy absorbed, (T_0) into a portion ($T_0 - T_d$) transferred to electronic systems, with an efficiency of $1/W_\beta$ for ion production, and a portion (T_d) transferred to atomic nuclei, with very little concomitant ion-production. Such a model does not bear scrutiny, since the ratio of cross-sections for excitation and ionization is velocity dependent, and may also vary with the type of particle in the pertinent velocity domain.

† This would be contingent on *several* features of the energetics of capture and loss processes, among them the kinetic energy of loss electrons and the magnitude of the difference between I_{gas} and the energy of recombination of He^+ or He^{++} with the captured electron. It would also require that the total energy lost by an α-particle via capture and loss cycles be at least a few per cent of T_0.

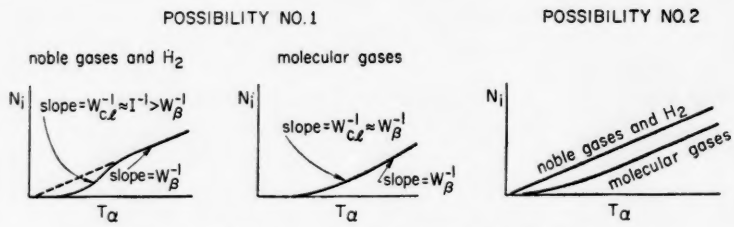

FIG. 1. Two possible explanations of the ratio W_α/W_β (schematic).

helium ion and gas ion involved in each of the two charge-exchange cycles. It may be noted incidentally that this compensation might play an even more important role in the ionization by heavier ions.

(ii) The uncharged component of the α-particle beam does not extend to as high an energy level in the noble gases and hydrogen as it does in the others. Such would be the case if the cross-section for electron capture by He^+ were smaller at intermediate energy (say, below 1 MeV) in the first gases than in the second. Accordingly, the total energy "wasted" in nuclear collisions would be smaller for the first group. A possible origin of this distinction is the contribution of molecular potential energy to the energy expended in extracting an electron, making possible a closer approach to resonance and therefore leading to a greater capture cross-section. (This is the same effect as that causing broad absorption and emission spectra in polyatomic molecules.) Hydrogen might fall with the noble gases because its molecular ion lacks a (Franck–Condon-accessible) state having excitation energy of $I_{He} - I_{H_2} = 9{\cdot}2$ eV. The importance of the resonance criterion in electron transfer to swiftly moving ions has been emphasized recently by the wonderful work of LINDHOLM[13].

These two possibilities are depicted schematically in Fig. 1. Another is mentioned below. It seems likely that the departure of W_α/W_β from unity may have different explanations for different gases—and, indeed, that the two categories of behaviour are not as clearly distinguished as presently available data suggest.

An energy dependence of W in the high-energy portion of the α-particle range is a question of equal importance. The experimental results are incomplete and still somewhat tentative (they are discussed in the following paper by Dr. Jesse), but they do indicate a slight energy-dependence of $\Delta T/\Delta N_i$ for α-particles in certain molecular gases, even above 4 or 5 MeV. Theoretically, such an energy dependence must exist: it stems from change in the degradation spectra, and therefore reflects the energy dependence of the *relative* cross-sections for excitation and ionization, as averaged over both α-particle and electron spectra. It may, indeed, account for part of the behaviour at the end of the range. We have inadequate information on the variability of this cross-section ratio to anticipate, or to understand, whether the atomic and molecular gases differ in the extent of energy dependence of W_α, excluding the end of the track, and whether or not this W is very close to W_β. Indeed, as already emphasized, information on excitation cross-sections for the most important transitions in *molecular* gases is almost entirely lacking.

5. THEORY OF W

(A) *Various formulations*

There are three different approaches to the calculation of total ionization (or, indeed, of any other products in aggregate). They have all been touched upon in the preceding paragraphs, and it may be helpful to collect the pertinent formulas at this point. For simplicity, the formulas are written for the

case of mono-energetic high-energy incident electrons, but generalization to other cases is simple.

(1) *Sequential counting: Direct calculation from cross-sections.*

$$N_i(T) = p_i(T) + \sum_n p_n(T) N_i(T - E_n) + \int_I^{(T+I)/2} p_i(T, E)\{N_i(T-E) + N_i(E-I)\}\, dE. \quad (2)$$

Here $p_i(T)$ is the probability of ionization in an inelastic collision, i.e. $p_i(T) = Q_i(T)/Q_{\text{in}}(T)$, where $Q_i(T)$ is the total cross-section for ionization, $Q_{\text{in}}(T)$ is the total cross-section for all inelastic collisions, $p_n(T)$ is the analogous probability for an excitation having excitation energy E_n, and $p_i(T,E)\, dE$ is the analogous probability for ionization with production of a secondary electron having a kinetic energy of $(E - I)$.

(2) *Calculation from the energy balance.*

$$T_0/N_i = \bar{E}_i + \bar{E}_{\text{ex}}(N_{\text{ex}}/N_i) + \bar{\varepsilon}. \quad (1)$$

3. *Calculation from the degradation spectrum.*

$$N_i(T_0) = N\int_0^{T_0} y(T) Q_i(T)\, dT. \quad (3)$$

Here $y(T)$ is the spectral density of all electrons ("primary" and "secondary") of kinetic energy T, as defined by SPENCER and FANO[2], and N is the density of molecules in the medium. The first and third methods can be used to calculate the average total number of any primary product—for example, the number of excitations to a particular state. Considering them in this general sense, the three equations are equivalent. However, they emphasize different aspects of the phenomena, and hence tend to supplement each other in the insight they afford. At the present time, analysis by all three methods has been achieved only for the case of helium.

(B) *Direct calculation from cross-sections*

Equation (2) derives from one developed long ago for this problem by R. H. Fowler. It can be solved, for example, by starting at $T = I$, where $N_i = 0$, and ascending (in T) by steps.

This method for theoretical calculation of W requires a knowledge of *all* of the pertinent individual cross-sections, and a solution of the bookkeeping problems. The latter require labour, and possibly some ingenuity, but in fact not a great deal of either. However, trustworthy information on cross-sections (particularly excitation cross-sections and secondary-electron distributions) is scanty: this is the major barrier that is preventing progress in the theory. Only in the case of helium has this difficulty been overcome. It can justly be said of most theoretical investigations that too much effort was devoted to mathematical treatment of the bookkeeping problems, and too little effort to the quest for accurate cross-sections.

Calculation of W for the case of hydrogen atoms was attempted in well-known early work by Bethe and by Bagge. More recently, DALGARNO and GRIFFING[14] have carried out a more detailed calculation. However, in this, as in the previous studies, purely theoretical cross-sections were used, and although these are certainly asymptotically correct at a high T-value, they are known to be incorrect at a low T-value—nor is there at present any adequate theory for the low-energy region. Hence calculations based entirely upon cross-sections from (Born-approximation) theory are of limited usefulness. Moreover, there are no experimental data on W for atomic hydrogen with which to compare the theory—nor are there likely to be in the forseeable future—and comparison with experiment is a particularly salutary practice in this field.

The only other case which has received careful attention is helium. Its large W-value was correctly anticipated by FANO[15] years before it was discovered in the laboratory. FANO demonstrated how H, He and other cases can be treated roughly by using a highly simplified, but none the less valid, system of bookkeeping, an his method remains a most instructive first approach. Detailed calculations from equation (2) were made later by ERSKINE[16]. However, the excitation cross-sections which he used were seriously in error,[17] and the excellent agreement with experiment of his resulting

VOL. 10 1961

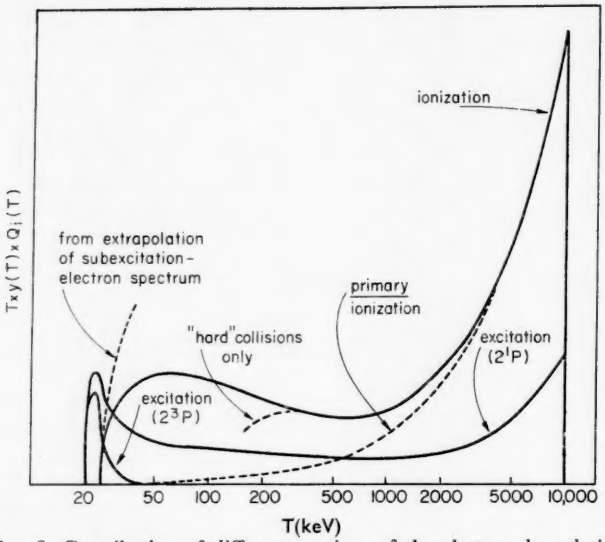

FIG. 2. Contribution of different portions of the electron degradation-spectrum to the total ionization and excitation: 10 keV electrons in helium gas.

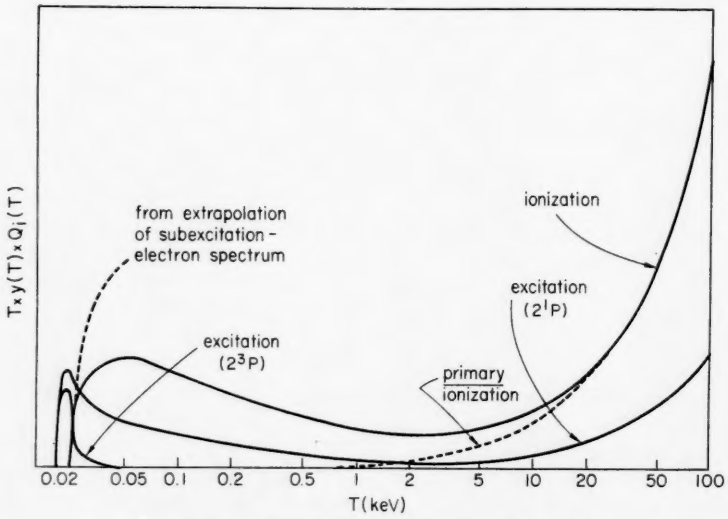

FIG. 3. Contribution of different portions of the electron degradation-spectrum to the total ionization and excitation: 100-keV electrons in helium gas.

W must therefore be regarded as at least partly accidental. MILLER[9,12] also used equation (2), and obtained the results for helium to which reference has already been made. This is perhaps the only accurate theoretical treatment of W thus far achieved.*

* ERSKINE's result for W of high-energy electrons was 38 eV/ion-pair, compared to an experimental value of about 42. MILLER's result was 46, which becomes 43 when corrected for artifact No. 3 (formation of dimeric ions). For a conclusive decision on the merits of the two calculations, it will be necessary to verify the extent to which higher excitations contribute to the measured ionization current in pure helium at atmospheric pressure.

Extension to other cases is urgently needed.

(C) *Calculation from energy balance*

This method, already discussed, focusses attention on aspects of the subject rather different from those emphasized by the other two. For instance, the interesting quantities $\bar{E}_{ex}/I$ and $\bar{E}_i/I$, although implicitly encompassed in equations (2) and (3), are well hidden there. It will be important to study these ratios independently of W-measurements, and through them to develop a more accurate command of equation (1).

(D) *Calculation from degradation spectra*

To illustrate the value of this method, we present two figures[18] (Figs. 2 and 3) which show the contribution to the *total* ionization in helium by electrons of all kinetic energies between T_0 and the threshold (i.e. the ionization potential). In order that the graph shall depict the integrand of equation (3) and have a logarithmic abscissa, the ordinate is $Tx\{y(T)Q_i(T)\}$. It is evident that the curve (denoted "ionization" on the Figures) is bimodal, with one major contribution in the neighbourhood of T_0 and another in the vicinity of 50 eV. However, the contribution from intermediate energies is also substantial. There is obviously no "typical" electron energy.

The curves in the Figures are probably somewhat inaccurate but should serve as a first approximation. Their basis is as follows: ionization cross-sections (Q_i) from experiment; excitation cross-sections from the work of MILLER[8]; $y(T)$ at $T \geqslant T_0/2$ taken equal to the reciprocal of the stopping power $S(T)$; $y(T)$ at high values of T by interpolation of data on the product $y(t) \cdot S(T)$ given by MCGINNIES[19]; $y(T)$ at very low values of T by extrapolation of the sub-excitation-electron spectrum[4]; and $y(T)$ in the intervening region by interpolation, under the requirement that the total ionization, as given by the area, shall be correct. Corresponding curves for several excitation processes are also shown. The tiny curve for triplet excitation is striking; its narrowness stems from the correspondingly narrow cross-section for spin-reversing excitation which has virtually a resonance character.

VOL. 10 1961

REFERENCES

1. PLATZMAN R. L. (CLAUS W. D., Ed.) *Radiation Biology and Medicine*, Chap. 2, Section 2.16. Addison-Wesley, Reading, Mass. (1958).
2. SPENCER L. V. and FANO U. *Phys. Rev.* **93,** 1172 (1954).
3. WEISSLER G. L. *Handbuch der Physik* Vol. 21, p. 318. Springer-Verlag, Berlin (1956).
4. PLATZMAN R. L. *J. Phys. Rad.* **21,** 843 (1960).
5. PLATZMAN R. L. *Radiat. Res.* **2,** 1 (1955).
6. PLATZMAN R. L. *Radiat. Res.* **3,** 340 (1955).
7. KRAUSS M., WAHRHAFTIG A. L. and EYRING H. *Ann. Rev. Nucl. Sci.* **5,** 241 (1955).
8. PLATZMAN R. L. To be published.
9. MILLER W. F. Dissertation, Purdue University (1956).
10. MILLER W. F. and PLATZMAN R. L. *Bull. Amer. Phys. Soc.* **2,** 227 (1957).
11. FANO U. *Phys. Rev.* **95,** 1198 (1954).
12. MILLER W. F. *Bull. Amer. Phys. Soc.* **1,** 202 (1956).
13. LINDHOLM E. *Z. Naturf.* **9a,** 535 (1954).
14. DALGARNO A. and GRIFFING G. W. *Proc. roy. Soc.* **A248,** 415 (1958).
15. FANO U. *Phys. Rev.* **70,** 44 (1946).
16. ERSKINE G. A., *Proc. roy. Soc.* **A224,** 362 (1954).
17. MILLER W. F. and PLATZMAN R. L. *Proc. Phys. Soc.* **A70,** 299 (1957).
18. PLATZMAN R. L. To be published.
19. MCGINNIES R. T. *Nat. Bur. Stand.* Circular No. 597 (1959).

technical notes

A Remote Sampling System for High-Level Gamma Sources*

(*Received* 1 *July* 1960)

A REMOTE-CONTROLLED mechanism for introducing and removing samples from the Georgia Tech. 12 kc cesium-137 irradiator† (Notre Dame type‡) has been designed and built with these primary features: (1) "fail safe" electrical system; (2) minimum radiation exposure to operating personnel and other experimenters in the area.

Operation

The lift mechanism (Fig. 1) is a solenoid which has a brass extension pinned and soldered to the core. Two ferromagnetic leaves are attached to the brass extension and are acted on by the magnetic field of the solenoid. These leaves are free to pivot outwards and are normally 15° from the vertical position (Fig. 2). The top of each sample carrier has a lip on it, and as the lift mechanism is lowered into the carrier the leaves close. When the brass extension reaches the bottom of the sample carrier the leaves fall open and engage the lip of the carrier. The unit can then be raised or lowered. To remove the lift mechanism from the carrier, the weight of the

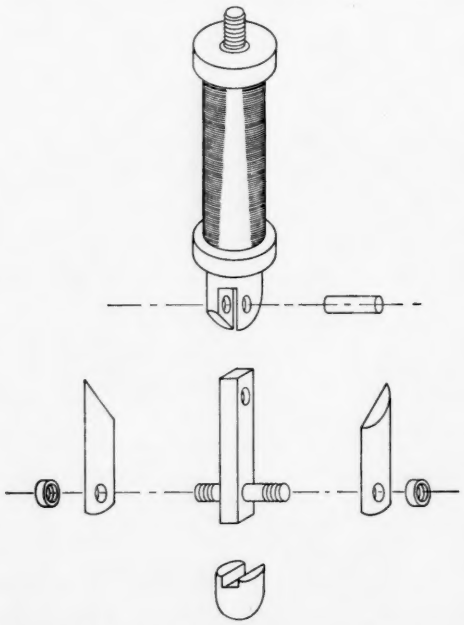

FIG. 1. Exploded view of solenoid mechanism.

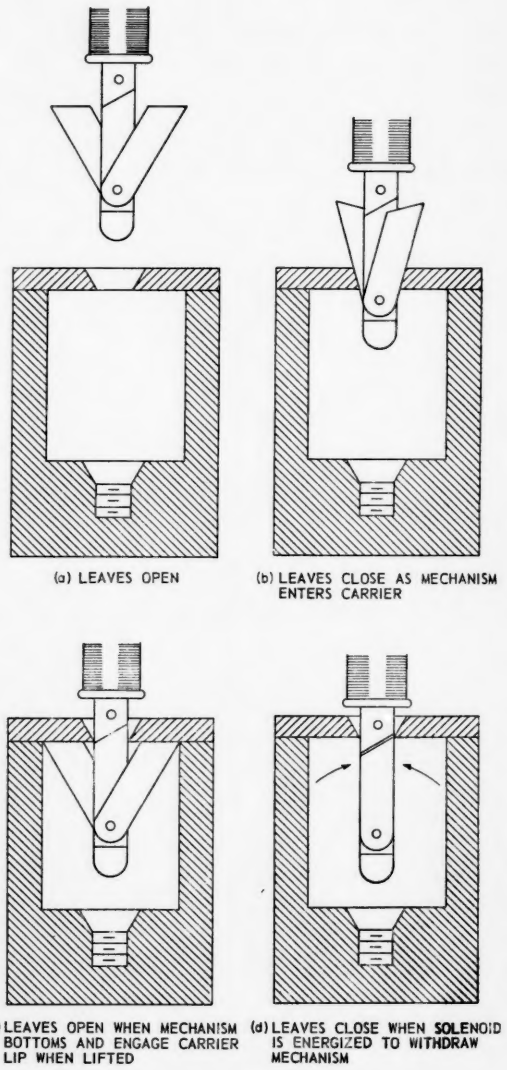
(a) LEAVES OPEN
(b) LEAVES CLOSE AS MECHANISM ENTERS CARRIER
(c) LEAVES OPEN WHEN MECHANISM BOTTOMS AND ENGAGE CARRIER LIP WHEN LIFTED
(d) LEAVES CLOSE WHEN SOLENOID IS ENERGIZED TO WITHDRAW MECHANISM

FIG. 2. Operation of solenoid mechanism.

* This work was supported in part by Office of Isotopes Development, U. S. Atomic Energy Commission, Contract No. AT (38-1)-202.

† A description of this irradiator has been accepted for publication in *Int. J. Appl. Rad. Isotopes.*

‡ *Nucleonics* **13,** 74 (1959).

VOL. 10 1961

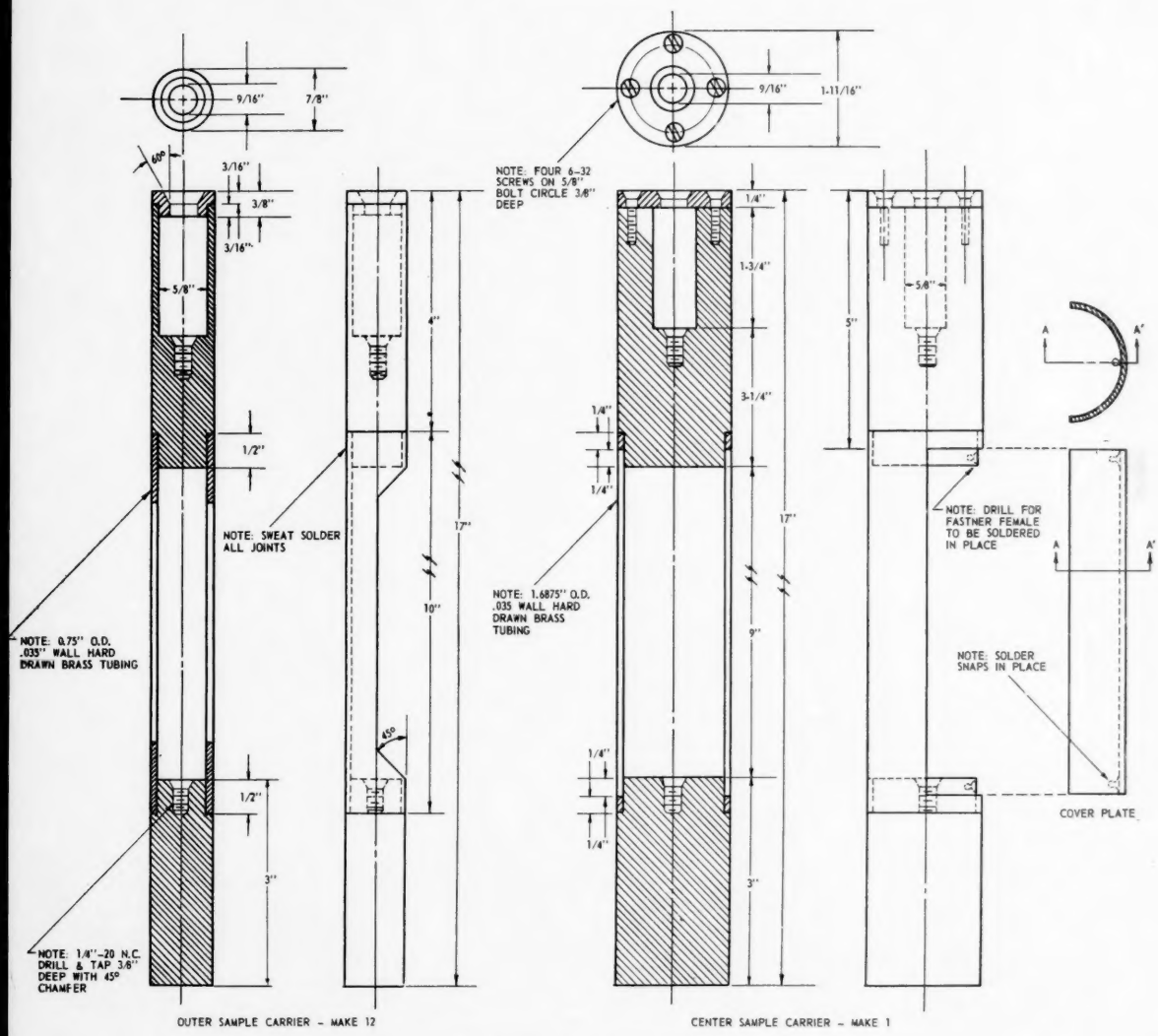

FIG. 3. Shop drawing of sample carriers.

carrier must be supported externally and not by the leaves, since the solenoid is not powerful enough to draw the leaves in against the weight of the carrier. This is a safety feature which prevents the carrier from being disengaged accidentally while moving it or loading it. The solenoid is energized with the weight off the leaves and the magnetic field causes the leaves to pivot in, so that the lift mechanism can then be extracted from the carrier. The solenoid can then be turned off.

Description of solenoid

The solenoid is composed of 600 turns of No. 20 enameled copper wire wound on a $\frac{1}{2}$ in. diameter high-permeability silicon–steel alloy core. Each layer of the winding was sprayed with clear plastic paint to help prevent insulation breakdown over a long period of continued use. The end washers confining the winding are $\frac{1}{4}$ in. wide. Since the solenoid operates on 10–12V a.c., these washers act as alternating current shim rings to prevent chatter in

the leaves. Both the solenoid and the leaf units are threaded to facilitate any maintenance necessary. The leaves are made from the same high permeability alloy as the core. It is important that they be able to rotate freely on the pivot pin to insure their engagement on the sample carrier lip.

Soft solder has been found to be the best method of attachment of the leaf components to the core extension. Screws tend to work loose during service, and bradding the pin ends will bind the leaves and hinder their rotation. Because the pivot pin supports the weight of the sample carrier, the mechanical strength of the solder is not taxed. No difficulty has been experienced since this method has been adopted.

Description of sample carrier

There are twelve outer sample carriers and one central sample carrier. The center carrier is fitted with two $\frac{1}{4}$ in. O.D. copper tubes for a temperature bath, two $\frac{1}{8}$ in. diameter copper tubes for gas lines and two $\frac{1}{4}$ in. holes for electrical leads (none shown on drawing). The smaller size of the outer carrier prevents the inclusion of such features in them.

Each sample carrier is fitted with a 3 in. plug of brass above and below the sample tube. This provides enough shielding to limit the maximum radiation level outside the source to 2–5 mr/hr regardless of sampler position (up or down), provided that the carriers are not removed entirely from the tube nest. Each of these plugs in turn is drilled and tapped, so that a threaded rod can be inserted down in the source to remove the sample carriers in case of breakage or power failure.

Sweat soldering is used throughout in the construction of the sample carriers with the exception of the lip ring of the center carrier, which is held in place with four 6-32 counter-sunk brass screws.

The center carrier has a cover plate which attaches to the carrier body by two snaps (Fig. 3). The outer carriers have no cover plate. Brass was chosen as the construction material since the tube nest is also made of brass, and such a choice would result in less wear on the tube nest.

The mechanism is raised and lowered on a $\frac{1}{8}$ in. steel cable with an electric hoist. This method has proven to be quite adequate, since the maximum weight of the center carrier when loaded is no more than 20 lb.

The system is very satisfactory and requires little, if any maintenance. The simplicity of the working parts makes the system very flexible. It can be adapted to any size or type of carrier, since the only necessary feature is the bore and lip upon which the leaves seat.

R. C. Palmer
D. K. Davis
W. V. Willis
Engineering Experiment Station
Georgia Institute of Technology
Atlanta, Georgia

The Preparation of Curie Quantities of S^{35}-Labelled Element Sulphur

(*Received* 13 *July* 1960)

In many syntheses of S^{35}-labelled compounds elemental sulphur is the starting material.

Usually the S^{35} is obtained by irradiation in a reactor of KCl according to Cl^{35} (n,p) S^{35}. The sulphur is isolated as sulphuric acid and finally available as a solution of carrier-free sulphuric acid which still contains a large excess of hydrochloric acid (1 N). It is thus desirable to prepare a stock quantity of elemental sulphur of high specific activity from this sulphate solution.

The described method, based on literature data, consists of two parts. First the reduction of the sulphate to hydrogen sulphide, and second the oxidation of the hydrogen sulphide to sulphur. Quantities of 5–25 mg.atoms of elemental sulphur with specific activities up to 100 mc/mg.atoms, or even higher, are easily obtained in 95–100 per cent yields. Carrier sodium sulphate is added to the sulphate-S^{35} solution in order to arrive at the desired specific activity.

The reduction of the sulphate[1–6] is essentially the method described by Kilmer and du Vigneaud.[1] A mixture of sulphate, hydrogen iodide, red phosphorus and formic acid is warmed in a slow stream of nitrogen, and the hydrogen sulphide evolved is absorbed in a dilute solution of sodium hydroxide. This method of reduction is less laborious than the method by which the sulphate is precipitated as $BaSO_4$ which has to be dried, powered and reduced with hydrogen at high temperatures to form BaS which finally gives the hydrogen sulphide when decomposed with an acid.[4,5,6]

The alkaline solution of sulphide is oxidized with a mixture of potassium ferricyanide and potassium carbonate in the presence of benzene. The oxidation has to take place gradually; then the benzene dissolves the sulphur immediately when formed and the precipitation of insoluble amorphous sulphur is avoided. A carefully adjusted quantity of potassium carbonate is added together with the potassium ferricyanide to maintain a pH 9 during the oxidation. Otherwise the solution would become acid, which would involve a loss of hydrogen sulphide.

In comparison with the often-used oxidation with iodine[1,3,4,5,6], which has to take place in acidic

VOL. 10 1961

solution, the oxidation with potassium ferricyanide offers another advantage, i.e. with the exception of sulphur none of the reaction products are soluble in benzene and a pure solution of sulphur in benzene is immediately obtained. The benzene solution is dried by removing the last traces of water by azeotropic distillation.

The sulphur separates out in beautiful crystals, when finally the benzene is evaporated in a slow stream of nitrogen.

Experimental

A preparation of 10 mg.atoms of sulphur with a total activity of 1 c is described. For the apparatus see Fig. 1.

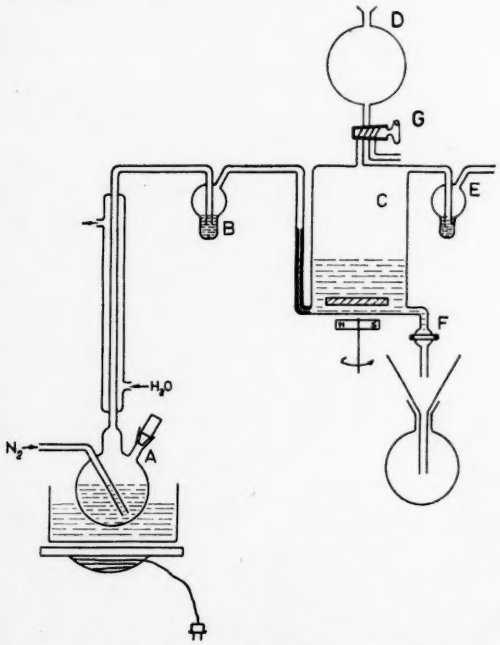

FIG. 1. Apparatus for the preparation of radioactive sulphur.

A solution of 1 c $H_2S^{35}O_4$ and carrier Na_2SO_4 (10 mM) is concentrated to 2 ml and brought into flask *A*. Red phosphorus (5 g), hydrogen iodide (33 ml of a 57% colourless solution) and formic acid (25 ml) are added, and the mixture is warmed up for 4 hr, during which period the temperature is raised from 90 to 150°C. A slow stream of nitrogen, passes through wash bottle *B* containing 2–3 ml of water eliminating traces of HI or HCl, then through the oxidation flask *C* where the hydrogen sulphide is absorbed in dilute sodium hydroxide (100 ml 0·3 N). Ten drops of saturated alcoholic thymol blue solution were added to check pH.

When the contents of flask *A* are back at normal temperature, benzene (100 ml) is added to *C* by way of funnel *D*, followed by the exact quantity of 1 N HCl to obtain a pH 9 (colour of the thymol blue changes to yellow). Excess of HCl solution in funnel *D* can flow off through the side tube of the two-way stop-cock *G*.

Next the oxidizing solution (22·5 mM $K_3Fe(CN)_6$ and 12·4 mM K_2CO_3 in 100 ml H_2O) is added dropwise, stirring the reaction mixture vigorously. Traces of hydrogen sulphide, which might escape during the oxidation, are absorbed in wash-bottle *E* which contains dilute sodium hydroxide. After the oxidizing solution is added, stirring is continued another 10 min. The water layer is separated by way of stop-cock *F*, the benzene layer is washed several times with water, and finally filtered through filterpaper to remove possible traces of insoluble amorphous sulphur and residual drops of water. The benzene solution is dried by distilling off a part of the benzene azeotropically. Finally, crystalline sulphur (304-320 mg) is obtained by evaporating the benzene in a slow stream of nitrogen. Last traces of benzene can be removed in high vacuum.

Centraal Laboratorium T.N.O. H. L. OTTO
Delft, Netherlands

Centre d'Etude de l'Energie Nucléaire M. WINAND
Mol-Donk, Belgium

References

1. KILMER G. W. and VIGNEAUD V. DU *J. biol. Chem.* **154,** 247 (1944).
2. WIELAND TH. and KRANTZ H. *Chem. Ber.* **91,** 681 (1958).
3. GUERONNIERE E. DE LA and HENRY R. Report CEA 858 (1958).
4. SELIGMAN A. M., RUTENBERG A. M. and BANKS H. *J. clin. Invest.* **22,** 275 (1943).
5. WOOD J. L., RACHELE J. R., STEVENS C. M., CARPENTER F. H. and VIGNEAUD V. DU *J. Amer. chem. Soc.* **70,** 2547 (1948).
6. MARKOVA Y. V., POZHARSKAYA A. M., MAIMIND V. I., ZHUKOVA T. F., KOSOLAPOV N. A. and SHCHUKINA M. N. *Dokl. Akad. Nauk SSSR* **91,** 1129 (1953); *Chem. Abstracts* **48,** 9921h.

Statistical Errors in Disintegration Rate Measurements by the Coincidence Technique

(*Received* 25 *July* 1960)

FOR certain radioactive nuclides the coincidence technique may be used to determine absolute disintegration rates. It has been pointed out that, if the

efficiency of one of the detectors approaches unity, the statistical variance of the measurement is not entirely determined by the number of counts accumulated in the coincidence channel.[1,2] In this note we give a simplified expression for the fractional standard deviation as a function of the efficiencies of both detectors. The deviation is applicable to any form of the coincidence technique; however we consider the case of 4π beta–gamma coincidence counting[3], where the efficiency of one detector can be made nearly equal to unity. For simplicity, backgrounds and accidental coincidences are neglected. Their effects are usually small and can be calculated in the conventional manner. The equations relating the counts accumulated in each channel to the total number of disintegrations, n_0, occurring within the counting period can be written

$$n_\beta = n_0\varepsilon_\beta$$
$$n_\gamma = n_0\varepsilon_\gamma$$
$$n_c = n_0\varepsilon_\beta\varepsilon_\gamma$$

and
$$n_0 = \frac{n_\beta n_\gamma}{n_c} = \frac{(n_c + X)(n_c + Y)}{n_c} \qquad (1)$$

where ε_β, ε_γ are the efficiencies of the beta and gamma detectors respectively, while X and Y are those counts in the beta and gamma detectors which do not lead to coincidence counts and hence are independent of one another and of n_c. It follows that

$$\varepsilon_\beta = \frac{n_c}{n_\gamma} \qquad \varepsilon_\gamma = \frac{n_c}{n_\beta} \qquad (2)$$

and
$$X = n_\beta(1 - \varepsilon_\gamma) \qquad Y = n_\gamma(1 - \varepsilon_\beta). \qquad (3)$$

Assuming n_c, X and Y are independent quantities, the absolute error, Δn_0, in n_0 can be calculated by the usual approximation for combining errors (for example see WORTHING and GEFFNER[4]) and is given by

$$(\Delta n_0)^2 = \left(\frac{\delta n_0}{\delta n_c}\right)^2 (\Delta n_c)^2 + \left(\frac{\delta n_0}{\delta X}\right)^2 (\Delta X)^2 + \left(\frac{\delta n_0}{\delta Y}\right)^2 (\Delta Y)^2$$

where the Δ's are the absolute errors in the corresponding quantities. This expression reduces to a number of forms; for example, the fractional standard deviation in n_0 is

$$\sigma = \left[\frac{1}{n_c}(2\varepsilon_\beta\varepsilon_\gamma - \varepsilon_\beta - \varepsilon_\gamma + 1)\right]^{\frac{1}{2}}. \qquad (4)$$

Clearly, for small efficiencies in both detectors the standard deviation approaches $(n_c)^{-\frac{1}{2}}$ as expected, while for $\varepsilon_\beta = 1{\cdot}0$ the error becomes $(n_\beta)^{-\frac{1}{2}}$ as suggested by SMITH[1] and GUNNINK *et al.*[2] Figure 1 shows a plot of equation (4). In order to demonstrate the variation of the standard deviation in a way which is independent of any total counts, we have plotted $\sigma(n_c)^{\frac{1}{2}}$ as a function of ε_β for a few values of ε_γ.

It is also of interest to determine the statistical error in an efficiency measurement using either of

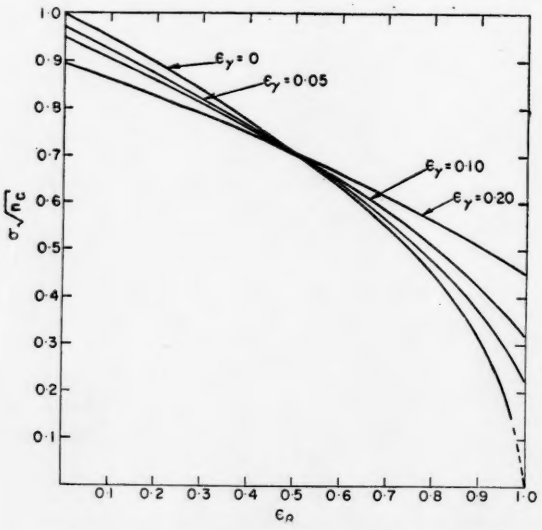

FIG. 1. The variation of $\sigma(n_c)^{\frac{1}{2}}$ as a function of beta detector efficiency, ε_β.

equations (2) above. The fractional standard deviation in the measurement of ε_β for example is:

$$\sigma = \left[\frac{1 - \varepsilon_\beta}{n_\varepsilon}\right]^{\frac{1}{2}}$$

which is zero for $\varepsilon_\beta = 1{\cdot}0$. Again, the contribution of statistical errors due to backgrounds, accidental coincidences and dead time corrections must be considered in practical cases.

P. J. CAMPION*
Atomic Energy of Canada Limited J. G. V. TAYLOR
Chalk River, Ontario

References

1. SMITH D. B. Atomic Energy Research Establishment Report I/R (1527).
2. GUNNINK R., COLBY L. J. JR. and COBBLE J. W. *Analyt. Chem.* **31**, 796 (1959).
3. CAMPION P. J. *Int. J. Appl. Rad. Isotopes* **4**, 232 (1959).
4. WORTHING A. G. and GEFFNER J. *Treatment of Experimental Data*, Wiley, New York (1943).

* Present address: The National Physical Laboratory, Teddington, England.

VOL. 10 1961

Zur Aktivierungsanalyse von Sauerstoff mit Hilfe der Reaktion $O^{16}(t,n)F^{18}$

(*Received* 22 *July* 1960)

Die Mehrzahl der Aktivierungsanalysen verwendet die (n, γ) Einfangreaktion. Dieser Prozess liefert beim Sauerstoff das Radionuklid O^{19}. Die Halbwertszeit dieses Nuklids ist so kurz (29 sec), dass eine chemische Abtrennung praktisch kaum durchführbar ist. Damit aber ist die analytische Brauchbarkeit der Reaktion auf solche seltenen Fälle beschränkt, bei denen die Aktivierung des Grundmaterials vernachlässigbar gering ist. Ist hingegen mit anderen Aktivitäten zu rechnen, so scheint die von Smales[1] vorgeschlagene Kettenreaktion:

$$_3Li^6(n,\alpha)_1H^3; \quad _8O^{16}(t,n)_9F^{18}$$

offenbar viel geeigneter, da das aus dem Sauerstoff gebildete Nuklid F^{18} die für eine radiochemische Abtrennung günstigere Halbwertszeit von 112 Minuten besitzt.

Osmond und Smales[2] haben die Brauchbarkeit der genannten Reaktion an Hand einer Sauerstoffbestimmung in Berylliummetallpulver geprüft. Dazu wurde Beryllium mit Lithiumfluorid vermischt, die Proben bestrahlt und anschliessend das gebildete F^{18} durch Destillation als Hexafluokieselsäure H_2SiF_6 vom bestrahlten Material abgetrennt. Die F^{18}-Aktivität wurde dann mit einem Endfensterzählrohr gemessen und durch Aufnahme der Abfallskurve identifiziert. Die Autoren berichten, dass die Grenze des Sauerstoffnachweises in Beryllium mit ihrem Verfahren bei 0,1 % liegt.

Diese relativ geringe Empfindlichkeit ist in erster Linie darauf zurückzuführen, dass das verwendete Lithiumfluorid auch nach mehrfacher Reinigung immer einen Restgehalt an Sauerstoff aufweist, der bei etwa 0,1 % liegt. Aus dieser Sauerstoffverunreinigung entsteht natürlich ebenfalls F^{18}, das dem aus dem Berylliumsauerstoff gebildeten F^{18} bei dessen radiochemischer Abtrennung folgt. Die entscheidende Begrenzung des Verfahrens liegt also darin, dass immer die Summe der F^{18} Aktivitäten gemessen wird. Zur Ermittlung der auf den unbekannten Sauerstoffgehalt des Berylliums zurückzuführenden F^{18} Aktivität muss von dieser Summe jeweils die aus dem Lithium stammende F^{18} Aktivität abgezogen werden. Es ist ersichtlich, dass diese Differenzbildung sehr ungenau wird, wenn der Sauerstoffgehalt des Berylliums kleiner als der des Lithiumfluorids wird.

Wir haben das Problem noch einmal aufgegriffen und mittels der oben beschriebenen Kernreaktionen Versuche zur Sauerstoffbestimmung in Metallpulvern durchgeführt. Über die ersten Ergebnisse der Untersuchungen wird im folgenden berichtet.

Für die Versuche stand uns als Neutronenquelle der Reaktor in München (Typ: swimming pool) zur Verfügung. Die Bestrahlungen wurden in unmittelbarer Nähe des Reaktorkerns im Wasser durchgeführt. Eine Wiederholung der Versuche von Smales zeigte, dass bei dem gegebenen Neutronenspektrum F^{18} auch noch auf Grund der Reaktion $F^{19}(n,2n)F^{18}$ entsteht. Damit war die Verwendung von Lithiumfluorid ausgeschlossen. Wir haben daher Lithiummetallpulver benutzt. Der Sauerstoffgehalt des metallischen Lithiums liegt natürlich mindestens in der Grössenordnung desjenigen von Lithiumfluorid. Durch eine wesentliche Abänderung des Aufarbeitungsverfahrens gelang es jedoch, diese, die Empfindlichkeit des Verfahrens so sehr einschränkende Schwierigkeit zu überwinden.

Nach beendeter Bestrahlung lösten wir das Lithium mit Methanol und Wasser aus dem bestrahlten Gemisch heraus. Durch diese Operation wird gleichzeitig die im Lithium aus dessen Sauerstoffverunreinigung gebildete F^{18} Aktivität, die als LiF^{18} vorliegen dürfte, mitherausgelöst und von der im zu untersuchenden Metallpulver gebildeten F^{18} Aktivität abgetrennt. Nach dieser Aufarbeitung wurde die interessierende F^{18} Aktivität in üblicher Weise als Hexafluokieselsäure abdestilliert und in geeigneter Form zur Messung gebracht.

Die Frage, ob das aus der Sauerstoffverunreinigung

des Lithiums stammende F^{18} etwa beim Löseprozess teilweise an der Oberfläche des zu untersuchenden Metallpulvers adsorbiert wird, wurde am besonders kritischen Beispiel von Thoriummetall experimentell geprüft. Es zeigte sich, dass die adsorbierte F^{18} Menge überaus gering ist und in dem unten angegebenen Empfindlichkeitsbereich nicht stört.

Experimenteller Teil

(1) *Reinigung des Lithiummetalls.* Um das käufliche Lithiummetall möglichst von anhaftenden Verunreinigungen, insbesondere Sauerstoff, zu befreien, wurde die Substanz in flüssigem Ammoniak gelöst und über eine IG 4-Fritte filtriert. Nach dem Verdampfen des Ammoniaks erhält man das Alkalimetall als ziemlich reines, fein verteiltes Pulver. Es wurde in einer Schutzgasatmosphäre von getrocknetem Wasserstoff gearbeitet.

Wie oben bereits betont und erläutert, enthält das so erhaltene Lithiummetall noch geringe Mengen Sauerstoff, die indessen wegen der besonderen Art der chemischen Aufarbeitung die Bestimmung nicht stören können.

(2) *Durchführung der Analyse eines Metallpulvers (Thorium).*

(a) Milligrammengen des Metallpulvers (Thorium) werden mit Lithiumpulver gemischt und nach Verpackung in Polyaethylen gleichzeitig mit einem Standard (ThO_2) 10 Minuten lang bei einem Neutronenfluss von 10^{12} cm^{-2} sec^{-1} bestrahlt.*

(b) Nach der Bestrahlung werden die Proben in Zentrifugengläser übergeführt, einmal mit Methanol und zweimal mit Wasser gewaschen, jeweils zentrifugiert und die überstehende Lösung abgegossen.

(c) Die verbleibenden Proben werden in eine Fluordestillationsapparatur übergespült. Nach Zusatz von 20 mg NaF (als Lösung) 50 ml halbkonzentrierter Schwefelsäure und 0,5 g Glaswolle wird das Fluor als Hexafluokieselsäure H_2SiF_6 mit Wasserdampf in eine Vorlage destilliert.

(d) Das Destillat wird mit zwei Tropfen Bromphenolblau als Indikator versetzt und dann solange Natriumacetatlösung zugetropft, bis die Lösung einen blauvioletten Farbton annimmt. Dann setzt man 100 ml Fällungsmittel hinzu und fällt das Fluor als Bleichlorofluorid PbClF.[3] Man lässt 30 min stehen und saugt dann auf einer Hahn'schen Nutsche über ein Blaubandfilter ab.

(e) Das Filter wird zusammengerollt und in ein Messgläschen gebracht. In einem Natriumjodid-(Tl)-Bohrlochkristall wird dann die F^{18}-Aktivität gemessen und durch Aufnahme der Abfallkurve identifiziert.

(f) Nach der Messung wird der PbClF-Niederschlag des Filters in Salpetersäure gelöst, durch Titration nach Volhardt der Chlorid-Gehalt und damit auch der Fluorid-Gehalt des Niederschlages quantitativ bestimmt.

(g) Dann wird aus den gemessenen Aktivitäten von Probe und Standard sowie aus den massanalytisch ermittelten Fluorgehalten der Bleichlorofluorid-Niederschläge in üblicher Weise der unbekannte Sauerstoffgehalt ermittelt.

(3) *Ergebnisse einer Bestimmung des Sauerstoffgehaltes von Thoriummetall.* Die Ergebnisse einer Bestimmung des Sauerstoffgehaltes von Thoriummetallpulver zeigt die Tab. 1. Als Vergleichspräparat diente Thoriumdioxyd.

Gleiche Bestrahlungsnummern wurden gleichzeitig und in gleicher Position bestrahlt. Vom Thorium

* Wir danken der Reaktorbetriebsgruppe des Instituts für Technische Physik der Technischen Hochschule München, insbesondere Herrn Dr. Köhler, für die zahlreichen Bestrahlungen am Reaktor.

TABELLE 1

Bestrahlungsnr.	Material	F^{18}-Aktivität in Imp/min berechnet auf Bestrahlungsende Einzelwerte	Mittelwert	Sauerstoffgehalt des Thoriums (g/g)
Probe				
1a	10 mg Thorium	$2{,}5 \cdot 10^3$	$1{,}95 \cdot 10^3$	0,005
1b	10 mg Thorium	$1{,}4 \cdot 10^3$		
2a	10 mg Thorium	$1{,}0 \cdot 10^4$	$1{,}2 \cdot 10^4$	0,0038
2b	10 mg Thorium	$1{,}4 \cdot 10^4$		
3a	10 mg Thorium	$1{,}2 \cdot 10^4$	$1{,}4 \cdot 10^4$	0,006
3b	10 mg Thorium	$1{,}6 \cdot 10^4$		
Standard				
1	5 mg Thoriumdioxyd	$4{,}6 \cdot 10^4$	—	0,12
2	5 mg Thoriumdioxyd	$3{,}8 \cdot 10^5$	—	0,12
3	5 mg Thoriumdioxyd	$2{,}8 \cdot 10^5$	—	0,12

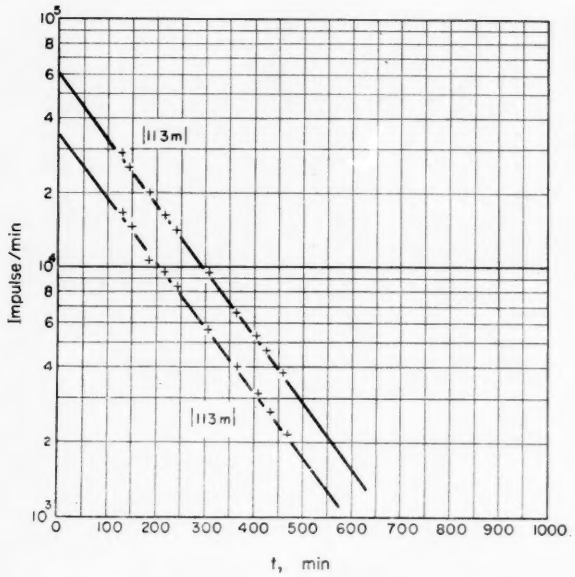

ABB. 1. Abfallkurven von F^{18}-Proben nach Abtrennung von bestrahlten Metallproben.

wurden bei jeder Bestrahlung zwei Proben exponiert (a und b).

Die radioaktive Reinheit des abgetrennten F^{18} erweisen die beigefügten Abfallskurven (Abb. 1) bei denen es sich um zwei willkürlich gewählte Beispiele handelt. Sie ist umso befriedigender, als bei der Bestrahlung der angegebenen Thoriummenge unter den beschriebenen Bedingungen eine Gesamtaktivität von ca. 10 mc entsteht.

Die verhältnismässig grosse Fehlerbreite bei dem angeführten Beispiel ist vorwiegend darauf zurückzuführen, dass die Lithium-Thoriummischungen wegen des grossen Dichteunterschiedes der beiden Substanzen schlecht reproduzierbar sind und mehr oder weniger grosse Inhomogenitäten aufweisen.

Diskussion

Das von OSMOND und SMALES[2] beschriebene Verfahren wurde in zwei wesentlichen Punkten abgeändert:

(1) Statt Lithiumfluorid wird Lithiummetall verwendet und nach beendeter Bestrahlung durch Waschen mit Methanol und Wasser von Probe und Standard abgetrennt. Gleichzeitig mit dem Lithium wird auch die seiner Sauerstoffverunreinigung entsprechende F^{18}-Aktivität entfernt.

(2) Die genannten Autoren[2] zählen die vom F^{18} emittierten Positronen im Endfensterzählrohr mit einer Effektivität von 12 %. Bei unseren Versuchen wurden die aus der Vernichtungsstrahlung stammenden γ-Quanten mit einer Effektivität von 45 % gemessen. Durch die erste Änderung wird die Empfindlichkeit des Sauerstoffnachweises erheblich verbessert, wie bereits oben diskutiert wurde. Durch die zweite Änderung wird die Nachweisgrenze infolge der Verbesserung der Messeffektivität noch einmal um den Faktor 3 herabgesetzt. Auch die Genauigkeit nimmt zu, da die zusätzliche Fehler bedingende Korrektur der Selbstabsorption überflüssig wird.

Unter den angegebenen Bedingungen wurden einige Promille Sauerstoff in 10 mg Thoriummetall bzw. 10^{-5} g Sauerstoff bestimmt. Eine um den Faktor 10 kleinere Sauerstoffmenge ist, wie aufgrund der in Tab. 1 angegebenen Aktivitäten ersichtlich, noch ohne weiteres nachweisbar. Ändert man die im experimentellen Teil beschriebenen Versuchsbedingungen durch Verlängerung der Bestrahlungszeit von 10 Minuten auf 2 Stunden (gleich einer Halbwertszeit des Radionuklids F^{18}) und verwendet man statt des natürlichen Lithiums das reine Li^6, so erhöht sich die Empfindlichkeit jeweils um den Faktor 10. Mithin sollte eine Menge von 10^{-8} g Sauerstoff noch bestimmbar sein. Da wegen der vorzüglichen Reinheit des abgetrennten Fluors keine Bedenken bestehen, die Einwaage der zu untersuchenden Probe auf ca. 1 g zu

VOL. 10 1961

erhöhen, so dürfte die Empfindlichkeitsgrenze für die Sauerstoffbestimmung mittels der beschriebenen Methode bei etwa 10^{-8} g/g liegen.

Dieses Verfahren kann auf alle Substanzen angewendet werden, die in Methanol unlöslich sind. Statt des Lithiummetalls kann auch Lithiumhydrid Verwendung finden.

Das Verfahren wird weiter ausgearbeitet. Insbesondere bedarf die Abhängigkeit der Aktivierung von der Homogenität der Mischungen, der Korngrösse und dem Mischungsverhältnis (vgl. 2) weiterer Prüfung. Ferner wird eine Übertragung auf die Untersuchung des Sauerstoffgehaltes von Oberflächen versucht.

H. J. Born
P. Wilkniss

Institut für Radiochemie
der Technischen Hochschule
München, Deutschland

Literatur

1. Smales A. A. *Ann. Repts. Chem. Soc.* **46,** 290 (1949).
2. Osmond R. G. und Smales A. A. *Analyt. chim. acta* **10,** 117 (1954).
3. Fischer und Peisker *Handb. analyt. Chem.* Bd. 7a, 156 (1950).

VOL.
10
1961

book reviews

The Thyroid Gland. British Medical Bulletin 16, May 1960. Medical Department, British Council, London. 86 pp., 20*s*.

THIS is a special issue of the British Medical Bulletin which was produced to coincide with The Fourth International Goitre Conference held in London in July 1960. It follows the usual pattern of such issues in that it consists of a collection of 15 articles each written by an authority in the particular field covered. These cover the basic biochemistry of the thyroid gland, transport of thyroid hormones, the relationship between the thyroid and other endocrine glands, genetic factors, thyroid auto-immunity, thyroid growths and there is a paper on naturally occuring goitrogens.

Only one of the papers deals specifically with radioactive iodine and this is an extremely competent survey of the diagnostic uses of radio-iodine by Dr. A. W. G. Goolden. However, a perusal of the other papers shows that isotopic tracer techniques and chromatography have contributed a great deal to the progress which has been made in the subject in the last decade and which is so well summarized by the present volume. Furthermore, the background knowledge on the biochemistry and physiology of the thyroid gland which is presented here is essential for the proper and intelligent interpretation of the radio iodine test results which are obtained in day-to-day clinical work.

In brief this series of papers maintains the high standard which has been set by preceding issues of the British Medical Bulletin.

N. VEALL

J. SHARPE: **Nuclear Radiation Measurement.** Nucl. Engng. Monographs No. VIII, Temple Press, 1960. 71 pp., 12*s* 6*d*.

THIS monograph presents the "basic physical operation of detectors" and is one of a series intended for university and technical college students and for research assistants and technical workers specialized in other fields. Mr. Sharpe, Research Director at EMI Electronics Ltd., and author of *Nuclear Radiation Detectors* (Methuen 1955), is well qualified to present such a survey. He has wisely excluded chemical dosimetry, devoted only a few lines to photographic techniques and restricted his field to electronic instruments.

Even with this restriction and the relegation of circuit details to the essential performance of "black boxes" the extent of the subject is formidable for so short an account.

Of five chapters, the first occupies little over a page of introductory matter. Chapters 2 and 3, on "Interaction of radiation with matter" and "Detectors—General considerations" and Chapter 5 on "Specific Applications" make up the bulk of the book; a short Chapter 4 being on "Ancillary apparatus."

The style is necessarily terse, sometimes almost at the expense of lucidity, but the pages are packed with concise and quantitative information. Numerous formulae are quoted (usually without derivation) and these and textual figures are liberally supplemented with tables of data. Inevitably, explanatory passages are scanty and some technical terms such as "Bragg curve", "pulse build-up", "dose", although intelligible enough to experts in the field, may discourage the unspecialized reader when used without introduction.

On the whole the standard of information is high, if condensed, though occasional inaccuracies occur (e.g. dead time in counters, beta back-scattering from lead) and there are more misprints than there should be. The references are in general adequate, though many are far from the most up-to-date, especially as regards absolute measurements of radioactivity.

This book cannot with advantage be read superficially: even numerical examples assume calculation by the reader. This being so, occasional lapses in precision of expression such as "a rather square cylindrical cathode" and "the rad is 100 ergs." are more noticeable.

What the reader gains from this little book depends very much on the effort he is prepared to expend in reading it. Its value to students is questionable unless as a basis for revision, but it is invaluable as a source of basic design information (in spite of the author's disclaimer) and there must still be few specialists in the field of radiation counting who cannot derive some fresh information from its pages.

J. L. PUTMAN

5A—(4 pp.)

R. S. ROCHLIN and W. W. SCHULTZ: **Radioisotopes for Industry.** Reinhold Publ. Corp. N.Y. (Chapman and Hall Ltd., London), 1959. x + 190 pp., 38*s*.

THE declared aims of this book enforce a purely descriptive approach throughout the text. The book is written for potential users of radioisotopes and serves to whet their appetite. Fundamental principles of radioisotope application are outlined and many specific applications are briefly described. No prior knowledge of radioactivity is assumed and the main text contains no mathematics. So far as readers of this journal are concerned the book will probably be regarded as too elementary for their own use but its existence is well worth noting when introducing the idea of radioisotope techniques to potential industrial users.

The first chapter consists of a short introduction to the U.S. economics of the uses of radioisotopes and emphasizes the huge dollar savings achieved by these techniques. Succeeding chapters on gauges and radiography contain a certain amount of repetition but this serves to stress the versatility and uniqueness of radioisotope applications. Furthermore, the applications are not confined to the use of radioactive samples prepared as chemical compounds for subsequent use; several examples being quoted of the use of high voltage machines to activate local areas of large components. Useful chapters presenting the wide range of wear testing and tracer applications (on a microscopic, macroscopic and bulk scale) lead to the sections concerned with the many applications of these techniques in manufacturing industries and commercial organizations. The majority of the large number of specific problems and their solution are drawn from American experience although a few British examples are cited.

Health and safety problems are mentioned, all recommendations refer to American codes of practice and safety standards. Four appendices listing useful radioisotope data (somewhat outdated), isotope production methods, thermal neutron activation yields and a fairly comprehensive classified bibliography conclude the volume.

R. A. ALLEN

VOL.
10
1961

Digest of IAEA Conference on Uses of Radioisotopes in the Physical Sciences and Industry Copenhagen, Denmark 6–17 September 1960

THE task of writing a condensed survey on such a large conference, which lasted 10 days and was attended by many potential readers of this comment, raises a number of points. First of all, a participant who did not attend all the sessions should thereby get a concentrated supplement to his own observations. Secondly, by reading the detailed papers one makes critical considerations concerning the work and hence, in our case, a re-examination of our own conference notes. Thirdly, the organizing bodies may be stimulated to strike a balance between digesting the information published at the conference and the enormous amount of work involved in organizing the meeting; a sacrifice which only the people in question can assess and which has been gratefully accepted by all participants in the Conference.

A digest of interesting items is necessarily a matter of subjective judgement. To avoid the danger of underrating important and topical information valuable to the average expert, the comment should preferably not be written by narrowly specialized insiders. Readers of this survey may be assured that the present reviewer does not suffer under too heavy a burden of special knowledge in the field of radioisotopes. They are invited to follow his impressions with critical interest and to supplement this in their own mind.

Several sessions made clear that radioisotopes do play and will play an important role in solving *geophysical problems*. To this category also belongs air movement and water transport. Interesting communications (49, 194)* even referred to the assessment of cosmic ray intensity distribution in outer space, based on the analysis of suitable meteorites. Development of better concentration methods and availability of refined counting techniques offer new prospects in those terrestrial instances where one would hesitate to spread undesirable amounts of radioisotopes (2, 205, 318). The possibility to apply natural and artificial radioactivity in meteorological research and the necessity of international collaboration in operations of that kind has been underlined in two evening lectures prepared and read by leading people of UNESCO's World Meteorological Organization (48, 292). Of course, dating investigations of geophysical or historical interest are being continued in many laboratories (37, 155, 315) and the range of the radioactive age determinations is still being enlarged (317).

In *nuclear physics*, the Mössbauer effect is offering new prospects for studies of resonance absorption of X-rays and of low-energy gamma rays. Extensive experiments on Fe^{57} have been described, giving information as to the strength of the absorption, line characteristics and polarization of the radiation (192).

Most of the work presented at the conference, however, was devoted to research directly or indirectly aiming at increased industrial efficiency or product quality. A number of *fundamental tracer investigations* in the field of *metallurgy and solid state physics* can be comprised in this larger concept of industrial isotope applications, since their results may sooner or later lead to improved processes. Interesting new autoradiographic procedures have been described (26), yielding good autoradiographs from relatively thick specimens and simplifying the interpretation of results.

Amongst applied *technological tracer studies*, special attention has been paid to *wear and friction*. Apart from the question of whether absolute wear under practical conditions can be extrapolated from short model experiments, there is a discussion as to the applicability of activated inserts into larger size test pieces. One paper described the activation in a pool-type reactor of a diesel engine cylinder lining of 1 m length (216), whilst other investigators were satisfied with activated plugs carefully applied to a similar lining (31) and, in another case (162), with radio-silver marks at certain parts of a huge bearing. Fast neutrons are of interest in the activation of systems containing iron and nickel, since (n, p)-reactions of these elements yield the useful radioisotopes of Mn^{54} and Co^{58} respectively (216). Oil additives should protect against corrosion and minimize friction. In addition to that, fine wear particles should be kept in suspension as much as possible. A Russian paper (305) described an ingenious technique for assessing the latter property by using a device in which labelled carbon black can be balanced and moved against gravity by an electric field applied between two GM-tubes which thus have the double function of being detectors as well as electrodes. The general impression is obtained that tracer techniques have been accepted as a useful tool in wear research. Whilst earlier studies have mainly been directed towards relative measurements of additive action or of total wear rates, the present trend is rather to distinguish between wear at different points of a machine or a tool (142) and to measure absolute wear.

* Bracketed figures refer to RICC-numbers of Conference Papers.

The well-known method of detecting critical *wear of refractory linings* has been subject to comment in a French paper (88). Utilization of long-lived isotopes which become dissolved in the metal or other product is legally restricted to a certain amount of activity per ton of product in several countries. The limiting amount should be fixed not only with respect to health hazard, but also in view of technical difficulties which will be encountered as soon as larger quantities of slightly contaminated steel etc. will spread all over the world. Low-activity measurements as well as production and use of photographic material would be disturbed by an increased background of uncontrolled variation.

Many other examples of fine tracer-work were presented including fundamental physical studies as well as technological research. It is difficult to elaborate points of general interest from these papers, since the principle of tracer methods is well established and all the ingenious work described refers to overcoming special difficulties or hazards and to obtaining accuracy and significance of results. The opinion has frequently been expressed that tracer-work should be reported in conferences and periodicals covering the field of application rather than at an isotope conference. An electrochemist will have a higher appreciation of information as to processes taking place during storage of a battery, than an isotope specialist who just listens to a new example of a (skilfully applied!) technique which has no fundamental secrets for him. Even a most difficult and careful investigation showing the fate of impurities during technical purification of silicon (143) is hardly noticed as a sensation by isotope people, although the importance of the subject is obvious.

The many applications based on *penetration, absorption and scattering of radiation* have been illustrated in a number of papers. In spite of the varied production of radioisotopes, there is a gap in the spectrum of available radiation of practical interest corresponding to mass attenuation coefficients in the range of 0·5–5g^{-1} cm^2. To obtain optimum conditions in gauging problems on objects of 0·3–3 g cm^{-2} surface weight, more penetrating rays than Y^{90} betas are needed, but softer ones than the mixed X- and γ-radiation of Tm^{170}. Much work is being carried out to construct suitable 50–200 keV X-ray sources consisting of high yield radioisotope–target combinations. Those X-rays, having mass attenuation coefficients in the required range, are also suitable as primary radiation in X-ray fluorescence assemblies used in analytical work.

Four papers (14, 108, 200, 203) discussed *X-ray spectra excited by different beta-sources* and compared experimental results with theoretical prediction. Since one is mostly interested in reducing the higher energy background as far as possible without losing too much of the desired characteristic frequencies, source constituents and source construction must be adapted to minimize the Bremsstrahlung component. As a matter of fact, X-ray excitation by suitable gammas would offer advantages in this respect. From the reported work on betas as a primary source, it is obvious that Pm^{147} deserves much attention amongst its competitors Kr^{85} and Sr^{90}, due to the available total and specific activities and its relatively low maximum beta-energy. As to the geometry of these sources, sandwich constructions with the target material on both sides of the beta-source and intimate source target mixtures seem to be approximately equivalent as far as X-ray yield in the desired energy region is concerned. Since Pm^{147} can act as its own target, a compressed disk of 200 c of promethium oxide can in principle yield a flux of about 10^6 K photons cm^{-2} sec^{-1} at 25 cm distance.

Contributions concerning *measuring techniques* have been scarce which is readily understood in view of the recent special I.A.E.A. symposium on metrology and the Stockholm meeting. The fact that *industrial thickness gauging* needs much care to avoid trouble from changing environmental conditions has been illustrated in three papers. All of them stress the necessity to compare the wanted signal with a standard signal and ingenious devices have been described to perform this in frequent alternation per second, at high temperature and for different detection chains (107, 110, 306). A special group of possible future applications, which was already casting its shadow in the Copenhagen Conference, depends on the very simple regulation of an electric current by a radiation field of varying strength, the intensity of which is controlled by the movement of a gamma source (27).

In a communication issued by a laboratory working on photographic materials, *autoradiography as a counting method* was compared with usual detector counting (38). In cases where many samples of low activity have to be counted, autoradiography is considered by the authors to be more effective than GM counting.

Radioactive detecting devices in gas-chromatography have been previously described. A German paper (152) discussed a method using a proportional counter opposite to a Sr^{90} source. With carrier gas alone, no signal is registered by the scaler, since the counter is kept well below its starting voltage. Chromatography fractions passing through the counter-cell lower the starting voltage and hence give rise to a signal, which turns out to have a linear relationship with the logarithm of the sought concentration.

An interesting *antistatic source* has been described (20) utilizing 10–20c of tritium which, in comparison with the usual effective beta- or alpha-sources,

causes the smallest radiation hazard. High specific activity compensates for the low particle energies.

Radioisotope methods have been generally adopted as an important tool in *analytical chemistry*. The trend is now towards adaptation of methods to more complicated systems (7), quicker procedures (202, 283) and even automation (11, 198). Most attention is still being paid to *neutron activation analysis*, since this principle is widely applicable in all fields where trace element or small constituent determination is needed. There is much work to be done in this respect and the many potential tasks form a stimulant to speed up the experimental procedure. There are two major bottle-necks in activation analysis, namely reactor irradiation and chemical after-treatment. To widen the first one, several experts (214, 283) have pleaded for more attention to short-lived isotopes, with the consequence that pneumatic installations and laboratory facilities close to a reactor or, alternatively, laboratory neutron sources of sufficient intensity are required. Sources yielding a fast neutron flux of the order of 10^8–10^9 n cm^{-2} sec^{-1} at practicable distance from the generator are being commercially developed, just as relatively simpler ones using sealed tube-generators to produce about one hundredth of that intensity, still sufficient for light element analyses. Chemical separation does not cause much delay in short-lived work, since by definition it must be performed in 15–30 min. In all other cases where direct spectrometry is not possible and chemical after-treatment constitutes a serious delaying factor, one should consider coincidence methods such as the described fast coincidence circuit (79). These complicated devices will, however, only pay in cases where many analyses have to be carried out. The same holds for the endeavour to evaluate analysis results by means of a computer in a quick and accurate way. This automated activation analysis (198) can be economical in routine cases, where the computer programme remains fixed.

Attention has been focused on fast neutrons as an activating tool not only in view of their possible generation in the laboratory, but also due to the various nuclear reactions which they add to thermal (n, γ)-reactions. Tracing Fe and Ni by (n, p) Mn^{54} and Co^{58}, respectively, has been mentioned above, to which can be added the determination of S as P^{32} (7) and many kinds of short-lived isotope work (283).

A nice example of *radiometric analysis* is worth while mentioning, although its applicability seems to be less fundamental than suggested by the authors (199). From Kr^{85}-clathrate, originated by British scientists and further developed in American laboratories, the radioactive gas can be set free by strong oxidizing agents, a reaction which can be used to determine reducing substances.

Isotope production is facing increasing demand. Oak Ridge reported (204) the production during the last 2 years of kilocurie quantities of Cs^{137}, Sr^{90}, Ce^{144} and Pm^{147}. Sixty grammes of pure Tc^{99} have been prepared, corresponding to about 1c of this unstable element. In Belgium, a continuous process for the isolation of Cs^{137} has been developed (4). There is interest for Be^7 produced by irradiating water with 150 MeV protons (92) or Li^7 with secondary protons or deuterons in a reactor (225). The Swedish group once more reported progress in their P^{33} programme (78). Russian contributions described the enrichment of Cl^{36} and Br^{82} (325) and the fixation of Sr^{90} in the shape of glass-like sources (326). The first objective has been reached by exposing to high neutron fluxes very stable compounds of the halogens with a ten- to seventy-fold amount of active charcoal, under which conditions recoil halogen nuclei are liberated and recombined in the carbon lattice. The specific activities obtained are 5–35 mc/mg of bromine and up to 230 mc/g of chlorine.

Apart from isotope production as such, much work was reported on labelled compound chemistry on the one hand and chemical tracer work on the other. The treatment of recoil problems has been restricted to an outstanding survey paper (290), in view of the separate recoil conference organized at Prague by I.A.E.A. New ways to obtain *labelled molecules* partly refer to efforts to improve the classical Wilzbach method. One tries to avoid high tritium concentrations and/or to shorten reaction times by applying additional energy sources such as electric discharge (182, 224), and electromagnetic energy in the form of ultraviolet as well as microwave and radiowave frequencies(224). Recoil tritium nuclei obtained by irradiating Li_2CO_3 have also been applied (321). All these papers claimed higher reaction yields, as compared with those obtained by the traditional Wilzbach procedure. On the other hand, where treatment of high tritium concentrations does not meet serious objection, reduction of reaction time offers but limited advantage, since the purification of reaction products constitutes the most time-consuming factor. More information as to the kind and amount of by-products formed under extra energy conditions will be needed to strike a balance between the advantages of decreased reaction time and relatively improved yield on the one hand and the complication of more complex reaction mixtures on the other. A trial to elucidate reaction kinetics under Wilzbach conditions has been reported (172) for the simplest case $T_2 + CH_4$. According to the author's discussion, extension of the investigation to more complicated systems, especially heterogeneous ones, offers poor prospects.

With reference to molecules labelled by radioisotopes other than tritium, several papers can be

VOL. 10 1961

mentioned. Labelling of cyclic hydrocarbons has been achieved by means of "hot" S^{35} atoms (322); aliphatic substances react with accelerated ionized $C^{14}O_2$ molecules to yield specific activities up to 200 μc/g (67); I^{131}-benzene and CH_3I^{131} have been obtained by reacting benzoic acid and ammonium acetate with fission recoil I^{131} (87). Purification of the required product forms a major difficulty in all these cases of "high impact" synthesis which necessarily leads to a gamut of by-products.

An interesting example of the "Wilzbach-technique" applied to a C^{14} system has been reported in a Russian paper (319). C^{14} is exchanged between $BaC^{14}O_3$ and KCN to equilibrium at 800°C within 2 hr. By using $BaCO_3$ of 60–70 mc/g, a KCN specific activity of more than 80 mc/g can be obtained. Unlike the case of tritium exchange, the change of high-activity carbonate into the depleted substance is a costly disadvantage partly negating the success of the good $HC^{14}N$ yield.

Many papers were devoted to *fundamental tracer work* in chemistry and physical chemistry. In inorganic chemistry much of the work reported referred to the formation and stability of complexes (81, 116, 185, 282). The study of *isotope effects* forms a common feature of a number of other tracer investigations (34, 153, 170, 171, 320); this, incidentally, shows the necessity in all tracer work to consider carefully the possible influence of isotope effects. Two difficult investigations (100, 278) illustrated the variety of products obtained by radiolysis of organic compounds showing the complexity of high-energy-radiation induced reactions, including direct radioisotope interaction as well as chemical reactions initiated by external radiation fields.

The organization of the conference was excellent and good technical facilities were provided. The availability of all summaries many weeks prior to the meeting and the distribution of practically all preprints at Copenhagen ensured maximum efficiency to all participants. Since "gouverner c'est prévoir", the organizing I.A.E.A. committee distributed a questionnaire asking for opinions as to the size and frequency of radioisotope conferences to be held in the future.

Finally, the present reviewer no doubt interprets the feelings of all the participants, when he expresses his gratitude to the Danish Atomic Energy Commission, to the city authorities and to the local conference officers. Everybody was made to feel perfectly at home in the beautiful city of Copenhagen.

Central Laboratory T.N.O. P. PLATZEK
Delft, Netherlands

SOUTHEASTERN CHAPTERS SOCIETY OF EXPERIMENTAL BIOLOGY AND MEDICINE SOCIETY OF NUCLEAR MEDICINE

Proceedings of Meeting held at Oak Ridge, Tennessee (28–29 *October*, 1960)

PROGRAM

Friday Morning 28 *October*, 1960

Symposium: *Virus-cancer interrelationships*

Chairman: S. ROGERS, University of Tennessee Memorial Research Center and Hospital, Knoxville

9:00 **Mammalian tumor viruses:** D. F. PARSONS, Biology Division, ORNL

9:45–10:30 **Avian myeloblast in cell culture:** G. S. BAUDREAU, CAROLINE BECKER and J. W. BEARD, Department of Surgery, Duke University Medical Center

10:45 **Morphology of avian myeloblastosis cells and virus:** R. A. BONAR, J. R. SOMMER, D. WEINSTEIN and J. W. BEARD, Department of Surgery, Duke University Medical Center

Friday Afternoon

Symposium: *New concepts and applications in radioisotope tracer methodology*

Chairman: H. K. EZELL, Special Training Division, ORINS

12:45 **The isotope effect:** G. A. ROPP, ORNL

1:15 **Relationship of the isotope effect to tracer experiments:** C. J. COLLINS, ORNL

2:00 **The neutron activation analysis equation:** ELIZABETH RONA, Special Training Division, ORINS

2:30 **Medical uses of activation analyses:** H. DOWLING, U.S.N. Hospital, Bethesda

3:10–3:35 **Activation analysis at Oak Ridge National Laboratory:** G. W. LEDDICOTTE, ORNL

General Sessions

Friday Afternoon

4:00

SNM

The direct determination of I^{131} in heterogeneous fecal specimens: A. F. DRATZ and J. C. COBERLY, VA Hospital, Atlanta, Ga.

SEBM

Pathological effects of nitrogen mustard on mouse tissue; protection with AET: M. ASANO, T. P. MCDONALD, and T. T. ODELL, JR., Biology Division, ORNL

4:15

SNM

The use of radioiodinated serum albumin in the localization of placental site: A. GILSON, D. CAVANAGH, E. POWE, University of Miami School of Medicine, Miami, Florida

SEBM

Further studies on the formation of phosphatidyl ethanolamine in liver preparations: C. ARTOM and H. B. LOFLAND, Bowman Gray School of Medicine, Winston-Salem, N. C.

4:30

SNM

Interruption of enterohepatic circulation of bile and its effect on the urinary and biliary excretion of I-131: Q. L. HARTWIG, Louisiana State University School of Medicine, New Orleans

SEBM

Origin of antibody-forming cells in the spleen of long-term homologous bone marrow and fetal liver chimeras: G. DORIA, J. W. GOODMAN, N. GENGOZIAN and C. C. CONGDON, Biology Division, ORNL

4:45

SNM

A comparative study of intravenous cerium, lutetium, and yttrium in cortisone-treated rats: E. A. DAIGNEAULT and G. C. KYKER, University of Tenn., Memphis

SEBM

Metabolic conversion of carbon tetrachloride to chloroform: T. C. BUTLER, University of North Carolina, Chapel Hill

5:00

SNM

The application of radioactive iodipamide in the determination of liver dysfunction: J. R. MCLAREN, J. T. GALAMBOS and H. S. WEENS, Grady Hospital, Atlanta

SEBM

Carbon-14 dioxide collection technique for liquid scintillation counting in conjunction with Warburg experiments: F. SNYDER and P. GODFREY, ORINS, Medical Division

5:15

SNM

The metabolism of Ca^{45} and P^{32} with reference to the ultrafilterable fraction of milk and plasma in dairy cows: T. H. KAMAL and R. G. CRAGLE, UT-AEC, Agriculture, Oak Ridge

SEBM

Some enzymic responses to rare earths: I. H. MILLER and G. C. KYKER, Meharry Medical College, Nashville, Tenn.

5:30

SNM

The discrimination exerted by bacteria between Ca^{45} and Sr^{90} and between S^{35} and Se^{75}: J. STERNBERG, University of Montreal, Canada

SEBM

The inhibition of DNA synthesis in the albino rat regenerating liver after partial hepatectomy: I. MESCHAN, Bowman Gray School of Medicine, Winston-Salem, North Carolina

5:45

SNM

Business Meeting

SEBM

Business Meeting

Saturday Morning 29 *October*, 1960

Symposium: *Current topics in radiobiology*

Chairman: A. C. UPTON, Biology Division, ORNL

8:45 **Primary processes in the interaction between radiation and biological materials:** J. S. KIRBY-SMITH, BiologyDivision, ORNL

9:10 **Effects of radiation on bio-chemical reactions:** G. C. NOVELLI, Biology Division, ORNL

9:35–10:00 **Effects of radiation on genes and chromosomes:** R. F. KIMBALL, Biology Division, ORNL

10:15 **Effects of radiation on cellular survival:** M. A. BENDER, Biology Division, ORNL

10:40 **Effects of radiation on animals and human beings:** G. A. ANDREWS, Medical Division, ORINS

11:05 **Modification of radiation injury: Protection and recovery:** C. A. CONGDON, Biology Division, ORNL

VOL. 10 1961

Abstracts of Contributed Scientific Papers (General Session)

The direct determination of I^{131} in heterogeneous fecal specimens: ARTHUR F. DRATZ and JAMES C. COBERLY, VA Hospital, Atlanta

A counting geometry incorporating sample rotation and graded attenuation makes it possible to accurately determine the I^{131} content of heterogeneous stools without prior processing other than the addition of water to an approximate total volume of 350 cm^3. Correction factors for variations in specimen size are not necessary. With this geometry even an extremely heterogeneous sample, i.e., a 1 cm^3 I^{131} source located anywhere within a 350 cm^3 volume of water, readily can be assayed with less than ± 7 per cent error.

A pint carton containing the specimen is rotated on a turntable at 20 r.p.m. A spectrally controlled 2×2 in. scintillation probe, symmetrically positioned four inches from and in a plane perpendicular to the axis of rotation, "sees" the specimen through a space between two vertical lead slabs which provide lateral attenuation. The width and point of interposition of this space are adjusted so that the response from a 1 cm^3 I^{131} source is independent of its radial position. The response from the source, however, continues to be dependent upon its vertical position and this varies over a ± 7 per cent range. At some sacrifice in sensitivity this error could be reduced by employing a greater crystal to specimen distance.

The use of radioiodinated serum albumin in the localization of placental site: ALBERT J. GILSON, DENNIS CAVANAGH and EDWARD POWE, University of Miami School of Medicine

A total of 50 patients in the third trimester of pregnancy were selected for study. All patients had either vaginal bleeding or were to undergo elective caesarean section the following day.

Five microcuries of radioactive serum albumin were injected intravenously. After a suitable mixing interval, counts were recorded over the heart and twelve preselected points over the uterus.

The count rate over the heart served as a control value indicating a known blood pool and was assigned a value of one hundred per cent. The count rate over the 12 uterine points was then compared to this value and percentages relative to the count rate were assigned to each point.

Interpretation and results of these 50 cases are reported.

Interruption of enterohepatic circulation of bile and its effect on the urinary and biliary excretion of I-131: QUENTIN L. HARTWIG, Louisiana State University School of Medicine, New Orleans

The influence of total external diversion of bile on the urinary and biliary excretion of intravenously administered I-131 as NaI^{131} was studied in the rat. The common bile duct of male rats was divided and polyethylene tubes were inserted into the proximal and distal ends of the duct to permit collection of bile and infusion of bile or tap water into the duodenum. Division and anastomosis of the bile duct over a polyethylene tube did not interfere with the urinary excretion of I-131 thus ruling out operative trauma as a factor in the experimental results.

Urinary excretion of I-131 was progressively decreased in the following groups of experimental animals: Group I, those simply starved; Group II, those with total biliary fistula given oral iodinated water; Group III, those with total biliary fistula given donor bile intraduodenally; and Group IV, those with total biliary fistula without supplemental bile or iodine. The I-131 content of the bile collected from rats in Groups II, III, and IV was essentially the same.

These studies raise the question of the role of bile in the excretion of I-131 *intravenously* administered.

A comparative study of intravenous cerium, lutetium, and yttrium in cortisone-treated rats: ERNEST A. DAIGNEAULT and GRANVIL C. KYKER, University of Tennessee, Memphis, and Medical Division, ORINS

Several hormones affect the acute fatty infiltration that occurs in the liver of rats treated with certain lanthanons. No explanation for these hormonal effects is known. We compared the effect of cortisone on the distribution and excretion of cerium, lutetium, and yttrium. This selection was an attempt to represent the lanthanons in groups according to atomic number and metabolic effect. Cerium represents the first five elements each of which causes fatty infiltration; others in the series above samarium do not elevate total liver lipids. Lutetium represents the upper end of the series and yttrium closely resembles certain intermediate lanthanide elements. The properties and availability of Ce^{144}, Lu^{177}, and Y^{90} as radioisotopic tracers also influenced the choice of elements. Two levels of dose were used. The lower dose of each element depended on the specific activity of the tracers and approximated

VOL. 10 1961

10^{-9}, 10^{-8}, and 10^{-12} mole of cerium, lutetium, and yttrium, respectively, per kg. The higher dose was adjusted to 10^{-5} mole per kg by additional carrier. The chlorides of each element adjusted to pH 4 were injected intravenously. Cortisone was given intramuscularly as the acetate derivative (25 mg/kg). Fasting was imposed throughout the 24-hr experimental period. Cortisone altered the distribution to some extent. This was more noticeable at the higher level of dose, and also for cerium. The effect on excretion was more variable and showed no consistent trend. In a few experiments we also compared the elements during treatment with corticosterone, insulin, dinitrophenol, and EDTA. Again no striking effects were observed, except the increased excretion during EDTA treatment. The EDTA was given subsequent to the metal and the enhanced excretion was accordingly less than that observed by others when a lanthanon is administered as its EDTA-complex. Typical results are presented and the effect of the various agents discussed.

The application of radioactive iodipamide in the determination of liver dysfunction: J. R. McLaren, John T. Galambos, and H. Stephen Weens, Grady Hospital, Atlanta, Ga.

Hepatic uptake of I-131 iodipamide, as assessed by external counting, is demonstrably different in patients with liver disease, compared to those without. Interpretation is based on the slope of the uptake curve. In nearly all patients showing a rising slope, the biliary tree is demonstrable by cholangiogram; in contrast, it will not be visualized in patients whose external counts fail to show hepatic concentration of the dye. Interfering factors such as obesity are discussed. In the light of the findings the radioiodipamide liver-uptake test appears to show promise.

The metabolism of Ca-45 and P-32 with reference to the ultrafilterable fraction of milk and plasma in dairy cows: T. H. Kamal and R. G. Cragle, UT-AEC Agricultural Research Laboratory, Oak Ridge

This study was undertaken to investigate the incorporation of the soluble inorganic Ca-45 and P-32 in the ultrafilterable and non-ultrafilterable fraction of blood plasma and milk after an intravenous injection of Ca-45 and P-32 in dairy cows. The concentration as well as the rate of decline of P-32 in plasma ultrafiltrate was similar to that of whole plasma during the first two to three hours after dosing, suggesting that most of P-32 in plasma was still in the soluble inorganic form. Thereafter, the P-32 concentration in both fractions leveled off with the ultrafilterable P-32 level in plasma being about 70 per cent of whole plasma P-32. After the first 2 to 3 hr, the tissues apparently begin to feed back P-32 in its various metabolized forms. The Ca-45 was determined directly after dosing to be about 70 per cent non-ultrafilterable and 30 per cent ultrafilterable probably due to an immediate binding of this portion of Ca-45 to plasma proteins. While most of plasma P-32 during the first 3 hr was in the ultrafilterable form, milk P-32 and Ca-45 were partitioned directly after dosing into ultrafilterable and non-ultrafilterable fractions. This indicates that both the organic and inorganic milk phosphorus are derived mainly from blood inorganic phosphorus and that the rate of metabolism of phosphorus in mammary gland exceeds that of other peripheral tissues. The endogenous Ca-45 and P-32 excreted in feces in 43 hr amounted to 22 and 15 per cent, respectively. During the same period, the amounts of Ca-45 and P-32 excreted in urine were 8 and 0·09 per cent, respectively, and those in milk were 16 and 6 per cent, respectively.

Pathological effects of nitrogen mustard on mouse tissue; protection with AET: M. Asano, T. P. McDonald, and T. T. Odell, Jr., Biology Division, ORNL

The purpose of this study was to determine the pathological effects of methyl bis (β-chloroethyl) amine hydrochloride (HN_2·HCl) on tissues of RF mice and to investigate the possible protective action of S,2 aminoethylisothiouronium·Br·HBr (AET), a radioprotective agent, against such damage. The LD_{50}/30 days of HN_2 in RF mice was found to be 0·127 mg/mouse. Immediate depression and prolonged atrophy of hemopoietic organs (bone marrow, spleen, lymph nodes and thymus) and damage to the intestinal epithelium and to the brain were observed. Damage to the brain was severe, sites of predilection being the neocortex, pyriform cortex, hippocampus, cerebellum and medulla oblongata. The most striking changes seen were selective neuronal shrinkage, hemorrhage, and necrosis. A comparison of brain injury with injury to other organs suggested that brain damage may have been a primary cause of death in HN_2-treated mice. In RF mice injected intraperitoneally with 9·0 mg of AET/mouse 20 min before intravenous injection of 0·10 mg of HN_2, there was less tissue damage, and recovery began earlier. Especially notable was a reduction in hemorrhage in bone marrow and brain, and a lessened depression of megakaryocyte number.

Further studies on the formation of phosphatidyl ethanolamine in liver preparations: CAMILLO ARTOM and HUGH B. LOFLAND, JR., Bowman Gray School of Medicine, Winston-Salem, N.C.

A comparative study of the *in vitro* incorporation of labeled ethanolamine (EA) and labeled phosphorylethanolamine (PEA) into the phospholipids of various liver preparations has been carried out. The results suggest that two different enzyme systems are present in rat liver. One of these systems is probably identical with that synthesizing cephalins (phosphatidyl EA) through the intermediate formation of PEA and cytidine diphosphate EA (Cyt-diP-EA), as postulated by KENNEDY and WEISS[1]. This system is stimulated by Mg^{++} and inhibited by Ca^{++}. For a sizable activity, the simultaneous presence of both mitochondria and their supernate is required. Addition of cytidine phosphates greatly enhances the incorporation of either EA, or PEA.

The second enzymatic system is predominantly located in the microsomes. It incorporates free EA into phospholipids by a pathway not involving PEA, or Cyt-diP-EA. It is strongly activated by Ca^{++} and is also clearly ATP-dependent. It is unaffected by Mg^{++}, as well as by the addition of cytidine derivatives. It is inhibited by Mn^{++}. This calcium-activated system is possibly similar to the one catalyzing an "enzymatic exchange" between free choline and lecithin.

Origin of antibody-forming cells in the spleen of long-term homologous bone marrow and fetal liver chimeras: GINO DORIA, J. W. GOODMAN, N. GENGOZIAN, and C. C. CONGDON, Biology Division, ORNL

A study is being made of the relative immune capabilities of the host and donor cells in chimeras sensitized against sheep RBC. The method is one in which lethally irradiated test mice are used as a culture medium for a known number of spleen cells from donors previously injected with sheep RBC. The irradiated recipients are injected with the test antigen at the time of the spleen cell transfer and bled 6 days later for serum titration of anti-sheep RBC agglutinins. The titer is a function of the number of transferred spleen cells; if the irradiated recipients have been pre-immunized to the donor no antibody-activity can be detected.

Homologous bone marrow and fetal liver chimeras [BDF_1 donor and $(101 \times C3H)F_1$ recipient] 120 days old and having only donor-type red cells, were injected intraperitoneally with sheep RBC. Eighteen days later spleen cells from fetal liver or bone marrow chimeras were injected intravenously into each irradiated recipient that also received sheep RBC intraperitoneally. The irradiated (900 r) recipients were BDF_1 and $(101 \times C3H)F_1$; BDF_1 pre-immunized against $(101 \times C3H)F_1$, and $(101 \times C3H)F_1$ pre-immunized against BDF_1. In both cases (fetal liver and bone marrow chimeras) the chimeric spleen cells gave positive titer in the first 3 groups of recipients and a negative one in the 900 r-$(101 \times C3H)F_1$ mice pre-immunized against BDF_1. These results provide evidence for the donor origin of antibody-forming cells in the spleen of homologous chimeras challenged with sheep RBC. The failure to detect activity of host-type cells can be due to their absence or functional impairment.

Metabolic conversion of carbon tetrachloride to chloroform: THOMAS C. BUTLER, University of North Carolina, Chapel Hill, N.C.

By gas chromatography small amounts of chloroform have been identified in the expired air of dogs that have received carbon tetrachloride by inhalation. Liver and kidney tissue *in vitro* have also been shown to produce chloroform from carbon tetrachloride. It is presumed that the carbon-chlorine bond undergoes homolytic fission, each fragment retaining one of the electrons comprising the covalent bond and attaining octet stability by acquisition of an electron from some other compound. Although the extent of the reaction is small, it is conceivable that the acquisition of electrons, e.g. from —SH groups of enzymes, might play a part in the toxic effects of carbon tetrachloride.

Carbon-14 dioxide collection technique for liquid scintillation counting in conjunction with Warburg experiments: FRED SNYDER and PAUL GODFREY, Medical Division, ORINS

A technique will be described for the collection of radioactive CO_2 in Hyamine and for subsequent liquid scintillation counting. At the end of a typical Warburg experiment the Hyamine is injected through a rubber cap covering the Warburg vessel into a small glass tube which has been positioned on top of the center well. Sulfuric acid is then poured from a side arm into the main compartment of the Warburg flask in order to release the carbon dioxide from the media. The transfer of CO_2 to the Hyamine is about

[1] *J. Biol. Chem.* **222,** 193 (1956).

97 per cent within 2–3 hr after the addition of hydrogen ion. The tube containing the Hyamine is then transferred *in toto* to a glass counting vial containing 0·4 per cent PPO and 0·01 per cent POPOP in toluene and the radioactive content is measured using an automatic Packard Tri-Carb Spectrometer.

This system has been used in a study of the oxidation of C^{14}-labeled fatty acids.

Some enzymic responses to rare earths: I. H. Miller, Jr. and Granvil C. Kyker, Meharry Medical College, Nashville, Tenn. and Medical Division, ORINS

VOL. 10 1961

The acute metabolic response of experimental animals to certain lanthanons poses questions of their effect on critical enzyme systems. Such effects are essentially undefined. A hepatic disorder caused by cerium in rats led us to examine the effect of this element on certain enzymes. Certain hydrolases were selected because of the availability of purified commercial preparations and because of the simplicity of assay procedures. Urease, invertase, amylase, pepsin, and phosphatase were studied under *in vitro* conditions. The levels of other hydrolases were compared in the serum and in the liver of normal and of cerium-treated rats; these include serum acid and alkaline phosphatase and hepatic esterases that hydrolyze ethylacetoacetate, monoproprionin, and phosphatidic acid. An inhibition of activity was observed for each of the commercial enzymes when cerium was added. The activities of acid phosphatase, invertase, and pepsin were inhibited by cerium at concentrations as low as 10^{-4} M, but amylase was inhibited by 10^{-6} M cerium. However, urease was not appreciably affected by cerium in concentrations of less than 10^{-2} M. In the *in vivo* comparisons, the levels of serum acid phosphatase and hepatic esterase (ethylacetoacetate) were much higher in cerium-treated than in saline-treated rats; the other three enzymes showed no differences. The increased levels of serum acid phosphatase and hepatic esterase are reflections of the response of the host to cerium and are not evidence for an effect of the metal on the enzymes.

The inhibition of DNA synthesis in the albino rat regenerating liver after partial hepatectomy: I. Meschan, A. D. Barton and Anne L. Barton, Bowman Gray School of Medicine, Winston-Salem, N.C.

The rat liver regenerates very rapidly following partial hepatectomy so that DNA synthesis begins approximately 18 hr after the operative removal of about 2/3 of the rat liver and DNA synthesis increases many fold by approximately 30 hr. Between 30 and 48 hr there is a very considerable increase in mitosis and the liver is almost completely regenerated to about 90 per cent of its former size in 7–10 days.

The rapid synthesis of DNA between the 18- and 30-hr interval after partial hepatectomy gives one an excellent experimental opportunity for studying possible DNA synthesis inhibition. Such synthesis inhibition has been accomplished by the injection intraperitoneally of liver homogenates obtained from normal rat livers as well as from livers which have been X-irradiated previously or regenerating livers of partially hepatectomized animals. Various fractions of liver homogenate have been studied in an effort to obtain greater isolation of the inhibitory factor or factors.

Discrimination between Periodic Relatives in Microorganisms S-35 and Se-75, Ca-45 and Sr-90: Joseph Sternberg, University of Montreal, Canada

The ability of microorganisms to discriminate between periodic relatives was studied in *Staphylococcus aureus*, *Mycobacteria* and the yeast-like fungus *Candida albicans*. Two pairs of periodic relatives were investigated: sulfur-35 and selenium-75, and calcium-45 and strontium-90; each isotope was added to the culture medium in the same concentration (4μc/ml.).

The microorganisms are unable to discriminate between sulfur-35 and selenium-75; the latter is taken up by the microbes in considerably larger amounts, especially when the uptake per mg cells is considered (*M. phlei* = 5–10 times, BCG = 20 times more Se-75 than S-35). Chromatographic analysis of cellular hydrolysates showed that Se-75 was integrated into methionine and cysteine, but probably the elaboration of proteins is inhibited; this explains the significant inhibitory action of selenium upon the microbial growth: the cell does not discriminate, but the seleniated amino-acid does not have the same metabolic properties as the sulphurated amino-acid. In *Staphylococcus*, the inhibitory action of selenium is less marked; in this case, sulphur (as sulphate) is almost exclusively concentrated in the cytoplasm, in opposition to selenium, which is taken up in significant amounts by the cell walls.

Young cells of BCG (7 days) are able to discriminate between Ca-45 and Sr-90; the uptake of Ca-45 (7·7%) is significantly higher than that of Sr-90 (0·6%); in older cultures (14 days), this discrimination disappears (Sr-90 = 15·5%; Ca-45 = 13·5%).

The opposite phenomenon is noted in *Mycobacterium phlei*, whose Sr-90 uptake (35·4%) is higher than that of Ca-45 (23·0%); chromatographic analysis showed that most of the isotopes are linked to glutamic and aspartic acids; a part of Sr-90 was present under mineral form.

In *Candida albicans*, the isotopes do not pass through the cellular membrane, the surface absorption seems to be predominant mechanism; although the uptake of both isotopes is small, it seems that Sr-90 is taken up in larger amounts (1·8%) than Ca-45 (0·05%). Sr-90 does not exert any inhibitory action upon microbial growth.

International Journal of Applied Radiation and Isotopes, 1961, Vol. 10, pp. 149–157. Pergamon Press Ltd. Printed in Northern Ireland

La Détermination du Cu, Cr, Zn et Co dans le Sérum par Radioactivation

J. PIJCK,* J. GILLIS et J. HOSTE
Laboratoire de Chimie Analytique, Université de Gand, Belgique

VOL. 10 1961

Les résultats d'expériences effectuées en vue de déterminer le comportement des éléments Sb, As, Cr, Co, Au, Fe, Cu, Hg, Pb, Mn, Mo, V, Ag et Zn sous forme de traces, pendant la destruction de matières biologiques, peuvent être résumés comme suit: la destruction par combustion sèche est à rejetter comme méthode générale. Pour la plupart des éléments précités il est en effet impossible d'effectuer une récupération quantitative, même à des températures relativement basses de 500 à 550°C. Par contre, en minéralisant les substrats organiques à l'aide du mélange d'acides HNO_3–$HClO_4$–H_2SO_4 (3 : 1 : 1) nous avons obtenu des résultats quantitatifs, sauf pour les éléments Sb, As, Au, Fe et Hg. Pour ces derniers l'emploi d'un réfrigérant à reflux s'impose.

L'examen des réactions secondaires gênantes $Zn^{64}(n, p)Cu^{64}$, $Fe^{54}(n, \alpha)Cr^{51}$, $Ni^{58}(n, p)Co^{58}$ fut effectué en irradiant des échantillons de Zn, Fe et Ni dans le flux central et dans la colonne thermique du réacteur. De ces expériences on peut conclure que l'interférence de ces réactions est négligeable pour le cas d'échantillons de sérum dans nos conditions d'irradiation bien déterminées.

Les oligo-éléments Cu, Cr, Zn et Co furent dosés dans le sérum par radioactivation. Pour le cuivre, le chrome et le cobalt une méthode de séparation sélective et quantitative fut employée, basée soit sur extraction liquide–liquide, soit sur distillation sélective. Pour le zinc par contre une séparation plus complexe s'avéra nécessaire dont le rendement fut calculé par gravimétrie ou par titrimétrie.

L'avantage principal des méthodes proposées consiste dans la réduction considérable de l'échantillon, qui fut de l'ordre de 250 à 25 λ.

THE DETERMINATION OF Cu, Cr, Zn AND Co IN THE SERUM BY RADIOACTIVATION

The results of investigations dealing with the loss of trace quantities of the elements Sb, As, Cr, Co, Au, Fe, Cu, Hg, Pb, Mn, Mo, V, Ag and Zn during destruction of biological material, prior to their determination by radioactivation analysis, can be summarized as follows: dry destruction by ignition is to be rejected as a general method as many of the metals investigated are lost to a considerable extend, even at relatively low temperatures of 500–550°C. With a liquid destruction mixture of HNO_3–H_2SO_4–$HClO_4$ in a ratio of 3 : 1 : 1, complete recovery can be obtained for all of the elements investigated, excepting Sb, As, Au, Fe and Hg. These can be quantitatively recovered if an efficient reflux condenser is used.

A number of possibly interfering (n, p) and (n, α) reactions, due to fast neutrons, were investigated, namely: $Zn^{64}(n, p)Cu^{64}$; $Fe^{54}(n, \alpha)Cr^{51}$; $Ni^{58}(n, p)Co^{58}$.

Interference was proved to be less than 1 per cent when irradiated in BR 1 at a flux of 5×10^{11} n/cm^2. sec.

Finally, trace quantities of the elements Cu, Cr, Zn and Co were determined in blood-serum by radioactivation analysis. Wherever possible, selective extraction methods were used. Results from series of determinations, which were compared with reliable spectrophotometric data, proved to be accurate and reproducible, whereas sampling could be kept down to the 25–250 λ range.

* Chercheur aggrée I.I.S.N.

ОПРЕДЕЛЕНИЕ Cu, Cr, Zn И Co В СЫВОРОТКЕ ПРИ ПОМОЩИ РАДИОАКТИВАЦИОННОГО АНАЛИЗА

Результаты исследования поведения следов элементов Sb, As, Co, Au, Fe, Cu, Hg, Pb, Mn, Mo, V, Ag, Zn во время деструкции биологического материала можно суммировать следующим образом:

Сухая деструкция прокаливанием непригодна, как основной метод, т.к. для большинства исследуемых веществ количественное выделение при этом невозможно, даже при таких сравнительно низких температурах как 500–550°C. При минерализации же органических субстратов при помощи смеси кислот HNO_3–$HClO_4$–H_2SO_4 (3:1:1) были получены количественные данные для всех элементов кроме Sb, As, Au, Fe и Hg. Для этих последних желательно применение противоточного конденсера.

Исследование нежелательных вторичных реакций $Zn^{64}(n,p)Cu^{64}$, $Fe^{54}(n,\alpha)Cr^{51}$, $Ni^{58}(n,p)Co^{58}$ проводилось путем облучения образцов Zn, Fe и Ni в центральном потоке и в термической колонке реактора. Из этих опытов можно вывести заключение, что для сыворотки в наших условиях вторичными реакциями можно пренебречь.

Cu, Cr, Zn и Co определялись в сыворотке при помощи радиоактивационного анализа. Для меди, хрома и кобальта был применен метод избирательного количественного разделения, основанный на экстракции или избирательной дистилляции. Выделение цинка оказалось более сложным и выход его определяли при помощи гравиметрии или титрования.

Принципиальное преимущество предложенного метода заключается в возможности значительного уменьшения образцов до величин от 250 до 25λ.

DIE BESTIMMUNG VON Cu, Cr, Zn UND Co IM SERUM MIT HILFE VON RADIOAKTIVIERUNG

Die Ergebnisse der Untersuchungen über den Verlust der Spurenelemente Sb, As, Cr, Au, Fe, Cu, Hg, Pb, Mo, V, Ag und Zn während der Veraschung von biologische Materie können in folgender Weise zusammengefasst werden: die Methode der trockenen Veraschung kann im allgemeinen nicht angewendet werden, da quantitative Wiedergewinnung eines Grossteiles der erwähnten Elemente selbst bei relativ niederer Temperatur von 500–550°C nicht möglich ist. Hingegen erhielten wir quantitative Ergebnisse bei der nassen Veraschung mit HNO_3–$HClO_4$ und H_2SO_4 (3:1:1), ausgenommen für die Elemente Sb, Au, Fe, und Hg. Die letzteren können mit Hilfe eines Rückflusskühlers quantitativ erhalten werden.

Um zu untersuchen wie weit störende (n,p) und (n,α) Prozesse, hervorgerufen durch schnelle Neutronen, auftreten können, besonders Zn^{64} (n,p) Cu^{64}, Fe^{54} (n,α) Cr^{51} und Ni^{58} (n,p) Co^{58}, wurden Proben von Zn, Fe und Ni im zentralen Fluss der thermischen Säule des Reaktors bestrahlt. Es zeigte sich, dass bei den während der Bestrahlung von Serumproben herrschenden Bedingungen die Störungen durch diese Reaktion vernachlässigbar klein sind.

Die Spurenelemente Cu, Cr, Zn und Co wurden schliesslich mit Hilfe der Aktivierungsanalyse bestimmt. Wo es möglich war, wurde die Methode der selektiven Extraktion verwendet. Die Ergebnisse der serienmässigen Bestimmungen erwiesen sich bei Vergleich mit verlässlichen, spektrometrischen Daten als genau und reproduzierbar.

Der Vorteil der vorgeschlagenen Methode besteht vor allem darin, dass die verwendeten Probenmengen auf 250–25λ herabgesetzt werden können.

1. INTRODUCTION

Le rôle important des oligo-éléments dans les processus biologiques et le dosage de ces bio-catalysateurs intéresse de plus en plus les biochimistes et les analystes.

Les méthodes de dosage sont malheureusement souvent très complexes et exigent de l'analyste une grande habilité et une longue expérience.

Nous avons essayé de doser divers éléments sous forme de traces dans les matières biologiques par la méthode par radioactivation. Cette technique relativement simple permet en effet par sa grande sensibilité de réduire considérablement l'échantillonage et possède en plus l'avantage d'être indépendante de contaminations accidentelles.

2. MINERALISATION DES SUBSTRATS ORGANIQUES

Avant de procéder aux analyses par activation, il a été jugé utile de controler le comportement de certains oligo-éléments pendant la destruction de matières biologiques. Il est en effet indispensable de minéraliser les substrats organiques avant de procéder aux séparations éventuelles et au dosage proprement dit. Au cours de cette minéralisation, des pertes considérables peuvent en effet se produire.[1,2,16,17]

L'emploi de traceurs radioactifs a permis d'obtenir d'une façon relativement simple les données nécessaires concernant le comportement d'un nombre d'oligo-éléments pendant la minéralisation des substrats organiques. En effet, en effectuant des mesures d'activité avant et après la destruction, il est facile de déterminer l'étendue des pertes éventuelles.

Un détecteur intégral à scintillations NaI(Tl) du type puits, suivi d'une échelle de comptage classique fut employé pour les comptages des divers isotopes émetteurs-gamma, à l'exception du Pb^{210}. Cet isotope émettant un rayon gamma de faible énergie (47 keV) il a été nécessaire d'intercaler un amplificateur linéaire dans la chaine de comptage. Le Tableau 1 résume les éléments examinés et leurs isotopes radioactifs correspondants, ainsi que les activités spécifiques employées.

Ces différents éléments furent soumis à une minéralisation par voie sèche, à des températures de 400, 500, 700 et 900°C en employant du sang comme substrat organique. Les temps de destruction furent variés de 3, 6, 12 à 24 hr afin de permettre une destruction complète. Les résultats obtenus sont résumés dans le Tableau 2.

Il apparait que pour la plupart des éléments, les pertes sont considérables, même à une température de destruction relativement basse. Ces pertes sont dues soit à l'absorption au creuset de porcelaine employé (Hg, Pb, Cu, Zn), soit à la volatilisation (Fe, As, Sb, Au, Hg).

Les mêmes éléments furent ensuite examinés au cours de la destruction par voie humide à l'aide d'un mélange d'acides HNO_3 (66%), $HClO_4$ (70%) et H_2SO_4 (98%) (3:1:1). Ce mélange permet une destruction totale et rapide de matériaux très divers et ne présente aucun danger. Les destructions par voie humide ont été exécutées en présence de matériaux divers, tels qu'urine, poudre végétale, tissu musculaire et sang entier. En général 5 ml du mélange des acides suffit pour la destruction complète de 500 mg de poudre végétale, 5 ml de sang, 25 ml d'urine et 2,5 g de tissu musculaire. La destruction s'opère dans des fioles micro-Kjeldahl d'un contenu d'environ 50 ml, chauffées électriquement. La durée de la

TABLEAU 1. Radio-isotopes employés

Composé	Isotope	Demi-vie	Activité spécifique (c.p.m/μg)	μg ajouté
$SbCl_3$	Sb^{122}	2,8 jours	5000	5
$NaAsO_2$	As^{76}	26,5 hr	25600	1
$CrCl_3$	Cr^{51}	27,8 jours	38000	2
$Co(NO_3)_2$	Co^{60}	5,25 ans	1500	6
$AuCl_3$	Au^{198}	2,69 jours	138000	1
$Fe(NO_3)_3$	Fe^{59}	45,1 jours	1200	6
$Cu(NO_3)_2$	Cu^{64}	12,8 hr	18000	3
$Hg(NO_3)_2$	Hg^{203}	47 jours	7000	5
$Pb(NO_3)_2$	Pb^{210}	22 ans	1000	10
$Mn(NO_3)_2$	Mn^{56}	2,58 hr	9000	3
Na_2MoO_4	Mo^{99}	68 hr	4200	4
V	V^{48}	16,2 jours	Carrier-free	—
$AgNO_3$	Ag^{110m}	270 jours	5600	4
$ZnCl_2$	Zn^{65}	245 jours	1600	7

TABLEAU 2. Minéralisation par voie sèche (% de traceur récupéré). (Nombre d'expériences entre parenthèses)

Elément	24 hr 400°C	12 hr 500°C	6 hr 700°C	3 hr 900°C
Sb	67 (4)	81 (4)	35 (4)	9 (4)
As	23 (3)	0 (6)	0 (6)	0 (6)
Cr	99 (6)	99 (6)	85 (6)	56 (6)
Co	98 (6)	75 (5)	67 (6)	30 (6)
Au	19 (4)	0 (5)	0 (5)	0 (4)
Fe	86 (4)	81 (4)	52 (5)	27 (3)
Cu	100 (5)	98 (4)	87 (4)	58 (5)
Hg	<1 (5)	0 (4)	0 (4)	0 (4)
Pb	103 (3)	70 (3)	32 (3)	13 (3)
Mn	99 (4)	96 (4)	85 (4)	79 (4)
Mo	100 (4)	97 (3)	85 (3)	83 (3)
V	102 (5)	99 (5)	70 (5)	60 (5)
Ag	65 (4)	67 (4)	45 (4)	21 (4)
Zn	100 (4)	98 (6)	69 (6)	30 (6)

TABLEAU 3. Minéralisation par voie humide
(% de traceur récupéré).
(Nombre d'expériences entre parenthèses)

Elément	Sang	Urine	Poudre végétale	Tissu musculaire	Réfrigérant à reflux
Sb	99 (4)	95 (5)	95 (5)	94 (5)	101 (4)
As	93 (6)	94 (4)	95 (6)	93 (5)	101 (4)
Cr	100 (6)	100 (6)	101 (6)	100 (6)	
Co	100 (11)	100 (6)	100 (6)	99 (6)	
Au	77 (4)	101 (6)	77 (6)	65 (4)	101 (4)
Fe	98 (17)	92 (5)	95 (6)	85 (6)	100 (12)
Cu	102 (5)	101 (5)	102 (5)	102 (5)	
Hg	24 (5)	87 (5)	45 (4)	30 (6)	100 (4)
Pb	100 (3)	101 (4)	101 (4)	101 (4)	
Mn	99 (5)	99 (5)	98 (4)	100 (5)	
Mo	101 (5)	101 (6)	101 (5)	101 (5)	
V	100 (5)	100 (5)	100 (5)	100 (5)	
Ag	100 (6)	101 (6)	100 (5)	100 (6)	
Zn	99 (12)	101 (6)	99 (5)	100 (6)	

destruction varie d'après le substrat organique, de 30 min à 2 hr. Les résultats sont résumés dans le Tableau 3.

Il apparait que la récupération des éléments précités est quantitative, à l'exception de Au, Fe, As, Sb et Hg. Pour ces derniers, l'emploi d'un condensateur à reflux s'impose.

3. ANALYSE PAR RADIOACTIVATION

Le principe de l'analyse par radioactivation a été suffisamment décrit dans la littérature.[7,8,9] Pour un grand nombre d'éléments, cette techniques est devenue une des plus sensibles dont dispose actuellement l'analyste. Elle est donc particulièrement indiquée pour l'analyse de traces.

Nous avons examiné le dosage du Cu, Cr, Zn et Co dans le sérum de cheval. Ce sérum fut obtenu par centrifugation du sang coagulé. En irradiant un échantillon de sérum de 250 λ (et même de 25 λ pour le cas du cuivre) dans le réacteur BR 1 à un flux de neutrons de $5 . 10^{11}$ à $8 . 10^{11}$ n/cm². sec, les activités obtenues furent amplement suffisantes pour permettre une détermination précise.

N'ayant pas le réacteur sur place, le choix c'est porté sur les isotopes de vie moyenne ou longue, c'est à dire, Cu^{64} (12,8 hr), Cr^{51} (27,8 jours), Zn^{65} (245 jours) et Co^{60} (5,2 ans), ce qui implique une durée d'irradiation assez importante (de 12 hr à 8 jours).

Après activation, l'échantillon irradié fut minéralisé par voie humide suivant la méthode décrite ci-dessus. L'élément à doser fut ensuite isolé du substrat irradié par une méthode de séparation sélective. L'activité obtenue fut comparée à celle d'échantillons-standard irradiés simultanément dans des conditions identiques. Ces standards, sous forme métallique ou d'oxyde, sont dissous dans un mélange d'acides, portés à 50 ml et dilués de 100 à 10·000 fois d'apres l'activité induite.

Après séparation des différents nuclides, leur pureté radiochimique fut controlée par spectrométrie-gamma et par analyse des demi-vies. La précision des résultats par radioactivation fut systématiquement comparée à celle obtenue par spectrophotométrie.

Dans les conditions d'irradiation dans le réacteur BR 1 c'est à dire, à un flux de neutrons de $5 . 10^{11}$ à $8 . 10^{11}$ n/cm². sec et dans une position à rapport-cadmium de 5, les neutrons rapides pouvaient engendrer les réactions (n, p) et (n, α) gênantes. Celles-ci peuvent éventuellement causer des erreurs considérables par formation simultanée du nuclide radioactif désiré à partir d'un autre

élément que celui dont le dosage est envisagé. Les sections efficaces pour ces réactions gênantes ont été déterminées par MELLISH *et al.*[6] Ces résultats, ne sont cependant valables que pour une position définie dans le réacteur. Nous avons donc préféré controler l'étendue des interférences pour nos conditions expérimentales.

(a). *Dosage du cuivre par radioactivation*

La détermination de traces de cuivre dans divers produits d'origine biologique ou géologique a été décrite par plusieurs auteurs.[15,18,19] Les méthodes employées étant relativement laborieuses, une séparation plus simple fut élaborée, basée sur l'extraction sélective du cuivre après irradiation. A cette fin des échantillons de sérum de 250 λ ou de 25 λ furent irradiés dans des capsules en polyéthylène pendant 24 hr à un flux de neutrons de $8 \cdot 10^{11}$ n/cm^2. sec. Simultanément, des échantillons-standard de cuivre de 5 à 10 mg furent irradiés dans des conditions identiques.

Les capsules furent ensuite minéralisées par voie humide et le cuivre extrait sélectivement par la 2:2′-diquinolyle (cuproïne) en solution isoamylique.[4,10]

Mode opératoire. Après ajoute de 2 ml d'une solution de $NH_2OH.HCl$ à 15 % au substrat minéralisé, neutralisation jusqu'à pH 3–7 à l'aide de NaOH, la solution est portée à 50 ml et extraite par 10 ml de réactif (0,02 % de cuproïne dans l'alcool isoamylique). Après centrifugation de la phase organique, l'activité de 4 ml est comparée à celle des standards en tenant compte des différents facteurs de dilution.

Le contrôle spectrophotométrique fut effectué à l'aide du même réactif sur des échantillons de sérum de 10 ml d'après la méthode de HOSTE *et al.*[4,10] Les résultats obtenus sont résumés dans le Tableau 4. Il apparait que la reproductibilité de la méthode par activation est du même ordre de grandeur que celle obtenue par spectrophotométrie (déviation moyenne ~ 1 %), les résultats absolus étant en moyenne supérieurs d'environ 3 %. Dans ces conditions il apparait également que la limite inférieure de la méthode n'est pas atteinte.

TABLEAU 4. Dosage du cuivre.
A. *Analyse par radioactivation*

Série no.	Éch. (λ)	Activité netto (c.p.m.)	Concentration (μg/%)	Concentration moyenne (μg/%)
1	250	4488	167	164,0 ± 0,8
	250	4327	161	Déviation
	250	4534	165	moyenne de
	250	4283	164	0,48 %
	250	4362	167	
	250	4183	160	
2	250	22044	172	165,0 ± 1,3
	250	20634	161	Déviation
	250	21659	169	moyenne de
	250	21263	165	0,78 %
	250	20618	160	
	250	20746	161	
3	25	2723	151	165,0 ± 3,2
	25	3209	178	Déviation
	25	2903	161	moyenne de
	25	2900	163	1,93 %
	25	2793	157	
	25	3220	181	

B. *Analyse spectrophotométrique*
Effectuée sur dix échantillons de 10 ml du même sérum, la concentration moyenne était de 158,8 ± 1,0 μg/%, ceci correspondant à une déviation moyenne de 0,63 %.

Le bruit de fond de nos compteurs étant de l'ordre de 300 c.p.m., il est possible de compter des activités du même ordre de grandeur. Ceci correspond à une quantité de cuivre de 0,005 à 0,01 μg.

L'influence de la réaction secondaire $Zn^{64}(n, p)Cu^{64}$ fut également examinée. A cet effet des échantillons de zinc contenant $2 \cdot 10^{-3}$ % de cuivre furent irradiés dans le flux central et dans la colonne thermique du réacteur.

Dans le second cas la teneur en cuivre du zinc, determinée par radioactivation, sera due exclusivement à la réaction (n, γ) tandis que l'irradiation dans le flux central donnera une teneur en cuivre apparante plus élevée, due aux réactions (n, γ) et (n, p) simultanées. L'expérience a montré que la teneur en cuivre obtenue dans le flux central n'était en moyenne supérieure que de 1 % à celle obtenue dans la colonne thermique. Il apparait donc qu'une proportion Zn/Cu de l'ordre de 50·000/1 ne cause qu'une erreur négligeable.

VOL. 10 1961

Dans le cas du sérum, cette proportion est de 1 et l'interférence due au zinc devient insignifiante.

(b). *Dosage du chrome par radioactivation*

A ce jour, aucune méthode de dosage du chrome dans des substrats biologiques par radioactivation, n'a été décrite.

Pour la détermination radiométrique de traces de chrome, des échantillons de sérum de 250 λ et des échantillons-standard de chrome (50 mg) furent irradiés pendant 3 jours à un flux de neutrons de $5 . 10^{11}$ $n/cm^2 . sec$. Après minéralisation par voie humide, le chrome fut séparé par distillation sous forme de chlorure de chromyle. Cette méthode permet en effet une séparation sélective et quantitative du chrome, comme l'ont démontré De Soete *et al.*[12]

Mode opératoire. Le substrat minéralisé est transféré dans le ballon à distillation (Fig. 1A) et l'eau est éloigné par distillation. On chauffe à 250° et on ajoute goutte à goutte 50 ml de HCl 11 N. As, Sb, Au et Hg qui distillent sous forme de chlorures, sont rejettés.

On remplace HCl par un mélange HCl (11N), HBr (66 %) 3:1 et on distille à une température de 250°C afin d'éliminer l'etain sous forme de bromure. On ajoute 30 ml de $HClO_4$ 70 %, le ballon à distillation est connecté au générateur de HCl (Fig. 1B) on chauffe à 300–350°C et on distille durant 30 min. Le chrome est receuilli sous forme de CrO_2Cl_2 dans 25 ml d'eau. On porte le distillat à un volume adéquat. L'activité de 4 ml de cette solution est comparée à celle d'un standard en tenant compte des facteurs de dilution. Les activites net obtenues n'étant que de l'ordre de 150 c.p.m.,

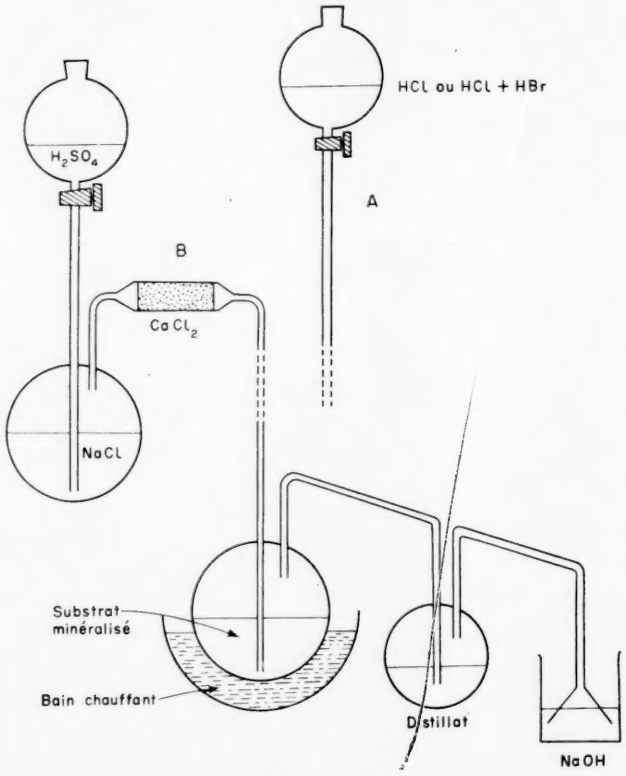

Fig. 1. Distillation du chrome.

les comptages des échantillons et du bruit de fond furent effectués durant 100 min. On obtient de cette façon une déviation moyenne de l'ordre de 2 %.

Le contrôle spectrophotométrique fut effectué à l'aide de la 1:5-diphénylcarbazide.[11] Les résultats obtenus sont résumés dans le Tableau 5. Il apparait que les analyses par radioactivation ont une reproductibilité correspondant à une déviation moyenne de 3 %, tandis que la spectrophotométrie permet d'atteindre une reproductibilité ayant une déviation de 0,5 %.

TABLEAU 5. Dosage du chrome
A. *Analyse par radioactivation*
(échantillons de 250 λ)

No.	Activité netto (c.p.m.)	Concentration (μg/%)	Concentration moyenne (μg/%)
1	163	24,6	20,8 $\pm$ 0,6
2	129	18,5	Déviation
3	131	20,0	moyenne de
4	172	21,4	2,88 %
5	169	20,1	
6	162	20,1	

B. *Analyse spectrophotométrique*
Effectuée sur dix échantillons de 10 ml du même sérum, la concentration moyenne était de 19,7 $\pm$ 0,1 μg/%, correspondant à une déviation moyenne de 0,50 %.

L'interférence possible de la réaction secondaire $Fe^{54}(n, \alpha)Cr^{51}$ fut également examiné. A cet effet des échantillons de fer exempt de chrome furent irradiés dans le flux central et dans la colonne thermique du réacteur. Après activation, le fer fut séparé par extraction à l'aide d'isoamylacétate en milieu HCl concentré.[5] Une double extraction en présence d'entraineur portant la concentration finale en fer à 1 mg/ml et en chrome à 0,2 mg/ml permet une séparation quantitative. Plusieurs séries d'expériences ont démontré que l'activité due au Cr^{51} n'est pas décelable dans les échantillons irradiés dans le flux central. La section efficace de la réaction $Fe^{54}(n, \alpha)Cr^{51}$ est donc négligeable.

(c). *Dosage du zinc par radioactivation*

Le dosage de traces de zinc dans les milieux biologiques fut effectué par BANKS *et al.*[2] ainsi que par BOWEN en 1959.[15] Il est proposé ici une méthode différente qui permet une séparation rapide du zinc.

Des échantillons de sérum de 250 λ et des standards de zinc de 50 mg furent soumis durant 3 jours à un flux de neutrons de 5. 10^{11} n/cm^2. sec. Après irradiation et ajoute de 10 mg de zinc comme ion entraineur, le substrat fut minéralisé par voie humide. Les ions des groupes I à III furent précipités par l'hydrogène sulfuré, tandis que le zinc fut extrait sélectivement de la solution par la méthyle-dioctylamine dans le xylol.[13,14] Après réextraction du zinc dans la phase aqueuse, il fut précipité sélectivement sous forme de $ZnHg(SCN)_4$, ce qui permit de calculer le rendement total de la séparation soit par gravimétrie, soit par titrimétrie.[20]

Mode opératoire. Le substrat minéralisé est neutralisé par NaOH 30 %. On ajoute 10 mg de Zn^{2+}, acidifie légèrement à l'aide de HNO_3 7 N et ajoute 10 mg des ions entraineurs suivants: Mn^{2+}, Fe^{3+}, Co^{2+}, Ni^{2+}, Cu^{2+} et Na^+.

On traite la solution par l'hydrogène sulfuré pendant 5 min, laisse reposer pendant 15 min et reprend le traitement par H_2S. On laisse reposer pendant 2 hr. Le précipité est rejetté tandis que le H_2S est élimine par ébullition. Après oxidation par quelque gouttes de H_2O_2 30 %, les hydroxydes insolubles sont précipités par l'ammoniaque gazeux. On centrifuge et on reprécipite après dissolution. Après centrifugation, la solution est évaporée à sec. On ajoute 10 ml de HCl 2 M et extrait par 20 ml de méthyle-dioctylamine dissoute dans le xylol (8 %). On extrait la phase organique par 10 ml de HCl 0,05 M. Le zinc est précipité dans la phase aqueuse en ajoutant 10 ml de $Hg(SCN)_2$ ($HgCl_2$, 27 g; HN_4SCN, 39 g; eau $\rightarrow$ 1000 ml). Le précipité de $ZnHg(SCN)_4$ est filtré, lavé et pesé ou titré. L'activité de l'échantillon est comparé avec celle d'échantillons-standard, compte tenu des facteurs de dilution et du rendement de la séparation. Le temps requis pour la séparation chimique est d'environ 3 hr. Les résultats sont repris dans le Tableau 6.

Le contrôle spectrophotométrique fut effectué à l'aide de la dithizone.[11]

Il apparait que la reproductibilité et la

VOL. 10 1961

TABLEAU 6. Dosage du zinc
A. *Analyse par radioactivation*
(échantillons de 250 λ)

No.	Poids du pp. (mg)	Rendement (%)	Facteur de correct.	Activité netto (c.p.m.)	Concentration (μg/%)	Concentration moyenne (μg/%)
1	46,59	61	1,64	3464	226,8	226,7 $\pm$ 2,3
2	44,29	58	1,72	3556	232,8	Déviation
3	31,31	41	2,44	3330	218,0	moyenne de
4	55,75	73	1,37	3249	212,8	1,0 %
5	48,88	64	1,56	3849	226,0	
6	51,17	67	1,49	4080	240,0	
7	39,71	52	1,92	3931	230,8	

B. *Analyse spectrophotométrique*
Effectuée sur dix échantillons de 10 ml du même sérum, la concentration moyenne était de 231,8 $\pm$ 1,3 μg/%, correspondant à une déviation moyenne de 0,58 %.

précision des résultats obtenus par radioactivation (déviation moyenne 1 %) sont comparables à ceux obtenus par spectrophotométrie (déviation moyenne 0,5 %).

(d). *Dosage du cobalt par radioactivation*

Le dosage de traces de cobalt par radioactivation fut décrit par SMALES *et al.*[18] qui effectuèrent la mesure de l'activité du Co^{60} (5,2 ans), tandis que KAISER et MEINKE[19] firent appel au Co^{60m} (10,5 min). Il fut jugé préférable d'employer l'isotope à longue vie (Co^{60}) et une méthode de séparation moins compliquée, basée sur l'extraction du complexe avec le β-nitroso-α-naphtol. Le contrôle spectrophotométrique fut effectué à l'aide du même réactif.

Il s'est avéré nécessaire, vu la longue demi-vie de l'isotope produit, d'irradier des échantillons de sérum de 250 λ et des standards d'oxyde de cobalt de 20 mg durant 8 jours à un flux de neutrons de $5 \cdot 10^{11}$ n/cm^2 . sec. Après 3 jours de refroidissement la minéralisation s'opèra par voie humide et le cobalt fut complexé au β-nitroso-α-naphtol et extrait au chloroforme.

Mode opératoire. Le résidue de la minéralisation est neutralisé par l'ammoniaque et ensuite légèrement acidifié par HNO_3 7 N. On ajoute successivement 10 ml de citrate de potasse (40 %), cinq gouttes de H_2O_2 (30 %) et 2 ml de réactif (1 % β-nitroso-α-naphtol dans l'acide acétique glacial. On ajoute 1 % de charbon activé et on filtre avant l'emploi) et laisse reposer durant 30 min. On extrait le complexe du cobalt en agitant successivement avec 25, 10 et 10 ml de chloroforme. Les extraits chloroformiques sont receuillés dans un ballon jaugé de 50 ml et dilués jusqu'au trait. L'activité de cette solution est comparée à celle d'échantillons-standard, compte rendu des facteurs de dilution.

Dans ces conditions le Hg(II) passe avec le cobalt dans la phase organique. Il ne gêne cependant pas le dosage, étant éliminé par volatilisation pendant la destruction préalable.

Les résultats des analyses par radioactivation et par spectrophotométrie sont représentés dans le Tableau 7. Il apparait que la

TABLEAU 7. Dosage du cobalt
A. *Analyse par radioactivation*
(échantillons de 250 λ)

No.	Activité netto (c.p.m.)	Concentration (μg/%)	Concentration moyenne (μg/%)
1	201	28,95	25,9 $\pm$ 0,5
2	188	27,10	Déviation
3	202	24,75	moyenne de
4	171	25,15	1,9 %
5	202	28,70	
6	185	26,24	
7	192	22,40	
8	202	23,85	

B. *Analyse spectrophotométrique*
Effectuée sur dix échantillons de 10 ml du même sérum, la concentration moyenne était de 27,3 $\pm$ 0,5 μg/%, correspondant à une déviation moyenne de 1,46 %.

précision des analyses par radioactivation (déviation moyenne de 1,9 %) est comparable à celle obtenue par spectrophotométrie (déviation moyenne de 1,5 %).

L'interférence éventuelle de la réaction gênante $Ni^{58}(n, p)Co^{58}$ fut également examinée. A cet effet une séparation Ni–Co fut effectuée après irradiation d'un échantillon de carbonate de nickel pur, exempt de cobalt.

Le nickel fut isolé par double précipitation par la diméthyle glyoxime, tandis que le cobalt fut précipité sous forme de CoS. L'échantillon étant examiné 2 jours après l'irradiation, aucune activité de nickel fut décelée. Il n'y a donc pas de formation d'isotopes de nickel à longue vie et le procédé de séparation proposé est efficace.

La fraction contenant le cobalt par contre était fortement radioactive, dû au Co^{58} qui fut identifié par spectrométrie-gamma. Il importe donc de tenir compte de cette interférence dans le cas de dosages de cobalt en présence de nickel. Il est néanmoins possible dans ces cas de compter sélectivement le Co^{60} à coté du Co^{58} en employant un discriminateur d'impulsions. Pour le cas du sérum, où le rapport Ni/Co est d'environ 0,1 la faute introduite par la réaction (n, p) reste de toute façon négligeable.

Ce travail fait partie du programme des recherches subsidiées par l'Institut Interuniversitaire des Sciences Nucléaires.

Remerciement—Les auteurs remercient Mme. Gorlee-Zels pour l'assistance technique au cours de ce travail.

VOL. 10 1961

BIBLIOGRAPHY

1. Pijck J., Gillis J. et Hoste J. *Meded. Kon. Vl. Akad.* **20,** No. 8 (1958).
2. Pijck J., Hoste J. et Gillis J. *Proceedings of the International Symposium on Microchemistry, Birmingham,* 1958, p. 48. Pergamon Press, London (1958).
3. Pijck J. Thèse Doctorat Sci. Pharm. Univ. Gand, Belgique (1959–1960).
4. Hoste J. *Verh. Kon. Vl. Akad.* **39,** 11 (1952).
5. Wells J. E. et Hunter D. P. *Analyst* **73,** 671 (1948).
6. Mellish C. E., Payne J. A. et Otlet R. E. *The Production of Threshold Reaction in a Graphite Reactor.* A.E.R.E.. Harwell (1957).
7. Gordon Ch. L. *Analyt. Chem.* **26,** 176 (1954).
8. Meinke W. W. *Analyt. Chem.* **28,** 736 (1956).
9. Meinke W. W. *Analyt. Chem.* **30,** 686 (1959).
10. Hoste J., Heiremans A. et Gillis J. *Mikrochim. Acta* **36–37,** 349 (1951).
11. Sandell E. B. *Colorimetric Determination of Traces of Metals.* (1950).
12. de Soete D., Hoste J. et Leliaert G. *Int. J. appl. Rad. Isotopes* **8,** 123 (1960)
13. Mahlman H. A., Leddicotte G. W. et Moon F. L. *Analyt. Chem.* **26,** 1939 (1954).
14. Morrison G. H. et Freiser H. *Solvent Extraction in Analytical Chemistry.* Wiley, N.Y. (1957).
15. Bowen H. J. M. *Int. J. appl. Rad. Isotopes* **4,** 214 (1959).
16. Gorsuch T. T. *Analyst* **84,** 135 (1959).
17. Costing M. *Meded. T.N.O.* 58-1 (1958).
18. Smales A. A., Mapper D. et Wood A. J. *Analyst* **82,** 75 (1957).
19. Kaiser D. G. *Progress Report No.* 8, Department of Chemistry, University of Michigan, p. 89 (1959).
20. Kolthoff I. M. et Belcher R. *Volumetric Analysis* Vol. 3. pp. 454–467. Interscience, N.Y (1957).
21. Banks T. E., Tupper R., White E. M. A. et Wormall A. *Int. J. appl. Rad. Isotopes* **4,** 221 (1958).

International Journal of Applied Radiation and Isotopes, 1961, Vol. 10, pp. 156–166. Pergamon Press Ltd. Printed in Northern Ireland

A Low-Background Laboratory

H. W. WILSON, D. E. WATT and D. RAMSDEN
Atomic Weapons Research Establishment, Aldermaston, Berks.

(*First received* 25 *July* 1960 *and in final form* 9 *September* 1960)

Consideration of the design, cost and construction of a low-background laboratory for the measurement of low specific activity samples leads to the choice of demineralized water as the main shielding material.

Background figures and spectra obtained for a range of proportional and scintillation counters in the completed laboratory, show that the shielding is slightly better than 12 in. of steel. It is deduced from energy and intensity measurements that the gamma-ray peaks occurring in the background spectrum arise mainly from ThC″ present in the counter construction materials.

UN LABORATOIRE A PETITE BASE RADIOACTIVE

La considération du dessin, du coût et de la construction d'un laboratoire ayant une petite base radioactive pour le dosage des échantillons de petite activité spécifique mène au choix de l'eau déminéralisée comme principal matériel de blindage.

Les chiffres de base et les spectres obtenus pour une rangée de compteurs proportionnels et à scintillement dans le laboratoire actuellement bâti indiquent que le blindage est légèrement supérieur à 12 in. (30 cm) d'acier. On déduit des mesures d'énergie et d'intensité que les maxima de rayons gamma qui paraissent dans le spectre de la base viennent pour la plupart du ThC″ qui se trouvent dans les matériaux de construction du compteur.

ЛАБОРАТОРИЯ С НИЗКИМ ФОНОМ РАДИОАКТИВНОСТИ

Рассмотрение схем монтажа, стоимости и устройства лаборатории с низким фоном, предназначенной для измерения образцов малой удельной активности, приводит к заключению, что наилучшим экранирующим материалом является деминерализованная вода.

Значения и спектры фона, полученные для ряда пропорциональных и сцинтилляционных счетчиков, показывают, что такое экранирование несколько более эффективно, чем экранирование сталью толщиной в 12 дюймов. Измерения энергии и интенсивности показывают, что максимумы в спектре гамма-лучей фона объясняются, главным образом, присутствием ThC″ в материалах, из которых изготовляются счетчики.

EIN LABORATORIUM MIT GERINGER HINTERGRUNDSTRAHLUNG

Überlegungen bezüglich Entwurf, Kosten und Konstruktion eines Labors mit geringer Hintergrundstrahlung für Messungen von Proben niederer spezifischer Aktivität, führen zu der Wahl von entmineralisiertem Wasser als hauptsächliches Abschirmungsmaterial.

Zahlenangaben über den Leerwert und über Spektren, welche mit Hilfe von Proportional- und Szintillationszählern im fertiggestellten Labor erhalten wurden, zeigen, dass diese Abschirmung etwas mehr leistet als 12 in. dicker Stahl. Aus Energie- und Intensitätsmessungen wurde geschlossen, das die im Spektrum der Hintergrundstrahlung aufscheinenden γ-Maxima hauptsächlich auf die Anwesenheit von ThC″ im Material der Zähler zurückzuführen sind.

1. INTRODUCTION

A LARGE number and variety of low-background proportional and scintillation counting equipments have been developed at the Atomic Weapons Research Establishment at Aldermaston over the past few years to provide assaying facilities for very low specific activity samples. The counters are usually accommodated in steel or lead shields

VOL.
10
1961

FIG. 1(a). Exterior view of the low background cell.

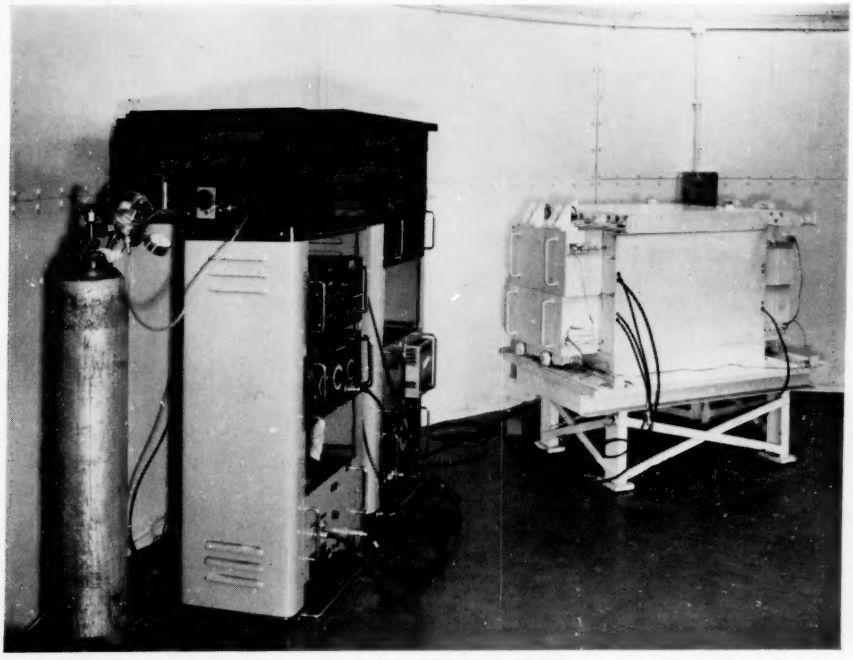

FIG. 1(b). Interior view of the steel cell. The electronic equipment and shielding are for temporary experiments and will be removed.

FIG. 2. The 12 ton steel door at the entrance to the steel cell.

VOL. 10 1961

assembled from 8 × 4 × 1 in. bricks. Each shield may occupy up to 20 sq. ft. of floor space, weigh several tons and take hours, or sometimes days, to build.

So much equipment proved to be necessary that it was decided to design and construct a special room or "low background cell" to provide the degree of shielding normally afforded by the best of the shields already in use. Such a cell has the following advantages.

(i) It is very convenient as the construction of shields is no longer necessary and experiments, especially those with large or complex counting systems, can be carried out with considerable saving in time and labour. Also, shielding bricks are expensive and always seem to be limited in number.

(ii) There is a considerable saving in floor area as conventional shields occupy more space than do the counters themselves.

(iii) Calibration sources can be more easily introduced although care must be taken in order not to affect counting rates in neighbouring systems.

(iv) Additional apparatus can be more easily brought up to the counter for special experiments.

In Section 2 there is a discussion of the various possible methods of construction followed by a description of the cell in its final form with an adjoining laboratory containing the electronic equipment associated with the counters. Experimental results on the performance of the cell compared with that of ordinary shields are given in the third section of the paper.

2. THE DESIGN OF THE LABORATORY

It was decided that the cell should contain only counters plus associated head amplifiers or cathode followers, the rest of the electronic equipment being accommodated in a separate laboratory. Two reasons for this were that the cost of a given floor area of the cell was considerably higher than that of an ordinary laboratory, and that all possible but unnecessary sources of contamination should be absent.

The first decision to be made was whether the cell should be on or below ground level. If underground, the cell would have to be fairly deep to obtain any advantage, and several inches of heavy shielding to reduce gamma background from the surroundings would still be necessary. This idea was too expensive, as there was no tunnel or mine available in the vicinity of the Establishment which could have conveniently been used for this purpose. A surface laboratory was thus the only real possibility. The following equivalent constructions were possible, each being the equivalent of 1 ft of steel for 1 MeV gamma radiation.

(i) Room with walls, floor and roof made of 1 foot of steel.

(ii) The equivalent of 1 ft of steel in the form of swarf or compressed scrap steel contained between thin steel walls.

(iii) Three feet of concrete lined with 3 in. of steel.

(iv) Two feet of barytes loaded concrete lined with 3 in. of steel.

(v) Six feet of water, preferably demineralized, contained between the walls of an inner and an outer steel tank.

In cases (iii) and (iv), the steel is present to reduce radiations arising from the concrete itself. It turned out that suggestion (i) was the most expensive and (ii) and (v) were the cheapest.

A compromise construction between (i), (ii) and (v) was chosen in that the walls and roof are shielded by demineralized water, the floor by 3 ft of concrete covered by 3 in. of steel whilst the door is made of 1 ft thick steel.

It proved simpler to construct a circular room 18 ft in diameter rather than a rectangular room. This is surrounded by an outer shell which permits 6 ft water shielding round the sides and 7 ft on top (Fig. 1). The door is of a bank safe type. Its dimensions are $7\frac{1}{2} \times 6\frac{1}{2}$ ft outside and $7 \times 5\frac{3}{4}$ ft inside; the gap between the sides and top of the door and of the frame is stepped to eliminate a direct path for radiation (Fig. 2). The floor below the door is not stepped in this way as it would have proved awkward to move

equipment in and out of the cell. Instead a steel barrier, just behind the door and normally flush with the floor, is raised automatically as the door is closed to seal this gap. The door can be operated either from inside or from outside the tank. As an extra safeguard, there is an emergency bell which can be operated from within the cell.

conditioning purposes but these have not yet proved necessary.

The cell was built at a total cost of some £20,000. This cost includes all services and air conditioning.

There was much discussion as to the advisability of bleeding in air which was "dead" (in a radioactive sense). This

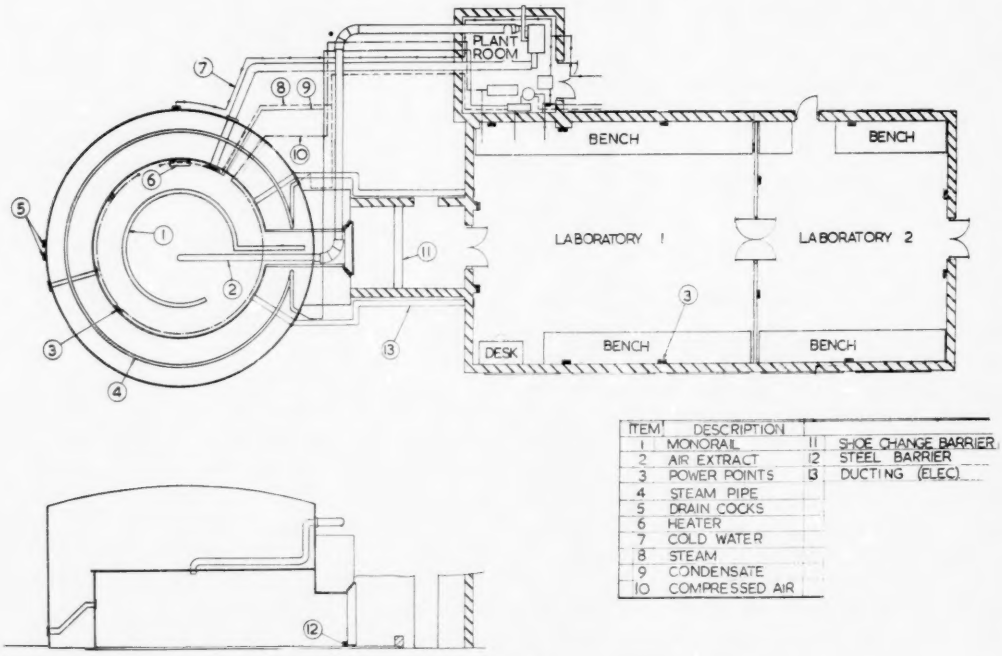

FIG. 3. Plan of low background cell and associated laboratory.

A principle which was applied in the construction was to exclude rigorously any possible path which did not pass through at least 1 ft of steel or its equivalent. Thus the passage between the door and the cell was provided with extra steel and concrete shielding as can be seen by a study of Fig. 3. Also all pipes leading into the cell through the water tank are S-shaped. Two of the pipes are permanently fitted with boards each containing twenty-five mixed single and multicore plugs which provide connexions from the electronics in the ordinary laboratory to the counters and probe units in the cell. Another two pipes are provided for air

discussion arose from the expectation of appreciable activity due to 1·8 hr A^{41} in the atmosphere arising from the operation of the Aldermaston research reactor, "Herald". Fortunately, the design of the reactor was changed in such a way that the A^{41} will no longer escape into the atmosphere.

The water in the tank is taken from Aldermaston supplies, is demineralized and treated with 1 p.p.m. of algaestat (2:3-dichloro-1:4-naphthaquinone) to prevent the growth of fungi. Heat to the water can be supplied by a steam coil fitted inside the tank to prevent possible freezing in winter and to reduce condensation inside the cell. Those

surfaces of the tank in contact with water were treated with bituminous paint which is made with an English coal tar base to ensure the absence of uranium-bearing material. The presence of such a large volume of water (60,000 gal) has not escaped the attention of the site fire brigade and the tank is fitted with two drain pipes and unions to take standard fire hoses.

All paints used in or about the tank were tested for activity by examining samples with a scintillation counter. In the case of cellulose and other carbon-containing paints, only those made from "dead" carbon were used, as the C-14 Bremsstrahlung from a large amount of paint could seriously affect the background.

The cell is shown diagrammatically in Fig. 3, a photograph of the interior in Fig. 1(b) and a photograph of the door in Fig. 2. The laboratory is conventional in design and was converted from an existing building 60 × 30 ft wide, divided into two rooms, 24 × 30 ft and 36 × 30 ft, the latter being next to the cell. Each room has the usual laboratory services, viz. electricity, gas, water, compressed air and cooling water. The layout is included in Fig. 3.

VOL. 10 1961

3. BACKGROUND EXPERIMENTS

Extensive trials followed the completion of the laboratory. The background and the background spectrum shape was examined for a variety of proportional and scintillation detectors operated in the tank and in the laboratory, with various combinations of shield and anti-coincidence counting techniques. A description of these experiments follows.

(a) *Scintillation counting*

Two scintillation counters were available for the background experiments. These were (i) a $2\frac{1}{2} \times 2\frac{1}{2}$ in. cylindrical well-type NaI crystal encapsulated in aluminium and mounted on a Dumont photomultiplier type 6363 and (ii) a 3 × 3 in. cylindrical well-type NaI crystal encapsulated in electrolytic copper and mounted on an EMI photomultiplier type 9531/0.

The background above 30 keV was measured for each crystal under various conditions of shielding in the ordinary brick laboratory and in the low background cell. The results are listed in Table 1 in which the errors represent the standard deviations of the count rate.

TABLE 1

Crystal position	Shielding	3 × 3 in. copper crystal	$2\frac{1}{2} \times 2\frac{1}{2}$ in. aluminium crystal
		Background (c.p.m.)	Background (c.p.m.)
Brick laboratory	None	13,240 ± 46	10,450 ± 2·6
Brick laboratory	8 in. steel		597 ± 2·0
Brick laboratory	12 in. steel	432 ± 3	349 ± 3·0
Brick laboratory	8 in. steel		302 ± 1·1
Tank (floor position)	None	482 ± 4	395 ± 1·2
Tank (4 ft from floor)	None		370 ± 5·0
Tank (4 ft from floor)	2 in. steel (below only)		363 ± 1·9
Tank	9 in. steel (below only)	398 ± 3·6	326 ± 3·3
Tank	8 in. steel	361 ± 2·7	284 ± 2·9
Tank (floor position)	Without water shielding		1433 ± 3·2

In order to obtain more detailed information on the nature of the crystal background, such as, for example, what fraction arises from radioactive contaminants in the crystal, photomultipliers, etc., and surroundings, the smaller crystal background spectrum in the energy range 30 keV to 8·0 MeV was examined for various shielding conditions in the laboratory, and in the steel tank. Typical spectra are shown in Fig. 4.

Seven gamma-ray peaks occur in the background spectrum at the following energies: 0·51, 0·58, 1·2, 1·45, 2·1, 2·6 and 3·2 MeV.

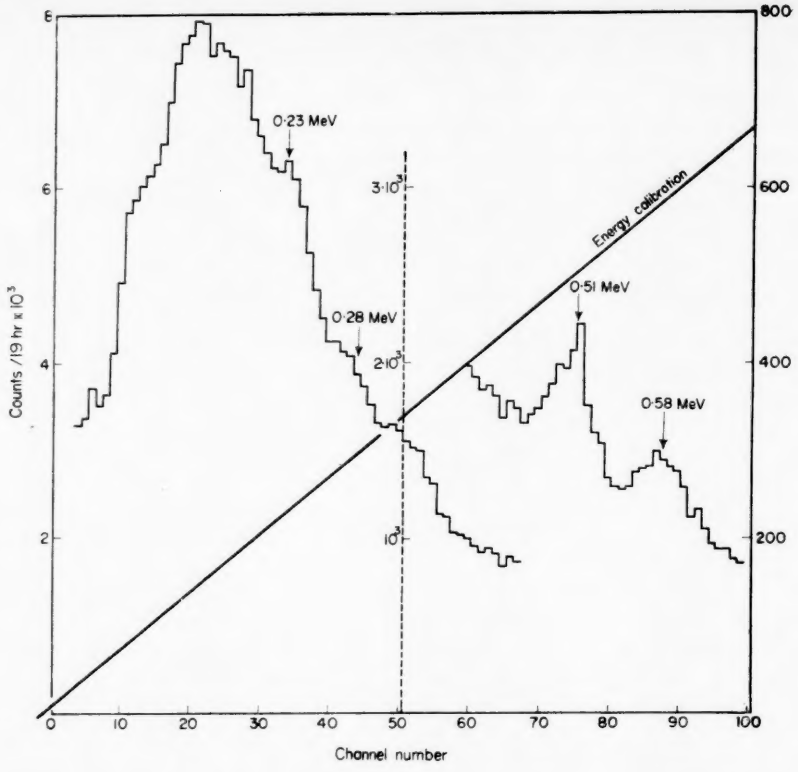

FIG. 4(a)

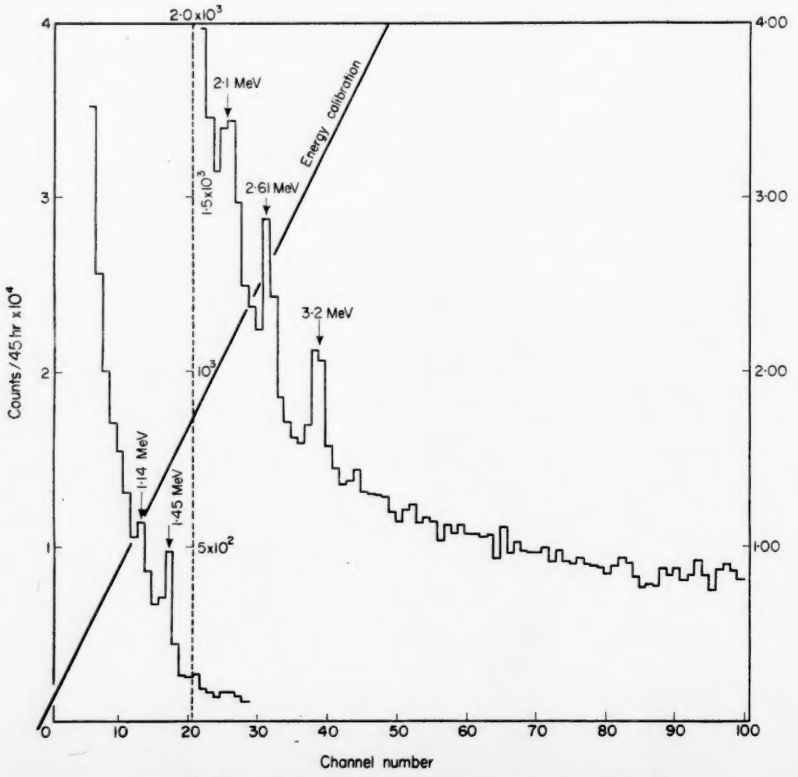

FIG. 4(b)

FIG. 4(a, b). Crystal background spectrum in the steel cell.

VOL. 10 1961

The intensities of the 0·51, 0·58, 1·2, 2·1, 2·6 and 3·2 MeV peaks remain at a constant value with added shielding inside the special tank. In the brick laboratory the intensities of these peaks are reduced considerably with shielding until a constant value equal to that found in the tank is attained. Consequently we deduce that the source of this gamma radiation is present to a large extent in the brick laboratory rather than in the cell, there being a residual effect in the crystal and its immediate attachments (viz. phototube and base, electronic components and the holder for the assembly).

ThC″(Tl^{208}) in equilibrium amounts can account for the presence of these gamma rays. The only other isotopes which could give rise to high-energy gamma rays of 2·6 and 3·2 MeV are short-lived fission products which would be identifiable by their decay. The peaks in the background spectrum do not decay appreciably in 6 weeks. The 3·2 MeV peak is attributed to the summation of 0·58 and 2·61 MeV gamma rays in ThC″. The 2·61 MeV peak is from the same source and gives rise to the 0·51 MeV annihilation line by pair production and the escape peak at 2·1 MeV.[1] May[2] has observed the 3·2 MeV peak and suggests this may be due to alpha particles. This is considered unlikely since the resolution of the peak is that expected for the 3·2 MeV gamma-ray summation peak already mentioned, and since there exists a 3·2 MeV level in ThC″. In addition, the ratio of the intensities of the 0·51, 0·58, 2·6 and 3·2 MeV peaks is constant within statistics, suggesting that these are gamma rays associated with one another and which arise from ThC″.

Since ThC″ is a beta emitter and the gamma rays are in coincidence with the beta rays, some of the contamination must subtend less than 4π solid angle at the crystal otherwise sharp peaks would not be observed because of the crystal integrating effect. These facts, taken together, indicate that ThC″ must be present in the immediate surroundings of the crystal and inside the shielding. The contributions to background arising from the $2\frac{1}{2} \times 2\frac{1}{2}$ in. crystal, the phototube and the phototube base including the resistor chain were determined by placing these in turn near another NaI crystal ($2 \times 1\frac{3}{4}$ in.) spectrometer, the background of which, above 30 keV, was 110 ± 1 c.p.m. It was found that these increased the background by $8{\cdot}0 \pm 0{\cdot}5$, $12{\cdot}0 \pm 0{\cdot}2$ and $8{\cdot}1 \pm 0{\cdot}2$ c.p.m. respectively.

The relatively high background of the $2\frac{1}{2} \times 2\frac{1}{2}$ in. aluminium canned crystal can only be explained, therefore, by assuming that the $8{\cdot}0 \pm 0{\cdot}5$ c.p.m. arise from impurity present in the actual crystal where the integrating effect will give a much larger contribution to the background of that crystal. It has not yet proved possible to identify the source of this background.

The 1·45 MeV peak is attributed to K^{40}. If this is assumed to be wholly inside the crystal then it will contribute 270 counts to the background. This is a much higher value than would be expected as the suppliers claim that the potassium content of their crystal is less than 2 p.p.m. It appears therefore that most of the potassium must be external to the actual crystal. The 1·2 MeV peak is due to Compton electrons arising from the K^{40} gamma ray.

(b) *Background measurements with proportional counters*

Because of the large residual background activity in the sodium iodide crystals, it is difficult to make an accurate comparison between the shielding properties of the special laboratory and an equivalent shield in the brick laboratory. Experiments were therefore carried out with gas-filled proportional counters for two reasons: (i) since these counters have low gamma-ray detection efficiency and are 100 per cent efficient for particle detection, direct comparison of the particle contribution to the backgrounds of the tank and the laboratory for different shielding conditions can be made; (ii) these counters normally are much less sensitive to natural contamination and are therefore capable of revealing more accurately the performance of the actual shielding.

Two types of counters were used: (i) a cylindrical brass counter 4 in. in diameter with a 0·002 in. tungsten wire anode and of

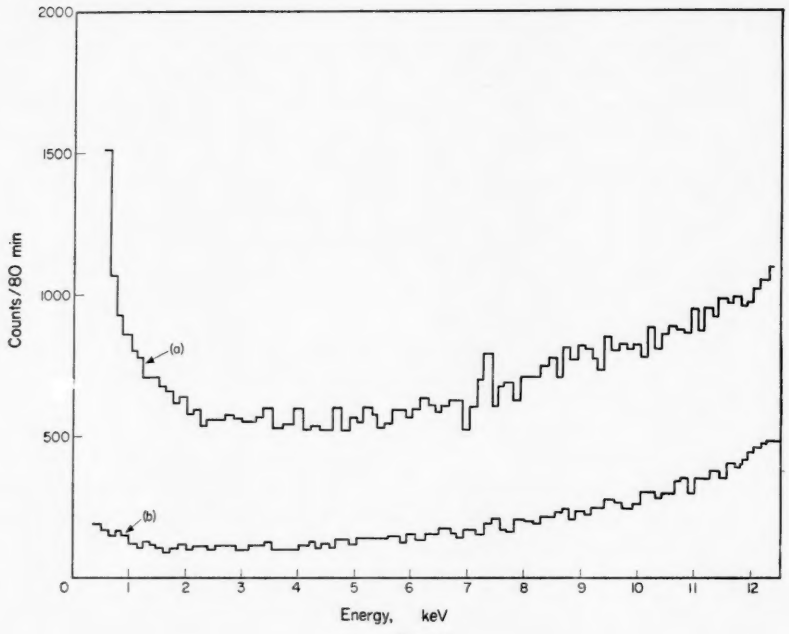

FIG. 5.

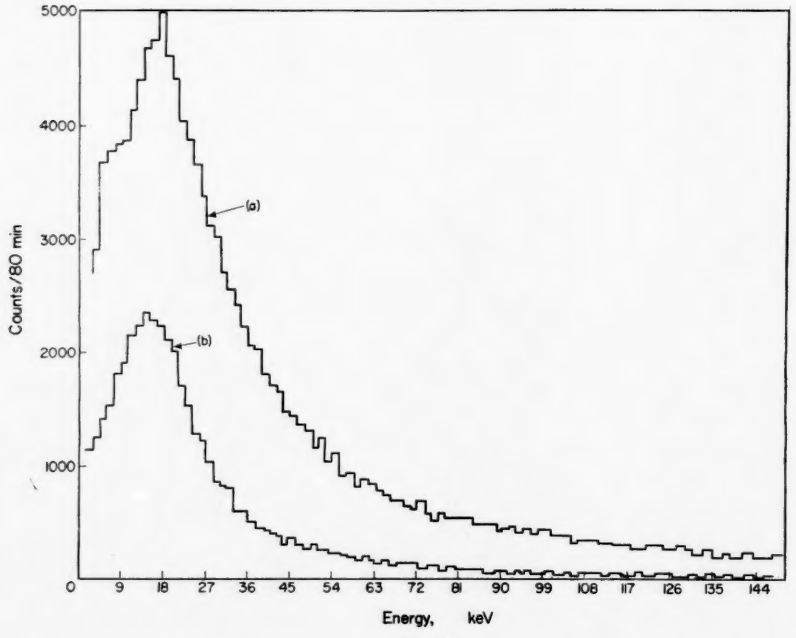

FIG. 6.

FIGS. 5 and 6. Proportional counter background spectra. (a) Spectrum in ordinary laboratory. (b) Spectrum in the low background cell.

TABLE 2. Five-litre brass proportional counter

Counter position	Shielding	Background (c.p.m.)
Brick laboratory	None	1564 ± 12
Brick laboratory	8 in. Fe	589·9 ± 3
Brick laboratory	8 in. Fe + Geiger ring in anti-coincidence	39·6 ± 0·5
Tank (floor position)	None	546 ± 2
Tank (4 ft from floor)	None	520 ± 2
	8 in. Fe	488·9 ± 2
	8 in. Fe + Geigers in a.c.	30·9 ± 0·5

TABLE 3. Multi-wire counter

(*a*) *With polystyrene wall and anti-coincidence ring operating*

Position	Shielding	Background
Brick laboratory	None	48·0 ± 1·2
Brick laboratory	12 in. Fe	5·31 ± 0·07
Tank (floor position	None	4·24 ± 0·06
Tank	8 in. Fe	3·23 ± 0·05

(*b*) *Without wall but with anti-coincidence ring operating*

Position	Shielding	Background
Brick laboratory	None	47·8 ± 1·5
	12 in. Fe	1·98 ± 0·04
Tank (floor position)	None	1·78 ± 0·04
	8 in. Fe	1·68 ± 0·03

5 l. counting volume, (this counter being filled to 760 mm Hg pressure with argon and 10 per cent methane); (ii) a wall-less type counter[3] with built-in anti-coincidence counters. This counter has 1·05 l. counting volume and can be operated either with or without a 0·005 in. polystyrene wall inserted between the anti-coincidence counters and the counting volume: it has the advantage that when operated without the wall it is virtually independent of any contamination of the construction materials and is capable of making very accurate measurements of cosmic-ray background changes.

Table 2 gives background figures for the 5 l. brass proportional counter in the brick laboratory without shielding, with 8 in. mild steel shielding and with 8 in. mild steel shielding plus a ring of Geiger counters operated in anti-coincidence. Similar results are given for inside the tank. These background results were obtained by operating on the flat part of the counter plateau and counting all energies greater than 200 eV.

Figures 5 and 6 show the background spectrum in the energy range 500 eV to 100 keV for the counter unshielded in the brick laboratory (a) and inside the tank (b). The broad peak observed in the spectrum at 9–12 keV is caused by high-energy particles, e.g. μ mesons, electrons or protons, passing through the counter and spending an average energy which is dependent on the dimensions of the counter and the gas pressure.

Table 3 contains the results for the multi-wire counter under its two operating conditions, i.e. with and without the polystyrene wall. It is clear that the tank is a definitely better shield than 12 in. of steel in the laboratory. The presence of the polystyrene wall increases the background as soft gamma rays can traverse the anti-coincidence ring undetected and convert in the wall to produce electrons which count in the main counter.

4. DISCUSSION AND CONCLUSIONS

To compare the shielding effect of the steel cell for a scintillation counter with an equivalent shield in the ordinary laboratory, it should be noted that there is only a 3 in. layer of steel above the concrete on the cell floor. Consequently, by placing an additional 9 in. of steel on the cell floor, the background obtained should be directly comparable with a 12 in. steel shield in the laboratory which also has a concrete floor. The result shows that the cell is slightly more efficient than theoretically expected.

Additional shielding inside the steel cell further reduces the continuous background spectrum whilst the contamination peaks remain at constant intensity. As it is assumed

VOL. 10 1961

that contamination from the constructional materials of the cell would give defined peaks and, also, would not give a spectrum beyond 4 MeV, it is deduced (i) that the continuous spectrum is due to cosmic rays and is being absorbed by the additional shielding and (ii) that the local contamination arises largely from the crystal and its accessories and not from the constructional materials of the cell.

Measurements show that the background contribution from the photomultiplier and tube base is small compared with the contributions from impurities in the actual crystal material, because of the greatly increased geometry for detecting the latter.

In general, the results show that the low-background laboratory is a better shield than 12 in. of local steel shielding in the brick laboratory for the gas proportional counters and is equivalent for the case of the scintillation counter.

Acknowledgments—We wish to thank the Director of the United Kingdom Atomic Energy Authority, Aldermaston, for permission to publish this paper. We also wish to acknowledge the part played in the design and construction of the cell by the engineering staff at Aldermaston, particularly, Mr. R. L. Bennetts and Mr. A. Osbaldeston.

REFERENCES

1. Heath R. L. Atomic Energy Commission Research and Development Report No. IDO-16408, 15 July (1957).
2. May H. A. Argonne National Laboratory Report No. 5919 p. 88 (1958).
3. Drever R. W. P., Moljk A. and Curran S. C. *Nucl. Inst.* **1,** 41 (1957).

International Journal of Applied Radiation and Isotopes, 1961, Vol. 10, pp. 167–176. Pergamon Press Ltd. Printed in Northern Ireland

The Radiotracer Testing Method in Metal Cleaning Studies

G. D. FATZER, J. M. SCHROEER and B. E. BLAKE
IBM General Products Division, Development Laboratory, Endicott, N.Y., U.S.A.

(*First received* 30 *September* 1960 *and in revised form* 15 *November* 1960)

VOL. 10 1961

A pre-requisite for obtaining reproducible results from friction, wear and resistance studies of rubbing surfaces is reproducible cleanliness of the metallic samples. This paper describes radiotracer studies for testing the effectiveness of several cleaning techniques. The contamination of metallic surfaces with sulfates, chromates and fatty acids was investigated. The detection sensitivities for $S^{35}O_4^=$, Cr^{51}, palmitic and stearic-1-C^{14} acids were respectively 3×10^{-8} g, $1{\cdot}5 \times 10^{-7}$ g, $3{\cdot}2 \times 10^{-9}$ g and $6{\cdot}2 \times 10^{-10}$ g. Results show that electropolished copper surfaces retained less than 3×10^{-8} g $SO_4^=$ and less than $1{\cdot}5 \times 10^{-7}$ g of Cr.

Toluene and chromic acid were found to be excellent cleaning agents for fatty acids. The quantity of fatty acid remaining on copper substrates after three successive immersions in toluene averaged 0·01 to 1 monolayer depending on the amount of the contaminant originally present. Less than 3×10^{-9} g of palmitic acid, i.e. $1{\cdot}6 \times 10^{-2}$ monolayer, or 6×10^{-10} g of stearic acid, i.e. 3×10^{-3} monolayer, remained on gold and copper surfaces after anodic polishing in chromic acid at 120°C for 2 min.

LA MÉTHODE D'ESSAI UTILISANT LES CORPS MARQUÉS DE RADIO-ISOTOPES POUR ETUDIER LE NETTOYAGE DES MÉTAUX

Pour obtenir des résultats reproductibles des études sur le frottement, l'érosion et la résistance des surfaces frottantes, une condition préalable est la propreté reproductible des échantillons métalliques. Cette communication décrit des études avec des corps marqués pour essayer l'efficacité de plusieurs techniques de nettoyage. On examina la contamination des surfaces métalliques avec des sulfates, des chromates et des acides gras. Les sensibilités de détection pour le $S^{35}O_4^=$, le Cr^{51}, les acides palmitique et stéarique-1-C^{14} furent 3×10^{-8} g., $1{,}5 \times 10^{-7}$ g., $3{,}2 \times 10^{-9}$ g. et $6{,}2 \times 10^{-10}$ g. Les résultats indiquent que les surfaces de cuivre polies électrolytiquement moins de 3×10^{-8} g. de $SO_4^=$ et moins de $1{,}5 \times 10^{-7}$ g. de Cr.

La toluène et l'acide chromique se trouvèrent excellents comme agents détersifs pour les acides gras. La quantité d'acide gras restant sur les couches inférieures du cuivre après trois immersions de suite dans la toluène moyenna 0,01 à 1 monocouche selon la quantité du contaminant présent au début. Moins de 3×10^{-9} g. d'acide palmitique, soit $1{,}6 \times 10^{-2}$ monocouche, ou 6×10^{-10} g. d'acide stéarique, soit 3×10^{-3} monocouche, restait sur des surfaces d'or et de cuivre après le polissage anodique dans l'acide chromique à 120°C pour 2 min.

ПРИМЕНЕНИЕ РАДИОАКТИВНЫХ ИНДИКАТОРОВ ПРИ ИССЛЕДОВАНИИ ЧИСТОТЫ МЕТАЛЛОВ

Воспроизводимая степень чистоты образцов металлов является обязательным требованием для получения воспроизводимых результатов при испытании на трение, износ и сопротивление трущихся поверхностей. В данной статье описано применение радиоактивных индикаторов для проверки эффективности некоторых методов очистки. Было исследовано загрязнение металлических поверхностей сульфатами, хроматами и жирными кислотами. В случае $S^{35}O_4^=$, Cr^{51}, пальмитиновой и стеариновой кислот чувствительность определения была, соответственно, 3.10^{-8} г., $1{,}5.10^{-7}$ г, $3{,}2.10^{-9}$ г и $6{,}2.10^{-10}$ г. Полученные данные показывают, что при электрополировке медные поверхности удерживают менее 3.10^{-8} г $SO_4^=$ и менее $1{,}5.10^{-7}$ г Cr.

Было найдено, что толуол и хромовая кислота прекрасно отчищают жирные кислоты. Количество жирной кислоты, остающейся на медных подложках после трех последов ательных погружений в толуол, составляло в среднем 0,01–1 монослой, в зависимости от количества первоначальной примеси. Золотые и медные поверхности, подвергнутые анодной полировке в хромовой кислоте в течение 2 мин. при 120 C°, удерживают менее 3.10^{-9} г пальмитиновой кислоты, т.е. $1{,}6.10^{-2}$ монослоя, или 6.10^{-10} г стеариновой кислоты, т.е. 3.10^{-3} монослоя.

RADIOINDIKATOREN-PRÜFMETHODE BEI UNTERSUCHUNGEN ÜBER METALLREINIGUNG

Die Vorbedingungen zur Erreichung reproduzierbarer Resultate bei Untersuchungen über Reibung, Abnützung und Widerstand bei reibenden Oberflächen ist die reproduzierbare Reinheit der metallischen Proben. Die vorliegende Arbeit beschreibt Untersuchungen mittels Radioindikatoren zur Prüfung der Wirksamkeit mehrerer Reinigungsverfahren. Die Verseuchung der metallischen Oberfläche mit Sulphaten, Chromaten und Fettsäuren wurde untersucht. Die Nachweisempfindlichkeit für $S^{35}O_4^=$, Cr^{51}, Palmitin- und Stearin-1-C^{14} Säuren betrug 3.10^{-8} g, $1{,}5 . 10^{-7}$ g, $3{,}2 . 10^{-9}$ g bzw. $6{,}2 . 10^{-10}$ g. Die Resultate zeigen, dass polierte Kupferoberflächen weniger als $3 . 10^{-8}$ g $SO_4^=$ und weniger als $1{,}5 . 10^{-7}$ g Cr zurückhält.

Toluol und Chrom-Schwefelsäure erwiesen sich als ausgezeichnete Reinigungsmittel für Fettsäuren. Die auf dem Kupfer verbleibende Fettsäuremenge nach drei aufeinander folgenden Bädern in Toluol betrug im Mittel 0,01 bis 1 monomolekulare Schichte in Abhängigkeit von der ursprünglich vorhandenen Menge, weniger als $3 . 10^{-9}$ g Palmitinsäure, d.h. $1{,}6 . 10^{-2}$ Monoschichten und $6 . 10^{-10}$ g Stearinsäure bzw. $3 . 10^{-3}$ Monoschichten verbleiben auf Gold- und Kupferoberflächen nach Polieren in Chrom-Schwefelsäure bei 120°C in 2 Minuten.

1. INTRODUCTION

Understanding the behavior of rubbing metals requires a thorough knowledge of the surface condition, primarily of contaminant surface films. Such films will tend to separate the surfaces so that a portion of the normal load will be borne by the intermediate surface contaminant. This contaminant layer can drastically alter the area of the contact and thus the friction, contact resistance and wear.

This paper describes experiments on the removal efficiency of certain lubricants from copper and gold metallic samples, in support of wear studies on gold and gold alloys. It is felt that under the experimental conditions of these wear studies the most probable lubricating compounds which could hinder reproducible wear data are inorganic residues (resulting from sample cleaning with various etching techniques) and fatty acids (resulting from the handling of the wear samples). The removal of these contaminant films by some cleaning process is desirable in rubbing surface studies. Radioisotopes are highly useful tools for testing the effectiveness of various cleaning methods used to prepare metallic samples. The extreme sensitivity attainable by radiotracer technique, often as low as 10^{-10} g, makes this method invaluable. Previous radiotracer work on metal cleaning effectiveness has been done by Harris *et al.*,[1,2] Hensley *et al.*,[3] Hensley,[4] Slater and Donahue.[5] These authors provided profitable insights and information on the various techniques.

Depending on the desired sensitivity, metal and glass cleaning techniques may be evaluated by one or all of the following three non-destructive methods: (1) the water break test; (2) the atomizer test; (3) radiotracer technique.

The first two methods rely on the property of hydrophobic layers to break up a thin water film. The contact angle of the water film will then indicate the cleanliness of the metallic sample. Both of these methods are fairly sensitive to organic contaminants. According to Feder and Koontz,[6] the water break test will detect contaminants in amounts of one or more monolayers while

the atomizer test is sensitive to a fraction of a monolayer.

The third method, the radiotracer technique, provides valuable information on the presence of both hydrophobic and hydrophylic contaminants. A sample is contaminated with a radioactive soil, and, after cleaning, the amount of residual contaminant is determined by measuring, with an appropriate device, the radioactivity level of the sample. The detection sensitivity of the radiotracer technique depends on the following factors: (1) specific activity of the radioactive contaminants; (2) measuring device; (3) type and energy of emitted radiation.

Considering the inherent advantages in the radiotracer technique, this method was investigated and the results compared with those obtained by the water break and/or atomizer test, which are available in previous publications.

VOL. 10 1961

2. EXPERIMENTAL CONSIDERATIONS

Our main interest was the preparation of 24 carat gold, solid or electroplated, wear samples. The standard cleaning technique for wear-sample preparation used by BLAKE and FATZER[7] consisted of (1) an anodic electroclean at high temperature in chromic acid, (2) a tap-water rinse, (3) a dip in KCN, (4) a boiling distilled-water rinse. The use of this cleaning technique posed two questions concerning (a) the possible contamination of the wear samples with inorganic material such as sulfate, dichromate or chromate ions, and (b) the efficiency of the method in removing organic material.

Concerning the first question, it must first be mentioned that solid or electroplated gold generally contains several base metal impurities. It thus becomes imperative to know the influence of these impurities on the cleanability and chemical properties (corrosion resistance) of solid gold wear members. This is investigated by studying bulk copper.

According to SIMNAD,[8] chromium, in chromate solutions, will exchange with metals such as silver, platinum, copper and nickel. Part of the initial metal goes into solution while chromium ions are reduced to elementary chromium. The factors governing this exchange are the local distribution of anodes and cathodes on the metal surface, the influence of oxygen and the relative positions of the exchange materials in the e.m.f. series. According to EISLER,[9] free sulfate ions are occluded in chromium coatings deposited from a chromic solution.

Sulfate and chromate and/or dichromate ions, coming from chromic acid and left on copper after cleaning, react with copper to form copper chromate and, copper sulfate. These various compounds may have lubricating properties and thus influence wear results; moreover, absorbed sulfate ions could initiate corrosion.

Thus, according to previous work, large chromium contamination can result on copper from exchange reaction in chromate solution. Secondly a chromic acid bath, may deposit adsorbed sulfate ions. The case of chromate and sulfate contamination of copper anodes is investigated in this work.

The effectiveness of organic material removal depends on the ability of the cleaning solutions to oxidize, saponify or dissolve the organic contaminant.

3. EXPERIMENTAL CONDITIONS

A. *Surface preparation*

In the two sets of experiments mentioned, precleaned and uncleaned gold (24 carat) and high conductivity oxygen-free copper samples were used. The copper samples ($1{\cdot}5 \times 2$ cm) were precleaned by an acid etch. This treatment gave a smooth bright surface on the copper samples.

The gold samples ($1{\cdot}5 \times 1{\cdot}5$ cm) were precleaned by anodic oxidation at high

current densities in chromic acid. Photomicrographs of the gold and copper surface are shown in Fig. 1.

All precleaned samples were cleaned to withstand the water break test. The radioactive contaminant was applied to the dry surface.

B. *Radioisotopes*

The cleaning bath, defined as the standard cleaning solution, was prepared by dissolving 100 g/l. of $K_2Cr_2O_7$ in 1 ÷ 1 sulfuric acid. The possible anionic contaminants were $SO_4^=$, $Cr_2O_7^=$ and their presence was tested by using S^{35}-tagged sulfuric acid and Cr^{51}-tagged sodium chromate.

Both polar and non-polar organic contaminants act as lubricants. However, only polar compounds were investigated and discussed in this paper. This category of compounds includes fatty acids, amines, etc. Carbon^{14}-tagged fatty acids are commercially available and these studies were carried out with palmitic, CH_3-$(CH_2)_{14}$-COOH, stearic CH_3-$(CH_2)_{16}$-COOH and oleic C^{14}-tagged acids.

C. *Radioactivity measurements*

The pure beta emitters (C^{14} and S^{35}) were detected and measured by liquid scintillation methods.

Chromium-51, both a gamma and X-ray emitter with energies of 320 keV (8%) and 5 keV (92%), was assayed by means of a scintillation spectrometer using a NaI (Tl) crystal.

The ultimate detection sensitivities were $1{\cdot}5 \times 10^{-7}$ g for chromium, 3×10^{-8} g for $SO_4^=$, and respectively 3×10^{-9} g and $6{\cdot}2 \times 10^{-10}$ g for palmitic and stearic acids.

4. DATA AND RESULTS

Two problems have been investigated and will be discussed: inorganic contamination of metallic surfaces due to cleaning solutions; efficiency of the cleaning solution for removal of polar organic contaminants.

A. *Inorganic contamination of metallic surfaces*

(1) *Chromium contamination.* Precleaned and uncleaned copper samples were cleaned in Cr^{51}-tagged chromic acid at 120°C for periods of 2 min. Some samples were cleaned by a simple dip in the acid. Others were etched by an anodic electropolish (50 mA/cm^2).

Because of limited sensitivity it can only be said that not more than $1{\cdot}5 \times 10^{-7}$ g of chromium was found on the copper surfaces following the standard cleaning procedure. This figure is valid both with and without current during etching.

It is interesting to note that SIMNAD[8] mentions the figures of $2{\cdot}3 \times 10^{-6}$ g and $6{\cdot}65 \times 10^{-6}$ g for annealed and etched copper in his exchange reaction in chromate solutions. However, SIMNAD's experiment time was 1 hr, compared to a time of two minutes for the above-mentioned experiments.

The techniques used in this experiment could be refined, if necessary, to obtain greater sensitivity by using greater Cr^{51} specific activity.

(2) *Sulfate contamination.* The influence of current (0·15–0·75 A/cm^2) and surface state (polished or etched samples) on the possible sulfate contamination of copper substrates was investigated using the complete standard cleaning procedure. Results are shown in Table 1.

These parameters seem to have little influence on sulfate sorption.

A step by step investigation of the standard cleaning technique was carried out to test the efficiency of the technique; results are shown in Table 2.

TABLE 1. Sulfate contamination of copper samples

	Current density A/cm^2	Activity (c.p.m.)	SO_4 mass (g)
Polished surface	0·15	19 ± 9	$5{\cdot}8 \times 10^{-8}$
Etched surface	0·15	14 ± 4	$4{\cdot}3 \times 10^{-8}$
Polished surface	0·75	8 ± 3	3×10^{-8}
Etched surface	0·75	23 ± 10	7×10^{-8}

The averages stated in Table 2 were

VOL.
10
1961

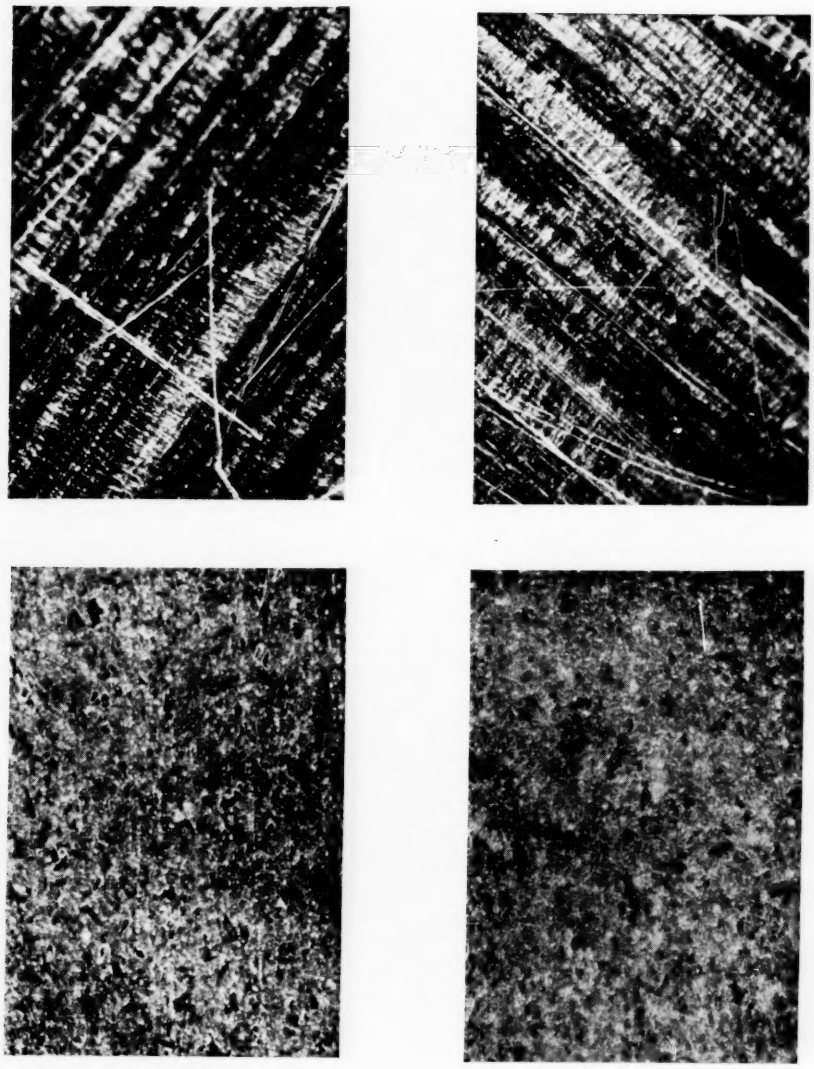

FIG. 1. Photomicrographs of gold and copper surfaces.

VC
1
19

TABLE 2. Sulfate contamination of copper samples*

	Activity (c.p.m.)	SO_4 mass (g)
1	36·5	$2{\cdot}2 \times 10^{-7}$
2	16	$9{\cdot}8 \times 10^{-8}$
3	1·7	1×10^{-8}
4	0	No detection
5	23	$1{\cdot}4 \times 10^{-7}$
6	0	No detection

* Where:
1 = 1 min in acid at 0·15 A/cm²—distilled water rinse
2 = 1 min in acid at 0·15 A/cm²—distilled water rinse —2 min tap water rinse
3 = 1 min in acid at 0·15 A/cm²—distilled water rinse —2 min tap rinse—2 min boiling distilled water rinse
4 = 1 min in acid at 0·15 A/cm²—distilled water rinse —2 min in KCN (6 g/l) at 70°C—2 min tap water rinse—2 min distilled boiling water—(complete standard cleaning)
5 = 1 min in acid (no current)—2 min tap water rinse
6 = 1 min in acid (no current)—2 min in KCN at 70°C—2 min tap water rinse—2 min boiling distilled water rinse.

VOL. 10 1961

calculated on a sample size of at least ten cleaning experiments.

Thus when the copper samples came out of the etching solution and were quickly rinsed, approximately $2{\cdot}2 \times 10^{-7}$ g of sulfate ions were left on the surface. By dipping in KCN and boiling the samples for 2 min the detection sensitivity was reached and sulfate ions could no longer be detected. This means that less than 10^{-8} g remains on the copper substrates. No characteristic difference was found in the post-cleaning contamination level (Cr and SO_4^{2-}) of precleaned and uncleaned copper samples.

B. *Efficiency of cleaning solution for organic contaminants*

Experiments were carried out by applying radioactive palmitic or stearic acid to precleaned and uncleaned gold and copper samples. The area covered by the acid was approximately 1·0 cm². The contaminated surfaces were cleaned with toluene or chromic acid.

(1) *Organic solvent (toluene).* Radioactive solutions are given in Table 3.

TABLE 3

Solution	Concentration mg/ml
(a) Palmitic	8·5
(b) Palmitic	2·8
(c) Palmitic	0·28
(d) Palmitic	$2{\cdot}8 \times 10^{-3}$
(e) Palmitic	$2{\cdot}8 \times 10^{-4}$
(f) Stearic	2·6

The radioactive samples were prepared according to the previously described procedure and placed in counting vials having a volume of 22 ml. The samples were counted three times, each time with new scintillation liquid. The discarded liquid washes were also counted for radioactivity.

Figure 2 shows the absolute decrease of the count rate of palmitic acid mass vs. the number of dips. The precleaned gold curves are systematically lower than the precleaned copper curves. This was to be expected since fatty acids may form soaps with copper and not with gold. One would expect the organic molecule to be highly adherent to the metallic surface in case of soap formation. It is also interesting that the curves, in the case of one surface, do not have the same slopes. They seem to be influenced by the amount of contaminant that was initially spread on the surface, implying an equilibrium condition between the palmitic acid on the surface and in the solvent.

Increasing amounts of contaminant were left on for increasing initial amounts of fatty acid. A relative plot of the count rate vs. the number of dips (Fig. 3) shows decreasing relative amounts left on for increasing initial amounts. Independently of the amount of contaminant put on (solutions *a*, *b* and *c*), a relatively constant percentage of acid was removed. The results obtained with solutions *d* and *e* show that detection sensitivity has been reached. Additional dips were carried out on the heavily contaminated samples. Even with solutions *a* and *b* two more dips in $C_6H_5CH_3$ brought the sample contamination level down to approximately background, i.e. 10 c.p.m.

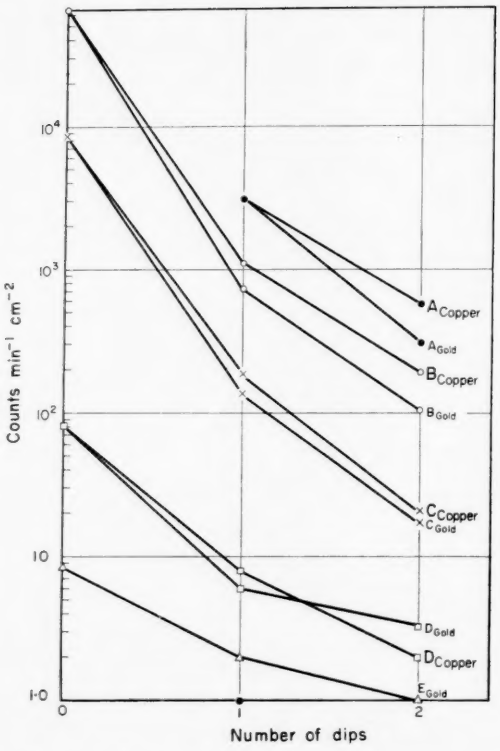

FIG. 2. Influence of the number of toluene dips on the removal of palmitic acid (gold and copper surfaces).

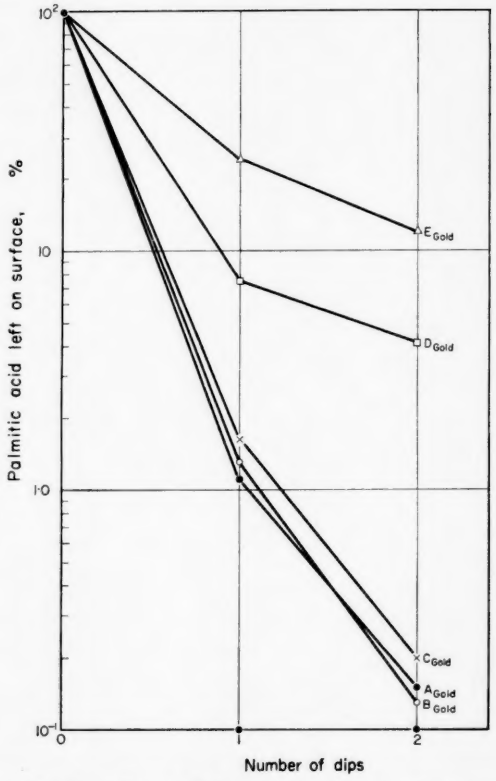

FIG. 3. Influence of the number of toluene dips on the removal of palmitic acid (gold surfaces).

(2) *Inorganic oxidant (chromic acid)*. Precleaned and uncleaned gold and copper surfaces were contaminated with 28 μg (solution *b*) of radioactive palmitic acid, or 26 μg (solution *f*) of stearic acid. The contaminated area was approximately 1 cm^2. To prevent contamination of the opposite side of the flat gold and copper samples, the back surfaces were masked with plater's tape.

Using anodic electropolish at (0·15) A/cm^2 in chromic acid the influence of time and temperature on the cleanability of the samples was investigated.

A sample size of at least nine cleaning experiments was used for each set of cleaning conditions.

After cleaning in chromic acid the samples were rinsed for 10 min in tap water, then rinsed for 2 min in boiling distilled water and finally air dried.

Figure 4 shows the absolute variations of the palmitic acid mass vs. cleaning time for precleaned and uncleaned copper surfaces. In both cases 2 min at 90°C was sufficient to decrease the contaminant mass below the detection sensitivity. This means that less than 3×10^{-9} g of palmitic acid or less than $1{\cdot}6 \times 10^{-2}$ monolayer was left on the copper samples. The curves are drawn through the averages for each set of conditions which explains the various changes of slope. The spread in measurement, which is dependent on the cleaning conditions, may be quite large. It was observed that palmitic acid was removed from uncleaned copper samples faster than from precleaned copper samples. This was to be expected. The cleaned

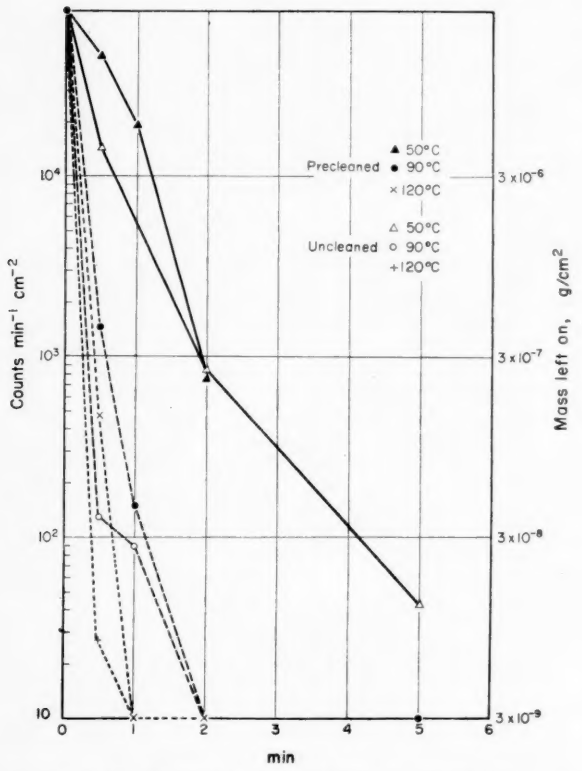

FIG. 4. Influence of time and temperature on the removal of palmitic acid with chromic acid (precleaned and uncleaned copper surfaces).

copper has affinity for fatty acids, thus cleans comparatively slowly.

Figure 5 shows the decrease of stearic acid mass vs. cleaning time for uncleaned copper and gold surfaces. Both palmitic and stearic acid are more readily removed from gold than copper surfaces.

For short cleaning times the solution's cleaning efficiency is two orders of magnitude greater for gold samples than for copper samples. Thus it can be said that copper contaminated gold (Cu $< 0{\cdot}1$ per cent) would have a cleaning efficiency which would fall near that of gold, between that of gold and copper. For longer cleaning times and high temperature (2 min at 120°C) detection sensitivities for the organic contaminants used are reached both for copper and gold surfaces. For practical purposes this means that the cleaning efficiencies for gold and copper are equivalent under these conditions. Thus, in this case copper impurities should not influence the cleanability of gold samples.

Figure 6 shows a comparison of the cleaning efficiencies for palmitic and stearic acid on copper surfaces. Since detection sensitivity for stearic acid was greater than that for palmitic acid, the stearic acid end points were lower. However, it can be seen on this figure that both acids were almost equally well removed by chromic acid.

Finally a comparison of the detection sensitivities of the three testing methods (1) water break test, (2) atomizer test and (3) radiotracer test is given in Table 4.

VOL. 10 1961

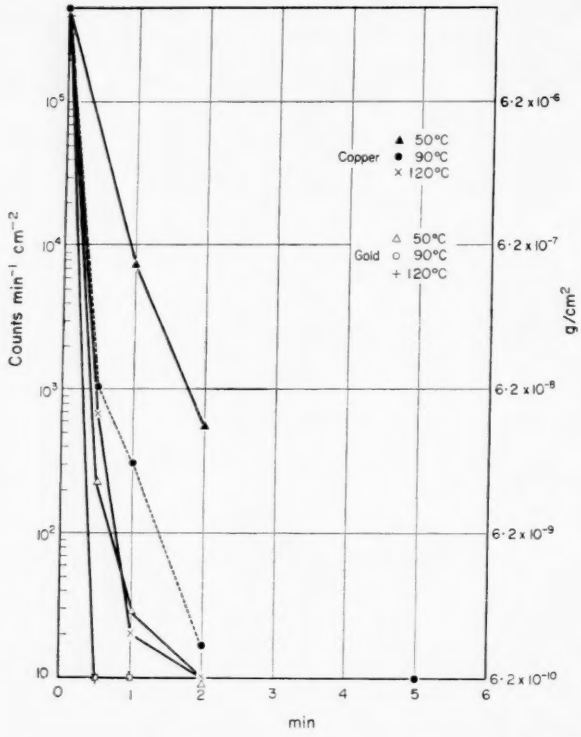

FIG. 5. Influence of time and temperature on the removal of stearic acid by chromic acid (uncleaned copper and gold samples).

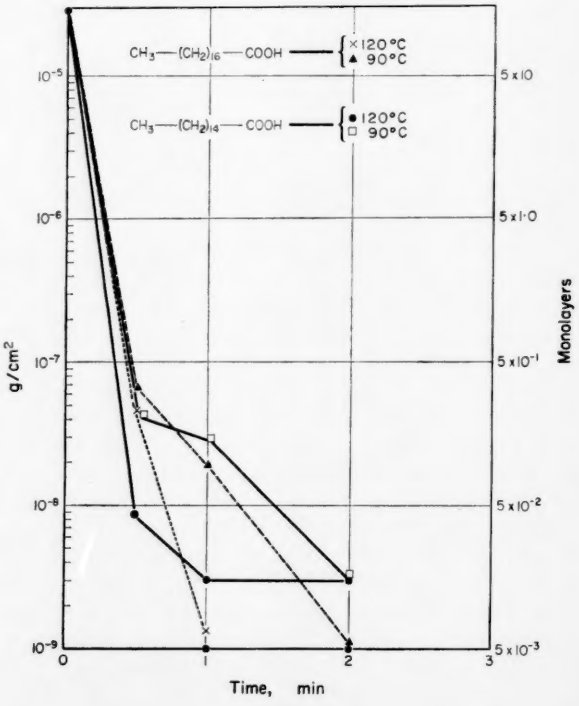

FIG. 6. Influence of time and temperature on the removal of fatty acids by chromic acid.

TABLE 4. Detection sensitivities of testing methods

	Water break test (g/cm^2)	Monolayers	Atomizer test (g/cm^2)	Monolayers	Radiotracer test (g/cm^2)	Monolayers
Stearic acid	$1{\cdot}1 \times 10^{-7}$	0·5	$0{\cdot}16 \times 10^{-7}$	0·075	$0{\cdot}006 \times 10^{-7}$	0·003*
Oleic acid	$1{\cdot}5 \times 10^{-7}$	1·5	$0{\cdot}18 \times 10^{-7}$	0·18	$0{\cdot}015 \times 10^{-7}$	0·015†
Palmitic acid	—	—	—	—	$0{\cdot}03 \times 10^{-7}$	0·016*

* The detection sensitivities of palmitic and stearic acids obtained with the radiotracer test could be increased by using radioactive material with higher specific activity.

† The data on oleic acid have been recently obtained and are included for completeness.

5. CONCLUSIONS

The data discussed show that a high state of cleanliness is obtained by electrocleaning in chromic acid.

Sulfate and chromate contamination of copper anodes is lower than the detection sensitivity of these ions. Chromic acid offers the additional advantage of removing most inorganic contaminants which might result from manufacturing operations.

The graphical data presented show that the efficiency of the chromic acid cleaning procedure for the removal of fatty acids is excellent, of the order of 99·99 per cent. By analogy, it is expected that fatty acid derivatives should clean equally well. In general, it may be said that these compounds, which are as readily oxidizable as fatty acids, should be as easily removable as fatty acids. This cleaning procedure may not be as effective on oxidation-resistant lubricants such as polysiloxanes as with fatty acids.

It was found that toluene is an efficient cleaning agent for fatty acids. The graphical data illustrate that the removal efficiency varies between 90 and 99·9 per cent depending on the initial amount of contaminant. It is interesting to note that the two cleaning techniques are more efficient on gold than on copper surfaces. Contaminant removal by toluene is dependent on solubility, thus no generalization can be made for fatty acid derivatives.

Comparison of the non-destructive testing methods for hydrophobic contaminants shows that, using the specific activities mentioned, the radiotracer technique is better by at least a factor of 10 than any of the wettability techniques. This increase in sensitivity could be still further enlarged by using higher specific activity radioactive material. The radio-tracer method further allows testing for hydrophylic contaminants which cannot be done with any of the wettability techniques.

The use of the standard cleaning technique is, of course, limited to solid metallic and glass samples; the technique should only be used when the metallic oxide produced on the sample dissolves in chromic acid. Plastic backed metals cannot be cleaned in this manner. Furthermore, this cleaning procedure is not recommended for metallic alloys since preferential etching is likely to result.

The tracer testing method provides the advantage of improved detection sensitivity for certain organic contaminants (fatty acids and derivatives) and offers a fast and accurate way of detecting hydrophylic contaminants. Shielding problems are non-existent where contaminants emitting only low-energy beta particles are used. The method also allows the qualitative and quantitative autoradiographic determinations of material distribution on the sample. This testing method may be easily used with any of the innumerable cleaning techniques that exist.

Given a well-instrumented laboratory, the limitations and/or disadvantages of this testing technique are few. First, the detection sensitivity will be limited by the specific activity of the material that is used and by the counting efficiency. For C^{14}-tagged organic materials, specific activities of 5 mc/mM, and counting efficiencies of 50–60 per

VOL. 10 1961

cent (liquid scintillation counting) may be obtained. The use of this method is not suggested in the case where porous materials are to be cleaned, since the amount of residual activity might be quite great after cleaning due to large amounts of contaminants left in the pores of the material. Finally, this method should not be used to test the cleanliness of any material, or part, for which residual activity, however small, would not be permissible.

Acknowledgments—The authors wish to thank MR. R. H. HOFFMAN for preparing and cleaning a large number of samples; and acknowledge the helpful suggestions offered by MR. W. D. KINSOLVING and the encouragement given by MR. H. B. ULSH.

REFERENCES

1. HARRIS J. C., KAMP R. E. and YANKO W. H. A.S.T.M. Bulletin No. 158, p. 49. TP75 (1949).
2. HARRIS J. C., KAMP R. E. and YANKO W. H. A.S.T.M. Bulletin No. 170, p. 82. TP308 (1950).
3. HENSLEY J. W., SKINNER H. A. and SUTER H. R. A.S.T.M. (Special Technical Publications). No. 115, p. 18 (1951).
4. HENSLEY J. W. *Iron Age* **170,** 151 (1952).
5. SLATER M. N. and DONAHUE D. J. A.S.T.M. (Special Technical Publications). No. 246, p. 146, (1959).
6. FEDER D. O. and KOONTZ D. E., A.S.T.M. (Special Technical Publications). No. 246, (p. 40) (1959).
7. BLAKE B. E. and FATZER G. D. *Pennsylvania State Seminar on Electrical Contacts* p. 39 (June 1959).
8. SIMNAD M. T. *Properties of Metallic Surfaces* p. 23. Institute of Metals, London (1953).
9. EISLER J. L., A.S.T.M. (Special Technical Publications). No 215, (p. 5) (1958).

International Journal of Applied Radiation and Isotopes, 1961, Vol. 10, pp. 177–180. Pergamon Press Ltd. Printed in Northern Ireland

Double Labelling of Sodium Monofluorophosphate with P^{32} and F^{18}

Y. ERICSSON
Clinical Laboratory, Royal Dental School, Stockholm, Sweden

(*First received* 5 *September and in revised form* 18 *September* 1960)

VOL. 10 1961

The preparation of $F^{18}P^{32}$-labelled sodium monofluorophosphate is described. The principles of this preparation are given in the second paragraph of this article. Different tests have demonstrated a high degree of purity of the preparations.

LE MARQUAGE DOUBLE DU MONOFLUOROPHOSPHATE DE SODIUM AVEC LE P^{32} ET LE F^{18}

On décrit la préparation du monofluorophosphate de sodium marqué du F^{18} et du P^{32}. Une exposition des principles de cette préparation se trouve au deuxième alinéa de cette communication. Des essais variés ont démontré la pureté très élevée des préparations.

ДВОЙНАЯ МЕТКА МОНОФТОРФОСФАТА НАТРИЯ ФОСФОРОМ-32 И ФТОРОМ-18

Дано описание получения препарата монофторфосфата натрия, меченого $F^{18}P^{32}$. Методика приводится во втором параграфе данной статьи. Различные испытания показали высокую степень чистоты полученных препаратов.

DOPPELMARKIERUNG VON Na-MONOFLUOROPHOSPHAT MIT P^{32} UND F^{18}

Die Präparation von $F^{18}P^{32}$-markiertem Na- Monofluorophosphat wird beschrieben. Die Grundlagen für diese Präparation werden im 2. Abschnitt dieser Arbeit angegeben. Verschiedene Teste erwiesen den hohen Grad der Reinheit dieser Präparate.

THE $P^{32}F^{18}$-labelling of Na_2PO_3F described below was performed in order to study the reactions of the PO_3F ion *in vitro* and the metabolism of this ion in the animal body. The separate determination of the P^{32} and F^{18} radiations forms no difficult problem and requires no discrimination of the different radiation characteristics owing to the short half-life of F^{18} of about 110 min, as compared to the half-life of 14·3 days of P^{32}.

Principles

P^{32}-labelled sodium metaphosphate, $NaPO_3$, is obtained by heating sodium dihydrogen orthophosphate, $NaH_2PO_4.H_2O$, in the presence of P^{32} as the orthophosphate.

F^{18}-labelled sodium fluoride, NaF, is obtained by evaporating a neutral or weakly alkaline solution of NaF containing F^{18} as the fluoride ion, carrier-free.

Na_2PO_3F is synthesized by fusing sodium metaphosphate, $NaPO_3$, and sodium fluoride, NaF, in stoichiometric proportions.

Practical example of a double labelling synthesis

$NaH_2PO_4.H_2O$, 276·2 mg, is weighed in a platinum crucible. Of P^{32}, as orthophosphate in essentially carrier-free form, 0·5 mc is added together with 4–5 ml of distilled water. Careful evaporation followed by heating in an electric furnace at 530° for 5 hr produces so-called sodium trimetaphosphate, $(NaPO_3)_3$.[1]

NaF, 84 mg, is added.

LiOH, 6 g, is irradiated overnight with a neutron flux of about 2×10^{12} n/sec per cm^2.

The reactions are

(1) $_3Li^6 + {}_0n^1 \rightarrow {}_2He^4 + {}_1H^3$

(2) $_1H^3 + {}_8O^{16} \rightarrow {}_0n^1 + {}_9F^{18}$.

The irradiated salt is glass distilled with 25 ml 70 % $HClO_4$ and 10 ml distilled water which removes radioactive contamination, mainly Na^{24}. The temperature is raised carefully until the salt is dissolved, in order to avoid bumping, and is then kept at about 140°. $NaClO_4$, 2–3 g, may be added to the distillation vessel if it is important to reduce the volatilization of $HClO_4$, which may have a toxic effect on experimental animals. With a slow air stream 10 ml distillate is obtained in about 20 min. The distillate is taken up in 1 ml 3 N NH_3.

F^{18} distills as the hexafluosilicic ion, which is completely hydrolysed with liberation of the fluoride ion at neutral or alkaline pH.[2]

The distillate is poured over the $NaPO_3$–NaF mixture in the platinum crucible and carefully and completely evaporated. F^{18} and the accompanying traces of silicon remain evenly and separately distributed in the residue after evaporation.

The crucible is put in an electric furnace preheated to about 800° and is kept there for about 1 min, which produces complete synthesis of $NaPO_3$ and NaF to Na_2PO_3F.[1,3] A lid is put on the crucible during cooling to protect against moisture.

Dissolution of the fused salt in 40 ml water gives the calculated concentration of 50 mM Na_2PO_3F. The solution is neutral and reported to be stable down to about pH 2·5; at lower pH values hydrolysis takes place.[4]

With our arrangements the above procedure, beginning with the F^{18} distillation, has taken about 1¼ hr. By the end of the procedure 0·1 ml of the 50 mM Na_2PO_3F solution has given about 800,000 c.p.m. for F^{18} and about 25,000 c.p.m. for P^{32} at the bottom of a Tracerlab P20B well-type scintillation detector with a 1 mm copper filter and an amplifier gain setting of 40. The copper filter is used to absorb the P^{32} beta radiation completely; only its Bremsstrahlung is registered by the scintillator.

If there is no call for minimizing the quantity of the double labelled salt (e.g. owing to its toxicity), separate batches of Na_2PO_3F may be labelled with P^{32} and F^{18}, respectively, otherwise following the above technique, whereafter solutions of the single-labelled batches are mixed. This may be a practical procedure especially when one preparation of P^{32}-labelled Na_2PO_3F can be used for mixing with several batches of the F^{18}-labelled salt, prepared for each day of experiment within the useful lifetime of P^{32}.

Tests on the chemical identity and purity of the double labelled substance

(1) *Weight tests.* $NaH_2PO_4.H_2O$, 276·2 mg, was weighed up in a platinum crucible. The salt was dissolved in 8 ml distilled water. After evaporation the crucible was heated at 530° for 5 hr. NaF, 84 mg, was added. The salts were dissolved in 10 ml 0·3N NH_3 which was evaporated to dryness. The salts were fused at 700°–800°. Weight after cooling: 288·8 mg (theoretical 288·0).

The same weight control in an experiment where the fused salt was double-labelled in exact accordance with the preceding chapter gave the final weight 292·1 mg of theoretical 288·0 mg.

(2) *Tests using infrared absorption.* The infrared absorption spectra of the following salts were studied: (1) sodium monofluorophosphate, commercial product, (2),(3) sodium monofluorophosphate, two preparations according to our technique, (4) sodium metaphosphate, prepared according to our technique, (5) calcium pyrophosphate, analytically pure commercial product.

The substances were pressed into potassium bromide disks, the sample concentrations being 0·25–0·5 per cent. A Perkin–Elmers infrared spectrometer with NaCl prism was used for the measurements. The resolution setting was 975, the gain 4·0 and scanning speed 5 min/μ.

The spectra of our monofluorophosphate preparations agreed with that of commercial sodium monofluorophosphate and with the absorption bands given by Corbridge and Lowe[5] with the exception of the 1205 μ absorption given by these authors. No traces of the metaphosphate or pyrophosphate spectra were found in the fluorophosphate

VOL. 10 1961

spectra. We are indebted to the Astra Pharmaceutical Co. for these spectrographic tests.

(3) *Precipitation tests with silver nitrate.* The heating of sodium metaphosphate with the weakly alkaline distillate in ammonia might be feared to involve some hydrolysis with the formation of orthophosphate or triphosphate. This was tested with silver nitrate which precipitates the latter ions but not trimetaphosphate.[6,7] No precipitate was formed when the salt, after the evaporation, was dissolved in water to give a 20 mM solution and mixed with an equal volume of 100 mM silver nitrate.

A more concentrated solution of the evaporated salt, 100 mM, on mixture with an equal volume 100 mM silver nitrate gave a slight opalescence. This was found to be soluble in weak ammonia and was not reprecipitated on addition of ethanol. The opalescence was thus not phosphate but probably traces of chloride from the distillation. There was thus no appreciable conversion of the metaphosphate.

(4) *Orthophosphate analysis.* Tests on the presence of orthophosphate ions were carried out on solutions of sodium monofluorophosphate, prepared according to our technique. The phosphate analyses were done according to a colorimetric molybdic acid method.

No orthophosphate was found in the solutions even after standing for a couple of days, while hydrolysis by boiling with strong nitric acid yielded the theoretically expected phosphate concentrations within the analytical errors.

(5) *Precipitation tests with calcium salts.* The solubility of the calcium salt of monofluorophosphate differs greatly from that of calcium fluoride (Fig. 1). Advantage can be taken of this fact to test the presence of free fluoride ions in a solution of Na_2PO_3F, prepared according to the description above. According to the diagram, a solution that is 50 mM PO_3F^{2-} and 2 mM Ca^{2+} should give no precipitate, provided that no hydrolysis of the PO_3F ions has occurred. Small concentrations of fluoride ions should be detected by precipitation.

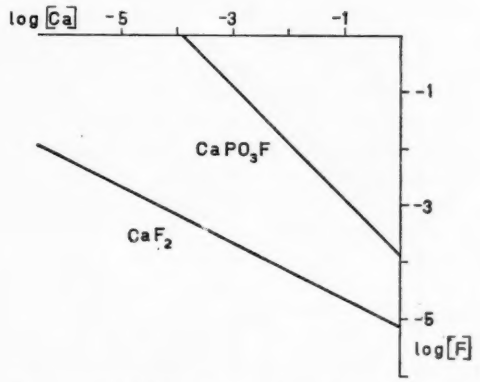

FIG. 1. Solubility diagram for calcium monofluorophosphate and calcium fluoride. Ionic concentrations corresponding to the areas above the solid lines cause precipitation.

Na_2PO_3F solutions were prepared of 100 mM concentration, (a) produced according to our double-labelling procedure but without the radioactive isotopes, (b) from commercial salt stated to be more than 95 per cent pure. Each solution was mixed with an equal volume of neutral 4 mM $CaCl_2$ and left standing overnight at 37°.

On the following day the pH values were determined, the mixtures were centrifuged and the supernatants were analysed for calcium using a complexone titration method.

The results are given in Table 1 together

TABLE 1. Precipitation tests with Na_2PO_3F preparations and calcium ions

		Own preparation	Commercial preparation
Analysed values	pH of solution	7·35	6·46
	Ca in solution (mM)	1·75	1·07
Calculated values	Ca precipitated (mM)	0·25	0·93
	F precipitated as CaF_2 (mM)	0·50	1·86
	F ions soluble together with analysed Ca concentration*, (mM)	0·15	0·20
	Total fluoride (mM) (precipitated F^- + soluble F^-)	0·65	2·06
	F^-/total F ("impurity")	0·013	0·041

* Solubility product of $CaF_2 = 4 \times 10^{-11}$.

with the fluoride ion concentrations calculated on the assumption, supported by the above-mentioned findings, that the calcium lost had not been precipitated as phosphates.

Even after standing overnight at body temperature, the impurity, as far as fluoride ions are concerned, was thus less than 2 per cent for our preparation against 4 per cent for the commercial preparation.

Further proof of the relative freedom of the produced Na_2PO_3F from fluoride ions was given by the fact, repeatedly confirmed, that shaking a solution of the F^{18}-labelled salt with solid calcium carbonate did not result in any loss of activity from the solution, in contrast to the rapid loss when a solution of F^{18}-labelled NaF was shaken with the calcium carbonate.

Acknowledgments—The author gratefully acknowledges the valuable suggestions and information obtained from Drs. Sven Ullberg and Gunnar Santesson.

The solubility diagram (Fig. 1) was kindly supplied by Prof. Arne Ölander.

Commercially prepared sodium monofluorophosphate was kindly supplied by Dr. Wayne White of the Ozark Mahoning Co., Tulsa, Oklahoma.

The investigation was financially supported by the Swedish Medical Research Council.

REFERENCES

1. Audrieth L. F. *Inorganic Syntheses* Vol. 3. McGraw–Hill, New York (1950).
2. Feldman I., Morken D. and Hodge H. C. *J. dent. Res.* **36,** 192 (1957).
3. White W. Personal communication (1958).
4. Van Wazer J. R. *Phosphorus and its Compounds*—I. *Chemistry.* McGraw–Hill, New York (1958).
5. Corbridge D. E. C. and Lowe E. J. *J. Chem. Soc.* **4,** 4555 (1954).
6. Mellor J. W. *Comprehensive Treatise on Inorganic and Theoretical Chemistry* Vol. 8, p. 987. Longmans, Green, London (1928).
7. Jones L. T. *Industr. Engng. Chem.* (*Anal.*) **14,** 536 (1942).

International Journal of Applied Radiation and Isotopes, 1961, Vol. 10, pp. 181–190. Pergamon Press Ltd. Printed in Northern Ireland

Gamma Radiolysis of Carbon-14 Labeled Isobutane

J. KIVEL* and A. F. VOIGT
Institute for Atomic Research and Department of Chemistry†
Iowa State University, Ames, Iowa, U.S.A.

(*Received* 13 *June* 1960)

VOL.
10
1961

The use of radioisotope labeled compounds and gas chromatographic techniques has been applied to a study of the decomposition of liquid and gaseous C^{14} labeled isobutane by cobalt-60 gamma radiation. Results are presented in terms of the G values of the radiation products. The specific activity of propane produced from isobutane-2-C^{14} was found to be about 1·5 times greater than that from isobutane-1-C^{14}. Similar results were obtained for propylene. Carbon-14 activity was not found in the methane product when isobutane-2-C^{14} was irradiated. The isobutene yield was unaffected by changing the labeled compound. The yield of neopentane was considerably greater than that of isopentane. Effects of temperature on hydrogen and methane formation are given and explained in terms of molecular and radical processes. Several mechanisms are presented for the formation of these radiation products.

LA RADIOLYSE GAMMA DE L'ISOBUTANE MARQUE DE C-14

L'emploi des composés marqués de radioisotopes et des techniques de la chromatographie gazeuse pour la recherche sur les produits de décomposition donnés par le rayonnement a été étudié. On a regardé la décomposition de l'isobutane à l'état liquide et à l'état gazeux, marqué de C^{14}, donnée par le rayonnement gamma du cobalte-60. On présente les résultats en termes des valeurs G des produits du rayonnement. L'activité spécifique du propane produit de l'isobutane-2-C^{14} se trouva environ 1,5 fois plus forte que celle de l'isobutane-1-C^{14}. Le propylène rendit des résultats semblables. On ne trouva aucune activité de carbone-14 dans le produit methene lors de l'irradiation de l'isobutane-2-C^{14}. Le rendement d'isobutene ne varia pas avec changement du composé marqué. Le rendement de néopentane fut fortement supérieur à celui d'isopentane. On indique les effets de la température sur la formation d'hydrogène et de méthane et on les explique en termes de procédés moléculaires et de ré actions entre radicaux. On présente plusieurs mécanismes pour la formation de ces produits du rayonnement.

ГАММА-РАДИОЛИЗ ИЗО-БУТАНА, МЕЧЕНОГО С-14

Рассматривается применение меченых соединений и газовой хроматографии для исследования продуктов радиационного разложения. Изучено разложение изо-бутана, меченого C^{14}, при облучении источником Co^{60} в жидкой и газовой фазе. Приводятся значения радиационных выходов (G) продуктов радиолиза. Найдено, что удельная активность пропана, полученного из изо-бутана-2-C^{14}, примерно в 1,5 раза больше, чем в случае изо-бутана-1-C^{14}. Аналогичные результаты были получены в случае пропилена. В метане, полученном при облучении изо-бутана-2-C^{14}, C^{14} обнаружено не было. Выход изобутола бутана не зависит от положения метки. Выход неопентана значительно превышает выход изопентана. Изучено влияние температуры на образование водорода и метана, которое объясняется на основе молекулярных и радикальных реакций. Предложено несколько механизмов образования радиационных продуктов.

* Present address: Honeywell Research Center, Hopkins, Minn.
† Contribution No. 903. Work was performed in part in the Ames Laboratory of the U.S. Atomic Energy Commission.

GAMMA-RADIOLYSE VON C-14 MARKIERTEM ISOBUTAN

Die Verwendung von radioaktiv markierten Verbindungen und gas-chromatographischen Methoden zur Untersuchung radiolythischer Zersetzungsprodukte wird beschrieben. Die Zersetzung von flüssigem und gasförmigem, C-14-markiertem Isobutan durch γ-Strahlung des Co-60 wurde untersucht. Die Ergebnisse werden durch die *G*-Werte der Strahlungsprodukte dargestellt. Die spezifische Aktivität von Propan aus Isobutan-2-C^{14} war 1,5 mal grösser als bei Verwendung von Isobutan-1-C^{14}. Ähnliche Ergebnisse wurden für Propylen erzielt. Es wurde keine Aktivität im Methan gefunden, wenn Isobutan-2-C^{14} bestrahlt wurde. Die Isobutene-Ausbeute blieb unbeeinflusst bei Änderung der markierten Verbindungen. Die Ausbeute an Neopentan war beträchtlich grösser als die des Isopentans. Der Einfluss der Temperatur auf die Wasserstoff- und Methanbildung wird angegeben und mit Hilfe von Molekülen- und Radikalprozessen erklärt. Es werden mehrer Mechanismen der Bildung dieser Strahlungsprodukte vorgelegt.

1. INTRODUCTION

THE possibility of attacking the problem of the mechanisms of radiation decomposition by the use of labeled compounds is an intriguing one. Until recent years the separation of the products and their radiochemical determination have been serious handicaps to such research. Recently the development of gas chromatography and in particular the use of a flow counter as an integral part of the gas stream[1,2] has made possible the ready identification and determination of the radioactive products of decomposition of labeled compounds. The availability at Iowa State University of a kilocurie Co^{60} source, in which time and temperature could be accurately controlled, made it possible to undertake such studies. In order to keep the products as simple as possible, a hydrocarbon system was studied. One of the most fundamental of these for which labeled compounds were available was isobutane, since compounds could be obtained in which the C^{14} label was in either the 1 or 2 position. Also recent studies by LAMPE[3] and HAMASHIMA *et al.*[4], on neopentane made the study of similar compounds such as isobutane of special interest.

2. EXPERIMENTAL

(A) *Materials*

Isobutane (Matheson Co., Joliet, Illinois, instrument grade, 99·9 per cent minimum purity) was used without further purification. Analysis by gas chromatography revealed only a trace of n-butane. Isobutane-2-C^{14} (Research Specialties Co., Berkeley, California) contained small amounts of radioactive propane, n-butane and isobutene. Isobutane-1-C^{14} (Orlando Research, Inc., Orlando, Florida) contained minor amounts of radioactive ethane, propane and isobutene but isobutene was the only impurity present in sufficiently large amounts to affect the results.

(B) *Sample preparation*

Standard vacuum techniques were used to transfer desired amounts of isobutane into the irradiation vials (ca.20 ml Pyrex glass vials, attached to a vacuum stopcock). In the studies involving labeled compounds, small amounts of the desired compound (specific activity 0·75 mc/g) were transferred to a McLeod gauge, measured and transferred to the irradiation vial, along with inactive isobutane, by immersing the vial in liquid nitrogen.

(C) *Sample irradiation*

Samples were irradiated at the cobalt-60 source of the Iowa State University Veterinary Medical Research Institute which contained 1380 c on 25 November 1959. The dose rate used in the investigations was determined to be 13,395 rad/min on this date by using the Fricke ferrous sulfate dosimeter. The value of *G* (ions of Fe^{II} oxidized per 100

VOL. 10 1961

eV energy absorbed) was taken as 15·45 as determined by SCHULER and ALLEN[5]. The dose rate was corrected for differences in electron density between the aqueous solution and the isobutane but was not corrected for the difference in effects in the two systems due to the interaction of the gamma rays with the glass sides of the irradiation vial.

Samples were irradiated for 15·5 hr to study the effects of temperature on methane and hydrogen formation, and for ca. 35 hr to study the other irradiation products. A thermocouple, placed within the sample chamber during the irradiation, actuated and controlled the temperature of circulating fluid reservoirs; these reservoirs maintained the sample chamber and sample at the desired temperature with a tolerance of 0·2°C.

(D) *Description of apparatus*

A gas chromatograph designed by W. A. Stensland and R. G. Clark of this Laboratory was used to separate the desired products. A Perkin–Elmer gas sampling valve (Perkin–Elmer Corp., Norwalk, Connecticut) was incorporated into the chromatograph for reproducible gas sampling, along with other liquid and gas sampling facilities. The carrier gas entered the apparatus through a low-flow rotameter, passed through the reference side of the thermal conductivity cell and flowed through the sampling system, where it picked up the gases to be separated, through the chromatographic column and the thermal conductivity cell. The gas stream was then mixed with a regulated amount of methane and passed into a proportional counter assembly, similar to that described by WOLFGANG and ROWLAND[2]. The output from the proportional counter was fed into a linear amplifier (Radiation Counter Laboratories Model 20701) through a discriminator into a scaler and rate meter (Nuclear Chicago Corporation, Models 162 and 1615A). It was found that a 20 ml counter chamber gave excellent results, independent of the nature of the center wire which was either 2 mil tungsten or 3 mil stainless steel. The operating voltage for the proportional counter was maintained by a separate high-voltage supply unit. A two-pen strip chart recorder (Bristol & Co.) was used to determine the thermal conductivity and rate meter response. In addition, the scaler was used to determine the radioactivity for calibration purposes. The areas under the thermal conductivity and radioactivity peaks were measured with a planimeter.

A two-stage column of 11 ft of 30 wt.% n-decane on Chromosorb (30/60 mesh) and 2 ft of activated charcoal (35/48 mesh) was used to separate hydrogen, methane, isobutane and traces of air. A three-way stopcock was fitted between the two segments of the column so that the isobutane could flow directly from the n-decane segment to the thermal conductivity cell. The other components passed through both segments of the column before entering the thermal conductivity cell. Table 1 shows the elution times obtained on this column.

For the analysis of the other radiation products of isobutane, columns of n-hexadecane, ethylacetoacetate and silica gel and of di-isodecylphthallate-dimethylsulfolane as described by FREDERICKS and BROOKS[6] were used.

(E) *Experimental procedure*

Samples of known volume ($\frac{1}{4}$ ml or 1 ml) of hydrogen, methane and isobutane were analyzed using the decane–charcoal column to determine the number of molecules of each per unit of area of the thermal conductivity peak obtained on recorder paper. The tracing from the rate meter was similarly calibrated to determine the counting rate per unit of area.

The irradiated isobutane vial was attached to one end of the sampling valve and the valve chamber was evacuated. The stopcock

TABLE 1. Elution times with a decane–charcoal column. Carrier flow rate, 20 ml/min argon. Temperature, 26°C

Component	Decane segment	Decane and charcoal
Hydrogen	3·4 min	4·0 min
Air	3·4 min	5·4 min
Methane	3·6 min	11·7 min
Isobutane	31·8 min	Undetectable

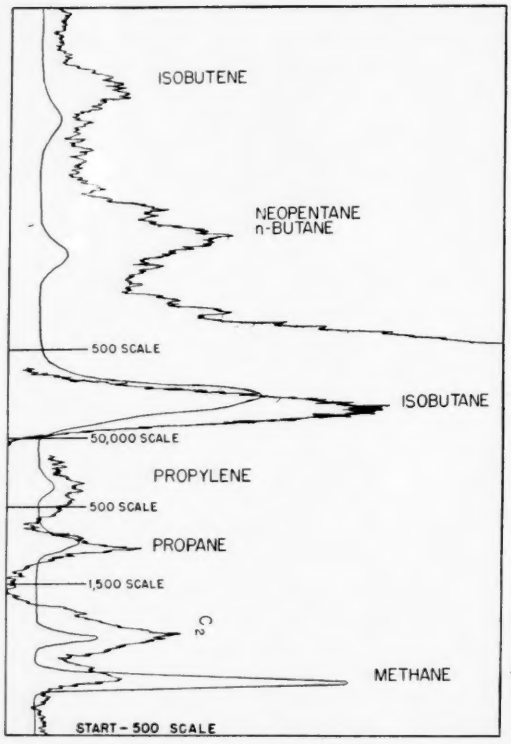

FIG. 1. Analysis of isobutane-1-C^{14} irradiated at $-16°C$ using a hexadecane column. Light line: thermal conductivity tracing; heavy line: counting rate tracing; scale ranges refer to count rate meter measurements.

on the irradiation vial was opened; the sample passed into the chamber and was injected into the gas chromatograph. A constant flow rate was maintained throughout the run; 20 ml/min of argon for the hydrogen and methane studies, and 15–25 ml/min of helium for the other substances. Although the flow rate could be maintained constant for short periods of time (the length of one run), it was impossible to keep it at the exact value for more than two successive runs. However, the relative thermal conductivity response of isobutane, methane and hydrogen for a mixture of different composition remained constant overflow rates of 15–25 ml/min. A typical dual tracing is shown in Fig. 1.

3. RESULTS

The values of $G(H_2)$ and $G(CH_4)$ obtained by thermal conductivity measurements for the radiolysis of isobutane are shown in Fig. 2. The conditions were as follows:

Dose rate	13,700 rad/min
Irradiation times	930 min
Dose	$1{\cdot}27 \times 10^7$ rad
Pressure of isobutane	745 mm.

In Table 2, the activity yields are listed for the irradiation of the two labeled isobutanes in the liquid and gaseous phases. The values are expressed in units which are proportional to the G value but which reflect the differences in radioactivity measurements, although the G value is independent of the amount of radioactivity. The unit of measurement is defined as the "activity G value" and is denoted by G_a. The relationship between G_a and G yields of component i is expressed by

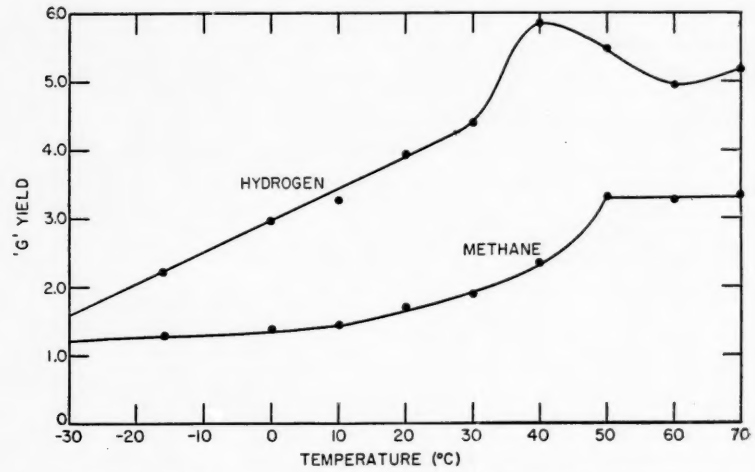

FIG. 2. The dependence of hydrogen and methane yield on temperature.

TABLE 2. Effect of physical state and carbon-14 position on activity yields

Temperature Physical state Labeled position	20°C Gas 2–C^{14}	−20°C Liquid 2–C^{14}	20°C Gas 1–C^{14}	−16°C Liquid 1–C^{14}
Compound	Activity yield (G_a)			
Methane	0·00	0·00	0·64 ± 0·12	0·42 ± 0·11
Acetylene	0·22 ± 0·06	0·30 ± 0·06	*a*	*a*
Ethylene	0·24 ± 0·04	0·24 ± 0·06	0·20 ± 0·06	0·16 ± 0·05
Ethane	0·24 ± 0·04	0·15 ± 0·06	0·68 ± 0·18	0·44 ± 0·15
Propyne	0·00	0·00	0·00	0·00
Propylene	1·39 ± 0·25	0·72 ± 0·20	0·88 ± 0·18	0·50 ± 0·16
Propane	3·61 ± 0·22	2·91 ± 0·36	2·51 ± 0·29	1·82 ± 0·36
Isobutene	1·87 ± 0·19	0·79 ± 0·12	2·0 ± 0·6	1·0 ± 0·5
Butene-1	0·00	0·00	0·00	0·00
Butene-2	0·00	0·00	0·00	0·00
n-Butane	1·02 ± 0·37	0·42 ± 0·11	0·85 ± 0·20	0·51 ± 0·06
Neopentane	0·92 ± 0·12	0·45 ± 0·08	1·34 ± 0·25	0·75 ± 0·12
Isopentane	*a*	*a*	0·37 ± 0·06	0·33 ± 0·05
n-Pentane	0·00	0·00	0·00	0·00

a—Not determined.

$G_a(i) = G(i) \times f$, where f is a constant equal to the ratio of the specific activities of i to isobutane. For example, if methane is formed by a methyl group which picks up a hydrogen after if is split from the isobutane-1-C^{14} molecule, the specific activity in the methane would be one third of that of the isobutane, or $f = \frac{1}{3}$.

4. DISCUSSION

(A) *Hydrogen*

The amount of hydrogen produced appeared to have a maximum G value of 5·87 at 40°C. The value of $G(H_2) = 2{\cdot}21$, obtained for the liquid state irradiation at −16°C can also be obtained by a straight line extrapolation of the gas phase irradiations between 0° and 30°C. This is to be expected since the

hydrogen radical is too small to remain trapped in a Franck–Rabinowitch cage, and therefore no dependence of phase should be expected. The value of $G(H_2) = 3{\cdot}92$, obtained in this investigation at 20°C, is, as expected, lower than the hydrogen yield obtained in straight-chain hydrocarbons[7–11], but is in agreement with the general trend of decreasing hydrogen with increasing branching. By extending the plot of $G(H_2)$ as a function of temperature to −30°C, a value of 1·6 was obtained; this is in good agreement with the value of 1·75 obtained by converting the yields obtained by KEENAN *et al.*[12] for the electron bombardment of liquid isobutane at −30°C to G values.

The several possible mechanisms by which hydrogen can be produced by the irradiation of isobutane can be considered to be in two general categories as due to hydrogen radical removal (equations 1 and 2) or hydrogen molecule removal (equation 3).

$$C_4H_{10} \xrightarrow{\gamma} C_4H_9 + H \qquad (1)$$

$$H + C_4H_{10} \longrightarrow C_4H_9 + H_2 \qquad (2)$$

$$C_4H_{10} \xrightarrow{\gamma} C_4H_8 + H_2. \qquad (3)$$

Processes involving hydrogen molecule production would be expected to be independent of temperature, since they do not involve interactions between molecules. Processes such as (1) and (2), in which a hydrogen radical is the first product, must involve a second reaction, and the latter step will be temperature dependent. It has been suggested[13] that, for unimolecular reactions, mass spectral data can give a good approximation of the relative importance of these radical and molecular processes. It may be assumed that the ratio of the mass spectral peaks at masses 56 and 57, which correspond to the removal from isobutane of a hydrogen molecule and hydrogen radical, respectively, are indicative of the ratio of molecular to radical processes. The ratio of these peak heights is reported[14] as $56/57 = 0{\cdot}44/3{\cdot}68$ or 11 per cent is attributable to molecular processes. If this ratio also applies for the radiation processes, the $G(H_2)$ value attributable to the molecular, temperature independent, process would be 11 per cent of 4 or about 0·5. The temperature dependence curve should then be essentially linear in the lower temperature range of these experiments. Since this is observed, the mass spectral data support those obtained in this investigation that the hydrogen was formed primarily by reactions such as (1) and (2) rather than molecular or hot radical processes.

(B) *Methane*

The yield of methane was found to be temperature dependent between −15 and +50°C. A maximum G value of 3·3 was observed above 50°C; a limiting value of $G(CH_4) = 1{\cdot}2$ was obtained by extrapolation of the yield–temperature plot. It was somewhat surprising that the $G(CH_4)$ value obtained for the liquid state irradiation falls on the same straight line as the G values in the gas. This may be indicative of the absence of a cage effect.

If the low-temperature limiting value of 1·2 for G is attributed to temperature-independent processes, 1·2/3·3 or 36 per cent of the total methane is produced by such reactions, while the remaining 64 per cent is produced by temperature-dependent processes. Mass spectral data on isobutane show that the ratio of mass peaks at 42 and 43 which correspond to the loss of methane and methyl radical is $42/43 = 0{\cdot}367$. Since methane would be removed by a molecular process and methyl by a radical process, this ratio also corresponds to the ratio of molecular to radical processes, or 27 per cent of the methane is formed by molecular processes. This value and the 36 per cent attributed to temperature-independent processes in these studies are in reasonable agreement, which can be taken as an indication that a reaction such as

$$C_4H_{10} \xrightarrow{\gamma} C_3H_6 + CH_4 \qquad (4)$$

is responsible for the temperature-independent processes while radical reactions such as

$$C_4H_{10} \xrightarrow{\gamma} C_3H_7 + CH_3 \qquad (5)$$

$$CH_3 + C_4H_{10} \longrightarrow CH_4 + C_4H_9 \qquad (6)$$

are responsible for the temperature-dependent processes.

VOL. 10 1961

In either of the two mechanisms postulated above, $G_a(CH_4)$ is expected to be zero with isobutane-2-C^{14} and one third of $G(CH_4)$ for isobutane-1-C^{14} (i.e. $f = \frac{1}{3}$). No activity was observed in the methane component for isobutane-2-C^{14} and the G_a/G ratios for isobutane-1-C^{14} were $0{\cdot}64/1{\cdot}70 = 0{\cdot}38$ in the gas phase and $0{\cdot}42/1{\cdot}29 = 0{\cdot}33$ in the liquid phase.

(C) *Acetylene, ethylene and ethane*

On the irradiation of isobutane-2-C^{14}, acetylene, ethylene and ethane were found to have almost identical G_a values at 20°C. The sum of the activity yields of the C_2 products was independent of the state of the isobutane, although the acetylene yield appeared to increase on going to the liquid state, while the yield of ethane decreased. It therefore appears that the C_2 products may be formed by temperature-independent processes.

The activity yield of ethane was approximately three times as large for isobutane-1-C^{14} as for isobutane-2-C^{14} in both the liquid and gas irradiations, although the ethylene yield was slightly less for the 1-C^{14} compound.

The presence of methyl radicals in the system would indicate the possibility of forming ethane by

$$CH_3 + CH_3 \longrightarrow C_2H_6 \qquad (7)$$

or

$$CH_3 + C_4H_{10} \longrightarrow C_2H_6 + C_3H_7. \qquad (8)$$

If these mechanisms are the only ones involved, no radioactivity would be expected in the ethane on the irradiation of isobutane-2-C^{14}. The greater activity yields of ethane in isobutane-1-C^{14} may indicate that these mechanisms are the predominant method of ethane formation.

Another possibility, not previously considered, is the ion–molecule reaction. This type of reaction, generally leading to rearranged products, may explain the activity obtained in the ethane fraction from isobutane-2-C^{14} as well as the formation of ethylene and acetylene. The temperature independence of the ethylene yield lends additional weight to this possibility.

TABLE 3. Activity yield ratios for propane and propylene

Compound	Temperature	G_a yields		
		2–C^{14}	1–C^{14}	Ratio
Propane	20°C	3·61	2·51	1·44
	−20°, −16°	2·91	1·82	1·60
Propylene	20°	1·39	0·88	1·58
	−20°, −16°	0·72	0·50	1·44

(D) *Propane and propylene*

The activity yields of propane and propylene and the ratio of these yields for isobutane-2-C^{14}/isobutane-1-C^{14} are listed in Table 3. In all cases this ratio was about 1·5. Possible mechanisms for the formation of propane and propylene are

$$C_4H_{10} \xrightarrow{\gamma} C_3H_7 + CH_3 \qquad (9)$$

$$C_3H_7 + C_4H_{10} \longrightarrow C_3H_8 + C_4H_9 \qquad (10)$$

$$C_3H_7 \longrightarrow C_3H_6 + H \qquad (11)$$

$$C_4H_{10} \xrightarrow{\gamma} C_3H_6 + CH_4. \qquad (12)$$

As the primary process in each case is the loss of a single carbon unit, the ratio G_a/G or f for isobutane-2-C^{14} would be 1, since each residue would contain the central labeled carbon. For isobutane-1-C^{14}, two out of three possible residues would contain C^{14} and f would be $\frac{2}{3}$. This, the activity ratio, 2-C^{14}/1-C^{14} would be expected to be 1·5.

No propyne was observed in these studies.

(E) C_4 *radiation products*

The large dependence of the isobutene yield on temperature and state tends to indicate that radical processes rather than molecular processes are responsible for the formation of most of the isobutene. Thus the reactions:

$$C_4H_{10} \longrightarrow C_4H_9 + H \qquad (13)$$

and

$$C_4H_9 \longrightarrow C_4H_8 + H \qquad (14)$$

appear to be more probable than

$$C_4H_{10} \longrightarrow C_4H_8 + H_2 \qquad (15)$$

which was also noted in the data on hydrogen production.

As would be expected, the isobutene yield is independent of isotope position, indicating that simple loss of hydrogen is more important than rearrangement or recombination of decomposition fragments. A comparison of the isobutene yield for the liquid and gaseous state irradiations, using the more precise data from isobutane-2-C^{14}, indicates that the difference between gaseous and liquid yields is $1{\cdot}87 - 0{\cdot}79 = 1{\cdot}12$. The hydrogen yield produced in this reaction must be decreased by a similar amount. If the $G(H_2)$ yields at 20° and at −16°C are similarly compared, the difference is $3{\cdot}92 - 2{\cdot}21 = 1{\cdot}71$. Thus, $1{\cdot}71 - 1{\cdot}12 = 0{\cdot}59$ is unaccounted for. This may be attributed in part to the reactions, such as (9) and (11), which produce propylene by the elimination of hydrogen since the formation of propylene also shows a large temperature dependence. It may also be partially due to the production of species of higher molecular weight with the general formula C_nH_{2n}, which were not studied in this investigation, but have been studied by others.[12]

No evidence was found for the formation of n-butenes but a surprisingly large amount of n-butane was observed. The formation of n-butane obviously involves rearrangement or recombination of fragments and could be explained by an ion-molecule mechanism, except that the n-butane yields were temperature sensitive while ion-molecule reactions are supposedly independent of temperature. Although it appears that the n-butane yields were independent of the position of the C^{14}, the data are not conclusive enough to present a mechanism for n-butane formation.

(F) C_5 *radiation products*

Normal pentane was not observed as a product of the irradiation of isobutane. This was to be expected since methyl radical substitution for hydrogen in isobutane should yield only isopentane and neopentane.

The reaction

$$CH_3 + C_4H_{10} \rightarrow C_5H_{12} + H \qquad (16)$$

should favor the formation of isopentane rather than neopentane. In addition, the steric effects of the methyl groups around the tertiary carbon atom should hinder the substitution for the tertiary hydrogen atom. Since for isobutane-1-C^{14} the ratio of neopentane to isopentane was found to be $1{\cdot}34/0{\cdot}37 = 3{\cdot}62$ at 20° and $0{\cdot}75/0{\cdot}33 = 2{\cdot}27$ at −16°C, it is not possible to reconcile the observed data with a mechanism such as reaction (16).

Observations on the mass spectra from isobutane[14] have shown that the tertiary hydrogen is removed 55 times more readily than the primary hydrogen. Also, the tertiary radical or positive ion has much greater stability than the corresponding primary radical or ion so that rearrangement of a primary intermediate to the tertiary analog might be expected. Thus, reactions of the types

$$C_4H_9 + CH_3 \longrightarrow C_5H_{12} \qquad (17)$$

$$C_4H_9 + C_4H_{10} \longrightarrow C_5H_{12} + C_3H_7 \qquad (18)$$

or similar reactions involving butyl carbonium ions would favor the production of neopentane rather than isopentane. These reactions, or related ones, are thus the probable mechanisms for the formation of pentanes.

On the basis of reactions (16,) (17) or (18), one can predict an expected ratio of G_a for neopentane from the two labeled isobutanes. In reactions (16) and (17), a methyl radical interacts with isobutane or an isobutyl radical; reaction (18) involves the transfer of a methyl radical from one isobutane group to another. In all three cases, this methyl group will have $f = \frac{1}{3}$ if isobutane-1-C^{14} is irradiated and $f = 0$ for isobutane-2-C^{14}. The value of f for the isobutyl group which enters the neopentane would be 1·0 for either compound. Thus, the total value of f for neopentane from isobutane-1-C^{14} would be 1·33 and from isobutane-2-C^{14}, 1·0. The activity ratio for neopentane (1-C^{14}/2-C^{14}) should be 1·33. The observed values are 1·46 for the gas at 20°C and 1·67 for the liquid at −16°C. In the latter case. the difference is beyond the experimental error, but no explanation is immediately apparent. Since the specific activity ratio f is one for neopentane from isobutane-2-C^{14},

the G value for neopentane is also 0·92 at 20° and 0·45 at −16°C.

It has been assumed that many of the products are formed by thermal free radicals. It is probable that the radiolysis involves radicals which have an energy distribution corresponding to a temperature somewhat higher than that of the irradiation. However, these reactions have been classified here as thermal rather than hot radical reactions. Other types of reactions may also play a fairly important part in the total picture, but the accuracy of the results is not sufficient to permit a choice of possible reactions other than the most important ones.

VOL. 10 1961

Conclusions

The production of hydrogen and methane by gamma radiolysis of isobutane was studied over the temperature range −20 to +50°C using thermal conductivity measurements in the gas chromatograph as the method of analysis. With the assumption that temperature-dependent processes involve radical formation as the primary step, while temperature-independent processes involve the direct removal of a molecule of hydrogen or methane, 36 per cent of the methane and much less of the hydrogen are produced by molecular processes. Since no radioactive methane was found in the irradiation of isobutane-2-C^{14}, the production of the substance by the complete breakdown of the irradiated molecule is not an important reaction. The isobutene yield is highly temperature dependent, another indication that the removal of hydrogen from isobutane is largely by radical rather than molecular processes.

The relative yields of radioactive ethane from the two labeled compounds indicates that much of the ethane is formed from a methyl radical, either reacting with another methyl radical or a methane molecule or extracting a second methyl group from an isobutane molecule. However, the yield of radioactive ethane from isobutane-2-C^{14} was not insignificant, indicating that other mechanisms must also be involved. The yields of the unsaturated C_2 hydrocarbons can possibly be attributed to ion-molecule reactions, but the data are not sufficient as yet to allow this possibility to be explored.

The relative yields of radioactive propane and propylene indicate that the principal mechanisms for their formation are the loss of methyl radical or methane. The yield of n-butane is unexpectedly large, but processes involved in its formation are too complicated to be understood on the basis of these data. The relative yields of radioactive pentanes is of considerable interest since the neopentane yield was 2·3–3·6 times the isopentane yield. Since reactions of methyl radical with isobutane would be expected to favor isopentane, it appears that these products are largely produced through the formation of isobutyl radicals as the first step.

Acknowledgments—The authors are especially grateful to Dr. J. C. Picken, Jr., and his co-workers of the Veterinary Medical Research Institute for the use of the Co^{60} source and for their invaluable cooperation and assistance. The Co^{60} source was obtained and installed in part through the aid of the U.S. Atomic Energy Commission.

The authors also wish to acknowledge their indebtedness to Mr. Richard Clark and Mr. Wayne Stensland of this Laboratory for designing the gas chromatograph and for assisting in the development of the auxiliary equipment.

REFERENCES

1. Evans J. B. and Willard J. E. *J. Amer. Chem. Soc.* **78,** 2908 (1956).
2. Wolfgang R. and Rowland F. S. *Analyt. Chem.* **30,** 903 (1958).
3. Lampe F. W. *J. phys. Chem.* **61,** 1015 (1957); *Nucleonics* **18,** No. 4, 60, (1960).
4. Hamashima M., Reddy M. P. and Burton M. *J. phys. Chem.* **62,** 246 (1958).
5. Schuler R. H. and Allen A. O. *J. chem. Phys.* **24,** 56 (1956).
6. Fredericks E. M. and Brooks F. R. *Analyt. Chem.* **28,** 297 (1956).

7. Lind S. C. and Bardwell D. C. *J. Amer. Chem. Soc.* **48,** 2335 (1926).
8. Tolbert B. M. and Lemmon R. M. *Radiat. Res.* **3,** 52 (1955).
9. Dewhurst H. A. *J. Amer. Chem. Soc.* **80,** 5607 (1958).
10. de Vries A. E. and Allen A. O. *J. phys. Chem.* **63,** 879 (1959).
11. Dewhurst H. A. *J. phys. Chem.* **61,** 1466 (1957).
12. Keenan V. J., Lincoln R. M., Rogers R. L. and Burwasser H. *J. Amer. Chem. Soc.* **79,** 5125 (1957).
13. Burr J. G. Jr. *J. phys. Chem.* **61,** 1483 (1957).
14. American Petroleum Institute, Project 44, *Catalog of Mass Spectral Data,* Spectrum Serial No. 64. National Bureau of Standards, Washington (1948).

International Journal of Applied Radiation and Isotopes, 1961, Vol. 10, pp. 191–197. Pergamon Press Ltd. Printed in Northern Ireland

Etude de l'Effet de Partenaires Solides sur la Polymérisation de l'Ethylène et sur la Télomérisation du Tétrachlorure de Carbone et de l'Ethylène Initiées par Rayonnement Gamma

VOL.
10
1961

C. MECHELYNCK-DAVID et F. PROVOOST
Centre d'Etude de l'Energie Nucléaire, Mol-Donk, Belgique

(*Received* 24 *August* 1960)

On a étudié la vitesse de disparition de l'éthylène engagé dans deux réactions initiées par rayonnement gamma en présence de partenaires solides. Les solides étudiés sont:

(1) des supports à grande surface tels que le silica-gel, l'alumine, les tamis moléculaires et des échantillons à base de charbon actif;

(2) des oxydes à surface faible tels que l'oxyde de zinc, le silica-gel calciné à 700°C et la laine de quartz;

(3) de la poudre de polythène.

Un accroissement de la vitesse de polymérisation de facteurs de 20 à 50 fois a été mis en évidence lorsqu'on polymérise $4{,}2 \cdot 10^{-3}$ mole d'éthylène en présence de 1 g de catalyseur microporeux á caractère polaire. Les catalyseurs polaires à faible surface n'ont pas d'effet sur la vitesse de polymérisation de l'éthylène tandis que le charbon actif est un inhibiteur de cette réaction.

En ce qui concerne l'addition de tétrachlorure de carbone sur l'éthylène, aucun effet de catalyse n'a été observé lorsque le milieu réactionnel est composé de $2 \cdot 10^{-2}$ mole de tétrachlorure de carbone, $1 \cdot 10^{-2}$ mole d'éthylène et 1 g de solide de n'importe quel type. On discute ces effets.

EFFECT OF SOLID ADDITIVES ON THE POLYMERIZATION OF ETHYLENE AND ON THE TELOMERIZATION OF CARBON TETRACHLORIDE AND ETHYLENE INITIATED BY GAMMA RAYS

The rate of disappearance of ethylene in the presence of solid additives was studied in two reactions initiated by gamma rays. The solids were:

(1) solids with large specific surface area such as silica gel, alumina, molecular sieves and activated charcoal;

(2) oxides with small specific surface area such as zinc oxide, silica gel calcined at 700°C and quartz wool;

(3) polyethylene powder.

The rate of polymerization of ethylene was increased 20 to 50 times when $4{\cdot}2 \times 10^{-3}$ mole ethylene was polymerized in the presence of 1 g of polar microporous solid. The polar catalysts of small surface area had no effect on the polymerization rate whereas charcoal was an inhibitor of this reaction.

For the addition of carbon tetrachloride to ethylene, no important catalytic effect was observed in a reaction medium containing 2×10^{-2} mole carbon tetrachloride, 1×10^{-2} mole ethylene and 1 g of solid of any type.

These effects are discussed.

ВЛИЯНИЕ ТВЕРДЫХ ДОБАВОК НА ПОЛИМЕРИЗАЦИЮ ЭТИЛЕНА И ТЕЛОМЕРИЗАЦИЮ ЧЕТЫРЕХХЛОРИСТОГО УГЛЕРОДА И ЭТИЛЕНА ПОД ДЕЙСТВИЕМ ГАММА-ЛУЧЕЙ

Скорость исчезновения этилена в присутствии твердых добавок была исследована для двух реакций, инициированных гамма-лучами. Были применены следующие твердые вещества:

(1) твердые вещества с большой удельной площадью поверхности, как например силикагель, алюминий, молекулярные сита и активированный древесный уголь;

(2) окислы с малой удельной площадью поверхности, как например окись цинка, силикагель, кальцинированный при 700°C, и кварцевая вата;

(3) порошок полиэтилена.

При полимеризации этилена в количестве $4{,}2 \times 10^{-3}$ молей, в присутствии 1 г полярного микропористого твердого вещества, скорость полимеризации повышалась в 20–50 раз. Полярные катализаторы с малой площадью поверхности не влияли на скорость полимеризации, в то время как древесный уголь ингибировал эту реакцию.

Добавление к этилену четыреххлористого углерода не вызывало заметного каталитического действия в реакционной среде, содержащей 2×10^{-2} моля четыреххлористого углерода, 1×10^{-2} моля этилена и 1 г любого твердого вещества.

Приводится обсуждение полученных результатов.

DER EINFLUSS VON FESTEN ZUSÄTZEN AUF DIE POLYMERISATION VON ÄTHYLEN UND AUF DEN ZUSATZ VON TETRACHLORKOHLENSTOFF ZU ÄTHYLEN UNTER GAMMA-STRAHLUNG

Die verbrauchsgeschwindigkeit von Äthylen unter gamma-Strahlung in Gegenwart von festen Zusatzkörpern wurde an zwei Reaktionen untersucht. Die verwendeten Festkörper waren;

(1) Stoffe mit grosser spezifischer Oberfläche wie Kieselgel, Aluminiumoxyd, Molecular Sieves, und Aktivkohle;

(2) Oxyde mit kleiner spezifischer Oberfläche wie Zinkoxyd, bei 700°C geglühtes Kieselgel und Quartzwolle;

(3) Polyäthylenpulver.

Eine 20 bis 50 fache Zunahme der Polymerisationsgeschwindigkeit, wurde erzielt, wenn $4{,}2 \cdot 10^{-3}$ mol Äthylen in Gegenwart von 1 g polarem mikroporösen Katalysator reagierten. Polare Katakysatoren von kleiner spezifischer Fläche hatten keinen Einfluss auf die Polymerisation, während Aktivkohle einen inhibierenden Einfluss hatte

In einem Reaktionsgemisch von $2 \cdot 10^{-2}$ mol Tetrachlorkohlenstoff, $1 \cdot 10^{-2}$ mol Äthylen und 1 g festen Material jeder Art, konnte man im Falle von Tetrachlorkohlenstoff zusätzen. Keinen katalytischen Einfluss auf die Reaktion war beobachtet.

Die verschiedenen Effekte werden erörtert.

La littérature récente mentionne l'effet de partenaires solides sur le déroulement de quelques réactions en chimie des radiations. L'introduction de solides microporeux à grande surface spécifique modifie le cours des réactions tant inorganiques qu'organiques, en phase gazeuse ou condensée.[1,2,3] L'addition de solides divisés tels que l'oxyde de zinc ou la poudre de polythène a également permis d'observer dans certains cas des effets intéressants.[4,5]

Dans ce qui suit, nous décrivons quelques résultats obtenus lors de l'étude de l'effet de partenaires solides sur deux réactions typiques en chaîne initiées par rayonnement gamma: la polymérisation de l'éthylène et la télomérisation de l'éthylène et du tétrachlorure de carbone.* L'étude de cette seconde réaction en l'absence de catalyseurs avait été préalablement réalisée dans ce laboratoire.[6]

Différents solides ont été étudiés:

(1) des supports à grande surface tels que le silica-gel, l'alumine, des alumino-silicates

* Une demande de brevet a été déposée par la Société Belge de l'Azote et des Produits Chimiques du Marly et le Centre d'Etude de l'Energie Nucléaire.

VOL. 10 1961

et des échantillons à base de charbon actif:

(2) des oxydes à surface faible tels que l'oxyde de zinc, le silica-gel calciné à 700°C et la laine quartz;

(3) de la poudre de polythène.

APPAREILLAGE ET PURIFICATION DES PRODUITS DE DEPART

Les produits de départ: éthylène et tétrachlorure de carbone contenaient moins de 30 p.p.m. d'oxygène et moins de 1000 p.p.m. d'autres impuretés. La quantité d'éthylène avant et après réaction a été mesurée par volumétrie gazeuse; l'avancement de la réaction a été calculé à partir de ces valeurs. La quantité initiale de tétrachlorure de carbone a été déterminée par volumétrie liquide à 20°C. Les solides ont été soigneusement dégazés sous vide à haute température avant le remplissage des ampoules; ils ont été préparés selon les procédés habituels.*

On trouvera dans le Tableau 1 une liste de leurs propriétés structurelles essentielles. L'ensemble des manipulations de vidange et de remplissage des ampoules a été effectué sous un vide de 10^{-5} mm de mercure en gaz résiduels autres que les réactifs. Les irradiations ont été effectuées dans des ampoules de quartz d'un volume de 5 ml environ et munies d'un "break-seal". La température d'irradiation a été mesurée à l'aide d'un thermocouple. La dosimétrie a été faite à l'aide du dosimètre au sulfate ferreux en utilisant la valeur de 15,5 pour le rendement radiochimique de disparition des ions ferreux par 100 eV dissipés dans le mélange. La vitesse de dose était habituellement de l'ordre de $3{,}5 \cdot 10^5$ r/hr. Les masses moléculaires ont été obtenues par mesure de la viscosité de solutions du polymère à 75°C dans le xylène.[7] La séparation silice-polymère a été effectuée par extraction au moyen de xylène bouillant.

TABLEAU 1. Caractéristiques des solides ajoutés

Type	Densité à l'hélium (g/cm^3)	Densité au mercure (g/cm^3)	Volume des pores ($ml.\ g^{-1}$)	Surface B.E.T. ($m^2\ g^{-1}$)	Granulométrie
Silicagel 1/174	2,17	1,29	0,316	625	Granules
Alumine 3/181	3,31	1,71	0,284	169,5	Granules
Charbon actif 7/18	2,087	0,818	0,743	1003,0	Granules
Charbon + oxyde d'uranium 7/160	2,713	1,318	0,390	730,0	Granules
Polythène	—	—	—	—	30–50 mesh
Laine de quartz	—	—	—	—	0,01 mm diamètre
Silice calcinée a 700°C	2,23	1,71	0,135	23,3	Poudre
Oxyde de zinc	5,17	1,56	0,446	2,40	Granules
Tamis moléculaire 5 A	2,53	1,22	0,426	365,3	Granules $\frac{1}{16}$ in.
Tamis moléculaire 4 A	2,41	1,24	0,396	10,85	Granules $\frac{1}{16}$ in.

RÉSULTATS EXPERIMENTAUX

Les résultats obtenus en l'absence et en présence de partenaires solides sont groupés dans les Tableaux 2 et 3. On a donné deux valeurs des rendements G. La première (le $G_{\text{réactif}}$) a été calculée en ne considérant que l'énergie dissipée directement dans les réactifs. Pour la seconde (le G_{apparent}) on a comptabilisé toute l'énergie dissipée dans le système additif-réactif. Pour réduire les fluctuations des résultats dues à des modifications de l'intensité du champ de radiation, le taux de réaction de l'addition du tétrachlorure de carbone sur l'éthylène a, de plus, été corrigé en admettant une variation

* La préparation des supports microporeux a fait l'objet d'un brevet déposé par la Société Belge de l'Azote et des Produits Chimiques du Marly (Belg. 573.657).

TABLEAU 2. Polymérisation

Essai No.	Additif 1 g	C_2H_4 mis* (mole $\times 10^3$)	C_2H_4 consommé (mole %)	Dose dissipée (rad $\times 10^7$)	Dose dissipée dans réactif (eV $\times 10^{-20}$)	$G_{réactif}$	Dose dissipée dans système (eV $\times 10^{-21}$)	$G_{apparent}$
30	—	4,16	6,9	3,3	2,37	73,4	—	—
32	—	3,93	22,4	11,6	7,92	66,7	—	—
27	Oxyde de zinc	4,03	23,9	11,6	8,14	71	8,02	7,3
101	Oxyde de zinc	4,13	26	11,14	8,0	81	7,72	8,5
63	Tamis moléculaire 4 A	4,21	69	2,6	1,90	927	1,80	97,7
88	Tamis moléculaire 4 A	4,02	61	2,6	1,82	815	1,79	82,4
90	Tamis moléculaire 5 A	4,16	82	2,6	1,87	1087	1,80	13,5
65	Tamis moléculaire 5 A	4,18	79	2,6	1,89	1056	1,80	110
68	Charbon actif + oxyde d'uranium	4,20	9,3	2,6	1,90	123	1,80	13,1
93	Charbon actif + oxyde d'uranium	4,21	9,5	2,6	1,90	126	1,80	13,3
57	Charbon actif	4,19	1,8	2,6	1,89	23	1,80	2,67
94	Charbon actif	4,24	4	13,3	9,84	11	9,25	1,10
59	Alumine	4,03	38	0,4	0,280	3288	0,276	333
91	Alumine	4,04	38	0,528	0,370	2540	0,365	259
62	Alumine	4,21	28	0,528	0,387	1906	0,366	200
60	Alumine	4,15	100	2,6	1,87	1334	1,80	139
61	Silice	4,23	50	0,528	0,388	3299	0,366	348
58	Silice	4,10	71	1,0	0,714	2444	0,692	252
92	Silice	3,85	95	2,6	1,74	1260	1,78	123
102	Laine de quartz	4,08	8,3	2,6	1,84	111	1,80	11,3
103	Silice calcinée	4,13	16,6	2,6	1,87	220	1,80	23

* Ces essais ont été effectués à 31°C (±1°C).

La vitesse de dose était $3{,}54 \cdot 10^5$ r/hr^{-1} à l'exception des essais 30, 32, 27 et 59 où elle valait $5{,}42 \cdot 10^5$ r/hr^{-1} et des essais 101, 94 et 60 pour lesquels elle n'a pas été determinée.

La pression d'éthylène est comprise entre 20 et 25 atm pour les ampoules ne contenant pas de solide ou contenant un solide à faible surface spécifique. Pour les polymérisations effectuées en présence de tamis moléculaires, l'examen des isothermes d'adsorption (Linde Molecular sieves data sheets) permet de calculer que la pression serait de l'ordre de 6 atm; elle serait inférieure à 15 atm pour la silice et inférieure à 4 atm pour le charbon.

des vitesses de réaction selon $\sqrt{I}$. Une meilleure concordance des résultats a ainsi été obtenue; elle confirme la validité de ce type de relation, d'ailleurs fréquent dans les réactions en chaîne initiée par rayonnement.[8] La mauvaise reproductibilité des résultats observée pour la polymérisation de l'éthylène en présence d'alumine peut vraisemblablement s'expliquer par des modifications du degré d'hydratation et de la surface apparaissant au cours du dégazage sous vide. Cet effet fait actuellement l'objet d'une étude.

L'ensemble des résultats obtenus montre que la présence de solides affecte peu le cours de la réaction d'addition du tétrachlorure de carbone sur l'éthylène dans les conditions expérimentales utilisées.

Par contre, les effets sont très importants lors de la polymérisation de l'éthylène. Ils peuvent se résumer de la manière suivante: en présence de silice, alumine et tamis moléculaire à grande surface la vitesse de disparition de l'éthylène est de 20 à 50 fois plus grande qu'en l'absence de solide; le charbon actif a un effet inhibiteur considérable. Par contre, l'incorporation d'oxyde d'uranium transforme cet effet inhibiteur en un léger effet accélérateur; l'oxyde de zinc, la silice à faible surface et la laine de quartz

TABLEAU 3. Téiomérisation

Essai No.	Additif	C_2H_4 mis (mole × 10^2)	CCl_4 mis (mole × 10^2)	C_2H_4 consommé (mole %)	Mole % corrigé	Vitesse de dose (r/hr × 10^{-5})	Gréactif	Gapparent
—	—	1,04	Extrapolé[6]	45	45	4,3	1158	—
17	Charbon + oxyde d'uranium 1 g	1,04	2,07	46	46	4,3	1133	880
83	Charbon + oxyde d'uranium 1 g	1,035	2,07	50	45,6	3,54	1232	955
15	Alumine 0,69 g	0,72	1,43	46	46	4,3	1130	879
20	Silicagel 1 g	1,04	2,07	48	48	4,3	1182	944
21	Silicagel 1 g	1,04	2,07	54,4	49,6	3,54	1336	1038
148	Oxyde de zinc 1 g	1,04	2,07	55,1	50,2	3,54	1354	1053
100	Oxyde de zinc 1 g	1,05	2,07	52	47,4	3,54	1287	1000
18	Charbon actif 1 g	1,04	2,07	38	38	4,3	945	733
82	Charbon actif 1 g	1,04	2,07	41	37,3	3,54	1003	778
24	Polythène 1 g	1,04	2,07	40,7	40,7	4,3	1002	779
140	Polythène 1 g	1,03	2,07	48,3	44	3,54	1174	914
85	Tamis moléculaire 4 A 1 g	1,04	2,07	46,7	42,5	3,54	1149	891
86	Tamis moléculaire 4 A 1 g	1,04	2,07	49,6	45,2	3,54	1222	947

Ces essais ont été effectuées a 27°C.

La dose dissipée était 10^6 r pour l'ensemble des essais.

La dose totale dissipée dans les réactifs était $2,55 \cdot 10^{20}$ eV et dans le système $3,28 \cdot 10^{20}$ eV pour l'ensemble des essais sauf l'essai 15 où ces doses valaient respectivement $1,99 \cdot 10^{20}$ eV et $2,26 \cdot 10^{20}$ eV.

La pression d'éthylène est comprise entre 25 et 30 atm pour les ampoules ne contenant pas de solide ou contenant un solide à faible surface spécifique. Elle est difficilement évaluable pour les solides à grande surface spécifique puisqu'il faut tenir compte à la fois de la solubilisation dans le tétrachlorure de carbone et de l'adsorption sur le solide.

sont sans effet appréciable. La présence de solide affecte considérablement la masse moléculaire moyenne du polymère.

En effet, pour l'essai 32, le polymère obtenu est une graisse de viscosité spécifique de l'ordre de $3,2 \cdot 10^{-3}$ l. g^{-1} de masse moléculaire moyenne en nombre inférieur à 700.

Le polymère obtenu sur silice au cours de l'essai 92 est un solide dont la viscosité spécifique vaut $2,87 \cdot 10^{-2}$ l. g^{-1} et dont la masse moléculaire moyenne en nombre est de l'ordre de 5000.[7]

DISCUSSION

Les effets les plus nets ont été observés avec des substances microporeuses et pour la réaction de polymérisation. On peut se demander comment la présence d'un solide à grande surface peut modifier dans une telle mesure le déroulement de la réaction.

Ces résultats ne peuvent s'expliquer par un changement des conditions physiques de l'irradiation tels qu'une liquéfaction de l'éthylène puisque les expériences sont réalisées à une température supérieure à la température critique de l'éthylène; aucune condensation capillaire n'a donc lieu dans les micropores des solides ajoutés.

Un autre hypothèse simple consisterait à penser que la réaction suit un déroulement normal dans les pores et micropores du solide et que la vitesse de la réaction d'initiation seule augmente; cette augmentation pourrait être due à une formation d'ions ou d'atomes et radicaux aux dépens de l'énergie dissipée dans le solide, mais les valeurs des G_{apparent} sont telles qu'une utilisation même quantitative de cette énergie par un phénomène de transfert solide–gaz serait insuffisante pour expliquer la grandeur de l'effet observé. L'augmentation de masse moléculaire observée lorsque la polymérisation

VOL. 10 1961

est effectuée en présence de catalyseurs semble elle aussi, montrer que l'augmentation de la vitesse de réaction n'est pas due à un accroissement de la vitesse d'initiation. En effet, un accroissement de la vitesse d'initiation augmenterait le nombre de chaînes croissantes et donc la vitesse de terminaison de chaîne. Ceci aurait pour conséquence une diminution de la masse moléculaire. Ces deux effets conjugués semblent prouver que l'on doive plutôt admettre que la polymérisation initiée par rayonnement ionisant en présence de substances microporeuses suit un mécanisme différent de celui de la phase gazeuse homogène. Il est d'ailleurs bien connu que la polymérisation de l'éthylène peut être réalisée thermiquement dans des édifices microporeux convenablement choisis renfermant un oxyde métallique.[9,10]

Un parallélisme entre la polymérisation thermique et la polymérisation initiée par rayonnement gamma en présence des même supports à grande surface existe vraisemblablement. On pourrait penser que dans les deux cas la polymérisation procède dans la phase adsorbée mais que la différence réside dans la nature du processus d'initiation. Pour la polymérisation thermique, l'oxyde métallique ou l'alkyl aluminium de Ziegler interviendrait; pour la réaction initiée par rayonnement gamma, la formation en surface d'espèces excitées ionisées ou radicalaires rendrait inutile la présence de l'oxyde ou de l'halogénure. Quoi qu'il en soit l'existence d'une grande surface développée est une condition nécessaire à l'existence d'un effet accélérateur; en effet on remarquera qu' aucun additif à faible surface (oxyde de zinc, silica-gel calciné à 700°C et laine de quartz) ne provoque un tel effet. Cette condition n'est cependant pas suffisante puisque la réaction en présence de charbon actif est très inhibée. Ce cas particulier illustre bien l'importance de la nature de la surface sur le déroulement de la réaction. Un phénomène similaire a déjà été observé pour la polymérisation thermique et catalytique du styrène, de l'acrylonitrile et de l'éthylène.[11,12,13] La présence de groupes quinoniques ou la structure électronique du charbon actif pourraient être invoqués pour interpréter cet effet inhibiteur qui disparait par la présence d'oxyde d'uranium dans les pores du charbon actif.[14]

En ce qui concerne la réaction de télomérisation, la présence d'additifs microporeux ne provoque aucun effet important sur la vitesse de transformation dans les conditions expérimentales utilisées. On peut considérer que dans ce cas la réaction se produit selon le mécanisme habituel, en phase condensée, partiellement dans les micropores de l'adsorbant, partiellement à l'extérieur. Sur tamis moléculaire, la stoechiométrie des produits de télomérisation est légèrement modifiée: la proportion de 1:1:1:3-tétrachloropropane augmente au détriment du 1:1:1:7-tétrachloroheptane. Une diminution de la pression en éthylène produirait le même effet.[6] Il y a lieu dans tous ces cas de tenir compte de la compétition entre la solubilisation de l'éthylène dans le tétrachlorure de carbone et son adsorption sur le support microporeux.

CONCLUSION

L'étude du comportement sous irradiation des systèmes mixtes solide dispersé-réactifs suscite actuellement de l'intérêt dans de nombreux laboratoires. On peut affirmer que, dans la plupart des cas, la présence d'un solide finement divisé modifie le déroulement de la réaction; l'interaction réactifs-solide en est la cause et la forme qu'elle prend dépendra du système étudié. Nous pensons que la polymérisation de l'éthylène initiée par rayonnement γ en présence de support microporeux suit un mécanisme voisin de celui mis en évidence dans les procédés Philips et Standard Oil Company. La nature des produits dépendra des paramètres physicochimiques du système. La structure particulière de l'additif constitue dans le cas étudié, un paramètre essentiel. Rappelons que les additifs les plus efficaces ont une structure caractérisée par des pores de

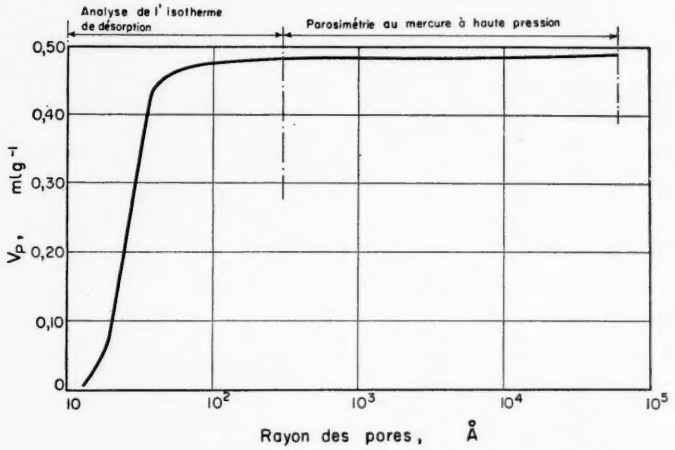

FIG. 1. Volume cumulatif des micropores d'un échantillon de silice.

quelques dizaines d'angströms. A titre d'exemple, nous donnons dans la Fig. 1[15] le spectre des pores de la silice utilisée. Des schémas cinétiques ont été proposés récemment pour expliquer la croissance des polymères en présence de solides finement divisés; la linéarité de la chaîne a été interprétée en admettant une croissance unidimentionnelle du polymère. La technique d'initiation par radiation permet d'étudier ces problèmes encore très mal connus dans des conditions particulièrement simples. Il devient ainsi possible de préciser l'incidence de la microstructure sur la nature du polymère formé en faisant varier celle-ci de manière systématique.

Remerciements—Nous tenons à remercier Monsieur P. GOSSELAIN, attaché aux Laboratoires de recherche de la Société Belge de l'Azote et des Produits Chimiques de Marly pour les nombreux échanges de vues que nous avons eus avec lui au cours de ce travail. Nous remercions également ses collaborateurs qui ont préparé et déterminé les propriétés des supports microporeux que nous avons étudiés.

REFERENCES

1. COEKELBERGS R. F. R., GOSSELAIN P. A. et SCHOTSMANS L. J. *Deuxième Conférence Internationale des Nations-Unies sur l'Utilisation de l'Energie Atomique à des Fins Pacifiques*. A/Conf. 15/P/1895 (1958).
2. HAISSINSKY M. et DUFLO M. *Deuxième Conférence Internationale des Nations-Unies sur l'Utilisation de l'Energie Atomique à des Fins Pacifiques*. A/Conf. 15/P/1233 (1958).
3. CAFFREY J. M. et ALLEN A. O. *J. Phys. Chem.* **62,** 33 (1958).
4. WORRALL R. et CHARLESBY A. *Int. J. appl. Rad. Isotopes* **4,** 84 (1958).
5. WORRALL R. et PINNER S. H. *J. Polym. Sci.* **34,** 229 (1959).
6. MECHELYNCK-DAVID C. *Tetrahedron* (1961) À paraître.
7. HARRIS I. *J. Polym. Sci.* **8,** 353 (1952).
8. WALLING C. *Free Radicals in Solution*. Wiley, N.Y. (1957).
9. GAYLORD N. G. et MARK H. F. *Linear and Stereoregular Addition Polymers*. Interscience, N.Y. (1959).
10. FRIEDLANDER H. N. *J. Polym. Sci.* **38,** 91 (1959).
11. KRAUS G., GRUVER J. T. et RALLMANN K. W. *J. Polym. Sci.* **36,** 564 (1959).
12. DONNET J. B. et HEINRICH G. *C.R. Acad. Sci., Paris* **246,** 3341 (1958).
13. FELLER M. et FIELD E. *Industr. Engng. Chem.* **51,** 155 (1959).
14. DRUSHEL H. V. et HALLUM J. V. *J. Phys. Chem.* **62,** 1502 (1958).
15. COEKELBERGS R., GOSSELAIN P., JULIENS J., SCHOTSMANS L. J. et VAN DER VENNE M. Communication Présentée à la Conférence de Varsovie de l'A.I.E.A. sur l'Utilisation des Sources Intenses de Rayonnement C.E.N.R./1788 (Fig 2), (1959).

VOL. 10 1961

International Journal of Applied Radiation and Isotopes, 1961, Vol. 10, pp. 198–209. Pergamon Press Ltd. Printed in Northern Ireland

The Cooperative Plant and Seed Irradiation Program of the University of Tennessee*

T. S. OSBORNE and A. O. LUNDEN

University of Tennessee-Atomic Energy Commission, Agricultural Research Laboratory, Oak Ridge, Tennessee, U.S.A.

(*First received* 14 *July* 1960 *and in final form* 10 *October* 1960)

The cobalt-60 plant and seed irradiation facility at the Atomic Energy Commission Agricultural Research Laboratory of the University of Tennessee at Oak Ridge is described. The facility, constructed in 1956, provides a source of gamma rays for plant geneticists of the agricultural experiment stations in the southern part of the United States; exposure to reactor neutrons is obtained at the Oak Ridge National Laboratory. Over 500 plant and seed samples, representing about 120 plant species, have been exposed to radiation under this program. These samples have been submitted by more than 100 research scientists in twenty-two states and five countries.

Results are summarized, based on sensitivity in the treated generation for about sixty species of plants. A summary of the observed genetic changes reported for about twenty species is included.

A method is described whereby dose-response at maturity may be predicted from seedling performance, following seed irradiation.

LE PROGRAMME CO-OPERATIF POUR L'IRRADIATION DES PLANTES ET DES GRAINES DE L'UNIVERSITÉ DE TENNESSEE

On décrit l'installation à cobalt-60 pour l'irradiation des plantes et des graines au Laboratoire des Recherches Agriculturelles de la Commission à l'Energie Atomique, de l'Université de Tennessee à Oak Ridge. Cette installation, construite en 1956, fournit une source de rayons gamma pour les généticistes de plantes des centres expérimentaux pour l'agriculture dans la partie méridionale des Etats-Unis; l'exposition aux neutrons de réacteur se fait au Laboratoire National à Oak Ridge. Plus de 500 échantillons de plantes et de graines, réprésentant environ 120 espèces de plantes, ont subi le rayonnement selon ce programme. Ces échantillons ont été soumis par plus de 100 hommes de recherche scientifique en vingt deux états des E-U et en cinq pays.

On donne un sommaire des résultats, basés sur la sensibilité de la génération traitée, pour environ soixante espèces de plantes; y compris un sommaire des observations de changements génétiques rapportés pour une vingtaine d'expèces.

On décrit une méthode par laquelle on peut prédire la réponse-à-dose à maturité selon la réaction de la jeune plante, suivant l'irradiation de la graine.

ОБЩИЙ ПЛАН ОБЛУЧЕНИЯ РАСТЕНИЙ И СЕМЯН В ТЕННЕСИЙСКОМ УНИВЕРСИТЕТЕ

Дано описание источника Co^{60} для облучения растений и семян в Сельскохозяйственной Лаборатории Комитета по Атомной Энергии при Теннессийском Университете в Оак Ридже. Установка, собранная в 1956 г., обеспечивает гамма-излучением генетические работы экспериментальных сельскохозяйственных станций юга США; облучение нейтронами производится в реакторе Национальной Лаборатории Оак Риджа. Согласно данному плану облучению было подвергнуто свыше 500 образцов растений и семян,

* This manuscript is published with the permission of the Director of the University of Tennessee Agricultural Experiment Station, Knoxville, Tennessee. The work was completed under Contract No. AT-40-1-GEN-242 between the University of Tennessee College of Agriculture and the U.S. Atomic Energy Commission.

представляющих в общем около 120 видов растений. Эти образцы были получены от свыше 100 ученых из 22 штатов и 5 стран.

Приводятся данные по чувствительности примерно 60 видов облученных растений одной генерации, а также данные по приблизительно 20 видам, претерпевшим генетические изменения.

Описан метод, позволяющий предсказывать чувствительность к облучению зрелой особи по поведению облученных семян.

DAS KOOPERATIVE PFLANZEN- UND SAMEN-BESTRAHLUNGSPROGRAMM DER UNIVERSITÄT TENNESSEE

Die Co-60 Pflanzen- und Samenbestrahlungsanlage des AEC Agricultural Research Laboratory der Universität Tennessee in Oak Ridge wird beschrieben. Die 1956 errichtete Anlage besitzt eine γ-Strahlenquelle für pflanzengenetische Untersuchungen der landwirtschaftlichen Versuchsstationen im südlichen Teil der USA. Bestrahlungen mit Reaktor-Neutronen werden im ORNL durchgeführt. Mehr als 500 Pflanzen und Samen von etwa 120 Gattungen wurden bestrahlt. Diese Proben wurden von mehr als 100 Wissenschaftlern aus 22 Staaten und 5 Ländern eingesandt. Die Resultate über die Strahlungsempfindlichkeit der behandelten Generation von etwa 60 Pflanzengattungen werden zusammengefasst. Ein zusammenfassender Bericht über die beobachteten genetischen Veränderungen an etwa 20 Gattungen liegt bei.

Eine Methode wird beschrieben, welche die Vorhersage der Dosiswirkung im Stadium der Reife aus dem Verhalten der Keime bestrahlter Samen gestattet.

VOL. 10 1961

INTRODUCTION

THAT ionizing radiations can cause hereditary changes in living material has been known for at least 35 years. Using this knowledge for the benefit of mankind, by deliberately inducing mutations in plants of economic importance, is a more recent development. This exploitation hinged largely on the realization, from painstaking research in many countries (notably Sweden), that most *but not all* such induced changes are injurious to the organism sustaining them, or to the function that organism serves. In economic terms, the cost of irradiating, growing, and examining two or more generations of plants must be balanced against the potential advantage of an improved variety. Discarding thousands of unwanted individuals is, to breeders of most plant species, trivial, if the chance of finding a desirable change is real.

The availability of large radiation sources, from radioactive nuclides, together with the knowledge that some induced mutations have agricultural value, has made radiation-breeding a technique of worldwide importance since the late 1940's. Any tissue that can be propagated is feasible irradiation material, and since some tissues (especially seeds) may be transported over great distances, one radiation device can easily serve many persons in a wide geographical area.

The widespread use of ionizing radiations to induce beneficial mutations in economic plants is emphasized by several recent reviews.[1–5] The varying and largely unpredictable nature of radiosensitivity in most species, tissues and metabolic states is well known, as shown by NILAN[6], and is a handicap in the commencing phase of any radiomutation program. The main purpose of the present paper is to contribute empirical knowledge in this regard.*

The plant and seed irradiation project of the University of Tennessee Atomic Energy Commission Agricultural Research Laboratory was organized in 1956, in part to provide radiation sources for plant geneticists of the Southern agricultural experiment stations. The kinds of radiations considered feasible were neutrons and gamma rays. Neutron irradiation was made available on a fee basis from a nuclear reactor at the Oak Ridge National Laboratory, and a source of gamma

* Since this paragraph was written, a very important finding has been reported by SPARROW and MIKSCHE (*Radiat. Res.* **12,** 474 (1960) abstract). Radiation sensitivity of plants receiving chronic gamma irradiation was said to be highly and positively correlated with nuclear volume (hence with DNA content) of cells of those species. If this correlation can also be found in dormant embryos, there will be less need for papers like the present one.

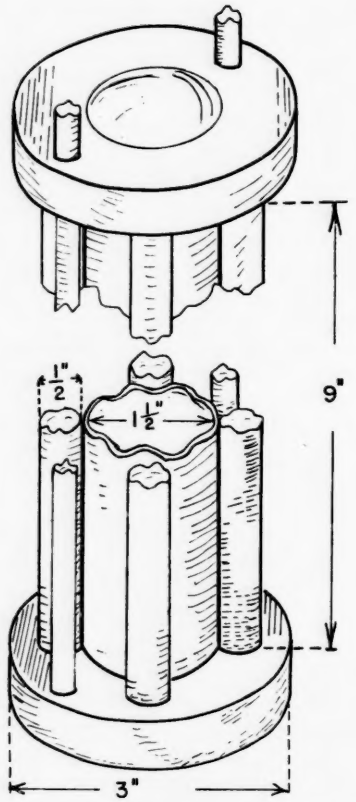

FIG. 1. Stainless-steel holder (cutaway view); Co^{60} pellets and inert spacers are arranged within the ½ in. pipes.

rays existed at the UT-AEC Laboratory. The latter is the unique "animal field" which is a multiple source device.[7] This outdoor facility provides several hundred square feet of space at a uniform flux and low intensity of radiation (about 50 r/hr in January 1960). The source was designed for whole-body irradiation of large animals, and could be used for treating actively growing plants and other materials of high sensitivity. A need existed for a high-intensity source of gamma rays, so one was designed and built.

Construction and description

The UT-AEC seed irradiation unit was constructed for gamma irradiation of dormant seeds and other materials requiring kiloroentgen dosages. It is an indoor device, located in an isolated area, utilizing only water and earth for shielding. The overall unit was designed and built by personnel of this Laboratory; the stainless-steel holder containing radioactive cobalt, by the Isotope Sales Division of the Oak Ridge National Laboratory. The unit consists of one concrete block building housing the source, and another housing the controls 64 ft away. The source is stored, except during use, at the bottom of a 10 ft water-filled well, and the source building is surrounded by earth fill. Access to the source building is by a concrete passageway at right angles to the building entrance. An electrically locked gate is to be installed to assure against accidental entrance.

The stainless-steel holder which houses the cobalt is represented by Fig. 1.

Radioactive cobalt cylinders (1 × 1 cm), totaling 110 ± 10c and separated by inert spacers, were placed in the four peripheral tubes and sealed with silver solder. The cobalt slugs and inert spacers were arranged to reduce any decrease of intensity at the tube ends. Overall length of the source holder is 9 in., with an external diameter of 5 in. and an internal diameter of 1½ in. The unit is designed to provide maximum intensity by intrasource irradiation, and a range of lesser intensities by sample placement outside the holder. The source holder is raised from the well by a hand-cranked cable extending to the control building. Electrical switches activate a series of lights in the control room enabling the operator to estimate the position of the source at any time. A flashing red warning light is also activated when the source leaves the bottom of the well.

Exposure procedures

This gamma-ray facility permits a wide range of intensities to be administered to samples of limited volume. Maximum intensity is achieved from intrasource irradiation. Samples are placed in a lucite cylinder, about 9 in. long and 1 in. across, which becomes surrounded by the source holder when the latter is raised. Dosimetry within

VOL. 10 1961

the cylinder was carried out on 17 August 1956, using the ferrous–ferric reaction with iron sulfate. Intensity at that time was 875 r/min ± 10 per cent for all points within the capsule; intrasource volume is approximately 120 ml.

Samples larger than 1 × 9 in. must be exposed outside the source, and can be placed from 3 to 84 in. from the source. On 5 November 1956, intensity was 21·0 r/min 11 in. from the source center, and considerable variation existed, especially in areas shaded by the vertical support pipes.

A rotating platform, constructed to equalize isodose curves and intrasample dosage (for externally irradiated samples), is represented in Fig. 2. The platform is constructed from plywood and consists of a main table revolving concentrically around the source and carrying a series of smaller tables, each of which revolves about its own axis. The platform is turned by an electric motor in a rim-drive manner, utilizing a simple friction drive to actuate the smaller tables. As the plywood has developed warpage with use, a new platform is being built of aluminum alloy with a chain-driven series of sprockets. The present source may be replaced or supplemented in the near future by another, tentatively planned to contain 500 c of cobalt-60. This would provide an initial intensity about five times that of the original system. Other nuclides have been considered but rejected.

Neutron exposures were made in the west animal tunnel of the Oak Ridge graphite reactor, with an enriched uranium-235 plate beneath the sample cart. It will be noted (Table 1) that although thermal neutrons constitute more than half the total flux, they contribute less than 3 per cent to the effective dose. This is, therefore, essentially a fast neutron source; gamma contamination is about 200 r/hr.

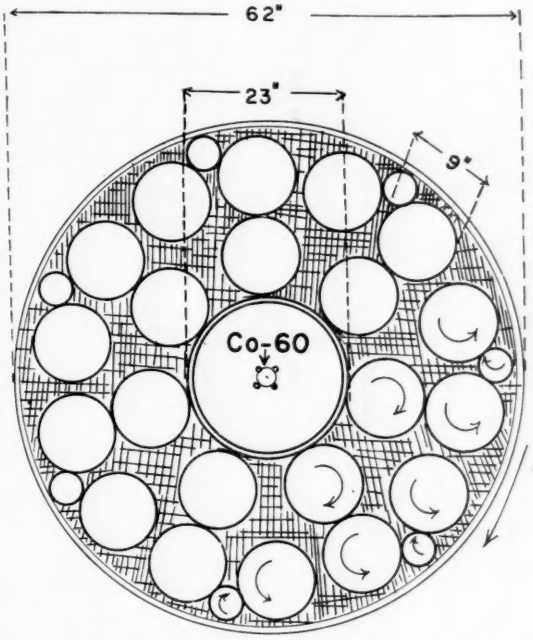

FIG. 2. Rotating table for low-intensity exposures, overhead view. Center rim (23 in. circle) is fixed; movements shown by arrows, including idlers (smallest circles), result from force applied to outer rim (62 in. circle).

TABLE 1. Neutron spectrum of reactor position used in these studies

Monitor foil	Minimum energy perceived (eV)	Neutrons per cm²/sec	Percentage of total flux	Rep/hr*	Percentage of total rep
Au	$2{\cdot}5 \times 10^{-2}$	$4{\cdot}2 \times 10^{8}$	54·5	43·2	2·9
Pu	$2{\cdot}5 \times 10^{4}$	$1{\cdot}9 \times 10^{8}$	24·7	280·8	19·0
Np	$7{\cdot}5 \times 10^{5}$	$1{\cdot}1 \times 10^{8}$	14·3	705·6	47·8
U	$1{\cdot}5 \times 10^{6}$	$3{\cdot}5 \times 10^{7}$	4·5	252·0	17·1
S	$2{\cdot}5 \times 10^{6}$	$1{\cdot}3 \times 10^{7}$	1·7	147·6	10·0
Al	$8{\cdot}6 \times 10^{6}$	$2{\cdot}4 \times 10^{6}$	0·3	46·8	3·2
	Totals	$7{\cdot}7 \times 10^{8}$	(100·0)	1476·9	(100·0)

* After HURST *et al.*[8].

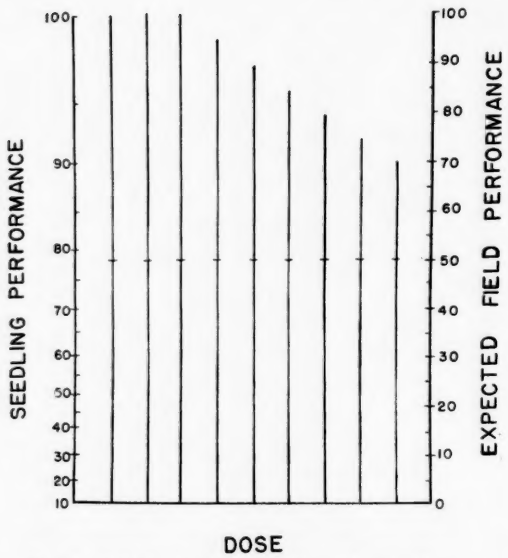

FIG. 3. Grid for predicting mature plant performance from seedling performance following seed irradiation. (See text).

Control of moisture

It was hoped at the outset that useful information on dose response of various species and tissues would be obtained from this cooperative program. It was realized that comparisons would be difficult due to differences in tissue, genotype and growth environment; these variables were considered uncontrollable. Other factors known or considered to be influential were studied for controllability and repeatability. These were, mainly, moisture content of seeds at the time of irradiation, and delay between irradiation and germination. The importance of these factors has been made clear by CURTIS *et al.*[9] (data generously provided before publication).

It was decided that, since very dry and very wet seeds were more sensitive to X-rays or gamma rays than were seeds of normal moisture, the most reasonable approach in such an undertaking—involving many species, persons and locations—would be to precondition all seeds at a moderate humidity. A cabinet containing about 12 cu ft was built for pre-radiation storage of seeds, to maintain a temperature of 70° ± 2° F and 65 ± 5 per cent relative humidity, with forced air. Repeated weighings showed most seeds to stabilize within about 2 weeks, although the water content at stabilization varied between species.

After stabilization, seeds were sealed in polyethylene, irradiated, and returned (still sealed) to the cooperator. Except for a few cases where time was insufficient, all seed samples reported here were preconditioned for moisture. Dates of irradiation and of planting were recorded.

Predicting radiosensitivity

The material most commonly submitted for exposure to radiation has been dormant seeds. Choice of dosages is of primary concern as it is generally desirable to provide exposures which will result in differential survival.

A great many factors influence radiosensitivity in seeds and plants. Some of these are age, moisture content, state of metabolism and, for neutron irradiation, chemical content. These factors may cause a ten- to twenty-fold difference in sensitivity between different kinds of seeds, thus a wide range of doses must be given to most material to insure reaching the "effective" level and not achieving complete lethality. When no data exist on sensitivity of seeds in a species, one is at a loss as to whether to start the dosages at, say, 2500 r of gamma rays or 25,000 r. An obvious possibility is to make a preliminary study, using germination and early growth as criteria of tolerance. In practice, this is of little help because virtually all seeds will sprout and elongate, even after doses sufficient to prevent cell division. A method is needed which accentuates small differences in seedling growth, and permits extrapolation to expected field survival.

We have devised a technique* which permits extrapolation from seedling performance to expected field performance, using a logarithmic basis. The technique is

* Semi-annual Progress Report of UT-AEC Agricultural Research Program, July-December 1956, University of Tennessee, Knoxville, Tennessee.

VOL. 10 1961

TABLE 2. Radiation treatments causing the indicated growth responses relative to untreated control

Scientific name	Common name	Variety	Investigator*	Observation†	Co^{60} γ r/min	Expected reduction in plant survival†			
						Kr of Co^{60} γ		Neutrons (hr)	
						25%	50%	25%	50%
SEEDS									
Alycicarpus vaginalis	Alyceclover	Common	(1)	(a)	1260	>64	—	4·0	5·0
Arachis hypogaea	Peanut	Spantex	(2)	(c)	1260	8	10	2·1	2·5
Asparagus officinalis	Asparagus	—	(3)	(h)	—	—	—	<2·0	2·2
Avena sativa	Oats	Clintland	(4)	(i)	—	—	—	0·5	1·0
Avena sativa	Oats	Forkedeer	(5)	(c)	840	18	27	0·2	0·4
Avena sativa	Oats	LeConte	(5)	(c)	840	7	17	0·2	0·4
Cajanus cajan	Pigeonpea	Kaki	(6)	(b)	1260	9	15	0·5	1·3
Capsicum frutescens	Pepper	Av. of 4	(7)	(b)	1260	13	24	0·6	0·8
Carica papaya	Papaya	—	(8)	(e)	650	10	12	1·8	2·2
Citrullus vulgaris	Watermelon	Sugar baby	(9)	(b)	1280	37	60	—	—
Clematis montana	Clematis	Rubens	(10)	(h)	—	—	—	0·1	0·2
Coffea arabica	Coffee	Av. of 10	(11)	(c)	721	—	<10	—	<1·0
Cucumis sativus	Cucumber	H-57-2	(12)	(b)	697	—	<20	<1·0	1·4
Dactylis glomerata	Orchardgrass	Common	(5)	(c)	844	8	11	0·6	0·8
Festuca elatior	Fescue	Ky. 31	(5)	(c)	844	17	19	0·4	0·7
Forsythia sp.	Forsythia	Beatrix Farrand	(10)	(h)	—	—	—	2·4	3·0
Glycine max	Soybean	Dorman	(13)	(c)	1260	3	11	1·1	2·0
Gossypium hirsutum and G. barbadense	Cotton	Av. of 4	(14)	(i)	1260	<10	11	<1·2	1·4
Gossypium hirsutum	Cotton	Av. of 2	(14)	(i)	612	18	29	>2·0	—
Gossypium hirsutum	Cotton	Blightmaster	(15)	(c)	775	13	21	0·8	1·0
Hemerocallis sp.	Daylily	—	(16)	(d)	752	14	17	—	—
Hibiscus esculentus	Okra	—	(17)	(c)	—	—	—	4·7	5·4
Hordeum vulgare	Barley	Av. of 2	(18)	(b)	850	14	18	0·3	0·5
Hordeum vulgare	Barley	236-3-46	(5)	(c)	844	12	20	0·1	0·3
Hordeum vulgare	Barley	50-112-38	(5)	(c)	844	6	13	0·1	0·2
Lespedeza cuneata	Sericea	Common	(1)	(a)	840	16	37	0·8	1·4
Lespedeza cuneata	Sericea	Ala. 1373	(19)	(b)	795	42	46	1·6	1·8
Lespedeza stipulacea	Korean lesp.	Climax 29A	(20)	(c)	795	—	<40	0·3	0·6
Lupinus angustifolius	Blue lupine	54-1092	(21)	(f)	750	<27	>40	—	<3·5
Lycopersicon esculentum	Tomato	Rutgers	(22)	(g)	1240	6	14	0·8	1·6
Lycopersicon esculentum	Tomato	Av. of 2	(23)	(c)	697	27	37	1·9	2·2
Lycopersicon esculentum	Tomato	Av. of 3	(24)	(c)	609	7	13	—	—
Medicago orbicularis	Buttonclover	Common	(5)	(c)	844	10	21	1·7	2·1
Medicago sativa	Alfalfa	Buffalo	(5)	(c)	844	52	62	1·5	1·8
Medicago sativa	Alfalfa	Dupuits	(5)	(c)	844	23	38	0·2	0·3
Melilotus sp.	Sweetclover	Common	(5)	(c)	844	49	59	1·7	2·3

TABLE 2 (*continued*)

Scientific name	Common name	Variety	Investigator*	Observation†	r/min Co^{60} γ	Expected reduction in plant survival†			
						Kr of Co^{60} γ		Neutrons (hr)	
						25%	50%	25%	50%
SEEDS									
Oryza sativa	Rice	Zenith	(25)	(c)	1260	—	<15	—	<1·2
Oryza sativa	Rice	Nato	(26)	(b)	1240	<15	23	0·7	1·5
Oryza sativa	Rice	Nato	(26)	(b)	775	<20	24	<1·0	1·2
Oryza sativa	Rice	Av. of 2	(27)	(c)	650	33	42	2·2	2·8
Paspalum dilatatum	Dallisgrass	B-230	(28)	(b)	—	—	—	0·8	1·2
Paspalum dilatatum	Dallisgrass	La. 430	(29)	(b)	1260	>64	—	4·6	5·7
Paspalum dilatatum	Dallisgrass	Ya-184	(29)	(b)	710	19	>32	>5·0	—
Paspalum dilatatum	Dallisgrass	Av. of 3	(28)	(b)	—	—	—	—	<2·0
Phaseolus vulgaris	Bean	Blue Lake	(30)	(b)	—	—	—	—	<1·2
Pinus sp.	Pine	Av. of 3 sp.	(31)	(f)	620	—	<10	—	—
Psidium guajava	Guava	Av. of 2	(32)	(b)	1240	9	17	0·3	1·3
Secale cereale	Rye	Gator	(33)	(a)	714	5	8	—	—
Secale cereale	Rye	Balbo	(5)	(c)	840	13	17	0·5	0·6
Secale cereale	Rye	Tetra Petkus	(5)	(c)	840	10	16	0·1	0·3
Sesamum indicum	Sesame	Nicaraguan	(34)	(c)	775	>40	—	>2·0	<6·0
Setaria italica	German millet	Common	(35)	(c)	760	<10	14	—	—
Sorghum halepense	Johnson grass	Av. of 5	(36)	(c)	—	—	—	—	<1·0
Sorghum vulgare	Grain sorghum	Av. of 2	(37)	(b)	1260	32	>40	—	—
Trifolium incarnatum	Crimsonclover	Dixie	(1)	(a)	1240	52	>64	>4·0	—
Trifolium incarnatum	Crimsonclover	Common	(5)	(c)	844	10	25	0·2	0·6
Trifolium pratense	Redclover	Kenland	(38)	(b)	1270	<30	35	—	—
Trifolium pratense	Redclover	Kenland	(38)	(b)	795	<30	42	—	<1·0
Trifolium pratense	Redclover	Kenland	(5)	(c)	844	7	43	0·2	2·0
Trifolium pratense	Redclover	Tenn. W.R.	(5)	(c)	844	84	>108	1·0	2·2
Triticum vulgare	Wheat	Av. of 4	(27)	(c)	3; 670	16	24	0·6	1·1
Triticum vulgare	Wheat	Av. of 4	(27)	(f)	3; 670	19	24	0·5	0·8
Triticum vulgare	Wheat	Seneca	(5)	(c)	840	15	25	0·6	0·9
Triticum vulgare	Wheat	46-1-1	(5)	(c)	840	6	14	0·2	0·5
Vicia villosa	Hairy vetch	Common	(5)	(c)	840	9	17	0·3	0·6
Vigna sinensis	Cowpea	—	(12)	(f)	1260	<4	11	6·6	7·3
Vitis rotundifolia	Grape	Av. of 2	(39)	(e)	1240	—	<4	—	<0·2
Vitis labrusca	Grape	Concord	(40)	(h)	800	>1	<4	—	—
Vitis vinifera X V. rotundifolia	Grape	Farrer 30	(39)	(b)	790	—	<5	—	—
Zea mays	Corn	Av. of 5	(41)	(c)	840	14	>15	1·3	1·9
Zea mays X Tripsacum dactyloides	Zea Tripsacum	BC_4 to Zea	(42)	(i)	790	—	<10	—	<1·0
POLLEN									
Aleurites fordii	Tung	Av. of 2	(43)	(j)	615	>3·2	—	—	—
Gossypium hirsutum	Cotton	Pope	(44)	(j)	1210	0·6	0·7	—	—
Gossypium sp.	Cotton	Av. of 3	(45)	(j)	1210	>3·2	—	—	—

VOL. 10 1961

TABLE 2 (*continued*)

Scientific name	Common name	Variety	Investigator*	Observation†	r/min Co^{60} γ	Expected reduction in plant survival†			
						Kr of Co^{60} γ		Neutrons (hr)	
						25%	50%	25%	50%
POLLEN									
Hibiscus syriacus	Shrubalthea	Snowstorm	(46)	(j)	756	>2·4	—	—	—
Zea mays	Corn	Av. of 2	(41)	(j)	1210	1·0	1·2	—	—
DORMANT BUDS									
Roots									
Ipomoea batatis	Sweetpotato	Av. of 3	(7)	(e)	—	—	—	—	<0·1
Ipomoea batatis	Sweetpotato	Porto Rico	(22)	(e)	11	>4	—	>0·5	—
Ipomoea batatis	Sweetpotato	Porto Rico	(22)	(e)	4	17	20	—	—
Budwood									
Prunus persica	Peach	South Haven	(47)	(l)	810	>8	—	>1·0	—
Cuttings									
Vitis labrusca	Grape	Concord	(40)	(k)	800	4	6	0·4	0·5
Vitis rotundifolia	Grape	Av. of 3	(39)	(h)	5	8	10	—	—
ACTIVE TISSUE									
Cuttings									
Ilex cornuta and I. crenata	Holly	Av. of 2	(48)	(k)	1 to 11	>20	—	—	—
Seedlings									
Pinus taeda	Pine	Loblolly	(39)	(h)	3	—	<1	>0·2	<0·5
Pinus taeda	Pine	Loblolly	(31)	(h)	—	—	<3	—	—

* Name and location of scientists:

(1) D. C. Bain — Mississippi Agr. Exp. Sta.
(2) B. C. Langley — Texas Agr. Exp. Sta.
(3) F. D'Amato — University of Pisa (Italy)
(4) K. J. Frey — Iowa Agr. Exp. Sta.
(5) T. S. Osborne — UT-AEC, Tennessee Agr. Exp. Sta.
(6) R. Abrams — Puerto Rico Agr. Exp. Sta.
(7) A. H. Dempsey — Georgia Agr. Exp. Sta.
(8) P. D. Ramirez — Puerto Rico Agr. Exp. Sta.
(9) V. M. Watts — Arkansas Agr. Exp. Sta.
(10) C. Dorsman — Boskoop, Holland
(11) T. Singh — Puerto Rico Agr. Exp. Sta.
(12) J. L. Bowers — Arkansas Agr. Exp. Sta.
(13) C. E. Caviness — Arkansas Agr. Exp. Sta.
(14) P. J. Lyerly — Texas Agr. Exp. Sta.
(15) L. L. Ray — Texas Agr. Exp. Sta.
(16) H. J. Teas — Florida Agr. Exp. Sta.
(17) W. J. Drapala and J. B. Edmond — Mississippi Agr. Exp. Sta.
(18) T. M. Starling — Virginia Agr. Exp. Sta.
(19) E. D. Donnelly and E. M. Clark — Alabama Agr. Exp. Sta.
(20) M. S. Offutt — Arkansas Agr. Exp. Sta.
(21) I. Forbes — USDA, Georgia Agr. Exp. Sta.
(22) H. D. Swingle — Tennessee Agr. Exp. Sta.
(23) W. R. Sitterly — S. Carolina Agr. Exp. Sta.
(24) L. F. Johnson — Tennessee Agr. Exp. Sta.
(25) T. H. Johnston — USDA, Arkansas Agr. Exp. Sta.
(26) M. T. Henderson — Louisiana Agr. Exp. Sta.
(27) J. F. Schuler — N. Carolina Agr. Exp. Sta.
(28) C. R. Owen — Louisiana Agr. Exp. Sta.
(29) E. C. Bashaw — USDA, Texas Agr. Exp. Sta.
(30) W. F. Jenkins — Mississippi Agr. Exp. Sta.
(31) T. S. Davis — Georgia Agr. Exp. Sta.
(32) J. Velez-Fortuno — Puerto Rico Exp. Sta.
(33) A. T. Wallace — Florida Agr. Exp. Sta.
(34) G. W. Rivers — USDA, Texas Agr. Exp. Sta.
(35) W. L. Settle — R. 1, Keystone, Indiana
(36) D. I. Dudley — Texas Agr. Exp. Sta.
(37) H. B. Harris — Georgia Agr. Exp. Sta.
(38) N. L. Taylor — Kentucky Agr. Exp. Sya.
(39) B. O. Fry — Georgia Agr. Exp. Sta.
(40) J. W. Fleming — Arkansas Agr. Exp. Sta.
(41) L. M. Josephson — USDA, Tennessee Agr. Exp. Sta.
(42) R. G. Reeves — Texas Agr. Exp. Sta.
(43) G. F. Potter — USDA, Bogalusa, Louisiana

TABLE 2 (*continued*)

(44) D. M. Simpson and J. B. Pate	USDA, Tennessee Agr. Exp. Sta.	(46) J. S. Alexander	Tennessee Agr. Exp. Sta.
(45) N. I. Hancock	Tennessee Agr. Exp. Sta.	(47) J. N. Moore	Arkansas Agr. Exp. Sta.
		(48) W. W. Wyatt	University of Tennessee

† Figures representing expected reduction in plant survival for observations (a) through (g) were calculated from the grid shown in Fig. 3; (h) through (j) are actual values:

(a) Laboratory germination X seedling height
(b) Greenhouse emergence X seedling height
(c) Field emergence X seedling height
(d) Laboratory germination
(e) Greenhouse emergence
(f) Field emergence
(g) Seedling height
(h) Field or greenhouse survival
(i) Plants producing seeds
(j) Flowers producing seeds
(k) Cuttings producing roots
(l) Survival of bud grafts

similar in principle to that proposed by ATWOOD and NORMAN[10] for a micro-organism, modified by our findings with multi-tissue systems. A graph is used (Fig. 3) with radiation dosage as the abscissa, and two ordinates: one, for seedling performance, from 10 to 100 on a reversed log scale; the other, for field performance, from 0 to 100 on an arithmetic scale. One obtains germination percentage multiplied by average seedling height, as per cent of control, and plots these data for different dosages using the log ordinate. Any point on the curve thus obtained is then read against the arithmetic ordinate, yielding a value for field performance—survival to maturity times fertility as percentage of control—expected for that dose of radiation. While this method is tentative, it is of immense help in choosing a "proper" dose-range from easily obtained germination data. If this logarithmic technique is valid, there are important implications concerning the mechanisms of radiation damage to dormant embryos.

RESULTS

The radiation sources have been used for treating several hundred samples covering wide ranges of materials and dosages. The materials include many types of seeds, both dormant and hydrated; dormant buds, tubers and rhizomes; potted plants, pollen and flowers. Treatments have been made for personnel of the Laboratory, cooperators in the Southern states, and interested persons in these and other states and other countries. Use of these sources is restricted to non-profit research, and exposures are carried out without charge.

Report forms are sent to each individual submitting material for treatment. These forms were designed to facilitate comparing

TABLE 3. Relative sensitivities of dormant seeds: exposures resulting in plant survival of about 50 per cent (species arranged in order of increasing resistance within and between groups)

A. *Cobalt-60 gamma-ray exposure*

1–9 Kr:	Grape, pine, coffee
10–18 Kr:	Peanut, soybean, cowpea, orchardgrass, papaya, German millet, rye, pigeonpea, corn, cucumber, guava, daylily, hairy vetch, barley
19–36 Kr:	Fescue, cotton, tomato, buttonclover, wheat, oats, pepper, rice
37–54 Kr:	Lespedeza, sesame, grain sorghum, blue lupine, sericea, dallisgrass, crimsonclover, alfalfa
55–72 Kr:	Redclover, sweetclover, watermelon, alyceclover

B. *Neutron exposure*

0·1–0·5 hr	Grape, clematis, coffee, barley, rye
0·6–1·0 hr	Oats, hairy vetch, lespedeza, fescue, orchardgrass, pepper, wheat, Johnsongrass, alfalfa
1·1–2·0 hr	Bean, pigeonpea, guava, cucumber, cotton, rice, sericea, redclover, tomato, corn, soybean
2·1–4·0 hr	Buttonclover, asparagus, papaya, sweetclover, crimsonclover, peanut, dallisgrass, forsythia, blue lupine
4·1–8·0 hr	Alyceclover, okra, sesame, cowpea

VOL. 10 1961

TABLE 4. Changes observed in R_2 and subsequent generations following irradiations by the UT-AEC Agricultural Research Laboratory

Material exposed	Radiation exposure		Changes appearing after treatment	Investigator*
	Type	Dosage		
Watermelon seeds	Co^{60} γ	8 Kr, 64 Kr	Nonpubescence, sterility (seedless melons), pale green foliage	V. M. Watts
Cucumber seeds	Co^{60} γ	20–60 Kr	Absence of tendrils, self-sterility, dwarfing, flower proliferation, absence of secondary branching	J. L. Bowers
Cucumber seeds	Neutrons	1–4 hr	Semi-erect growth habit, dwarfing	J. L. Bowers
Soybean seeds	Co^{60} γ	8–20 Kr	Disease resistance (*Pseudomonas glycines*), upright growth habit, coarse leaves, sterility	C. E. Caviness
Soybean seeds	Neutrons	2·5–5 hr	Disease resistance (*Pseudomonas glycines*), sterility	C. E. Caviness
Cotton pollen	Co^{60} γ	0·4–3·2 Kr	Early prolific type, earliness, sparse branching, large leaves, large plants, small leaves, small bolls, sterility, delayed maturity, pointed bolls, curled leaves, dwarfing, light green foliage	N. I. Hancock
Cotton seeds	Co^{60} γ Neutrons	10–15 Kr 1·2–5 hr	Earliness, height differences, cluster types, large leaves, green stemmed Pima type in upland cotton, miniature plants, sterility, chlorophyll deficiencies, velvety leaves, crinkled leaves, small corolla glands	P. J. Lyerly
Cotton seeds	Co^{60} γ	10–30 Kr	Sterility, chlorophyll deficiencies malformed cotyledons, probable chromosomal derangements	L. L. Ray
Cotton seeds	Neutrons	1 hr	Malformed cotyledons, probable chromosomal derangements	L. L. Ray
Sweetpotato roots	Co^{60} γ	10–40 Kr	Color changes in roots (first generation growth only)	T. P. Hernandez (1)
Tomato seeds	Co^{60} γ	16–64 Kr	Mild resistance to Southern blight (*Sclerotium rolfsii*), dwarfing, chlorosis	P. A. Young
Tomato seeds	Neutrons	1 and 4 hr	Mild resistance to Southern blight (*Sclerotium rolfsii*), large plants, entire leaflets (*e*-allele type) lanceolate leaves with parallel veins, purple seedlings, sterility, lethality, dwarfing, chlorosis	P. A. Young
Tomato seeds	Co^{60} γ	20 Kr	Delayed maturity, profuse dichotomous branching	T. P. Hernandez (1)
Lespedeza seeds	Co^{60} γ	40–80 Kr	Prostrate growth habit, narrow leaflets, thick dark leaves (possible tetraploid), five leaflets, sterility, dwarfing, chlorophyll deficiencies, flower color variants	M. S. Offutt

TABLE 4 (*continued*)

Material exposed	Radiation exposure		Changes appearing after treatment	Investigator*
	Type	Dosage		
Tobacco seeds	Co^{60} γ	50 Kr	Resistance to black shank	J. L. Apple (2)
Rice seeds	Co^{60} γ	30 and 40 Kr	Sterility, dwarfing, chlorophyll deficiencies	N. E. Jodon (3)
Rice seeds	Co^{60} γ	35 Kr	Tall plants	T. H. Johnston
Rice seeds	Neutrons	2 and 2·5 hr	Purple hulls, short strawed types, leaf stripe on seedlings	T. H. Johnston
Dallisgrass seeds	Neutrons	0·5–3 hr	Yellow anthers, narrow leaves, delayed maturity, chlorophyll deficiencies	C. R. Owen
Dallisgrass seeds	Co^{60} γ	4–64 Kr	Prostrate growth habit, yellow anthers, narrow leaves, fine stems, reduced vigor, dwarfing, deformed inflorescences	E. C. Bashaw
Dallisgrass seeds	Neutrons	1·2–5 hr	Prostrate growth habit, narrow leaves, fine stems, yellow anthers, reduced vigor, dwarfing, deformed inflorescences	E. C. Bashaw
Sesame seeds	Co^{60} γ	20 and 50 Kr	Earliness, long capsules, red stems and capsules, profuse branching, dwarfing, "potato" leaves	G. W. Rivers
German millet seeds	Co^{60} γ	10–40 Kr	Large plants and spikes, delayed maturity, enlarged stalks, elongated pedicels, adventitious roots from four lowest nodes, seeds borne on setae	W. L. Settle
Redclover seeds	Co^{60} γ	30–150 Kr	Self fertility, sterility	N. L. Taylor
Grape plants	Co^{60} γ	0·6–11·7 Kr	Increased vigor, earliness, large leaves, apparent tetraploidy (large fruit, large dark green leaves, and thick stems) (first generation)	B. O. Fry
Corn seeds	Co^{60} γ	10 and 15 Kr	Short plants, chlorophyll deficiencies	L. M. Josephson
Corn seeds	Neutrons	0·5–4 hr	Short plants, ribbon leaf, small seeds, no seeds, chlorophyll deficiencies	L. M. Josephson
Wheat seeds	Neutrons	0·5 hr	Two R_3 progenies resistant to *Septoria nodorum* in the variety "Seneca"	T. S. Osborne

* Addresses given in Table 2 unless otherwise indicated.
(1) T. P. Hernandez, Louisiana Agr. Exp. Sta.
(2) J. L. Apple, North Carolina Agr. Exp. Sta.
(3) N. E. Jodon, USDA, Louisiana Agr. Exp. Sta.

biological injury and genetic changes in the many types and species of material treated with different kinds and amounts of radiation.

Cooperators have returned reports describing post-irradiation observations for about 30 per cent of the 507 seed and plant samples exposed in the 4 years. Most reports describe effects upon seedling growth and plant development from treated seeds, while the remainder pertain to effects of exposure

VOL. 10 1961

of other plant parts and to radiation-induced genetic changes. The data in Table 2, arranged alphabetically by genera, represent first-generation effects from exposure of seeds and other plant parts. The designated levels of gamma rays or neutrons refer to the total dosages which resulted in 25 per cent and 50 per cent reductions in survival. The investigator reporting each set of data and the specific growth characteristics reported are designated parenthetically. Direct comparisons should be tentative because of differences in features studied, environmental conditions, methods of planting and care, and kinds of notes taken, as well as variations in seed moisture, genotype and post-radiation storage.

The dosage levels giving relative effects as stated can be used as approximate values regarding sensitivity to radiation. The data in Table 2 provide only two points on each dose-response curve, but these indicate the range of dosages which might be used to obtain differential survival for certain species and tissues.

Table 3 contains a summary of the apparent sensitivity of certain species, based on growth response following irradiation of seeds. The groups are arranged in order of increasing radioresistance, as are the species within groups.

Certain general observations can be made on the basis of the tabulated values. Small-seeded legumes and dallisgrass appear to be very resistant to both neutrons and gamma rays, while rice, tomato and cotton are moderately resistant. Rye and barley are moderately sensitive; coffee and grape appear to be very sensitive. Peanut, soybean and cowpea are especially sensitive to injury from gamma radiation while being resistant to neutrons, and the opposite condition exists for oats, wheat and lespedeza. Treatments involving pollen, buds and plants were not included in this tabulation.

Observations of induced changes in R_2 and subsequent generations from exposure of seeds or pollen, except for treatments involving grape and sweetpotato, are listed in Table 4. First-generation observations are reported in these two species, in which vegetative tissues were treated. Some of the variants listed here are of potential economic value, although most are obviously undesirable. The majority of changes occurred following dosages producing approximately 50 per cent reduction in performance of R_1 plants.

Acknowledgments—In such a large, cooperative undertaking as this, the number of persons contributing is inevitably too large to be listed completely. Besides those cooperators who generously permitted our using their data (see Tables 2 and 3), thanks are due to present and former personnel of the Oak Ridge and Brookhaven National Laboratories, especially Dr. Seymour Shapiro of the latter institution, for advice in the early stages of the program.

REFERENCES

1. Torssell R. (Ed.) *Acta agric. Scand.* **43,** 359 (1954).
2. Shapiro S. In: *Conference on Radioactive Isotopes in Agriculture*, U.S. Atomic Energy Commission, TID-7512, 141 (1956).
3. Smith H. H. *Bot. Rev.* **24,** 1 (1958).
4. Sparrow A. H. and Konzak C. F. In: *Camelia Culture*. (Edited by Tourje E. C.) p. 425. Macmillan, N.Y. (1958).
5. Brock R. D. *J. Aust. Inst. agric. Sci.* **23,** 39 (1957).
6. Nilan R. A. In: *Conference on Radioactive Isotopes in Agriculture*, U.S. Atomic Energy Commission, TID-7512, 151 (1956).
7. Wilding J. L., Simons C. S. and Rust J. H. *Nucleonics* **10** (5), 36 (1952).
8. Hurst G. S., Harter A. J., Hensley P. N., Mills W. A., Slater M. and Reinhardt P. W. *Rev. Sci. Instrum.* **27,** 153 (1956).
9. Curtis H. J., Delihas N., Caldecott R. S. and Konzak C. F. *Radiat. Res.* **8,** 526 (1958).
10. Atwood K. C. and Norman A. *Proc. Nat. Acad. Sci.* **35,** 696 (1949).

technical notes

Precision Plating of Stearic Acid-1-Carbon-14 from Benzene Solutions*

(*Received* 18 *July* 1960)

THE precision of counting replicate samples of organic compounds labeled with carbon-14 suffers materially because of the large effects of sample geometry, self-absorption and backscatter in counting "soft beta" radiation. Due to its low maximum energy (0·155 MeV) and short range, the beta radiation from C^{14} is largely absorbed by layers of inert material or carrier between the radioactive atoms and the counter. The general equation given below shows the large factor due to self-absorption in counting low-energy radiations.[1]

$$I = I_0 e^{-\alpha d}$$

where I = the observed radiation intensity
I_0 = the intensity with no absorber
α = absorption coefficient = $5/l_0$
d = absorber thickness in mg/cm^2
and l_0 = range of the most energetic beta rays in $\frac{\text{milligrams of Al}}{\text{square centimeters}} = (1/150)E^{5/3}$, where E is the upper energy limit in kilovolts.

The authors required a quick and precise method of counting benzene solutions of stearic acid with a thin end-window Geiger counter. The technique of converting organic compounds to barium carbonate for counting mounts of infinite thickness has been used with fatty acids.[2] However, it is a measure of specific activity, while the requirement was to determine different concentrations of stearic acid having the same specific activity. A procedure developed by FREEMAN and HUME[3] for precision counting of beta radiation from strontium-90 solutions was not applicable because the lacquer applied on top of their liquid samples could be penetrated by only a small portion, if any, of the low-energy beta rays emitted by carbon-14. (Beta rays from strontium-90 are relatively energetic, with a maximum energy of 0·61 MeV.) The use of a dip type of counter would avoid the necessity of plating the solutions but did not seem advisable since the counter itself, according to COOK and RIES,[4] could sorb as much as 0·3 of a monolayer of stearic acid on its surface. A liquid scintillation counter, which also makes sample plating unnecessary, was not available.

Experimental

Stearic acid-1-carbon-14 (purchased from Tracerlab, Inc., Waltham, Mass., and from Volk-Radiochemical Co., Chicago) was dissolved in dry benzene and added to solutions of inert stearic acid to obtain the desired specific activity. A 0·1 ml Mohr measuring pipette, filled and emptied by means of a thumbscrew type of pipette filler (Adams Suction Apparatus), was used to transfer 0·1 ml solution aliquots to detergent-cleaned 25 mm watch glasses or $1\frac{1}{4}$ in. Teflon discs that had been chilled in a refrigerator. The chilled substrates were kept cold on a bed of cracked ice during the plating process and were returned to the refrigerator for slow solvent evaporation. The Teflon discs were examined carefully before use and those having scratched surfaces were discarded because of the unfavorable effect of scratches on the shape of the stearic acid deposit. As shown in Table 1, the average deviation in replicate plates obtained by this technique was usually under 2 per cent and often less than 1 per cent.

To correct for self-absorption, back-scatter of radiations and differences in deposit diameter obtained from 0·1 ml aliquots of different concentrations, an empirical correction curve was constructed for each specific activity of interest. A stearic acid solution of the desired specific activity was diluted with dry benzene to several different concentrations. Four 0·1 ml aliquots of each concentration were plated on chilled watch glasses as described above and counted with an end-window Geiger counter. The data were corrected for dead time[5] and tube response and were plotted as concentration vs. counts per minute. From the resulting curve the concentrations of unknown solutions could be determined as long as their specific activity and plated volumes were the same as those used for the standard curve and if their concentrations did not exceed about 20 g/l. At higher concentrations the curve rises sharply as the plated aliquots approach "infinite thickness," and all concentrations above some critical concentration give a constant maximum count except when there are differences in deposit diameter. In addition, the higher concentrations are more difficult to plate uniformly. Consequently, if counts from a sample fall above the point for 20 g/l.

* The work reported herein was made possible by Office of Isotopes Development of the U.S. Atomic Energy Commission, Contract No. AT (38-1)-202. Reproduction of this article in whole or in part is permitted for any purpose by the United States Government.

TABLE 1. Deviation in replicate samples of radiostearic acid plated from benzene solutions

Specific activity of stearic acid (mc/g)	Substrate	Solution concentration (g/l.)	Average sample count (c/m)	Number of plates	Average deviation in plates (%)
0·219	Watch glass	8·615	12,458 ± 79	4	1·5
0·219	Teflon	8·615	14,238 ± 84	4	1·0
0·219	Teflon	8·615	15,762 ± 73	13	2·5
0·278	Watch glass	10·79	17,225 ± 90	10	2·4
0·278	Watch glass	0·108	1,929 ± 31	3	0·9
0·278	Teflon	10·79	19,984 ± 82	3	1·5
0·278	Teflon	10·79	20,498 ± 83	6	1·3
0·278	Watch glass	10·0	14,804 ± 86	12	1·0
0·246	Watch glass	4·064	12,174 ± 50	5	1·1
0·248	Watch glass	2·14	3,726 ± 18	3	1·7
0·248	Watch glass	2·10	3,663 ± 29	4	1·7
0·248	Watch glass	2·86	5,623 ± 36	4	1·2
0·248	Watch glass	3·13	6,183 ± 37	4	2·6
0·248	Watch glass	4·02	7,928 ± 42	4	1·7
0·248	Watch glass	2·59	4,673 ± 31	5	1·7
0·248	Watch glass	4·027	7,268 ± 40	5	0·3
0·248	Watch glass	4·027	7,124 ± 39	5	1·5
0·248	Watch glass	1·98	3,498 ± 27	5	1·5
0·246	Watch glass	3·86	11,592 ± 51	4	0·3
0·127	Watch glass	2·87	6,036 ± 35	5	1·2
0·481	Watch glass	3·07	13,790 ± 79	4	1·8
0·481	Watch glass	3·31	14,856 ± 79	5	0·9
0·127	Watch glass	7·854	11,972 ± 73	4	1·3
0·127	Watch glass	3·941	6,212 ± 53	4	1·0
0·127	Watch glass	4·620	7,520 ± 56	5	1·1
0·127	Watch glass	6·283	9,732 ± 66	4	1·7
0·127	Watch glass	1·919	3,173 ± 37	4	2·4
0·127	Watch glass	1·094	1,892 ± 25	4	1·6
0·127	Watch glass	3·023	4,942 ± 47	4	1·2
0·246	Watch glass	8·15	16,530 ± 100	6	1·1
0·246	Watch glass	7·55	15,287 ± 101	4	1·8
0·246	Watch glass	7·44	15,071 ± 100	4	1·5
0·246	Watch glass	7·06	14,346 ± 94	5	1·8
0·246	Watch glass	7·25	14,696 ± 100	4	1·4
0·246	Watch glass	7·61	15,445 ± 95	9	1·9
0·246	Watch glass	7·26	14,122 ± 97	4	1·1
0·246	Watch glass	7·55	14,711 ± 99	4	1·9
0·246	Watch glass	8·15	15,828 ± 73	4	2·0
0·246	Watch glass	2·77	6,267 ± 37	4	1·2
0·246	Watch glass	4·065	9,197 ± 45	4	1·5
0·246	Watch glass	3·52	10,677 ± 49	4	1·8
0·246	Watch glass	3·59	9,900 ± 47	4	1·1

on the correction curve, the unknown solution should be diluted and replated.

Discussion

During a given series of analyses, either Teflon discs or watch glasses were used. A solution plated on Teflon gave higher counts than when plated on watch glasses. Greater self-absorption in the thick portion of the deposit at the center of the watch glass and the closer approach to the counting tube of the flat disc than the concave watch glass account for this difference.

When benzene-stearic acid solutions are plated on solid substrates, the cleanliness of the surface and its wettability by benzene are important. Also, since benzene is highly volatile, the speed of precipitation and consequently the physical characteristics of the

VOL. 10 1961

deposit are affected by the ambient temperature, drafts from windows or air conditioners, and the speed of ejection from pipette or syringe. These factors should be controlled as much as possible.

M. C. KORDECKI
M. B. GANDY

Georgia Institute of Technology
Atlanta
Ga., U.S.A.

References

1. LIBBY W. F. *Analyt. Chem.* **19,** 2 (1947).
2. TIDWELL H. C., DUNKELBERY C., WOOD W. A. and BURR W. W. JR. *J. biol. Chem.* **220,** 733 (1956).
3. FREEDMAN A. J. and HUME D. *Science* **112,** 461 (1950).
4. COOK H. D. and RIES H. E. JR. *J. phys. Chem.* **63,** 226 (1959).
5. TOMLINSON J. D. *J. chem. Educ.* **31,** 203 (1954).

A Nomogram for Calculating Autoradiograph Exposures

(*Received* 8 *September* 1960)

CURRENT work in this laboratory with I^{131}-labelled proteins requires that autoradiographs of different paper electrophoretograms should receive the same radiation dose to facilitate visual comparisons. Each sample would contain the same total activity, if corrected for decay, but the different papers only become available for preparing the autoradiographs at different times, varying by a week or more. Furthermore, the exposure required is not short compared with the half-life of the isotope, so that it is not sufficient to apply a simple decay factor appropriate to the start of the exposure.

To permit equalization of exposures a nomogram has been constructed, based on the following considerations applicable to any radioactive isotope. Let an isotopically labelled sample contain N_0 atoms of the radioactive species at time t_0. Then at time t_1 there will remain $N_0e^{-\lambda t_1}$ atoms, where λ is the decay constant of the isotope in question, and similarly for other times t_2, t_3, t_4. Thus the number of atoms that have decayed during time t_2–t_1 is $N_0(e^{-\lambda t_1} - e^{-\lambda t_2})$, and the number that have decayed during time t_4–t_3 is $N_0(e^{-\lambda t_3} - e^{-\lambda t_4})$. The condition that an autoradiograph exposed for time t_2–t_1 should receive the same total radiation dose as one exposed for time t_4–t_3 is therefore:

$$N_0(e^{-\lambda t_1} - e^{-\lambda t_2}) = N_0(e^{-\lambda t_3} - e^{-\lambda t_4})$$

so that

$$e^{-\lambda t} - e^{-\lambda t_2} = e^{-\lambda t_3} - e^{-\lambda t_4}. \qquad (1)$$

The nomogram is based on this equation. It can be constructed in terms of half-lives, so as to be applicable to any isotope, but for practical purposes it is more useful to have the scales graduated in days for use with one specific isotope. The example shown (Fig. 1) is for use with I^{131}, and also includes half-life scales for the general case.

Scale A is based on a linear plot of $e^{-\lambda t}$ extending from zero (for $t = \infty$) to unity (for $t = 0$); scale C is similar but inverted. For each isotope, values of $e^{-\lambda t}$ for different values of t can be calculated or, with sufficient accuracy for the present purpose, read off from a semilogarithmic decay plot, in which $e^{-\lambda t}$ equals unity for $t = 0$ and equals 0·5 for $t = T_{\frac{1}{2}}$. The non-linear scale for t can thus be drawn. Scale B is half the length of A and C and is equi-distant from them.

A straight line joining t_1 on scale A with t_2 on scale C intersects scale B at a point corresponding to $e^{-\lambda t_1} - e^{-\lambda t_2}$, that is, the fraction of the initial radioactivity (at time $t = 0$) that has decayed during time t_2–t_1. If another line is drawn through the same point on B, but cutting scale A at t_3 and scale C at t_4, then equation (1) is satisfied by t_1, t_2, t_3, t_4, and the nomogram can be used to find one of the t's when the other three are known.

In the example shown, an autoradiograph exposed from 2 days to 5 days 4 hr has received 0·2 of the

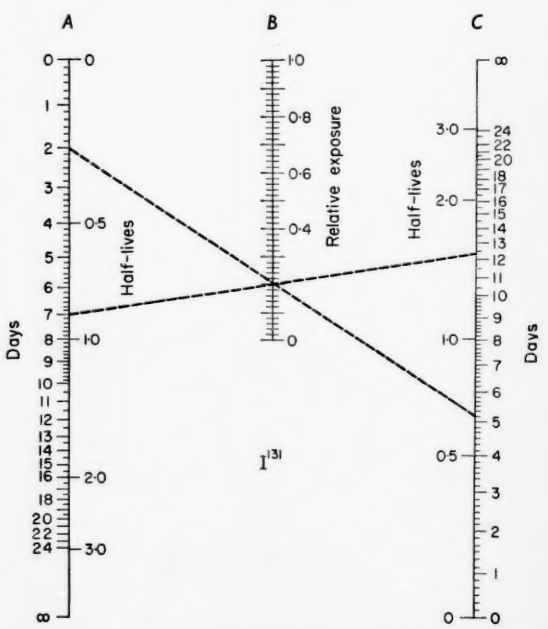

FIG. 1. Example of a nomogram for calculating autoradiograph exposures.

initial radioactivity. A second autoradiograph is to receive the same radiation dose and exposure is to start on day 7. A line drawn from day 7 on *A* through 0·2 on *B* shows that the exposure must finish at 12 days 8 hr. It may be noted that all times are calculated from some convenient arbitrary zero which can often be taken as the start of exposure of the first autoradiograph.

Graduations on scale *B* are not necessary for the purpose of equalizing exposures, but they make the nomogram more versatile; it can thus be used for calculating exposures so that one autoradiograph should have a radiation dose differing from that of another by a required factor, or for counting calculations with short-lived isotopes, when the period of counting a sample is not short compared with the half-life.

In calculating autoradiograph exposures by this method, the possibly non-linear response with time of the photographic emulsion should not be overlooked. Thus prolonged exposure, beyond say 2 or 3 weeks, may lead to latent image fading.

W. G. Duncombe

The Wellcome Research Laboratories
Beckenham, Kent

VOL. 10 1961

letters to the editors

Assay of Radioactive CO_2 in Geiger Counters

(*Received* 23 *February* 1961)

Boyce and Cameron have now reported a method for Geiger counting of radioactive carbon dioxide[1]. They add 1 cm of alcohol vapour and obtain, at a CO_2 pressure of 10–15 cm, a plateau of 160 V with a slope of 2 per cent/100 V or less. The length of the plateau decreases sharply with increasing pressure of CO_2, and disappears at a pressure of 25 cm.

It may be pointed out that we have been using gas counting of CO_2 for nearly ten years without having to add a foreign gas.[2–6] The CO_2 is not purified specially. Plateaus of 400–500 volts, with negligible slope, have been obtained regularly with a modified Neher-Pickering quenching circuit. We have now found that these plateaus are situated largely in the region of limited proportionality.

More recently, another type of circuit, based on new principles, has been introduced. This circuit is distinguished by high sensitivity and high quenching power.[7] With this circuit, unpurified CO_2, again without addition of a foreign gas, can be measured at any pressure between 20 cm and 76 cm Hg, and presumably (if sufficient voltage were available) also at even higher pressures. At 76 cm, the length of plateau is 1200 V with an average slope of 0·25 per cent/100 V. These results are described in detail in papers to be published shortly.[8,9]

Acknowledgment—Our work has been supported by the Jane Coffin Childs Memorial Fund for Medical Research.

B. Kalab
E. Broda

Institute for Physical Chemistry
The University
Vienna

References

1. Boyce I. S. and Cameron J. F. *Int. J. appl. Rad. Isotopes* **9,** 133 (1960).
2. Rohringer G. and Broda E. *Z. Naturf.* **8b,** 159 (1953).
3. Reinharz M., Rohringer G. and Broda E. *Acta phys. Austr.* **8,** 285 (1954).
4. Broda E. and Rohringer G. *Z. Elektrochem.* **58,** 634 (1954).
5. Broda E. *J. Inorg. Nucl. Chem.* **1,** 412 (1955).
6. Suschny O., Kellner G., Broda E., Figdor B. and Rücker W. *Exper. Cell Res.* **14,** 316 (1958).
7. Kalab B. *J. Sci. Instrum.* In press.
8. Broda E. and Kalab B. *Mikrochim acta.* In press.
9. Kalab B. and Broda E. Unpublished.

VOL.
10
1961

book reviews

LIESELOTT HERFORTH und HARTWIG KOCH: **Radiophysikalisches und Radiochemisches Grundpraktikum.** VEB Deutscher Verlag der Wissenschaften Berlin, 1959. 468 Seiten, DM 29,20

DIE Anwendung radiochemischer Messmethoden über den engen Bereich einiger Spezialinstitute hinaus ist heute bereits so weit verbreitet, dass man jeden Versuch begrüssen sollte, für die Teilnehmer entsprechender Praktika eine handliche kritische Übersicht über Messmethoden und Anwendungsbereiche zu schaffen. In der deutschsprachigen Literatur herrscht bisher ein empfindlicher Mangel an derartigen Praktikumsleitfäden. Der vorliegende Band ist wie aus dem Vorwort zu entnehmen ist, aus der Laboratoriumspraxis heraus unter Mitwirkung verschiedener Mitarbeiter entstanden. Im 1. Teil (bis Seite 225) hat der Physiker das Wort, und es werden ausführlich und kritisch die verschiedensten Messmethoden und ihre Auswertung besprochen, so dass er jedem Teilnehmer an einem radiochemischen oder physikalischen Lehrgang empfohlen werden kann. Jedes einzelne Kapitel enthält eine allgemeine Einführung, die Aufgabenstellung, eine Besprechung der theoretischen Grundlagen, die Angabe des zum Versuch erforderlichen Arbeitsmaterials, eine Arbeitsanleitung und die Besprechung und Auswertung eines Versuchs. Diese übersichtliche und vorbildliche Einteilung ist konsequent auch für den 2. Teil des Buches beibehalten worden. Leider ist das beinahe auch das einzige, was man am 2. Teil als vorbildlich ansprechen kann. Abgesehen von einer ganzen Anzahl von Vorschriften, die bestimmt nicht von einem Analytiker und vermutlich nicht einmal von einem Chemiker gegeben worden sind, sind in den Berechnungen und Auswertungen Fehler unterlaufen, die vermuten lassen, dass es sich bei den experimentellen Ergebnissen des 2. Teils um eine praktisch unkontrollierte Zusammenstellung von Praktikumsprotokollen handelt. Die dadurch bedingte Entwertung des Buches ist umsomehr zu bedauern, als gute zuverlässige Anleitungen zum Arbeiten mit radioaktiven Substanzen für den Chemiker von wesentlich grösserer Bedeutung sein können als für den Physiker.

Die Art der Entstehung dieses Buches lässt allerdings hoffen, dass die vorliegende Form von den Verfassern nicht als endgültig angesehen wird, so dass die Möglichkeit gegeben scheint, bei der nächsten Auflage das radiochemische Praktikum in seinem Wert den radiophysikalischen Übungen anzugleichen.

F. STRASSMANN

A. J. SWALLOW: **Radiation Chemistry of Organic Compounds.** Pergamon Press, London & New York, 1960, 380 pp.

DR. Swallow's monograph is the first published volume reviewing the field of organic radiation chemistry. This part of the subject was inevitably neglected during that period following the last war when, as a result of the Atomic Energy Programme, radiation chemistry received a considerable impetus. The demands of this programme, however, lead to considerable emphasis being placed on the radiolysis of water and aqueous solutions, and only comparatively recently has there been a revival of interest in organic radiation chemistry.

The book reviews in general terms the interaction of radiation with matter, followed by a chapter on experimental methods. It is to be noted from the introduction to the volume, that it forms part of a series on radiation effects on materials, the first member of the series, *Atomic Radiation and Polymers* by A. Charlesby having already been published. Since this first volume also reviews the principles of the interaction of high energy radiation with matter, and also contains a lengthy chapter on experimental methods, it is, in the reviewer's opinion, at least debatable whether this repetition is desirable in all the individual volumes in a series. Following these two introductory chapters, there is a further chapter reviewing briefly the radiolysis of water and aqueous systems, after which follows the meat of the book. The radiation behaviour of most of the common classes of aliphatic and aromatic compounds is considered, and there are chapters on the effect of radiation on polymers, dyestuffs and substances of biological interest such as steroids, carbohydrates, amino acids, thiols, proteins, nucleic acids, etc. Finally, there is a chapter which includes a discussion on possible industrial uses of radiation in the chemical industry and its use for the sterilization of food and pharmaceuticals.

On the whole, the author is to be congratulated on his review of the above fields, although again, in view of the detailed description of radiation effects on polymers contained in the first volume of the series it is questionable whether or not the chapter on the effect of radiation on polymers is redundant. The reviewer feels that the publishers of the two volumes have erred in not ensuring the correct sequence of volumes in the series, since as it stands, Swallow's book makes an excellent introduction to the field of

organic radiation chemistry which might well have been followed up by Charlesby's book.

The book is apparently free of major errors although there are a number of minor ones: for example, on page 2, "dimerization" can hardly be called "condensation polymerisation". These minor defects do not detract from the value of the book: they have, however, been communicated to the author.

There is evidence in the book, from the references quoted, that some considerable time has elapsed between the presentation of the final manuscript and the publication of the volume. There are relatively few references to journals published at the beginning of 1959. Such a delay in publication is obviously undesirable, particularly in a rapidly expanding subject such as radiation chemistry.

The reviewer finds the referencing system tedious, since it is difficult, when only initial letters are used, to decipher from the text who the author referred to is, and reference must therefore be made to the end of the book.

This book can be well recommended to those interested in a general review of oragnic radiation chemistry. There is, however, a need for more detailed monographs on radiation chemistry generally.

R. ROBERTS

Radioactivity for Pharmaceutical and Allied Research Laboratories. Edited by ABRAHAM EDELMAN. Academic Press, New York and London, 1960, 171 pp.

THIS volume contains the proceedings of a symposium sponsored by the Nuclear Science and Engineering Corporation. Although it is obviously designed to promote the wider use of ionizing radiation and radioactive tracers in a particular branch of industry this collection of papers should also prove to be of interest to research workers in fields such as pharmacology, bacteriology and biochemistry.

There are several survey papers which deal with the basic principles of techniques such as activation analysis, isotope dilution methods and tracer studies designed to follow the distribution and metabolism of labelled drugs. In general, the subject matter of these papers is covered more adequately in standard text books. Of greater interest are the papers which form the major part of the book and which deal with the application of these principles to specific problems. Since the emphasis throughout the book is on technology rather than academic research it is probable that any given paper will only be of direct interest to a comparatively narrow group of readers. On the other hand, it is hardly necessary to point out to readers of this journal that radioisotope techniques often have much wider applications than those for which they were originally designed. This reviewer is of the opinion that the papers dealing with the use of previously irradiated rats as sensitive preparations for the bioassay of drugs which may have a granulocytopenic effect, the analytical methods for the determination of sterols and gamma hexane by isotope dilution in natural or crude products, and the "isotopic profile" method for studying the effects of antibiotics on bacterial metabolism come within the above-mentioned category. However, this selection of subjects for particular mention is so subjective as to be almost arbitrary.

Some of the papers, notably the one dealing with the use of radiation for the sterilization of pharmaceutical preparations may prove to be particularly illuminating to many research workers, since they show that the industrial application of a laboratory process raises many economic and administrative problems which can only be overcome by bitter experience. This book undoubtedly contributes towards bridging the gap between the academic worker and the technologist; it also provides some evidence that this problem is a real one in that there are now signs of a language barrier arising. For example, the reviewer had to re-read several paragraphs before realizing that the noun "soil" when used by a detergent chemist has no earthy connotation; and the word "beer" has an esoteric significance in penicillin production.

N. VEALL

J. S. MITCHELL: **Studies in Radiotherapeutics.** Blackwell Scientific Publications 1960. 216 pp., 52*s.* 6*d.*

THE author is a man of great ability in mathematics, physics, chemistry, radiotherapy and medicine. The reader might therefore be afraid that he would have to be well-versed in all these subjects fully to understand the book. In fact, Professor Mitchell, while he reveals himself as an authority in many fields, has written a book which can be profitably read and easily understood by any radiotherapist with a good scientific background, and by many clinicians as well as by the research worker.

It will be recognized as an excellent work if we realize that its scope is intended to be limited. It is not a text-book or general reference book. It provides a survey in considerable detail of a few subjects only, and in fact one-seventh of the book consists of a very full bibliography to allow detail to be followed up.

The volume is divided into three chapters. They

VOL. 10 1961

are three separate essays, each with its own bibliography, and any one of them may be read separately.

The first chapter discusses the *Mechanisms of the Therapeutic Actions of Radiations*. It is a survey of present knowledge, including description of the disturbances of cellular metabolism and nuclear structures, reinforced by results obtained in the writer's own department, e.g. the effects of microbeam irradiation of the nucleolus. The chapter concludes with a clear and concise summary of the modes of action and a statement of general principles.

The second chapter deals with *Some Clinical and Laboratory Studies of Chemical Radiosensitisers, Including the Design and Conduct of Clinical Trials*. In contrast to the first chapter, the general survey of the subject is here quite short, and most of the space is given up to Mitchell's account of his own investigations and search for sensitisers, especially syncavit and allied compounds. The chapter will be read particularly for the authors' experience in a subject which he has made especially his own.

The last chapter is wholly an account of *Some Investigations of Problems of Practical Interest*, and is mainly a description of various techniques developed in the author's own department. Among many points of interest, the comparison of the comparative cost of different sources of external radiation is worth mention.

R. C. TUDWAY

R. D. RUSSELL and R. M. FARQUHAR: **Lead Isotopes in Geology.** Interscience Inc., New York, 1960. viii +243 pp., $9.

THE progress of the past 22 years in the study of the isotopes of lead is reviewed in this timely, well-written volume. The authors, both able and well-recognized investigators in the field, have done a commendable service in summarizing objectively the contributions of many scientists from the first mass spectrometric analyses of the lead isotopes by Nier in 1938 to papers published during 1960. Each of the eight chapters is followed by suggestions for further reading, and throughout, the volume is carefully documented by footnotes and terminal references.

The problem of the known variations in isotopic composition of lead minerals is introduced in Chapter 1 which reviews briefly the origin of lead through decay of uranium and thorium. The authors point out that the problems pertaining to the interpretations of the natural variations of the lead isotopes are fundamentally geologic ones.

Chapter 2 considers the measurement of the lead isotope ratios. Comparative results obtained in different laboratories for a number of University of Toronto samples are given. The methods of analysis are considered, and some of the analytical problems, particularly in the precise determination of Pb^{204}, are clearly presented.

The age of the earth is considered in Chapter 3, and strong arguments are given for accepting Patterson's value of 4.5×10^9 years, obtained from isotopic analyses of lead in meteorites, as the best presently available. The dating of galenas is discussed in Chapter 4 with a discussion of the models of Holmes-Houtermans, Russell-Farquhar-Cummings, and Russell-Stanton-Farquhar. Limitations of the models are indicated.

The discussion of anomalous leads in Chapter 5 is particularly valuable. The usage of terms in this area of investigation has gradually changed with increased understanding of the complexity of the prob!em. The authors define anomalous lead as a type resulting from additions to ordinary lead of amounts of radiogenic lead in a manner that cannot be explained by the formulae now being used.

In Chapter 6, data from lead-isotope analyses are applied to three mining districts: Sudbury, Ontario; Thunder Bay, Ontario; and Broken Hill, New South Wales, Australia. Chapter 7 considers various extensions of the Holmes-Houtermans model and reviews the contributions of Bate, Damon, Marshall, and others. Chapter 8 reviews briefly the methods and some of the problems of lead-uranium-thorium age determinations.

A valuable feature of *Lead Isotopes in Geology* are the 12 appendices in which data on lead isotopes are listed by laboratories. Russell and Farquhar have ably handled a difficult subject in a manner to be of great service to many disciplines, and their book is a valuable addition to the libraries of geologists, geophysicists, geochemists, geochronologists, and to all scientists who are interested in the problems of the constitution and origin of the earth. They have succeeded not only in presenting the available information, but also in indicating the great promise for future investigations. This is indeed a scholarly effort.

S. S. GOLDICH

Radioactive Sources; Radioactive Chemicals. The Radiochemical Centre, Amersham, Bucks., England.

THESE catalogs, dated 1959, became available in 1960. Both describe products and services of the Radiochemical Centre at Amersham, an establishment which supplies radioisotopes and radioactive sources as does Oak Ridge in the U.S.A.

Radioactive Sources contains 36 pages, 12 drawings of good quality, and 9 photographs. The illustrations are useful in indicating the structure of the sources and in showing the facilities necessary for working with such materials. Alpha sources include radiolead, polonium, radium, and radiothorium in amounts ranging from a fraction of a millicurie to a curie (polonium). Beta-emitter sources contain strontium cerium, promethium, thallium, ruthenium, and tritium. These are used for research, clinical, and industrial purposes. Cesium gamma sources are supplied which contain a wide range of activities, 1 mc to 500 curies. Other gamma sources contain cobalt, indium, thulium, tantalum, gold, radium, and radon. Encapsulated neutron-emitting mixtures include polonium-, radium-, and antimony-beryllium. Reference sources, intended for calibration of instruments, include alpha, beta, gamma, and neutron emitters. It was noted with interest that solutions of five nuclides, particularly intended for calibrating liquid counters, are available. Information is given on prices, service irradiations at Harwell, and details on methods of ordering, necessary approvals, and delivery.

Radioactive Chemicals is a catalog of radioisotope preparations (mostly in solution) and labelled compounds. It also contains a listing of reference sources and information on service irradiations and procurement of materials, as does the first catalog. It consists of 40 pages, 2 drawings, and 7 photographs. The table of "primary isotopes" lists 96 different radioisotopes, several in more than one form (specific activity or solution). In the section on labelled compounds, about 200 carbon-14-tagged materials are listed, plus about 127 tagged with phosphorus-32, 28 with iodine-131, and 42 with tritium. Further, a few compounds tagged with radioactive antimony, bromine, chlorine, cobalt, and other elements are listed.

S. A. Reynolds

Joseph Selman: **The Basic Physics of Radiotherapy.** C. T. Thomas, Springfield, Ill., 1960. 671pp., 105*s*.

Among a number of interesting text books now available on this subject for students of radiotherapy, this volume has the distinction of having been written by a radiotherapist. It covers a wide range of topics from elementary mathematics to nuclear and radiobiological theories. The practical aspects of the planning of X-ray treatments and the calculation of doses in radium and isotope therapy are treated in considerable and valuable detail.

The author begins with a chapter on mathematics, which, if it is not evaded by the student, will prove of great use. All those who have taught physics to radiotherapy students will know of the tedious circumlocations made necessary by their lack of knowledge, not to say deep suspicion, of mathematics. In particular if the section on the use of the slide rule encourages students to be more familiar with this instrument, it will have performed a very useful service. So often one has seen the interest of revealing even simple numerical relationships between variables in experimental work completely clouded for students by the tedium of the arithmetic involved, if a slide rule is not used. It is difficult, however, to understand why the author expends a good deal of space on simple proportion, but assumes that his readers can take exponentials in their stride.

One wonders why authors still continue to present graphs of X-rays spectra in terms of wave-length when most of the properties of radiation encountered in radiotherapy are only comprehensible in terms of its particulate nature. Spectral distribution shown in terms of wave-length give an entirely wrong impression of the amount of soft radiation present in X-ray beams and this is of importance in the appreciation of the significance of differential bone absorption. It is a pity, too, that in a book published in 1960 the röntgen is considered the primary unit of dose. However debatable the question of its continued use in clinical practice still may be, the subject is surely easier to understand both logically and historically if energy absorption is treated as the primary concept and ionization measurements considered as a means of estimating this quantity.

It is always difficult to teach electrotechnology and to describe the interaction of radiation with matter in elementary terms and yet retain sufficient detail to be of use in understanding radiotherapy practice and this has led to several oversimplifications and half-truths. Simple nuclear theory seems to be easier in this respect and here the author gives a clear account of nuclear reactors and their uses. Later chapters include a short account of the effects of radiation on the living cell, the uses of radioisotopes in diagnosis and therapy and finally a discussion of some of the problems of personnel protection. In all this, experimental results, theory and clinical practice are closely and clearly linked.

Indeed the main feature which would lead to the recommendation of this book is its essentially practical approach. Its price, however, is greater than many students will be willing to spend on a single textbook.

J. C. Jones

The Fourth Japan Conference on Radioisotopes

(*To be held in Tokyo, October* 1961)

I. Purpose of the Conference

THE purpose of the Japan Conference on Radioisotopes is to exchange scientific knowledges and experiences on research and application of radiation and radioisotopes in different fields including physics, chemistry, medical science, agriculture and industry, and to contribute to technological progress and spread of knowledge in this field that would result in increase of industrial productivity and improvement of public welfare.

It should be mentioned particularly that 1961 is a significant year for holding such a conference in that a look at the world's nuclear activities in the previous year reveals effort to revise their respective programmes or to make them fit to the realistic needs and thus the programmes in new shapes are going to be implemented in the year 1961. For Japan, too, 1961 is the first year of implementation of the new long range programme for atomic energy development and utilization and, in this light, the Conference would greatly help realize what is being purported in new programmes.

The Conference will be immensely benefited by having participants from Asian and Pacific countries since it would expedite development of peaceful uses of atomic energy through international exchange of knowledge and experience and would also tighten and promote international friendship.

II. Date and Place

1. *Date:* October 17 (Tuesday) through 19 (Thursday), 1961.
2. *Place:* International Hall, 5th floor, Tokyo Sankei Kaikan, Tokyo, Japan.

III. Official Language

Japanese and English.

IV. Remarks

(i) The sponsoring body is planning to invite experts in the field concerned also from the International Atomic Energy Agency, the United States, the United Kingdom and other countries.

(ii) Overseas participants are also requested to present research papers.

(iii) The details of the Conference and related subjects will be informed later.

VOL. 10 1961

VOL.
10
1961

TABLE 1. Exposure in the ORINS tot

(1) Select the desired exposure; (2) choose the lowest filter number to approximate the desired time. Tim
studies. (Ion chamber—Victoreen #605—NBS

r/min	4·77	4·00	2·86	2·34	2·13	1·78	1·36	1·13	0·90	0·74	0·57	0·49	0·46	0·39	0·314	0·271	0·17
Filters "in" r Exposure	0	1	2	3	4	5	6	7	8	9	10	11	12	13	14	15	1
25	00:05	00:06	00:09	00:11	00:12	00:14	00:18	00:22	00:28	00:34	00:44	00:51	00:54	01:04	01:20	01:32	02:
50	00:10	00:12	00:17	00:21	00:23	00:28	00:37	00:44	00:56	01:08	01:28	01:42	01:49	02:08	02:39	03:04	04:
75	00:16	00:19	00:26	00:32	00:35	00:42	00:55	01:06	01:23	01:41	02:12	02:33	02:43	03:12	03:59	04:37	07:
100	00:21	00:25	00:35	00:43	00:47	00:56	01:14	01:28	01:51	02:15	02:55	03:24	03:37	04:16	05:18	06:09	09:
150	00:31	00:38	00:52	01:04	01:10	01:24	01:50	02:13	02:47	03:23	04:23	05:06	05:26	06:25	07:58	09:14	14:
200	00:42	00:50	01:10	01:25	01:34	01:52	02:27	02:57	03:42	04:30	05:51	06:48	07:15	08:33	10:37	12:18	19:
250	00:52	01:02	01:27	01:47	01:57	02:20	03:04	03:41	04:38	05:38	07:19	08:30	09:03	10:41	13:16	15:22	23:
300	01:03	01:15	01:45	02:08	02:21	02:49	03:41	04:25	05:33	06:45	08:46	10:12	10:52	12:49	15:55	18:27	28:
350	01:13	01:28	02:02	02:30	02:44	03:17	04:17	05:10	06:29	07:53	10:14	11:54	12:41	14:57	18:35	21:32	33:
400	01:24	01:40	02:20	02:51	03:08	03:45	04:54	05:54	07:24	09:01	11:42	13:36	14:30	17:06	21:14	24:36	38:
450	01:34	01:52	02:37	03:12	03:31	04:13	05:31	06:38	08:20	10:08	13:09	15:18	16:18	19:14	23:53	27:40	43:
500	01:45	02:05	02:55	03:34	03:55	04:41	06:08	07:22	09:16	11:16	14:37	17:00	18:07	21:22	26:32	30:45	47:
550	01:55	02:18	03:12	03:55	04:18	05:09	06:44	08:07	10:11	12:23	16:05	18:42	19:56	23:30	29:12	33:50	52:
600	02:06	02:30	03:30	04:16	04:42	05:37	07:21	08:51	11:07	13:31	17:33	20:24	21:44	25:38	31:51	36:54	57:
650	02:16	02:42	03:47	04:38	05:05	06:05	07:58	09:35	12:02	14:38	19:00	22:07	23:33	27:47	34:30	39:58	62:
700	02:27	02:55	04:05	04:59	05:29	06:33	08:35	10:19	12:58	15:46	20:28	23:49	25:22	29:55	37:09	43:03	67:
750	02:37	03:08	04:22	05:21	05:52	07:01	09:11	11:04	13:53	16:54	21:56	25:31	27:10	32:03	39:49	46:08	71:
800	02:48	03:20	04:40	05:42	06:16	07:29	09:48	11:48	14:49	18:01	23:24	27:13	28:59	34:11	42:28	49:12	76:
850	02:58	03:32	04:57	06:03	06:39	07:58	10:25	12:32	15:44	19:09	24:51	28:55	30:48	36:19	45:07	52:16	81:
900	03:09	03:45	05:15	06:25	07:03	08:26	11:02	13:16	16:40	20:16	26:19	30:37	32:37	38:28	47:46	55:21	86:
950	03:19	03:58	05:32	06:46	07:26	08:54	11:39	14:01	17:36	21:24	27:47	32:19	34:25	40:36	50:25	58:26	91:
1000	03:30	04:10	05:50	07:07	07:49	09:22	12:15	14:45	18:31	22:31	29:14	34:01	36:14	42:44	53:05	61:30	95:

S total-body irradiator (1960–1961).
Time is read as *xx*:*yy*, when *xx* = hours and *yy* = minutes. This is the "nominal dose" for all clinical
-NBS calibration, 22° C, 760 mm pressure)

0·174	0·147	0·115	0·099	0·094	0·081	0·067	0·059	0·053	0·049	0·041	0·037	0·036	0·034	0·032	0·030
16	17	18	19	20	21	22	23	24	25	26	27	28	29	30	31
02:24	02:50	03:37	04:12	04:26	05:09	06:13	07:04	07:52	08:30	10:10	11:16	11:34	12:15	13:01	13:53
04:47	05:40	07:15	08:25	08:52	10:17	12:26	14:07	15:43	17:00	20:20	22:31	23:09	24:30	26:02	27:47
07:11	08:30	10:52	12:38	13:18	15:26	18:39	21:11	23:35	25:31	30:29	33:47	34:43	36:46	39:04	41:40
09:35	11:20	14:30	16:50	17:44	20:34	24:52	28:15	31:27	34:01	40:39	45:03	46:18	49:01	52:05	55:33
14:22	17:00	21:44	25:15	26:36	30:52	37:19	42:22	47:10	51:01	60:58	67:34	69:27	73:32	78:08	83:20
19:09	22:40	28:59	33:40	35:28	41:09	49:45	56:30	62:54	68:02	81:18	90:05	92:36	98:02	104:10	111:07
23:57	28:21	36:14	42:05	44:20	51:26	62:11	70:37	78:37	85:02	101:38	112:37	115:44	122:33		
28:44	34:01	43:29	50:30	53:11	61:44	74:38	84:45	94:20	102:02						
33:31	39:41	50:43	58:55	62:03	72:01	87:04	98:52	110:04							
38:19	45:21	57:58	67:20	70:55	82:18	99:30	113:00								
43:06	51:01	65:13	75:45	79:47	92:36	111:56									
47:54	56:41	72:28	84:10	88:39	102:53										
52:41	62:21	79:43	92:36	97:31											
57:28	68:02	86:57	101:01	106:23											
62:16	73:42	94:12													
67:03	79:22	101:27													
71:50	85:02														
76:38	90:42														
81:25	96:22														
86:12	102:02														
91:00															
95:47															555:56

2

3